RESEARCH

UDOT CONNECTING COMMUNITIES

Utah Department of Transportation - Research Division
4501 South 2700 West, Box 148410 - Salt Lake City, Utah 84114-8410

Report No. UT-10.18

DYNAMIC PASSIVE PRESSURE ON ABUTMENTS AND PILE CAPS

Prepared For:

Utah Department of Transportation Research Division

Submitted By:

Brigham Young University
Department of Civil & Environmental Engineering

Authored By:

Kyle M. Rollins
Travis M. Gerber
Colin R. Cummins
Joshua M. Pruett

August 2010

THIS PAGE INTENTIONALLY LEFT BLANK

1. Report No.	2. Government Accession No.	3. Recipient's Catalog No.
UT-10.18		

4. Title and Subtitle	5. Report Date
DYNAMIC PASSIVE PRESSURE ON ABUTMENTS AND PILE CAPS	August 2010
	6. Performing Organization Code

7. Author	8. Performing Organization Report No.
Travis M. Gerber, Kyle M. Rollins, Colin R. Cummins, and Joshua M. Pruett	

9. Performing Organization Name and Address	10. Work Unit No.
Civil & Environmental Engineering Dept. Brigham Young University 368 CB Provo, UT 84602	11. Contract or Grant No. 06 9148

12. Sponsoring Agency Name and Address	13. Type of Report & Period Covered
Utah Department of Transportation 4501 South 2700 West Salt Lake City, Utah 84114-8410	FINAL
	14. Sponsoring Agency Code UT05.703

15. Supplementary Notes

Prepared in cooperation with the Utah Department of Transportation and Federal Highway Administration.

16. Abstract

This study investigated the lateral load response of a full-scale pile cap with nine different backfill conditions, more specifically being: 1) no backfill present (baseline response), 2) densely compacted clean sand, 3) loosely compacted clean sand, 4) densely compacted fine gravel, 5) loosely compacted fine gravel, 6) densely compacted coarse gravel, 7) loosely compacted coarse gravel, 8) a 3-ft wide densely compacted fine gravel zone with loosely compacted clean sand backfill, and 9) a 6-ft wide densely compacted fine gravel zone with loosely compacted clean sand backfill. The pile cap was loaded using a combination of hydraulic load actuators and an eccentric mass shaker. The actuators were used to slowly push (statically load) the pile cap to incrementally larger target displacement levels. At each displacement level, the actuators were used to cyclically displace the pile cap a small distance, and the shaker was used to apply a dynamic loading on top of the static holding force from the actuators. Hence, the results presented in this report address static, cyclic, and dynamic loadings. The results of this study include horizontal load versus displacement relationships for the pile cap with differing backfill conditions and earth pressure distributions along the pile cap face. The results also include comparisons between measured and theoretically-based or calculated values. Additional results include descriptions of vertical displacement, horizontal displacement and cracking of the backfill. The stiffness and damping for the pile cap with the different backfill conditions were also determined.

17. Key Words	18. Distribution Statement	23. Registrant's Seal
Passive Force, Abutment, Pile Cap, Lateral Load Tests, Static Loading, Dynamic Loading, Cyclic Loading	UDOT Research Division 4501 S.2700 West-Box 148410 Salt Lake City, Utah 84114	

19. Security Classification	20. Security Classification	21. No. of Pages	22. Price
Unclassified	Unclassified	223	

THIS PAGE INTENTIONALLY LEFT BLANK

DISCLAIMER

The authors alone are responsible for the preparation and accuracy of the information, data, analysis, discussions, recommendations, and conclusions presented herein. The contents do not necessarily reflect the views, opinions, endorsements, or policies of the Utah Department of Transportation or the U.S. Department of Transportation. The Utah Department of Transportation makes no representation or warranty of any kind, and assumes no liability therefore.

THIS PAGE INTENTIONALLY LEFT BLANK

ACKNOWLEDGEMENTS

Funding for this project was provided by Contract No 069148 “Dynamic Passive Pressure of Abutments and Pile Cap” with the Utah Department of Transportation as part of a pooled-fund study supported by Departments of Transportation from California, Oregon, Montana, New York and Utah. Daniel Hsiao served as the project manager for UDOT. Additional support for this shared-use project was also provided by the National Science Foundation under Award Number CMS-0421312, and the George E. Brown, Jr. Network for Earthquake Engineering Simulation (NEES) which operates under NSF Award Number CMS-0402490. This support is also gratefully acknowledged.

THIS PAGE INTENTIONALLY LEFT BLANK

TABLE OF CONTENTS

THIS PAGE INTENTIONALLY LEFT BLANK

LIST OF FIGURES

THIS PAGE INTENTIONALLY LEFT BLANK

LIST OF TABLES

TABLE OF EQUATIONS

THIS PAGE INTENTIONALLY LEFT BLANK

EXECUTIVE SUMMARY

Building and bridge structures are often founded upon pile groups connected with a concrete cap, an arrangement which increases resistance to lateral loads and overturning moments and decreases lateral displacements. Lateral loadings and displacements, along with accompanying overturning moments, can be induced by wind or earthquakes. Interaction between the soil and the piles, as well as passive earth pressure from the backfill material against the pile cap, provides the lateral resistance of a pile cap foundation.

The ultimate passive pressure of backfill materials surrounding pile cap foundations can be calculated for static loading conditions using Rankine, Coulomb, or log-spiral theories. However, the development of passive pressure as a function of soil-foundation displacement is less-well defined. Some relationships assume a simple linear elastic relationship while others specify non-linear (often hyperbolic) relationships. Unfortunately, nearly all of the existing load-displacement relationships for soils are based on static or slowly applied loadings. Under seismic loading conditions, both dynamic and cyclic effects are present which alter the load-displacement relationship. Cyclic loadings will usually reduce the strength of a soil (also referred to as soil softening) whereas dynamic loading effects tend to produce an apparent increase in soil resistance due to damping and other factors. Because there is a lack of well-defined load-displacement relationships which address the effects of both cyclic and dynamic loading, the engineering community has often applied static load-displacement relationships in seismic design.

This study was undertaken to help quantify the effects of cyclic and dynamic loadings, and develop appropriate load-displacement relationships, for different backfill soils. The research consisted of two major parts: performing the field testing, and analyzing and interpreting the test results. The field testing consisted of laterally loading a full-scale pile cap (5.5 ft high by 11 ft wide) with various backfill conditions. The different backfill conditions consisted of: 1) no backfill present (also referred to as a baseline response); 2) loosely compacted clean sand; 3) densely compacted clean sand; 4) loosely compacted fine gravel; 5) densely compacted fine gravel; 6) loosely compacted coarse gravel; 7) densely compacted coarse gravel; 8) a 3-ft (0.91-m) wide zone of densely compacted coarse gravel between the cap and

loosely compacted clean sand; and 9) a 6-ft (1.83-m) wide zone of densely compacted coarse gravel between the cap and loosely compacted clean sand.

The loading of the pile cap was accomplished using a combination of hydraulic load actuators and an eccentric mass shaker. The actuators were used to slowly push (statically load) the pile cap to incrementally larger target displacement levels. At each displacement level, the actuators were used to cyclically displace the pile cap a small distance and the shaker was used to apply a dynamic loading on top of the static holding force from the actuators.

The analysis and interpretation of the data collected during testing produced various results associated with static, cyclic, and dynamic loading conditions. These results include horizontal load versus displacement relationships for the pile cap with differing backfill conditions and earth pressure distributions along the pile cap face. Results also include comparisons between measured and theoretically-based or calculated values. Additional results include descriptions of vertical displacement, horizontal displacement and cracking of the backfill, as well as estimates of cyclic and dynamic stiffness and damping for the pile cap with different backfill conditions.

The test results show that there is a dramatically different load-displacement response between loosely and densely compacted backfill soils. Consequently, it is recommended that engineering professionals should take significant measures to assure that backfill compaction requirements are met and that those requirements result in a high relative density if significant passive earth force is required. For the design of concrete foundations and abutments backfilled with well-compacted granular materials, say on the order of 95% modified Proctor density or 75% relative density, it is suggested that the log-spiral approach can be used with a soil friction angle of 40° and a δ/□ ratio of 0.6 to 0.75 to determine the passive earth force. These parameters should give a lower-bound solution to the passive response of backfill subjected to static, cyclic, and dynamic loadings. The designer who has performed field shear strength testing and is confident in the resulting parameters can use them in determining a larger passive earth force, noting that calculated passive earth coefficients increase 10 to 15% for each 1° increase in □beyond 40°.

In the case of loosely compacted granular fills, say on the order of 85 to 90% modified Proctor or 35% relative density, it was found that Rankine passive earth theory may be used to determine the passive earth force. However, the Rankine method may underestimate the

capacity of granular backfill soil as the failure mode transitions from punching to general shear. Alternatively, shear strengths can be reduced by a factor ranging from 0.6 to 0.85 (perhaps increasing with relative density) when using the log-spiral method to compute the passive earth force. This approach is similar to that suggested by Terzaghi and Peck (1967) for the bearing capacity of loose to medium dense granular soils. For densely compacted granular backfills, the test results confirm that the load-displacement response can be modeled as a hyperbolic curve and the ultimate passive force is realized at a displacement-to-height ratio of approximately 3 to 4%. Computer programs such as PYCAP and ABUT can be used to reasonably calculate hyperbolic load-displacement relationships for densely compacted granular backfills.

Under cyclic and dynamic loadings, the passive earth force acting on the face of a pile cap or abutment can contribute a significant portion of the overall resistance and stiffness. The response of pile cap structures subject to variable frequency loadings can be quantified using an average damping ratio of at least 15%, but the precise ratio will vary as inertial and total earth forces act in and out of phase. Consideration should be given to changes in structural period due to changes in dynamic stiffness and damping ratio with forcing frequency and displacement amplitude.

Other findings suggest that placement of a relatively narrow zone of densely compacted gravel immediately adjacent to a foundation where the surrounding soil is otherwise relatively loose can significantly increase the passive resistance provided by the soil backfill. A nominal 3 ft (0.91 m) wide (i.e., horizontal) zone of densely compacted gravel should provide at least 50% of the ultimate capacity otherwise expected if all of the material surrounding the pile cap had been composed of the densely compacted gravel. The densely compacted backfill should also extend vertically below the bottom of the foundation 25% of the pile cap height. The effect of a wider zone of densely compacted gravel is less certain and requires more analysis.

Lastly, when accounting for the effect of wall height on the ultimate passive force and backfill stiffness, the results of this study indicate that both parameters should be scaled by the square of the ratio of the wall heights.

THIS PAGE INTENTIONALLY LEFT BLANK

1.0 INTRODUCTION

1.1 Background

Building and bridge structures are often founded upon pile groups connected with a concrete cap, an arrangement which increases resistance to lateral loads and overturning moments and decreases lateral displacements. Lateral loadings and displacements, along with accompanying overturning moments, can be induced by wind or earthquakes. The interaction between the soil and the piles, as well as the passive earth pressure provided by the backfill material against the sides of the pile cap, provide the lateral resistance of a pile cap foundation.

The ultimate passive pressure of backfill materials surrounding pile cap foundations can be calculated for static loading conditions using Rankine, Coulomb, or log-spiral theories. However, the development of passive pressure as a function of soil-foundation displacement is less well defined. Some relationships assume a simple linear elastic relationship while others specify non-linear (often hyperbolic) relationships. Unfortunately, nearly all of the existing load-displacement relationships for soils are based on static or slowly applied loadings. Under seismic loading conditions, both dynamic and cyclic effects are present which alter the load-displacement relationship. Cyclic loadings will usually reduce the strength of a soil (also referred to as soil softening) whereas dynamic loading effects tend to produce an apparent increase in soil resistance due to damping and other factors. Because there is a lack of well-defined load-displacement relationships which address the effects of both cyclic and dynamic loading, the engineering community has often applied static load-displacement relationships in seismic design.

1.2 Description and Objective of Research

The research presented in this report was undertaken to help quantify the effects of cyclic and dynamic loadings, and develop appropriate load-displacement relationships, for different backfill soils. The research consisted of two major parts: performing the field testing, and analyzing and interpreting the test results.

The field testing consisted of laterally loading a full-scale pile cap with different backfill conditions. The different backfill conditions consisted of: 1) no backfill present; 2) loosely compacted clean sand; 3) densely compacted clean sand; 4) loosely compacted fine gravel; 5) densely compacted fine gravel; 6) loosely compacted coarse gravel; 7) densely compacted coarse gravel; 8) densely compacted clean sand with MSE walls; 9) 3-ft (0.91-m) wide zone of densely compacted coarse gravel between the cap and loosely compacted clean sand; and 10) 6-ft (1.83-m) wide zone of densely compacted coarse gravel between the cap and loosely compacted clean sand.

The lateral loading of the pile cap was effectuated by a combination of hydraulic load actuators and an eccentric mass shaker. The actuators were used to slowly push (statically load) the pile cap to incrementally larger target displacement levels. At each displacement level, the actuators were used to cyclically displace the pile cap a small distance and the shaker was used to apply a dynamic loading on top of the static holding force from the actuators.

The analysis and interpretation of the data collected during testing produced various results associated with static, cyclic, and dynamic loadings. The results include horizontal load versus displacement relationships for the pile cap with differing backfill conditions and earth pressure distributions along the pile cap face. These results also include comparisons between measured and theoretically-based or calculated values. Additional results include descriptions of vertical displacement, horizontal displacement and cracking of the backfill. The stiffness and damping for the pile cap with the different backfill conditions were also determined for both cyclic and dynamic loading conditions.

1.3 Organization of Report

This report is organized as follows. A description of the testing methods is presented in the next chapter, including the test setup and the site and backfill characteristics. Subsequently, the particular methods used to analyze the test data are discussed, including the methods of data reduction as well as the use of models to estimate passive resistance for comparison with the measured data. Chapters following the presentation of data analysis methods describe the results from each of the different backfill conditions examined for this study. The final chapter presents conclusions and recommendations based on this research effort.

2.0 TESTING METHODS

2.1 Site Description

Testing was performed at a site located approximately 1000 ft (300 m) north of the control tower at the Salt Lake City International Airport, in Salt Lake City, Utah. Multiple research efforts have occurred at this site, including testing of single piles, pile groups, and drilled shafts (for examples, see Johnson (2003) and Rollins et al. (2005a, 2005b)). An aerial photograph of the test site and the surrounding area is shown in Figure 2-1.

This previous testing has provided a large amount of data pertaining to the subsurface conditions of the site. In general, the surface of the test site is covered by approximately 5 ft (1.5 m) of imported clayey to silty sand and gravel fill. Underlying soils consist of multiple silt and clay layers with occasionally interbedded sand layers. An excavation was made and a 5.5-ft (1.68-m) high pile cap was constructed such that its top elevation matched that of the surrounding ground surface. Adjacent soils were excavated away from the cap such that only one face of the cap was in contact with the backfill soil. The water table during testing was located essentially from zero to 2 in (50 mm) above the base of the pile cap.

Figure 2-1 Aerial photograph of test site

2.2 Subsurface Characteristics

As previously mentioned, the test site has been used in several full-scale pile and drilled shaft tests which have provided substantial subsurface soil information. The first extensive subsurface investigation was conducted in 1995 by Peterson (1996). A variety of in-situ tests (such as SPT and CPT) as well as extensive laboratory shear strength and index property testing have been performed. Figure 2-2 shows locations of subsurface tests in relation to the previously existing pile groups and drilled shafts. The pile cap used in this research was constructed on the 9-pile group, but with the middle row of

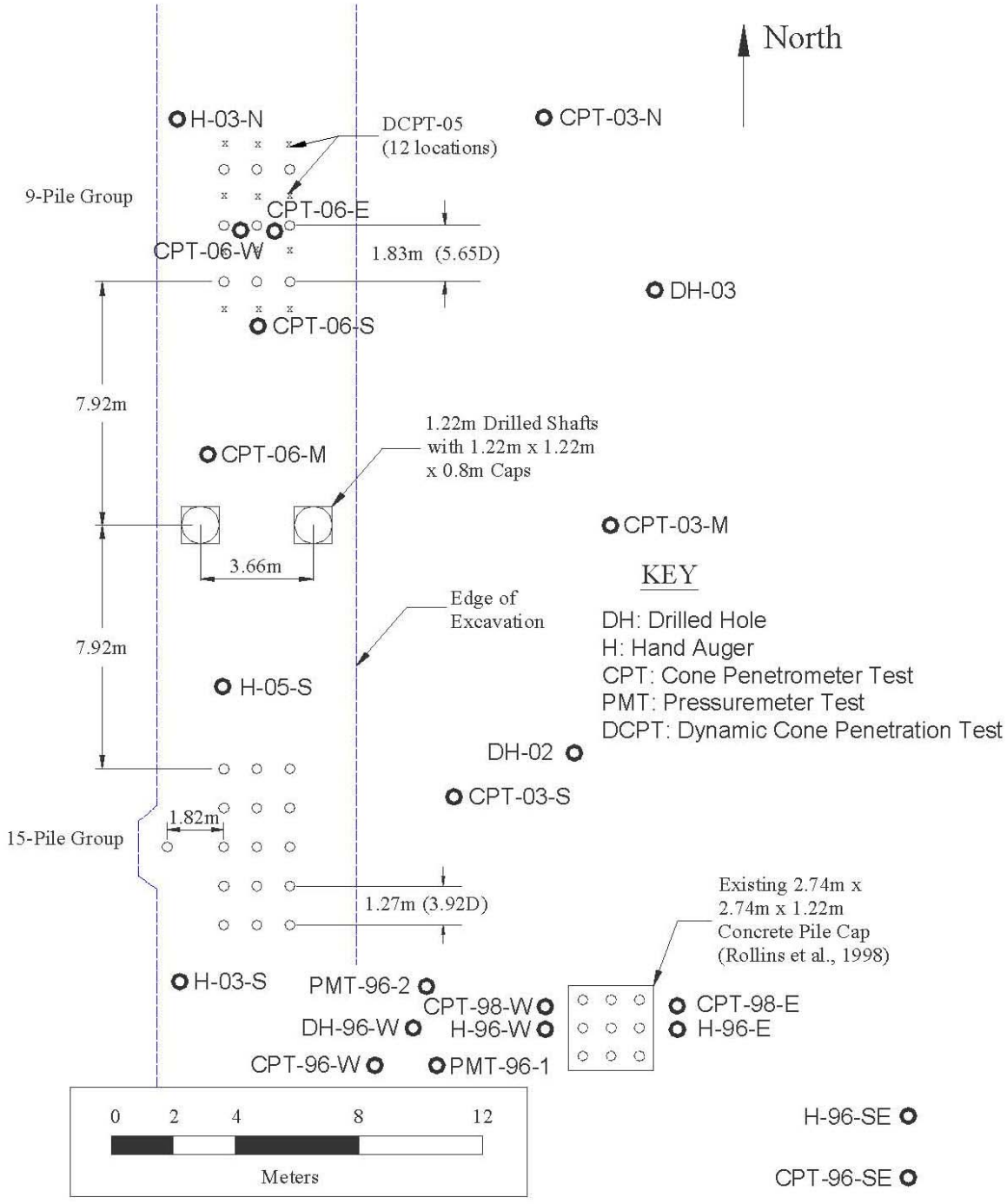

Figure 2-2 Entire test site with locations of subsurface tests (Christensen, 2006)

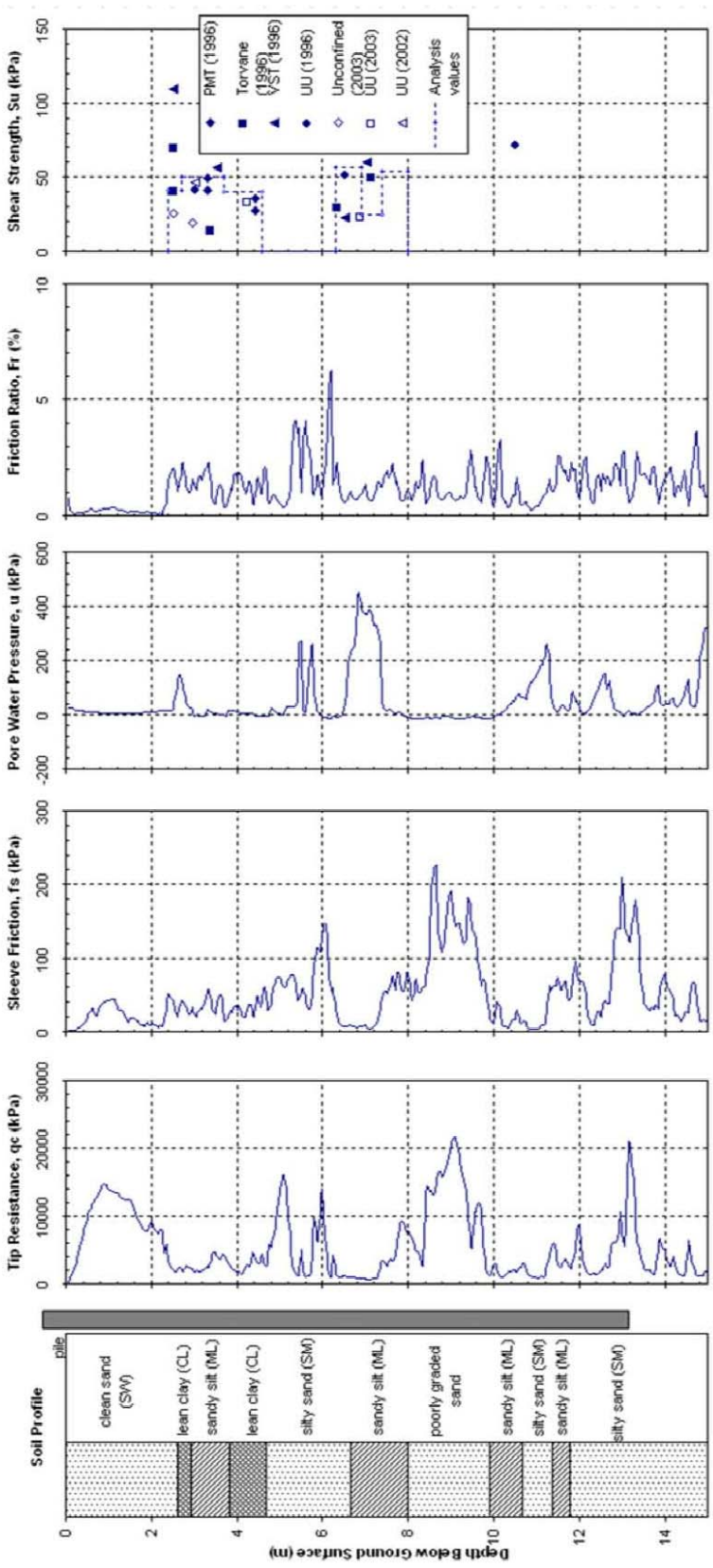

Figure 2-3 Idealized soil profile with CPT data (Christensen, 2006)

piles removed. Because this research focuses on the effects of the near-surface backfill, complete data from all previous subsurface investigations focusing on deep foundations will not be presented here, but reference can be made to Peterson (1996), Rollins et al. (2005a, 2005b), Christensen (2006), and Taylor (2006). However, a simplified subsurface profile (largely based on Peterson and presented by Christensen), together with results of a CPT conducted in the vicinity of the pile group upon which the pile cap was built, is shown in Figure 2-3. The layer of clean sand near the ground surface (which replaced previously imported materials) was removed and the piles cut off below the ground surface in order to construct the pile cap. Soils underlying the cap down to a depth of about 33 ft (10 m) consist of various layers of lean clay and sandy silt with two 5 to 6.5 ft (1.5 to 2 m) thick silty sand and poorly graded sand layers. Deeper soils consist of interbedded sandy silts and silty sands.

2.3 TESTING LAYOUT, EQUIPMENT AND PROCEDURE

2.3.1 General

The basic features of the test site consist of a reaction foundation, a test pile cap, and the backfill soil zone. Figure 2-4 shows a plan and profile view of the test site and equipment. Additional views are provided in the photos presented in

Figure 2-5. Characterization of the backfill materials is provided in Section 2.4.

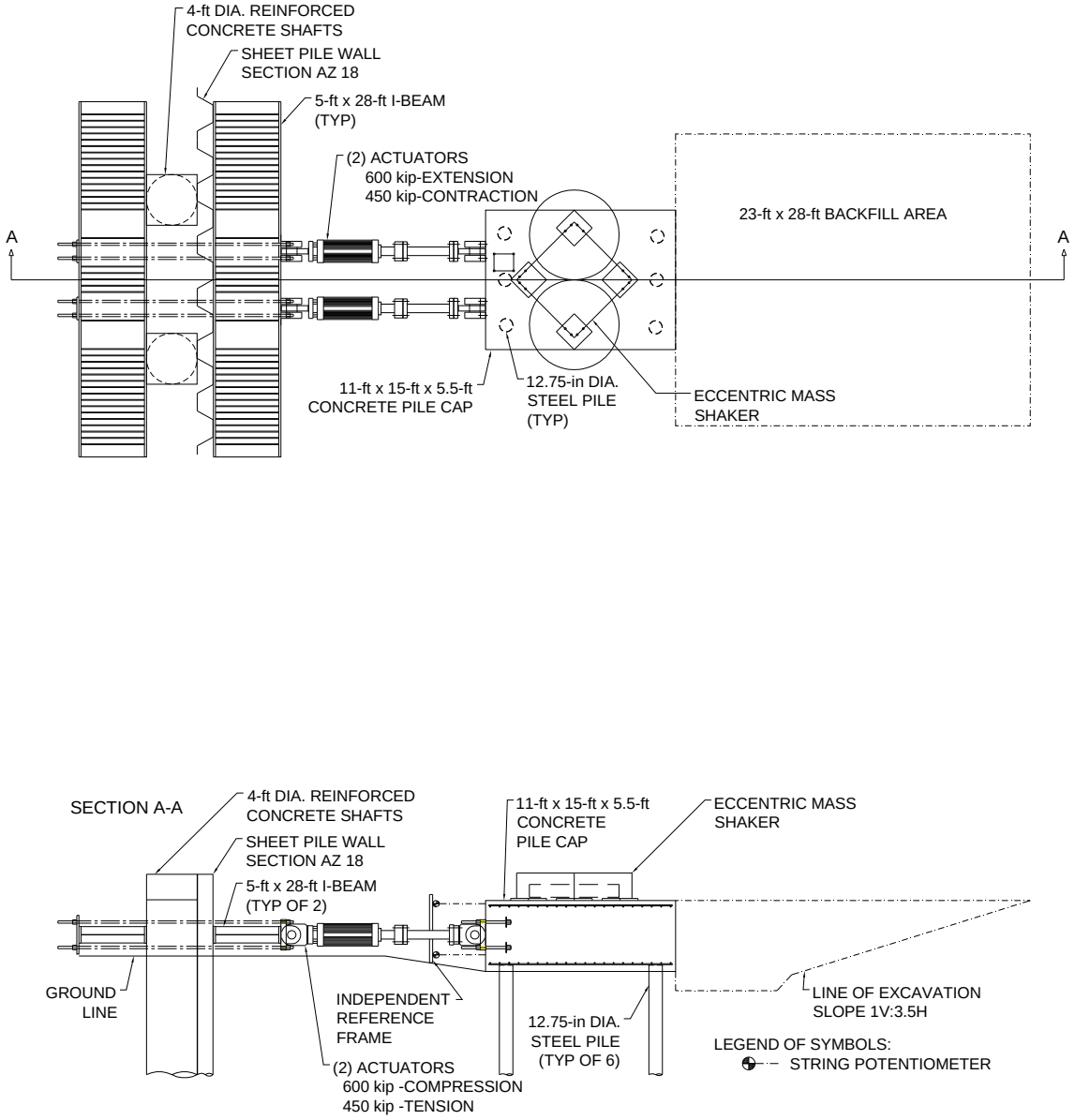

Figure 2-4 Plan and profile view of test setup

Figure 2-5 Photos of test site and equipment setup

2.3.2 Reaction Foundation

The reaction foundation was composed of the two existing 4-ft (1.2-m) diameter drilled shafts, spaced 12 ft (3.66 m) center to center, that were buttressed with a sheet pile wall and two reinforced steel I-beams. The top 2 ft (0.61-m) length of shaft above the ground surface are finished as a 4-ft (1.2-m) square cap to facilitate loadings from previous testing. The west and east shafts extend to depths of 55 ft (16.8 m) and 70 ft (21.3 m), respectively. Shaft reinforcement consists of eighteen #11 (#36) vertical bars extending to a depth of 35 ft (10.67 m) below ground. These bars are wrapped with a #5 (#16) spiral pitched at 3 in (75 mm) with a 4.75-in (120-mm) clear cover of concrete. Half of the vertical bars extend from 35 to 55 ft (10.67 to 16.76 m) with a spiral pitched at 12 in (300 mm). The average compressive strength of the concrete in the shafts is 6000 psi (41 MPa).

To increase the lateral capacity of the shafts being used as a reaction foundation, a sheet pile wall was installed on the north side of the drilled shafts. AZ-18 sheet piling constructed of ASTM A-572, Grade 50 steel was used, being selected from sections readily available in the local area. Installation depth was controlled by the 40 ft (12.2 m) length of the available stock. The piling, as built, extended to depths of 33.5 to 35.5 ft (10.24 to 10.85 m) below the excavated ground surface. The sheet pile was installed by vibratory hammer, and the sheet piling was kept as vertical and flush with the faces of the shafts as possible.

To help ensure a composite behavior and proper load distribution, two 28-ft (8.53-m) long, 64- by 16-in (1626- by 406-mm) I-beams with numerous stiffeners were placed with the web horizontal on either side of the shafts and sheet piling as shown in Figure 2-4. The reaction foundation was tied together with eight 2.5-in (64-mm) diameter high-strength threaded bars that were post-tensioned to 10 kip (45 kN).

2.3.3 Piles and Pile Cap

The previously driven piles are made of ASTM A252 Grade 3 (i.e., 45 ksi (310 MPa) minimum yield strength) steel pipe, with an outside diameter and wall thickness of 12.75 and 0.375 in (324 and 9.5 mm), respectively. The piles were driven closed ended to a depth of approximately 0.5 in (13 m) below the ground surface. After the removal of three (the middle row) of the original nine piles the remaining piles were spaced 12-ft (3.66-m) center to center in

the direction of loading. The tops of the piles were cut-off, leaving an approximate embedment of 6 in (150 mm) into the future cap. The piles were filled with 6000-psi (41-MPa) concrete and attached to the cap with a rebar cage consisting of six #8 (#25) vertical bars and a #4 (#13) spiral at a 6-in (152-mm) pitch. The 18-ft (5.49-m) long cages extend approximately 5 ft (1.47 m) into the cap and support the upper mat of horizontal reinforcement. Inclinometer tubes and shape array tubes were placed in the center north and center south piles.

The final cap dimensions are 15-ft (4.57-m) long, 11-ft (3.35-m) wide and 5.5-ft (1.68-m) tall. The concrete used in the cap has a compressive strength of 6000 psi (41 MPa). The cap is reinforced primarily with a mat of transverse and longitudinal reinforcing bars placed in both the top and the bottom of the cap. Each mat consists of #6 (#19) bars placed at 8 in (203 mm) on center, each way. Threaded bars to be used as connectors for the shaker and actuators were set into place during construction so as to be integral with the cap.

2.3.4 Loading Equipment

A pair of 600 kip (2.7 MN) capacity hydraulic actuators was used to apply horizontal force to the south side of the pile cap, pushing the cap northward. Each actuator was attached to the reaction foundation system with the threaded bars also used to tie the I-beams together. Each actuator was attached to the test pile cap by four threaded bars embedded in the cap during construction. Both ends of the actuators have free- swiveling heads, providing moment-free loading conditions. Hydraulic pressure was provided by a 60 gpm (227 l/min) pumping unit. Load from the actuators was applied at the mid-height of the cap, which corresponds to a depth of approximately 2.75 ft (0.84 m) below the backfilled ground surface. To help span the distance between the test cap and reaction foundation, 4-ft (1.22-m) long extensions were added to the actuators.

An eccentrically loaded mass shaker was used to provide dynamic loading to the pile cap. This piece of equipment was provided by the Network for Earthquake Engineering Simulation (NEES) equipment site located at UCLA. The shaker was oriented on the pile cap so that the maximum force vector was perpendicular to the reaction frame and parallel to the actuator load. The magnitude of force generated by the shaker is based on Equation 2-1:

$$F = 0.102 \times (WR) \times f^2 \qquad \text{Equation 2-1}$$

Where F is force (lb), WR is the weight-distance (i.e., moment) of the shaker basket (lb-in), and f is the shaker frequency (Hz). The weight and eccentricity of the shaker baskets can be changed by adding or subtracting 18.2 lb (0.08 kN) steel blocks which can be variously positioned within the baskets. Note that as written, the coefficient in Equation 2-1 is dimensionally dependent. With the configuration of steel blocks used during testing, the WR parameter was equal to 9820 lb-in (110.97 kN-cm) which gave a shaker capacity of 100 kip (446 kN) of force at a maximum frequency of 10 Hz.

2.3.5 Instrumentation

An independent reference frame was used to provide a non-moving datum from which to measure movement of the pile cap. The frame was located between the pile cap and the reaction foundation. The frame was embedded in the ground with concrete, and steel guide cables were used to reduce movement within the long-spanning frame.

Four string potentiometers were mounted to the primary frame and attached to the four corners of the southern pile cap face (the face to which the actuators were attached), with two near the top (29 in (740 mm) above the load point) and two close to the bottom (19 in (480 mm) below the load point) of the cap. Seven additional string potentiometers were mounted on the top of the pile cap near the backfilled face. These potentiometers were attached to metal stakes driven into the surface of the backfill, thus providing a measure of relative movement between the cap and points within the backfill.

Triaxial accelerometers were mounted to the top of the pile cap at each corner, with an additional accelerometer located near the center of the backfilled face of the cap. Because the reference frame is mounted to the ground, it responded dynamically when the shaker was used and data from the string potentiometers was expectedly unreliable. During the operation of the shaker, pile cap displacement was determined by double integrating the accelerometer data. Data was processed using a forward and backward FIR filter to eliminate phase distortion. A sampling frequency of 200 samples per second (sps) was used to capture the pile cap response up to 10 Hz.

The amount of resistance provided by the soil backfill can be determined in two ways. In the first way, the pile cap is load tested both with and without the backfill in place, and the difference between the two responses can be assumed to be the load-displacement response of the backfill. The second way consists of using pressure cells to measure the earth pressure directly and then using contributory areas based on the location of the pressure cells on the pile cap face to determine the resisting force from the backfill. The pressure cells have the obvious advantage of also providing a pressure distribution along the cap face. Six pressure cells were used, spaced at depths of 5.5, 16.5, 27.5, 38.5, 49.5, and 60.5 in (0.14, 0.42, 0.70, 0.98, 1.26, and 1.54 m) in the center portion of the pile cap. These stainless steel pressure cells were designed with a reinforced backplate to reduce point loading effects when directly mounting the cell to a concrete or steel structure, and the cells utilize a semi-conductor pressure transducer rather than a vibrating wire transducer to more accurately measure rapidly changing pressures. The cells were cast integrally with the pile cap so their top surfaces were flush with the concrete face.

To further document changes in the backfill during testing, a 2-ft (0.61-m) square grid was painted on the backfill. After cyclic and dynamic testing at each displacement level, cracking of the backfill was mapped by visual inspection with the aid of the grid. Vertical displacements were measured at grid nodes using traditional surveying equipment at the beginning and end (i.e., at the maximum displacement) of each testing sequence.

2.3.6 General Testing Procedures

Load testing of the pile cap was generally performed according to the following procedure. After placement of backfill materials (if any), the hydraulic load actuators were used to load and displace the pile cap to its initial target displacement level. The typical initial target displacement was 0.25 in (6.3 mm). After a several-second pause to manually record verification data, the actuators were used to apply 15 small amplitude displacement cycles (typically on the order of 0.1 in (2 mm) (single amplitude) at 0.75 Hz). After returning the actuators to their starting pre-cycling positions, the lengths of the actuators were fixed, causing each actuator to act as a strut between the reaction and test foundations. The shaker was then activated and a dynamic stepped-ramp loading was applied. The ramped loading consisted of dwelling on a specified frequency for 15 cycles and then ramping as fast as possible to the next dwell frequency. The dwell frequencies ranged from 1 to 10 Hz, in 0.5 Hz increments.

Afterwards, the shaker was allowed to ramp back down. The duration of shaker operation was typically about 3½ minutes, which includes the ramp up and the ramp down to the stopped position.

After some data processing and inspection of the backfill, the actuators were extended again to push the pile cap to the next displacement level. Upon reaching the target displacement level, rather than having the actuators cycle first as was performed previously, the shaker was used with the actuator lengths fixed. After the shaker loading was completed, the actuators applied their cyclic loading. Hence, the use of cyclic actuator loads and dynamic shaker loads was alternated between each target displacement level throughout the testing program until the maximum target displacement was reached.

In general, target displacement levels occurred in 0.25 in (6.3 mm) increments, ranging up to 1.75 and 3.0 in (44 and 76 mm) of displacement (the actual maximum displacement depended upon the load capacity of the actuators, the behavior of the reaction foundation, and the functionality of all the other equipment). Because the displacement control of the actuators included the displacement of both the reaction foundation and the test foundation, setting an appropriate displacement in the actuator control program for each loading increment depended upon our knowledge of the relative stiffnesses of the two different foundations, both of which were not precisely known a priori for the entire range of displacement. Hence, the actual displacements of the test pile cap vary from the targeted displacement levels. In some instances (particularly with those tests involving less compacted backfills), inspection of the load-displacement curve at the time of testing suggested that the incremental displacement for a given displacement level was insufficient to cause the load-displacement curve to reach the static backbone curve (i.e., the curve that would have been produced had the loading been applied monotonically rather than in a stepped fashion). In these instances, cyclic and dynamic loading was omitted and the pile cap was pushed to the next target displacement level so that the load path was closer to the backbone curve, as evidenced by a flattening of the load path after an initially steep reloading path during the initial portion of the loading increment.

Data during testing was acquired using a sampling rate of 200 samples per second (sps). Data files resampled at 1 sps were prepared to facilitate data screening and to use in analyses for portions of the testing involving relatively static loading conditions.

After cyclic and dynamic loading at each pile cap displacement interval, the equipment was briefly inspected and manual readings were taken before the cap was pushed to the next target displacement level. During the tests that involved backfill soil, any observed cracking of the backfill soil was mapped with the aid of the grid painted on the ground surface; therefore, the progression of cracking with increasing pile cap displacement was captured. Before initially loading the cap, the vertical elevations of the grid nodes were surveyed and inclinometer readings were taken for the center piles in the front and back rows of the pile cap. These measurements were again taken when the cap was at the maximum displacement level. Elevation surveys and inclinometer readings were not taken at intermediate displacement levels because of time constraints, whereas shape array data was collected throughout the test.

2.3.7 Summary of Tests

During our testing, a total of 12 individual tests were conducted. The backfill conditions for each test are shown in Table 2-1. The results of Test #9 with clean sand and a mechanically stabilized earth wall are presented elsewhere and will not be presented in this particular report.

Table 2-1 Summary of tests conducted

Test Number	Test Date	Backfill Condition
1	18-May-07	Free Response (Condition Cap)
2	25-May-07	Densely Compacted Clean Sand
3	29-May-07	Loosely Compacted Clean Sand
4	1-Jun-07	3-ft wide Gravel Zone with Loosely Compacted Clean Sand
5	1-Jun-07	No Backfill (Free Response)
6	4-Jun-07	6-ft wide Gravel Zone with Loosely Compacted Clean Sand
7	6-Jun-07	Loosely Compacted Fine Gravel
8	11-Jun-07	Densely Compacted Fine Gravel
9	18-Jun-07	Mechanically Stabilized Earth (MSE) Wall with Dense Clean Sand
10	21-Jun-07	Loosely Compacted Coarse Gravel
11	21-Jun-07	No Backfill (Free Response)
12	26-Jun-07	Densely Compacted Coarse Gravel

2.4 BACKFILL SOIL CHARACTERIZATION

Three types of soil were used in our testing and are referred to as 1) clean sand, 2) fine gravel, and 3) coarse gravel. This terminology is consistent with that used by Rollins and Cole (2006) and Cole and Rollins (2006) in describing similar testing conducted at the nearby I-15 Test Bed site at South Temple in Salt Lake City, Utah.

These three soils were placed and tested in both loosely and densely compacted states, with the former intending to represent a modest compactive effort (perhaps on the order of 90 to 95% of standard proctor) and a good compactive effort (perhaps on the order of 96% of modified proctor), respectively. In addition, two tests were performed with a 3- and 6-ft (0.91- and 1.83-m) wide zone of densely compact fine gravel between the pile cap and an otherwise loosely compacted clean sand.

2.4.1 Clean Sand Backfill

The clean sand backfill material used during testing is classified as a well graded sand (SW) using the Unified Soil Classification System. The AASHTO classification of the material is A-2-6(0). Figure 2-6 shows the particle distribution of the clean sand backfill material. This material is commonly used as fine aggregate for concrete; hence, the gradation limits for ASTM C-33 concrete sand are included on the chart. Table 2-2 provides a summary of the grain size distribution and other properties of the clean sand backfill material.

Table 2-3 provides the optimum moisture content and maximum dry density of the clean sand material using standard and modified effort, respectively. Tests were performed on the material in two separate compaction states: loosely compacted and densely compacted. Several compactors were used to reach the desired compaction

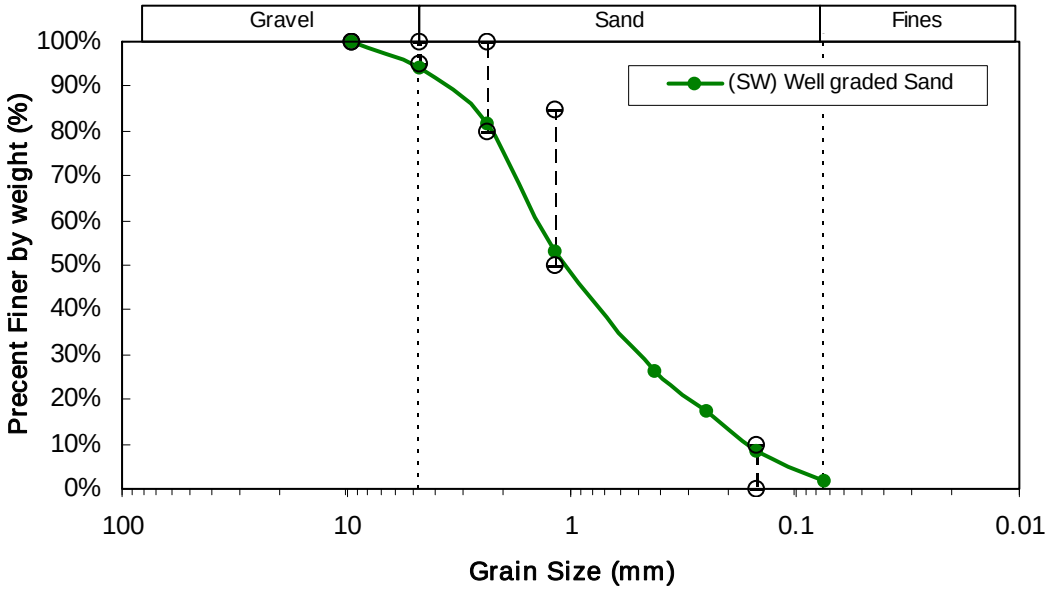

Figure 2-6 Particle size distribution for clean sand backfill material with qualifying limits for ASTM C-33 concrete sand

Table 2-2 Index properties for clean sand backfill material

Backfill Type	Gravel (%)	Sand (%)	Fines (%)	D_{60} (mm)	D_{50} (mm)	D_{30} (mm)	D_{10} (mm)	C_u	C_c
Clean Sand	6	92	2	1.50	1.11	0.56	0.17	8.7	1.2

levels, including a vibrating drum compactor, a vibrating plate compactor, and a jumping jack compactor. Several nuclear density gauge readings were taken for each lift to verify the degree of compaction and moisture content. Histograms illustrating the density distribution of densely compacted clean sand and loosely compacted clean sand are shown in Figure 2-7 and Figure 2-8, respectively. Table 2-4 summarizes the average in-situ unit weight properties of the clean sand backfill. The densely compacted clean sand has an average dry density of about 96% of the Modified Proctor maximum dry density.

Table 2-3 Compaction characteristics of clean sand backfill

Backfill Type	USCS	Standard Effort		Modified Effort	
		w_{opt} (%)	γ_d (pcf)	w_{opt} (%)	γ_d (pcf)
Clean Sand	SW	17	105	15	111

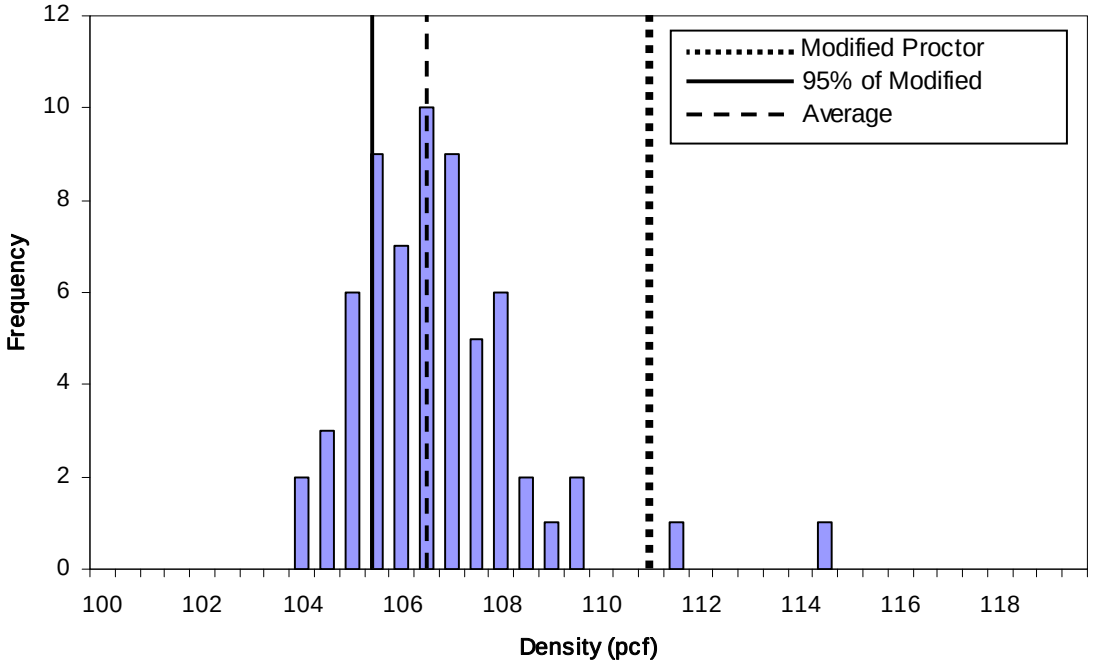

Figure 2-7 Density distribution of densely compacted clean sand backfill

The loosely compacted clean sand has an average dry density of about 94% of Standard Proctor maximum dry density or about 89% of Modifued Proctor density. Using the correlation developed by Lee and Singh (1971), relative density can be estimated from relative compaction (i.e. percentage of modified Proctor density). On this basis, the densely and loosely compacted fine gravel materials have estimated relative densities of approximately 80% and 44%, respectively. Cole (2003) used a similar sand backfill for which he reports maximum and minimum index densities of 17.8 and 13.4 kN/m^3, for which he reports maximum and minimum index densities of 17.8 and 13.4 kN/m^3, respectively. Based on these values, the average relative

densities of the loosely and densely compacted clean sand are calculated to be about 57 and 84%, respectively.

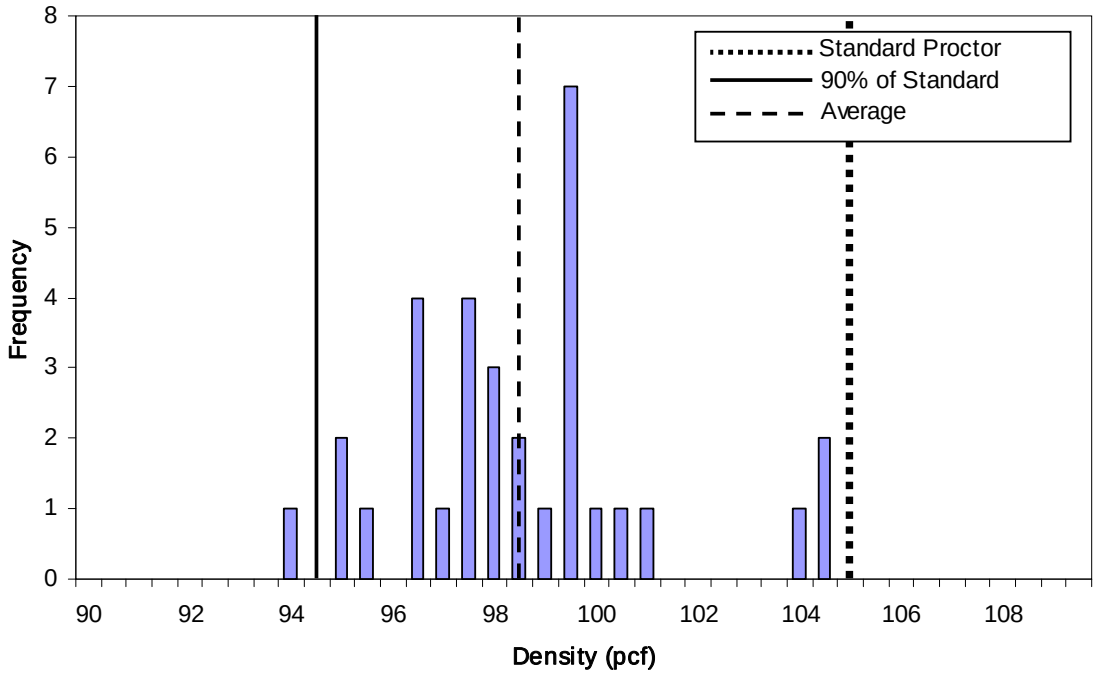

Figure 2-8 Density distribution of loosely compacted clean sand backfill

Table 2-4 Average in-situ unit weight properties for clean sand backfill

Backfill Type	$\gamma_{d,avg}$ (pcf)	w_{avg} (%)	$\gamma_{m,avg}$ (pcf)	Relative Compaction
Densely Compacted Sand	106.6	9.1	116.3	95.9% of modified
Loosely Compacted Sand	98.6	8.0	106.5	93.6% of standard (88.7 % of modified)

Direct shear tests were performed in the Brigham Young University soil mechanics laboratory to determine the shear characteristics of the sand at both of the aforementioned compaction levels. The direct shear tests were done in general accordance with ASTM D 3080.

The normal stress during the tests ranged from about 730 psf to about 6000 psf (35 kPa to about 290 kPa). Shear strength envelopes for the densely and loosely compacted clean sand are shown in Figure 2-9.

Failure envelopes for both peak and ultimate values were evaluated. Table 2-5 gives a summary of the engineering characteristics of the clean sand backfill based on the direct shear tests performed in the lab. These properties are used in subsequent analyses and interpretation of the test results.

Along with the normal direct shear tests, a series of modified tests were performed to quantify the interface friction angle (δ) between the concrete and the densely compacted clean sand. The interface friction angle was determined by placing a concrete sample of comparable roughness to the face of the pile cap into the bottom half of the shear box, filling the top half of the box with fine gravel compacted to the appropriate density, and shearing the composite sample under the same normal stress range as the internal friction angle tests. The interface friction angle determined from the ultimate stress points was approximately 29 degrees for densely compacted clean sand against concrete. The δ/φ ratio based on ultimate value results is about 0.72, which generally agrees with the value of 0.77 determine by Cole and Rollins (2006) for a similar sand material.

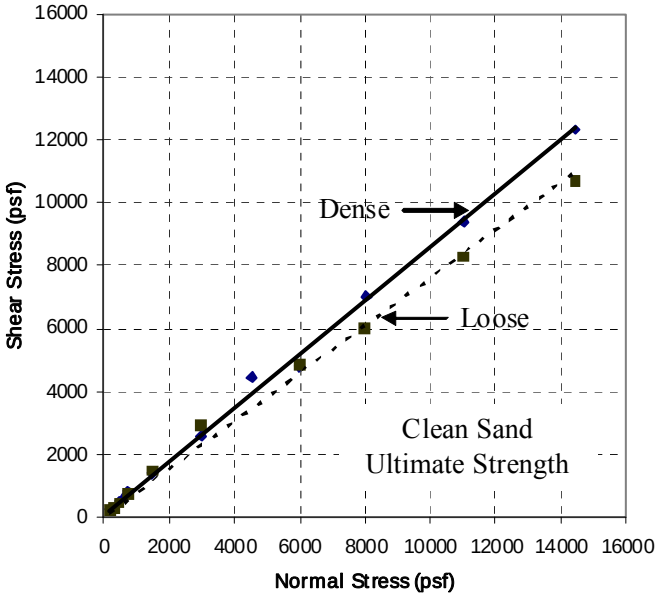

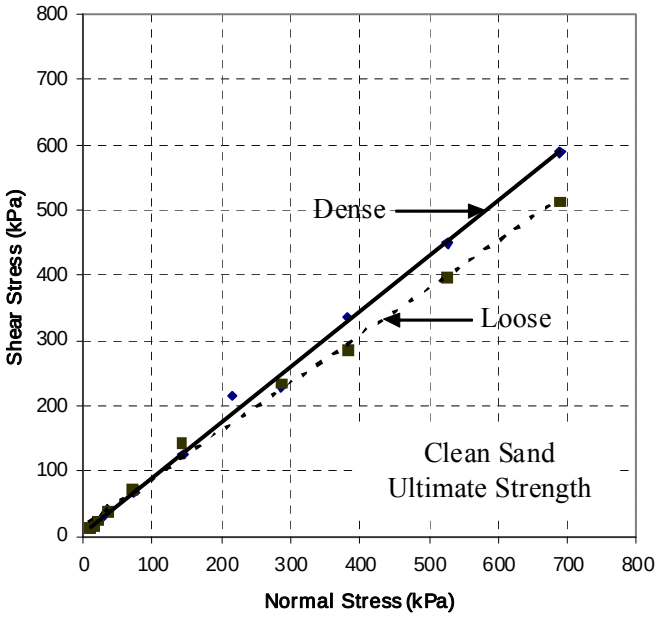

Ultimate Strength

0 to 689 kPa (0 to 14400 psf)

Dense	Loose
φ' = 40.2°	φ' = 36.2°
c' = 7 kPa	c' = 14 kPa
(144 psf)	(284 psf)

287 to 689 kPa (6,000 to 14,400 psf)

Dense	Loose
φ' = 40.5°*	φ' = 37.0°*
c' = 0 kPa*	c' = 0 kPa*
(0 psf)	(0 psf)

* φ' and c' values determined by forcing the cohesion intercept to pass through 0.

Figure 2-9 Direct shear results for densely compacted and loosely compacted clean sand backfill

Table 2-5 Direct shear summary for the clean sand backfill material

Backfill Type	Peak Values		Ultimate Values	
	ϕ (°)	c (psf)	ϕ (°)	c (psf)
Densely Compacted Sand	43.3	0	40.5	0
Loosely Compacted Sand	37.3	0	37.0	0

2.4.2 Fine Gravel Backfill

According to the USCS, the fine gravel classifies as a well graded sand with gravel (SW). The AASHTO classification of the fine gravel material is A-1-a. While the name given for the "fine gravel" appears to be a misnomer on the basis of the USCS, since AASHTO uses the #10 sieve rather than a #4 sieve to distinguish between gravel and sand, this roadbase material would appropriately be identified as a fine gravel in the AASHTO soil classification system. Figure 2-10 shows the particle distribution of the fine gravel backfill material. The gradation limits shown in the figure correspond to the gradation limits for locally used UDOT roadbase material. Table 2-6 provides a summary of the grain size distribution for the fine gravel backfill.

Table 2-7 shows the optimum moisture content and maximum dry density of the clean sand material using standard and modified effort, respectively. Testing was performed on the material in two separate compaction states: loosely compacted and densely compacted. A jumping jack and a robust trench compactor were used to bring the soil to the desired compaction levels. Several nuclear density gauge readings were taken for each lift to verify the degree of compaction and moisture content. Histograms showing the density distribution of densely compacted fine gravel and loosely compacted fine gravel are shown in Figure 2-11 and Figure 2-12, respectively. Table 2-8 provides the average in-situ unit weight properties of the fine gravel backfill. The densely compacted fine gravel has an average dry density of about 95% of the Modified Proctor maximum dry density, while the loosely compacted fine gravel has an average dry

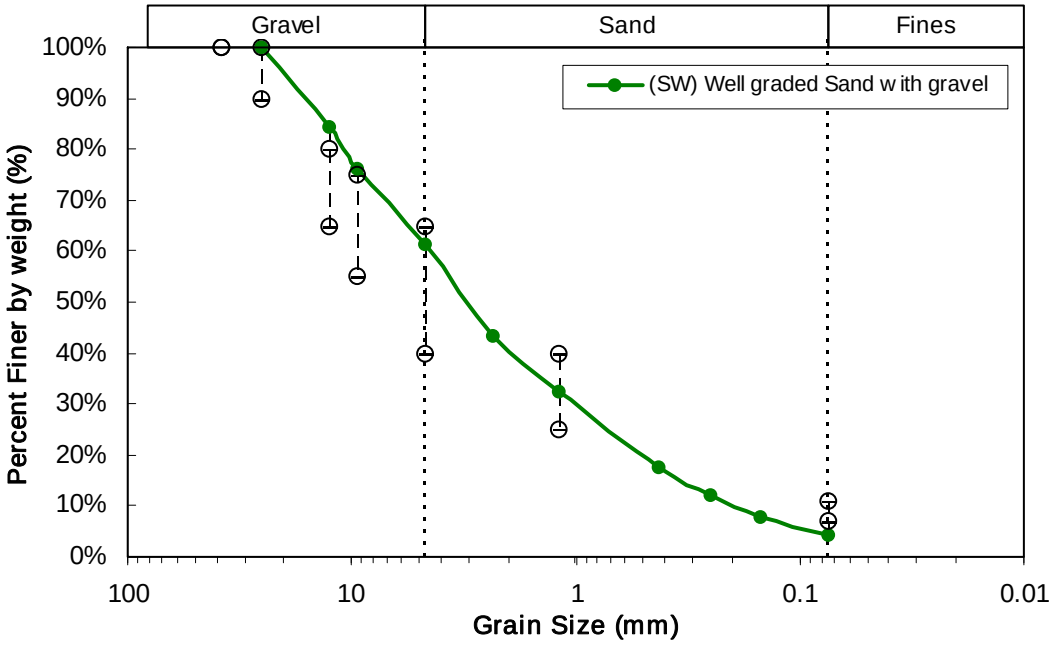

Figure 2-10 Particle distribution for fine gravel backfill with gradation limits for UDOT roadbase

Table 2-6 Index properties for the fine gravel backfill material

Backfill Type	Gravel (%)	Sand (%)	Fines (%)	D_{60} (mm)	D_{50} (mm)	D_{30} (mm)	D_{10} (mm)	C_u	C_c
Fine Gravel	39	57	4	4.5	3	1.03	0.2	22.5	1.2

density of about 94% of Standard Proctor maximum dry density or about 87% of Modified Proctor density. Using the correlation developed by Lee and Singh (1971), relative density can be estimated from relative compaction (i.e. percentage of modified Proctor density). On this basis, the densely and loosely compacted fine gravel materials have estimated relative densities of approximately 74% and 35%, respectively.

Table 2-7 Density characteristics of the fine gravel backfill material

Backfill Type	USCS	Standard Effort		Modified Effort	
		w_{opt} (%)	γ_d (pcf)	w_{opt} (%)	γ_d (pcf)
Fine Gravel	SW	8	122	7	131.8

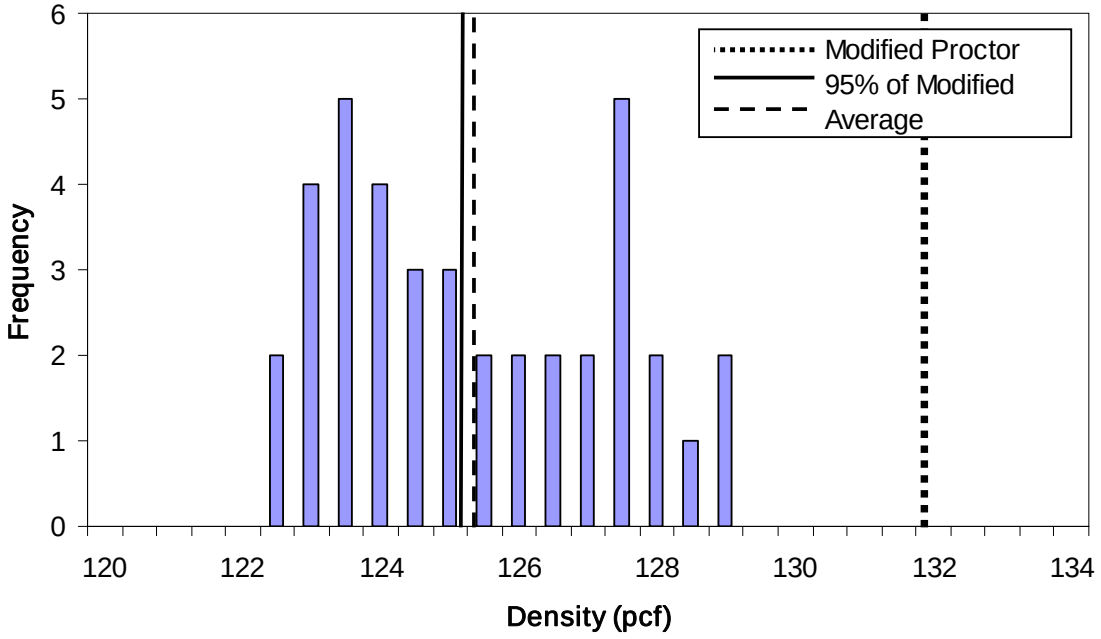

Figure 2-11 Density distribution of densely compacted fine gravel backfill

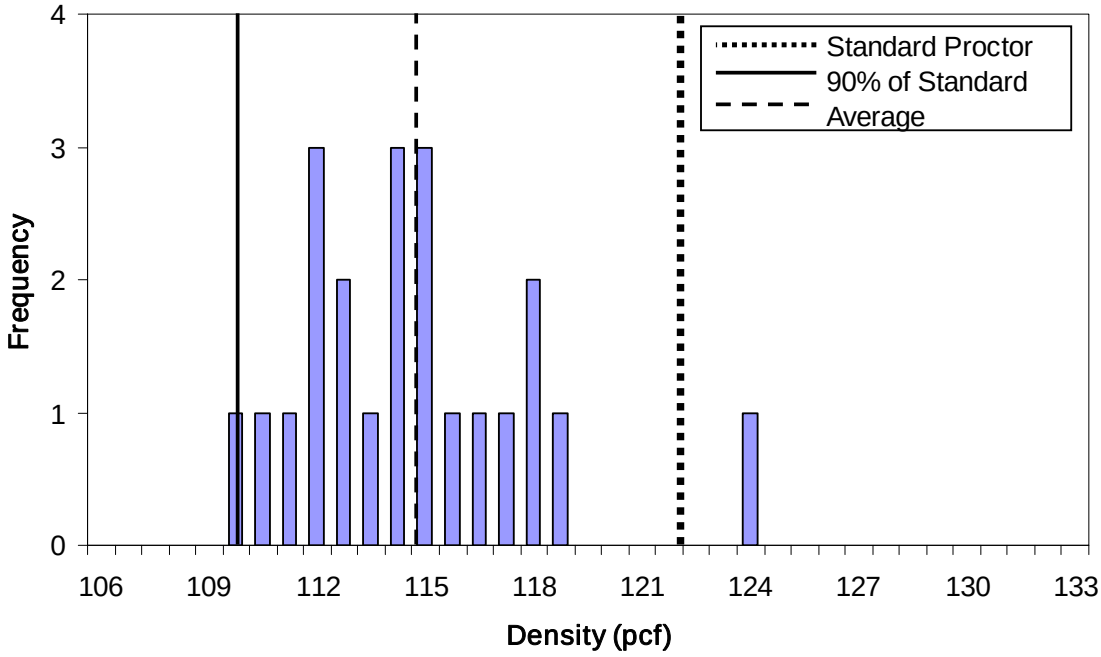

Figure 2-12 Density distribution of loosely compacted fine gravel backfill

Table 2-8 Average in-situ unit weight properties for fine gravel backfill

Backfill Type	$\gamma_{d,avg}$ (kN/m^3)	w_{avg} (%)	$\gamma_{m,avg}$ (kN/m^3)	Relative Compaction
Densely Compacted Fine Gravel	125.4	9.7	137.6	94.8% of modified
Loosely Compacted Fine Gravel	114.7	6.6	122.3	93.9% of standard (87.0% of modified)

Direct shear tests were performed in the Brigham Young University soil mechanics laboratory to determine the shear characteristics of the fine gravel backfill material at both of the aforementioned compaction levels. The normal stress during the tests ranged from about 200 psf to about 8000 psf (10 kPa to about 380 kPa). The shear strength envelopes for the densely and loosely compacted fine gravel backfill are shown in Figure 2-13. Failure envelopes for both peak and ultimate values were evaluated. In-situ direct shear tests were also performed on the fine gravel material at the time of testing. In these tests, an 18-in (0.46-m) square, 9-in (0.23-m) high steel box is positioned over a progressively carved-out sample of the material and loaded from the side with a hydraulic jack. Normal stresses during the in-situ tests ranged from about 210 psf to about 670 psf (10 kPa to 30 kPa). The in-situ direct shear tests are staged (i.e., the specimen is sheared to the point of apparent failure under one normal stress, whereupon additional normal stress is added to the same specimen and the specimen is sheared again) so a single specimen can be used for all the points on the failure envelope. A summary of the engineering characteristics of the backfill soils based on the direct shear test results is presented in Table 2-9. The soil friction angle and cohesion intercepts for the laboratory and in-situ direct shear tests are different from each other. Unfortunately, there are issues with both tests. In the lab direct shear test, the strength parameters could be artificially high due to the relatively large particle sizes present in the reconstituted specimen (the specimen as tested had a thickness-to-maximum-particle-size ratio of 3 rather than the normal 6 or more, while its diameter-to-maximum-particle-size ratio was just at the specified threshold of 10). Because these diameter ratios were not fully met, the lab-based test results should be somewhat discounted. Repeated loading of dilative soils (e.g. dense sands and gravels) during staged testing may lead to a reduction in resistance as the test progresses to higher stages. Hence, for in-situ direct shear tests, this may lead to lower friction parameters than if a fresh specimen was evaluated for each confining pressure.

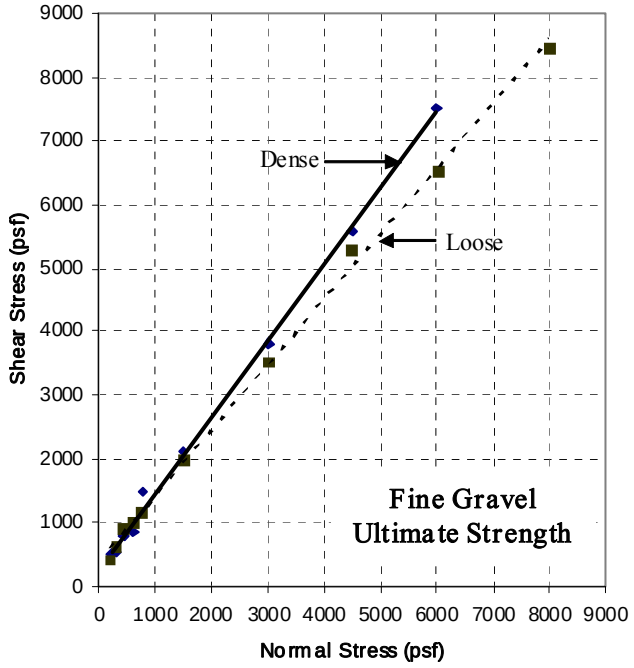

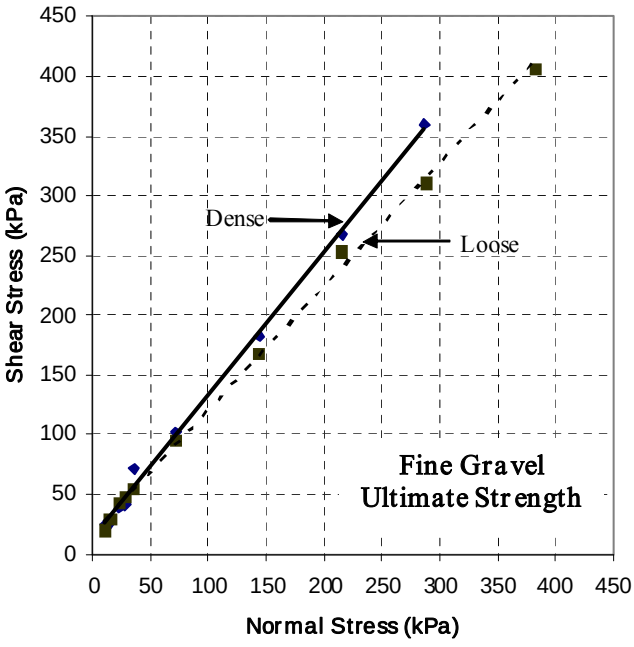

Ultimate Strength

0 to 287* kPa (0 to 6000 psf)

	Dense	Loose
φ' =	50.3°	45.8°
c' =	11 kPa	18 kPa
	(231 psf)	(375 psf)

72 to 287* kPa (1500 to 6000 psf)

	Dense	Loose
φ' =	50.0°	44.9°
c' =	13 kPa	27 kPa
	(275 psf)	(566 psf)

*383 kPa (8000 psf) for Loose Fine Gravel

Figure 2-13 Direct shear results for densely compacted and loosely compacted fine gravel backfill

Table 2-9 Direct shear summary for the fine gravel backfill material

Backfill Type	Laboratory Values				In-situ	
	Peak		Ultimate			
	ϕ (°)	c (psf)	ϕ (°)	c (psf)	ϕ (°)	c (psf)
Densely Compacted Fine Gravel	52.0	270	50.0	275	44.3	410
Loosely Compacted Fine Gravel	45.8	370	44.9	566	43.0	100

Along with the normal direct shear tests, a series of modified laboratory direct shear tests were performed to quantify the interface friction angle (δ) between the concrete and fine gravel. The interface friction angle was determined by placing a concrete sample of comparable roughness to the face of the pile cap into the bottom half of the shear box, filling the top half of the box with fine gravel compacted to the appropriate density, and shearing the composite sample under the same normal stress range as the internal friction angle tests. The interface friction angle determined from the ultimate stress points was 30.5 degrees for densely compacted fine gravel against concrete. The δ/φ ratio for the densely compacted fine gravel based on ultimate value results is 0.61 (as compared to a typically assumed value of 0.75).

2.4.3 Coarse Gravel Backfill

According to the USCS, the coarse gravel classifies as a poorly graded gravel with sand (GP). AASHTO classifies the coarse gravel as an A-1-a soil. Figure 2-14 shows the particle distribution of the coarse gravel backfill material. The coarse gravel is currently used locally as P-154 material, as specified by the FAA, the gradation limits for which are shown alongside the particle size distribution in the figure below. Table 2-10 provides a summary of the grain size distribution and other properties for the coarse gravel backfill material.

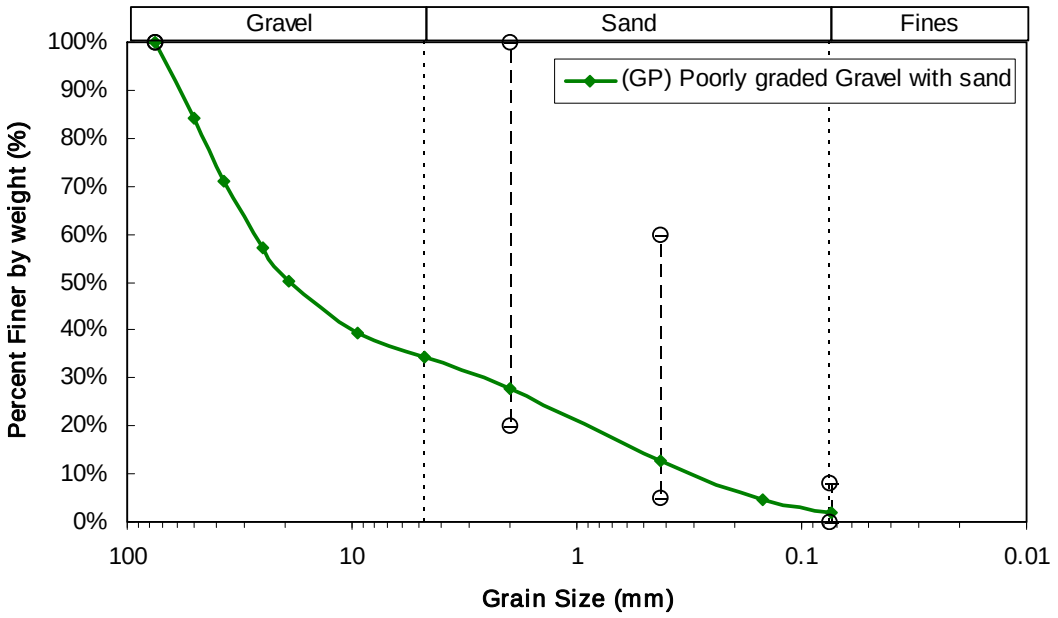

Figure 2-14 Particle distribution for coarse gravel backfill with gradation limits for P-154 material

Table 2-10 Index properties for the coarse gravel backfill material

Backfill Type	Gravel (%)	Sand (%)	Fines (%)	D_{60} (mm)	D_{50} (mm)	D_{30} (mm)	D_{10} (mm)	C_u	C_c
Coarse Gravel	66	33	2	27	19	2.7	0.3	85	0.8

Table 2-11 gives the optimum moisture content and maximum dry density of the coarse gravel material using standard and modified effort, respectively. Testing was performed on the material in two separate compaction states: loosely compacted and densely compacted. A jumping jack and a robust trench compactor were used to bring the coarse gravel backfill to the desired compaction levels. Nuclear density gauge readings were taken for each lift to verify the degree of compaction and moisture content. The histograms in Figure 2-15 and Figure 2-16 illustrate the density distribution of densely compacted coarse gravel and loosely compacted coarse gravel, respectively.

Table 2-11 Compaction characteristics of the coarse gravel backfill material

Backfill Type	USCS	Standard Effort		Modified Effort	
		w_{opt} (%)	γ_d (pcf)	w_{opt} (%)	γ_d (pcf)
Coarse Gravel	GP	8	132.1	6	139.9

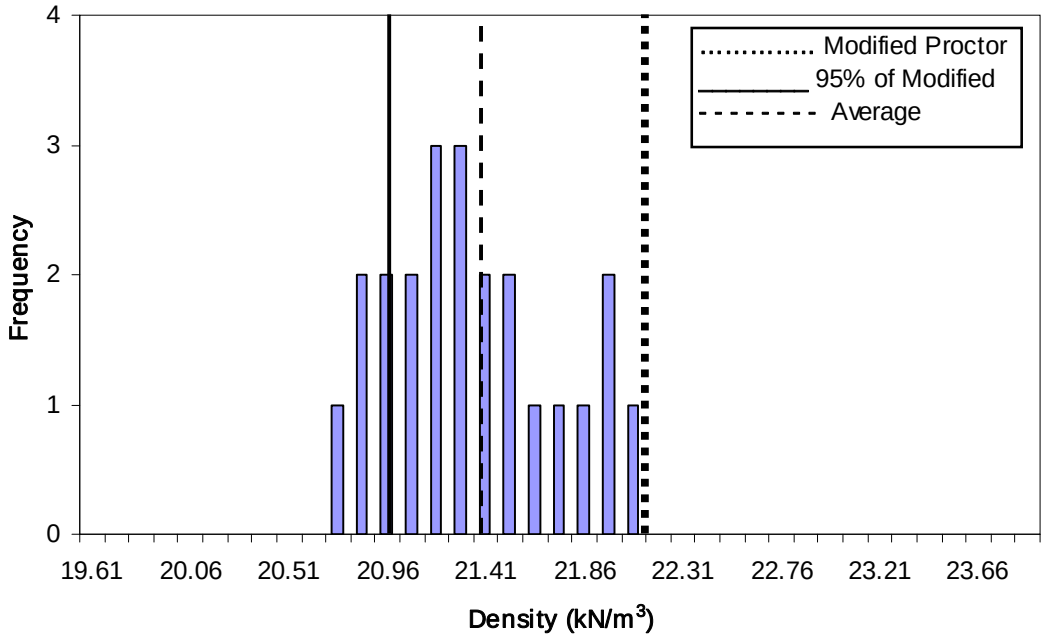

Figure 2-15 Density distribution of densely compacted coarse gravel backfill

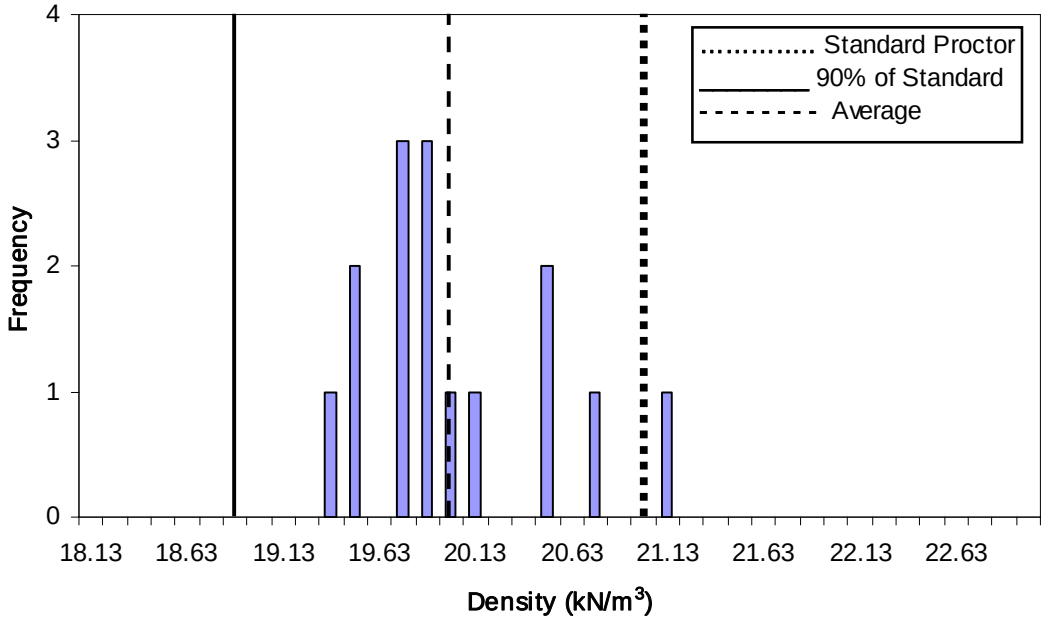

Figure 2-16 Density distribution of loosely compacted coarse gravel backfill

Table 2-12 Average in-situ unit weight properties for coarse gravel backfill

Backfill Type	γd,avg (pcf)	wavg (%)	γm,avg (pcf)	Relative Compaction
Densely Compacted Coarse Gravel	135.0	2.9	138.8	96.4% of modified
Loosely Compacted Coarse Gravel	126.3	1.9	128.7	94.9% of standard (89.5% of modified)

The densely compacted coarse gravel backfill material has an average dry density of about 96% of Modified Proctor maximum density. The loosely compacted coarse gravel backfill has an average dry density of about 95% of Standard Proctor maximum density or about 89.5% of Modified Proctor density. Table 2-12 summarizes the in-situ compacted properties of the coarse gravel backfill.

Direct shear testing of the coarse gravel in the laboratory was not possible using conventionally sized testing equipment due the relatively large particle sizes. Consequently, friction angles for the coarse gravel in its loosely compacted and densely compacted states were determined using relationships developed by Duncan (2004) based on a relatively large database

of sand, gravel, and rockfill, together with relative compaction (i.e., percent modified proctor) serving as a proxy for relative density based on the correlation developed by Lee and Singh (1971). Relative density can be estimated using this correlation as 82% for the densely compacted coarse gravel and about 48% for the loosely compacted coarse gravel. Friction angles obtained for the fine gravel using these correlations were compared to direct shear test results, yielding good agreement between the two approaches, which helped confirm the appropriateness of using the Duncan (2004) relationships to estimate the friction angle of the coarse gravel.

In-situ direct shear tests were also performed on the coarse gravel material at both levels of compaction. In these tests, an 18-in (0.46-m) square, 9-in (0.23-m) high steel box encloses a sample of the material and is loaded from the side with a hydraulic jack. Because of the relative coarseness and poorly graded nature of the gravel, it was not possible to carve the box into place as is normally done; rather, a lift of soil was compacted in and around the box and then the outside soil was removed. Normal stresses during the in-situ tests ranged from about 220 psf to about 670 psf (10 kPa to about 30 kPa). The in-situ direct shear tests are staged so a single sample can be used for all the points on the failure envelope. Repeated loading of dilative soils during staged testing may lead to lower resistance as the test progresses to higher stages. This may lead to lower friction parameters than if a fresh specimen was tested for each confining pressure. A summary of the engineering characteristics of the coarse gravel backfill material based on the correlation and the in-situ direct shear results is presented in Table 2-13.

Table 2-13 Direct shear summary for the coarse gravel backfill material

Backfill Type	Correlated		In-situ	
	φ (°)	c (psf)	φ (°)	c (psf)
Densely Compacted Coarse Gravel	54.0	0	40.6	286
Loosely Compacted Coarse Gravel	50.0	0	39.7	0

An initial estimate of the interface friction angle for the coarse gravel backfill material against concrete was obtained by using the δ/φ ratio from testing the fine gravel material against concrete. For the correlated engineering properties, that ratio means an interface friction angle between 32 and 33 degrees for the densely compacted coarse gravel and about 30 degrees for the

loosely compacted coarse gravel. Using the same ratio for the in-situ direct shear-based properties the interface friction angle is between 24 and 25 degrees for the densely compacted coarse gravel and about 24 degrees for the loosely compacted coarse gravel.

2.4.4 Backfill Dimensions

The soil backfills were placed against the 11-ft (3.35-m) wide by 5.5-ft (1.68-m) high side of the pile cap, resulting in a loaded face with an aspect ratio of 2. As shown in the plan view portion of Figure 2-4, the backfill zone was approximately 23 ft (7.0 m) wide and 28 ft (8.5 m) long. The cross-sectional view in Figure 2-4 shows that the soil within the first 8 ft (2.44 m) from the cap within the excavation extends to a depth of approximately 7 ft (2.16 m), after which the base of the excavation slopes up to its exit point at the ground surface. The dimensions of the backfill zone were selected to minimize the amount of backfill soil needed while still enclosing the anticipated shape of a log-spiral failure plane in three dimensions.

In two tests, a limited width of densely compacted fine gravel backfill was placed adjacent to the pile cap and the remainder of the excavation was filled with loosely compacted clean sand. The gravel zones in these tests extended 3 and 6 ft (0.91 and 1.83 m) from the face of the pile cap. The gravel zones also extended laterally beyond the edges of the pile cap by the same dimensions. The gravel was placed to the full depth of the excavation.

3.0 DATA ANALYSIS METHODS

3.1 General

This chapter describes the methods used to analyze data collected during the pile cap load tests. Results derived from these methods will be presented for each respective backfill condition in its own subsequent chapter.

3.2 Load-Displacement Response and Passive Earth Force

The most basic data generated during our tests was horizontal load versus displacement relationships for the pile cap with differing backfill conditions. Due to the actuator cycling and the rotations of the eccentric mass shaker, these relationships do not follow a smooth curve that describes the system response due to the loading and displacement of the pile. The load-displacement response of the system can be found by picking the peak load at the end of each static actuator push, before any cyclic or dynamic testing has begun, and finding the displacement that corresponds to each load. The series of points obtained from this process becomes the coordinates of the load-displacement response of the system for a given backfill condition.

The passive earth force from the backfill material can be determined by taking the load-displacement response of the pile cap with the backfill in place and subtracting the response of the pile cap without any backfill. The response of the pile cap without any backfill in place is referred to in this study as the "baseline" response of the pile cap. Hence, the baseline response reflects the pile cap resistance provided by pile-soil interaction. The pile cap response with no soil present is shown in Figure 3-1 and is based on the test conducted on June 21, 2007. As shown previously in Table 2-1, there were two other tests conducted without backfill present; however, they were not used as the baseline for several reasons. The first test involved the initial loading of the cap and this initial loading would not be comparable to a reloading of the cap until softening of the pile-to-cap connections had occurred after the first few complete load-displacement cycles of up to 3.5 in (90 mm of displacement). In fact, this "conditioning" of the

cap was the purpose of the first load test. Later comparisons of the slopes of the load-displacement curves during the pulling of the cap back to its starting position at the end of each backfill test showed generally consistent values, indicating that the cap was well conditioned and that the baseline response of the cap was relatively consistent between

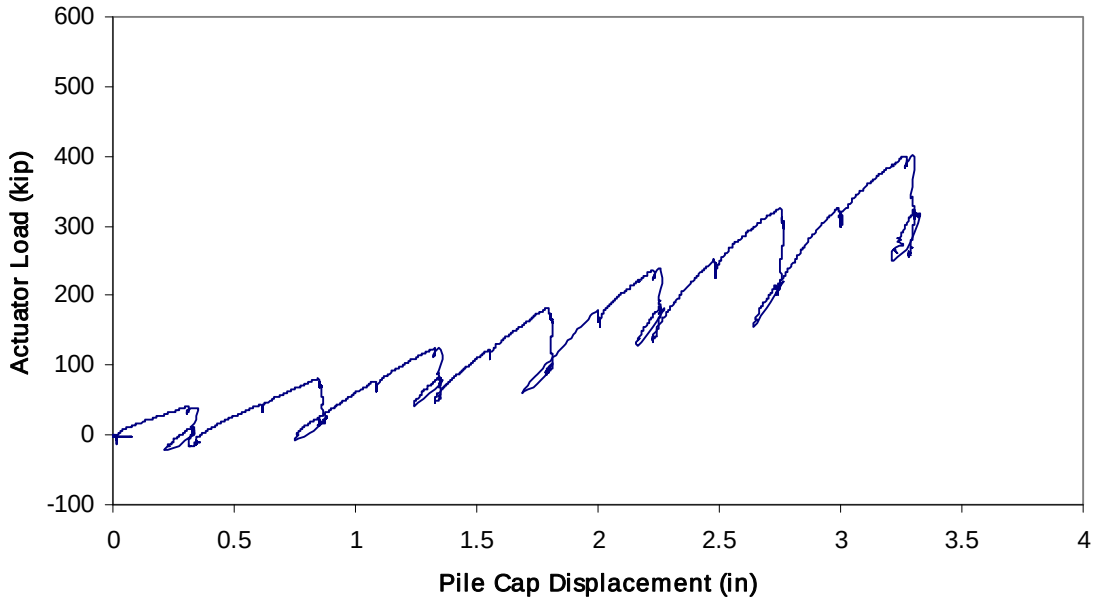

Figure 3-1 Load versus displacement relationship for pile cap with no backfill materials present (baseline test)

tests. The test on June 1, 2007 did not have any dynamic effects in the load-displacement relationship because the shaker had experienced a malfunction; also, there were fewer intervals at which cyclic actuator loading were applied. The behavior of the cap suggests that the baseline response is non-linear, with the cyclic and dynamic loadings contributing particularly to this at lower displacement levels.

To quantify the non-linear baseline response, a fifth order polynomial curve was fitted to the peak points of the response (i.e., the maximum load and displacement before any cyclic loading was applied to the cap) and forced through zero. The fitted curve is shown in Figure 3-2 along with the measured response curve. The equation was used to quantify the baseline response at the peak points of other tests. Due to the high order of the polynomial, caution must be taken when extrapolating beyond the 3.25-in (83 mm) maximum displacement from the baseline test.

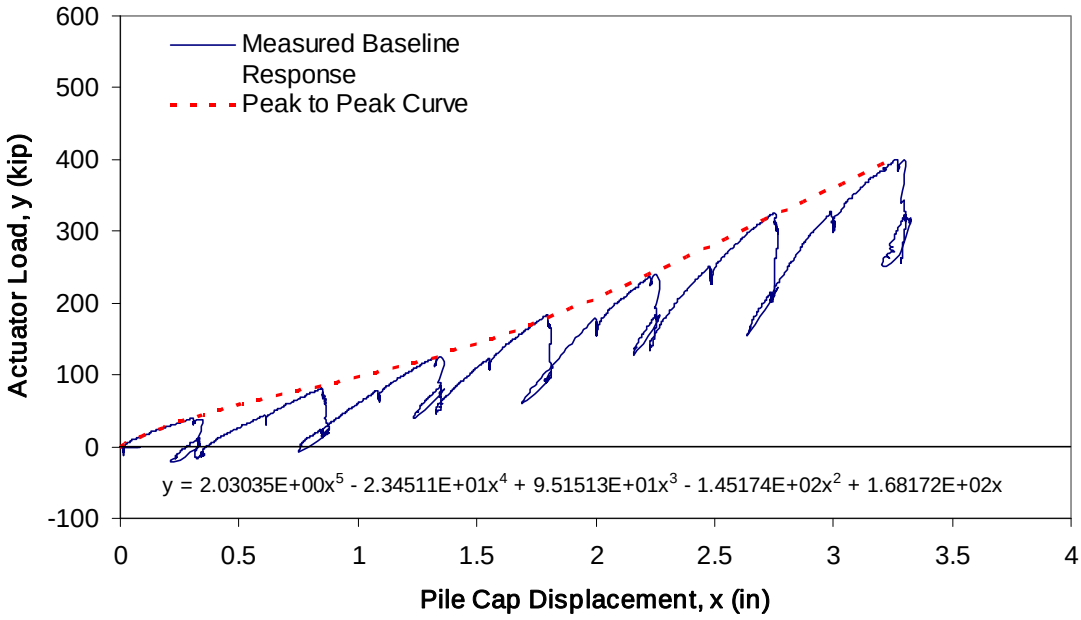

Figure 3-2 Measured baseline response with modeled baseline response

Plots of passive earth force for the backfill soils developed by subtracting the baseline response of the pile cap from the measured pile cap response with backfill in place are shown in subsequent chapters for each backfill condition. The total measured response of the pile cap and the baseline response from which the passive earth force was developed are also shown in these figures. To facilitate understanding of these figures, the loading sequence (or loading path) has been color coded. Portions of the loading path which occur as the actuators are being used to slowly push the pile cap to the next target displacement level are shown in green. These portions are also referred to in this text as "static pushes." Portions of the loading path in which the actuators are being used to apply 15 cycles of small amplitude cyclic loading are shown in blue. Portions of the loading path in which the eccentric mass shaker is being used to apply a dynamic loading to the pile cap are shown in red. Because of the extremely large quantity of data otherwise involved, these plots are based on 1-sps datasets and hence do not fully reflect the cyclic and dynamic portions of the test. Also, the load shown in the figures is the combined load applied to the pile cap by the two actuators. To find the total load acting on the cap, the shaker load, inertial load, and any backfill reaction would need to be superimposed; thus, a detailed analysis of each dynamic loading loop would be required (and, incidentally, the overall slopes of

the red portions of the load paths would become reversed). Such analyses are presented later in this report, but for the sake of providing an overall perspective of each test, just the actuator loads have been used to produce these figures.

During the loading of the pile cap, a differential in cap displacement was observed between the east and west sides of the cap. The maximum differential during the first test with backfill, based on the top two string potentiometers, was 0.17 in (4.3 mm), with the west side leading. The differential displacement can be explained in part by the different stiffness of the drilled shafts used in the reaction foundation. The west shaft is somewhat stiffer than the east shaft (see Taylor, 2006), causing the west side of the pile cap to move more than the east side. We attempted to mitigate this differential movement by applying uneven loads in the actuators, but some differential movement still occurred. The reported pile cap displacements are based on the median displacement measured by the string potentiometers mounted to the pile cap.

3.3 Calculated Passive Earth Force

Several methods were used to calculate the passive force versus displacement relationship for the backfill soils. In this study, passive earth pressures were calculated using a modified version of the spreadsheet program PYCAP developed by Duncan and Mokwa (2001), which implements the classical log-spiral solution for passive force with a hyperbolic displacement curve; the computer program entitled ABUTMENT, which implements the Log Spiral Hyperbolic (LSH) approach presented by Shamsabadi et al. (2007); and the CALTRANS standard design method. Comparisons of these methods to the measured earth pressures will be shown in subsequent chapters.

3.3.1 PYCAP Methodology

Duncan and Mokwa (2001) presented a method in which the ultimate passive force (pressure) from a soil backfill is determined using the log-spiral method while the force versus displacement curve is based on a hyperbolic load-displacement relationship where initial loading stiffness (k_{max}) is based on the solution for a laterally loaded plate embedded in an elastic half-space (Douglas and Davis, 1964). The methodology has been implemented by Mokwa using an EXCEL spreadsheet entitled PYCAP.

Input parameters include soil properties such as soil friction angle (ϕ), cohesion (c), soil-foundation interface friction (δ), an adhesion factor ( ), initial soil modulus (E_i), poisson's ratio (ν), and in-situ unit weight (γ). The inputs describing the foundation geometry are the foundation height (H), width (b), embedment depth (z), surcharge (q) and failure displacement divided by cap height (Δ_{max}/H).

The soil friction angle and cohesion, as well as the interface friction angle, were generally determined from direct shear testing. Initial soil modulus was found using the stress-strain unloading/reloading curve of a one-dimensional consolidation test and confirmed by comparing with typical values. Values for Poisson's ratio were selected from typical values. Specific values for each parameter used in analyses will be presented subsequently. Three-dimensional loading effects are accounted for using the factor (R_{3D}) developed by Brinch-Hansen (1966), but with a limiting value of 2.

Along with a load-displacement curve of the passive earth pressure, PYCAP has several other outputs, including the soil loading stiffness (k_{max}), the hyperbolic failure ratio (R_f) which is derived from Δ_{max}/H, and the coefficient of passive earth pressure (K_p) from the log-spiral method of calculating passive soil resistance.

The initial soil moduli used in the analysis of the gravel backfill soils in this study were determined from oedometer tests and correlations. The range of suggested values given in Duncan and Mokwa (2001) is presented in Table 3-1. A synopsis on how each modulus value used in analysis compares to these ranges will be given subsequently for each backfill condition in its respective chapter.

Table 3-1 Suggested ranges for horizontal initial soil modulus, Ei, at shallow depths (Mokwa and Duncan, 2001)

Density	Dr	N_{60}	Normally loaded	Preloaded or compacted
Loose	40%	3	Ei = 200 - 400 ksf	Ei = 400 – 800 ksf
Medium	60%	7	Ei = 300 – 500 ksf	Ei = 500 – 1000 ksf
Dense	80%	15	Ei = 400-600 ksf	Ei = 600 – 1200 ksf

3.3.2 ABUTMENT (LSH) Methodology

In this methodology, the ultimate pressure of the backfill is determined by dividing the backfill soil into slices and then satisfying force-based, limit-equilibrium equations for mobilized logarithmic-spiral failure surfaces. Displacement is determined using a modified hyperbolic stress-strain relationship. This methodology, referred to as the LSH method and developed by Shamsabadi et al. (2007), has been incorporated by Shamsabadi into the computer program ABUTMENT.

Input parameters for the LSH method are soil properties and foundation geometry. The soil properties needed are internal friction angle (ϕ), soil cohesion (c), soil-foundation interface friction (δ), in-situ unit weight (γ), Poisson's ratio (ν), and strain at 50% strength (ε_{50}) (ideally determined from triaxial testing). An additional failure ratio (R_f) parameter must be defined which helps control the sharpness of the hyperbolic curve. Different from the R_f values used in some hyperbolic soil models, this value typically ranges from 0.95 to 0.98. Output from the program includes the load-displacement curve and the passive horizontal earth pressure coefficient. Most of the soil input parameters were selected in the same way that they were chosen for the analyses using PYCAP. The strain parameter is difficult to precisely define but was estimated using the stress-strain loading curve of a one-dimensional consolidation test and then compared with values shown for similar backfill materials in Shamsabadi et al. (2007). Within the computer program, the log-spiral force method of calculation was used with the "composite" option while the stresses and strains were calculated using the "modified hyperbolic" option. Three-dimensional end effects were accounted for using an effective foundation width determined using the same Brinch-Hansen (1966) relationships as used in the PYCAP-based analyses.

3.3.3 CALTRANS Methodology

Based on full scale tests conducted at UC Davis (Maroney 1995), CALTRANS developed a method to determine the initial stiffness and ultimate passive resistance for abutment backfill to use in standard design work. The initial stiffness (K_{abut}) and ultimate force (P_{ult}) are determined using Equation 3-1 and Equation 3-2:

$$K_{abut} = 20\frac{kip/in}{ft} \times w_{abut} \times \frac{h}{5.5}$$ Equation 3-1

$$P_{ult} = 5.0\,ksf \times A_{abut} \times \left(\frac{h}{5.5}\right)$$ Equation 3-2

where w_{abut} is the width of the abutment, h is the height of the abutment and A_{abut} is the area of the abutment (with dimensions of length expressed in terms of meters). The load-displacement relationship follows the initial stiffness and then becomes constant when the ultimate pressure is exceeded. The method scales different abutment heights linearly to the height of the test abutment and does not account for changes in backfill material. In fact, no explicit soil properties are used in the method. For the geometry of the test pile cap, this method indicates the initial slope is to be 220 kip/in (39 kN/mm) and the ultimate passive resistance is to be approximately 305 kip (1360 kN).

3.4 Response to Cyclic Actuator and Dynamic Shaker Loadings

During testing, the pile cap was subjected to slow cyclic loadings from the actuators and a cyclically applied dynamic loading from the eccentric mass shaker. The behavior of the pile cap was analyzed by resolving the forces acting on the test cap during testing and isolating the test setup to the right of the actuators shown in Figure 2-4. To the right of the actuators, the only forces to be considered are those affecting the pile cap. These forces include the actuator force; the shaker force; the damping, stiffness, and inertial forces from the cap by itself; and the damping, stiffness, and inertial forces from the backfill. The net damping, stiffness, and inertial forces from the reaction foundation system are accounted for by the actuator loads.

The inertial force for the pile cap system during dynamic loading was calculated using measured acceleration data from the cap and a constant, single lumped-mass representation of the test pile cap, the shaker, a portion of the piles (the upper eight pile-diameters), one of the actuators, and the backfill (if any) assuming a log-spiral failure geometry. The total weight of the test components without any backfill was 159 kip (707 kN). The mass representing the densely compacted backfill was determined from the log-spiral shape of the failure mass

computed using the modified version of the PYCAP program and then adjusted by the three-dimensional factor to account for the fanning of the failure wedge out beyond the edges of the pile cap. For the densely compacted clean sand backfill, a mass equivalent to 170 kip (750 kN) was used. For the loosely compacted clean sand backfill where the failure wedge was poorly defined, half of the densely compacted backfill weight was used. For the densely and loosely compacted fine gravel, 320 and 80 kip (1420 and 360 kN), respectively, were used as the backfill weight, whereas for the densely and loosely compacted coarse gravel, 380 and 95 kip (1690 and 420 kN), respectively, were used. In the case of the slowly applied actuator-based loadings, inertial forces are negligible.

The inertial force was combined with the shaker and actuator forces such that the resulting force-displacement loops represent the combined internal stiffness and damping effects of the pile cap with whatever backfill was present. During cyclic testing with the actuators, system stiffness and damping were calculated for the median loop of the 15 loading loops. During dynamic testing with the eccentric mass shaker, system stiffness and damping were calculated from the median loop of the 15 loops recorded at each dwell frequency ranging from 1 to 10 Hz, at 0.5 Hz intervals.

Stiffness of the system, *k*, was calculated using the average peak-to-peak slope of the force-displacement loops as shown in Figure 3-3 and Equation 3-3:

$$k = \frac{\left(P_{\max} - P_{\min}\right)}{\left(u_{\max} - u_{\min}\right)} = \frac{P_{amp}}{u_0} \qquad \textbf{Equation 3-3}$$

where u_{max} is the maximum displacement, u_{min} is the minimum displacement, P_{max} and P_{min} are the loads associated with the maximum and minimum displacements (which are not necessarily the maximum and minimum loads during the loop), and P_{amp} is the load amplitude. Since the shaker force was applied in ramped manner, it is difficult to discretely isolate the effects of the number of loading cycles. Also, due to the nature of the ramped loading, the calculated stiffness is a reloading, rather than an initial loading, stiffness.

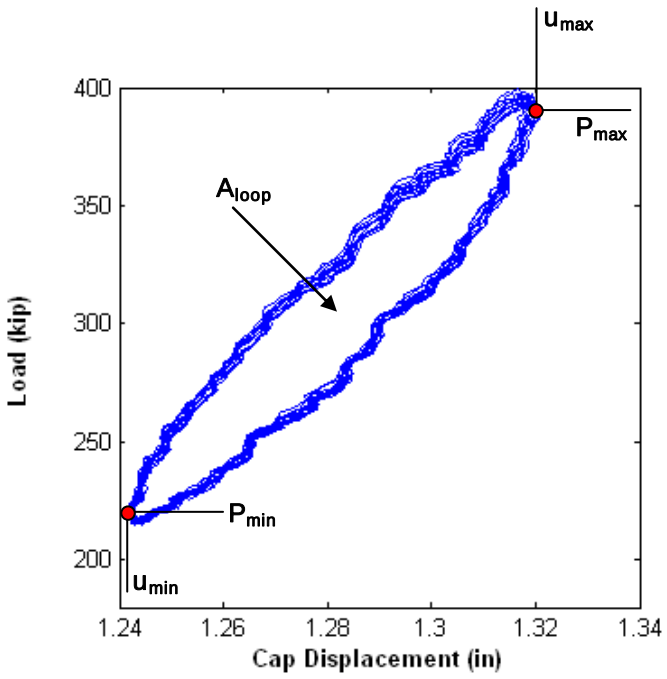

Figure 3-3 Example of actuator-based load-displacement loops

Damping under dynamic loading conditions can be assessed using either the half-power bandwidth method or by directly using the area and slope of the force-displacement loops. In the half-power bandwidth approach, the measured dynamic displacement is plotted versus the frequency ratio, □/□n (where □ is the circular frequency of the forcing function and □n is the natural circular frequency of the structure). The two frequencies, □1 and □□ , on opposing sides of □/□n = 1 whose displacement amplitudes correspond to 1/√2 times the resonant displacement amplitude are then selected and used to determine the amount of damping, ξ, by satisfying the expression shown below.

$$\left(\frac{\omega}{\omega_n}\right)^2 = \left(1-2\xi^2\right) \pm 2\xi\sqrt{1-\xi^2} \qquad \textbf{Equation 3-4}$$

Often this equation is simplified to following relationship by the assumption of a small damping ratio: $\frac{\omega_b - \omega_a}{\omega_n} \cong 2\xi$

Equation 3-5

However, if damping is large (> 20% is the value typically cited) this latter equation becomes unreliable. It should also be noted that the former equation cannot be used if damping exceeds approximately 38% because with increased damping, the spread between □₁ and □□ increases, and □₁would need to be less than zero for that amount of damping to be present. Due to limitations of the testing equipment, the dynamic displacement amplitude versus frequency curves commonly did not extend to a range high enough to identify □□.

In attempting to use the more rigorous solution with various extrapolations of the measured response curve to estimate □□, it was found that the dynamic displacement amplitude versus frequency curves (with displacement amplitude normalized by the net applied load from the shaker and actuator in order to establish a relatively stationary forcing function), exhibited an atypical shape in which □□ - □n was greater than □n - □₁, thus preventing a solution to Equation 3-5 which was consistent with the measured data. This behavior is attributed to a changing of stiffness and/or damping with respect to shaker frequency because of material non-linearity.

Damping during dynamic loading, ξ, was evaluated directly from the force-displacement loops using Equation 3-6:

$$\xi = \frac{1}{4\pi}\frac{A}{E_s}$$

Equation 3-6

where A is the area of the resistance force-displacement loop; E_s is the stored strain energy which equals 0.5 $k\,u_o^2$, in which case k is the slope of the loop and u_o is the single peak displacement amplitude.

Plots showing displacement amplitude, stiffness, loop area, and damping, as a function of frequency and static pile cap displacement level are presented in subsequent chapters for each pile cap backfill condition. At low frequency levels, shaker forces and the resulting pile cap displacements are very small; therefore, it is difficult to distinguish between real load and

instrumental noise. Because of this, results have not been presented for frequencies less than 4 Hz.

In general, the cyclic actuator data exhibits a saw-tooth shaped trend in stiffness and damping, The stiffness is higher when the actuator cycles are performed before the shaker cycles because of the softening of the soil during dynamic loading (i.e., when the actuator loading occurs second, the soil has already experienced the dynamic loading from the shaker). A related trend is observed in Figure 3-4, which shows typical load-displacement loops when the actuator cycles are initiated first or second (second meaning that the actuator cycles are performed after the dynamic loading from the shaker). When the static actuator cycles are performed first, there is an increase or drift in the cap's position with little change in stiffness for each progressive loop. However, when the static cycles are performed second after the dynamic shaker loading, no drift is observed. This drift is due to the softening or relaxing of the soil during cyclic loading.

During the dynamic shaker loadings, stiffness and damping fluctuate in terms of frequency and displacement amplitude. One reason for this is due to the nature of the force displacement loops. As mentioned previously, the shaker was incapable of producing large forces or displacements at low frequencies, therefore causing the load-displacement loops to be influenced by small differences. At about 4 Hz, the load displacement loops become more distinct but their size and orientation change significantly through the remainder of the test. The changes in the load-displacement loops are also significantly affected by the order of the shaker and actuator cycling. Figure 3-5 shows typical load-displacement loops from the dynamic shaker loadings.

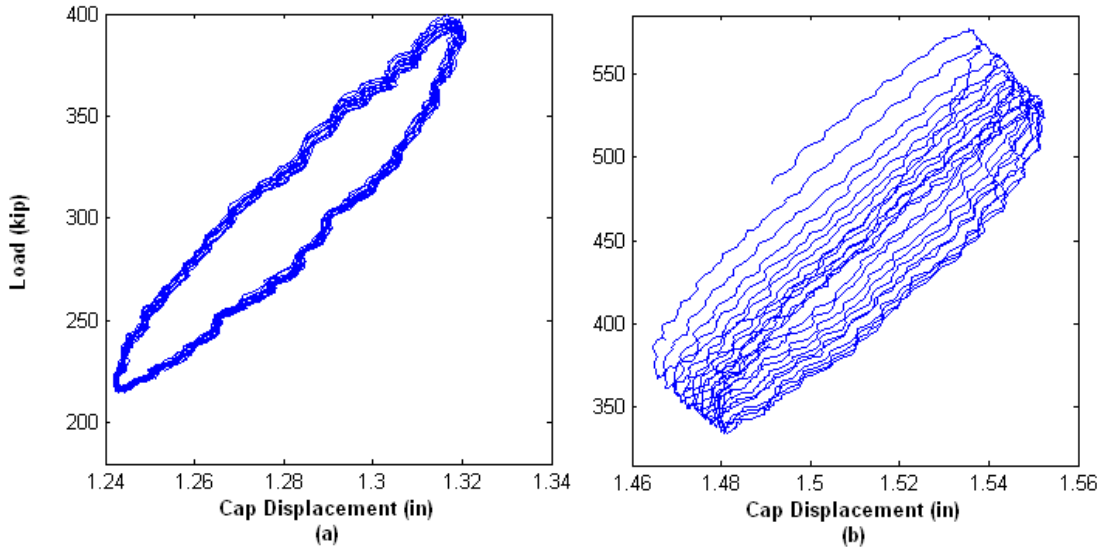

Figure 3-4 Typical actuator loops when actuator cycles are applied (a) second and (b) first

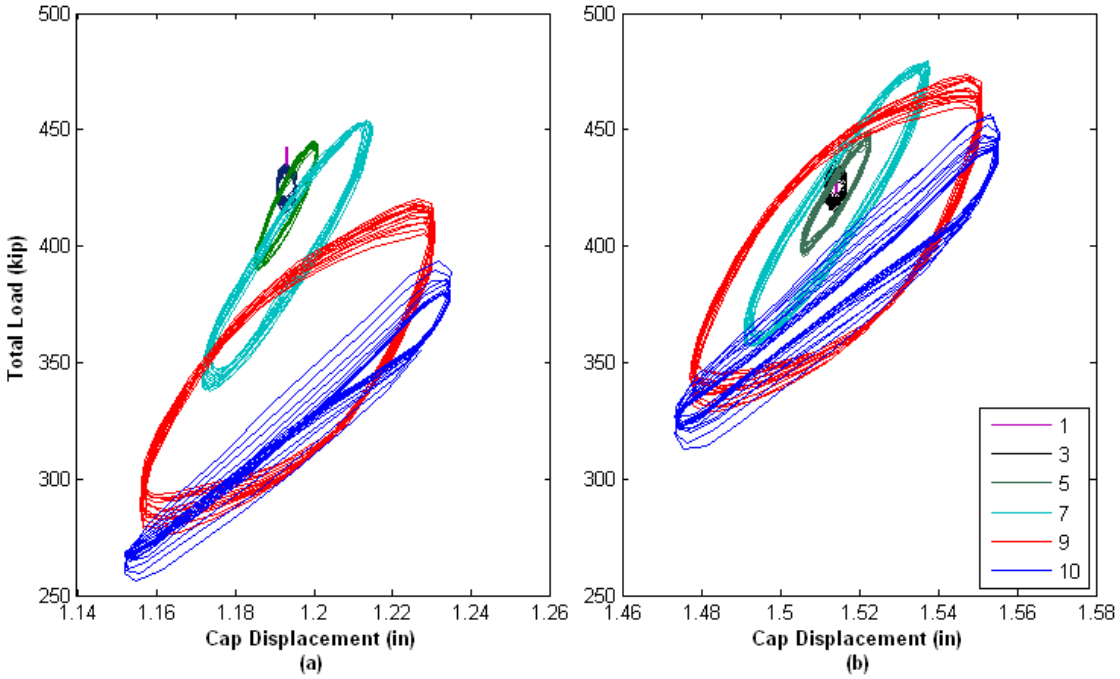

Figure 3-5 Typical load-displacement loops when shaker cycles are applied (a) second and (b) first

3.5 Passive Earth Pressure Distributions

In addition to the load-displacement response data from the actuators, passive earth pressure from the backfill soil was measured directly with a vertical array of six earth pressure cells evenly distributed in the central portion of the pile cap face. Plots of earth pressures as a function of pile cap displacement for the different backfill soil conditions are shown in subsequent chapters for each backfill test.

The lower-most pressure cell typically exhibited irregular behavior in relation to the other cells in the array in many of the tests. While this pressure cell does appear to measure increasing pressure for the first couple of displacement levels, subsequent pressure measurements tend to drop off, returning to relatively small values. This behavior may be indicative of pile cap rotation effects with the top of the cap rotating further out into the backfill soil. However, in comparing the relatively small amount of cap rotation that occurred during the test to that required to obtain such a pressure distribution based on an elastic pressure distribution acting on a vertically embedded plate as developed by Douglas and Davis (1964), the actual amount of cap rotation was significantly less than the rotation needed to produce such a significant decrease in pressure at the bottom of the pile cap. Consequently, we believe that the low pressures at the base of the cap do not appear to be due in a significant way to rotation effects. It is possible that the pressure cell was damaged in some way or that, being near the location were a pile is embedded into the cap, an interaction between the end of the embedded pile and the concrete of the cap near the cell produced stress on the back side of the pressure cell which lead to inaccurate measurements.

By simply multiplying each pressure cell reading by the contributory area across the face of the pile cap and then summing the resulting forces, passive earth forces can be determined. These pressure cell-based forces can then be compared to passive earth forces determined from the load actuators which were determined by subtracting the baseline response of the pile cap from the measured pile cap response with the backfill in place. Although the actual soil pressure distributions are generally irregular with depth, the plots of force calculated using these pressure cells have shapes which are consistently similar, albeit generally lower in magnitude, to the passive earth forces curves derived from the actuator-based measurements. Comparison between pressure cell- and actuator-based passive earth forces are shown in subsequent chapters for each backfill test.

The systemic differences between pressure cell- and actuator-based passive earth forces may be attributable to differing pressure conditions outside the spatial coverage provided by the pressure cells, particularly those areas near the edges of the pile cap. In analyzing a uniformly loaded strip foundation, Borowicka (1938) determined that the distribution of contact pressure near centerline could approach 67% of the net average pressure distributed across the full width of a very rigid foundation. Similar pressure distributions with higher pressures near the edges of a foundation and lower pressures in the central portions are seen in elastic stress distributions such as that developed by Douglas and Davis (1964) for a vertically loaded plate embedded in an elastic half-space.

In an analysis conducted using the pressure-based forces at the end of the static actuator pushes (before cyclic and dynamic loads are applied) for each displacement interval for all of the backfill soil types, the correlation between pressure cell-based and actuator-based forces was found to be approximately 0.6 (i.e., the pressure cell-based measurements are 60% of the force-based measurements). This correlation is shown in Figure 3-6. If the lower-most pressure cell is frequently in error as suspected and it is subsequently corrected such that a resultant force is produced which is consistent with an elastic stress distribution along the center of a vertical plate, the correlation improves to about 0.7.

3.6 Cracking and Vertical Movement of Backfill

At each pile cap displacement level and after any cyclic and dynamic loadings, cracking within the backfill was visually mapped using the grid painted on the ground surface. Additionally, vertical surveys were performed at the beginning of each test and at the maximum displacement level in order to assess vertical changes in backfill elevation. The elevations were surveyed at the node points of the grid to the nearest 0.01 ft (3 mm); however, the actual tolerance is somewhat greater due to variations in making measurements along an irregular soil surface with varying particle sizes. Paired

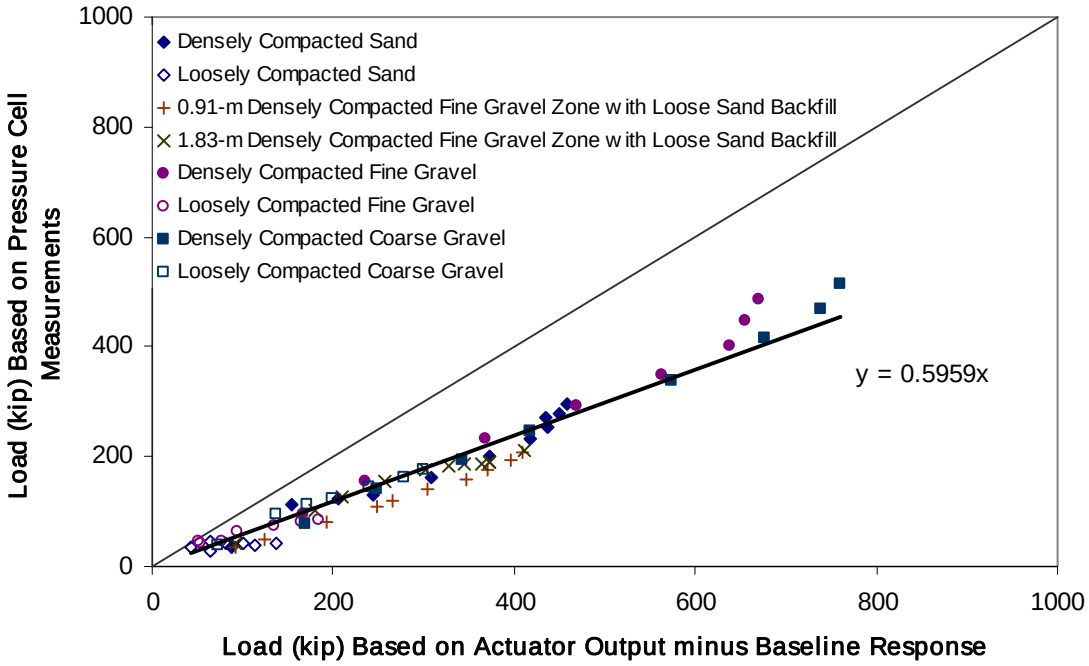

Figure 3-6 Passive earth loads based on pressure cells versus load actuators

sets of backfill cracking maps and backfill heave (or settlement) contours for each of the backfill soil types are shown in subsequent chapters for each backfill test.

3.7 Horizontal Movement of Backfill

String potentiometers mounted on the pile cap and attached to steel stakes installed at various points in the backfill material were used to measure relative movement along the top surface of the backfill throughout each test. These stakes were located at the following distances from the pile cap face: 2, 4, 6, 9, 12, 15, and 18 ft (0.61, 1.22, 1.83, 2.74, 3.66, 4.57, and 5.49 m) . By knowing the relative movement between the cap face and the location of the stakes, as well as the absolute movement of the pile cap, absolute displacement of the backfill and strain in the backfill can be computed.

The changes in length recorded by the string potentiometers correspond to the total amount of compression between the cap face and the monitoring stakes. Negative change in length represented shortening of the string and positive change in length represented lengthening.

Movement of the monitoring positions was calculated by subtracting the negative of the string potentiometer change in length from the displacement of the pile cap, effectively subtracting the magnitude of the backfill compression from the maximum total movement. When performed for each monitoring point, this method yielded the net movement of the stake. The data shown in subsequent plots are based on pile cap and stake positions at the end of each displacement interval (i.e., the time immediately after the pile cap had just been pushed to a new displacement level with the actuators).

To calculate the strain in the backfill material, the backfill was segmented into intervals bounded by the stakes. This segmentation produced seven intervals, one between the cap face and the first stake and the remaining between any two adjacent stakes. By normalizing the change in interval length by the initial interval length strains were calculated in each of the seven segments with positive values corresponding to compression.

In some cases, small negative displacements or strains (indicative of expansion) may be shown. These values likely result due to the limited precision with which the data could be collected and processed; any tilting of the steel monitoring stakes or differential movement between the far ends of the pile cap along which the different string potentiometers were mounted could result in small errors in the data. Also, in some instances, there were unexplained short-duration jumps in the string potentiometer readings, and these readings were corrected manually by adjusting the affected data to match the data trend before and after the jumps.

Paired sets of plots showing the displacement of the backfill (as a function of distance away from the pile cap) and the calculated strains (as a function of pile cap displacement level) are shown in subsequent chapters for each backfill test.

4.0 PILE CAP WITH NO BACKFILL PRESENT (BASELINE RESPONSE)

4.1 General

As shown previously in Table 2-1, three load tests were performed with no backfill in place. As explained in Section 3.2, the test performed on June 21, 2007 was used as the baseline response. The results of this test are presented in this Chapter. Table 4-1 summarizes the test in terms of loads and displacements measured at the end of each "static push" with the actuators. The table also indicates the order in which cyclic loads from the actuators and dynamic loads from the shaker were applied. No significant deviations from the general test procedure occurred during this test.

Table 4-1 Summary of test with no backfill (Test 11; June 21, 2007)

Displacement Interval	Displacement (in)	Actuator Load (kip)	Actuator Cycles	Shaker Cycles
1	0.28	40.0	First	Second
2	0.63	42.5	None	None
3	0.83	82.0	Second	First
4	1.06	77.6	None	None
5	1.30	124	First	Second
6	1.54	123	None	None
7	1.77	183	Second	First
8	1.97	178	None	None
9	2.24	240	First	Second
10	2.44	252	None	None
11	2.72	326	Second	First
12	2.95	327	None	None
13	3.27	401	First	Second

4.2 Load-Displacement Response

Figure 4-1 shows the entire actuator load verses pile cap displacement relationship for the test, with static pushes, actuator cycles and shaker cycles being represented by green, blue, and red data points, respectively. Section 3.2 provides some discussion relative to the details of

interpreting this data. Because no backfill was present, the horizontal load versus displacement relationship shown is the result of the resistance of the piles, the pile-soil interaction, and any friction due to contact of the pile cap with the underlying soil.

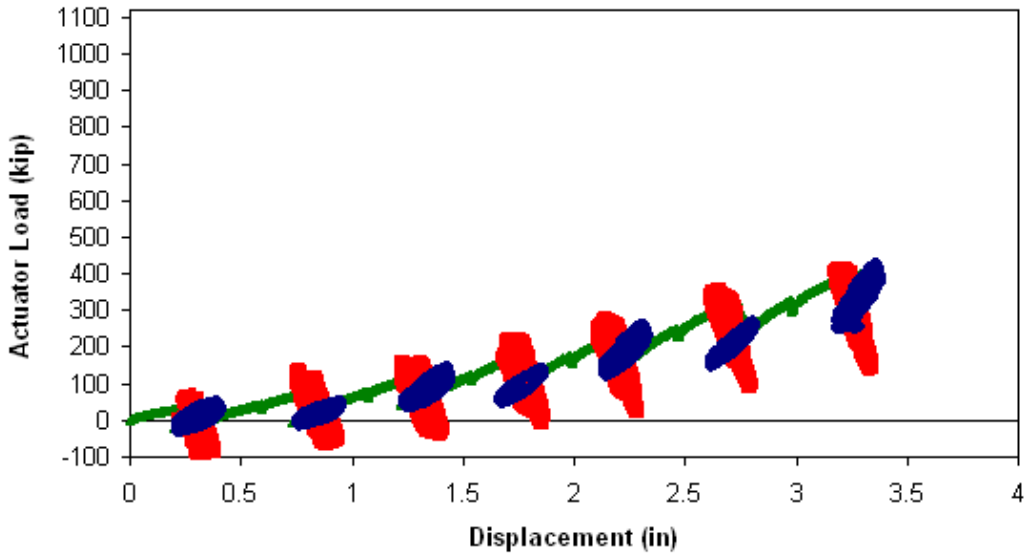

Figure 4-1 Actuator load versus pile cap displacement with no backfill (Test 11; June 21, 2007)

Figure 4-2 shows the equivalent monotonic response of the pile cap isolated from the data shown in Figure 4-1. As seen in Figure 4-2, the overall baseline response is somewhat non-linear, being concave up (increasing stiffness per loading interval as the pile cap displacement is increased). Slight decreases in load are observable at the intermediate pushes while manual data points were being recorded. The decrease is believed to be a relaxation of the soil acting on the piles and is not due to a decrease in pile cap displacement (pile cap displacement actually increases minutely). These effects are observed to be much more pronounced when backfill soils are present and contribute to a larger portion of the overall pile cap resistance. See Section 3.2 for additional discussion of this load-displacement curve and its use as the baseline response for the pile cap.

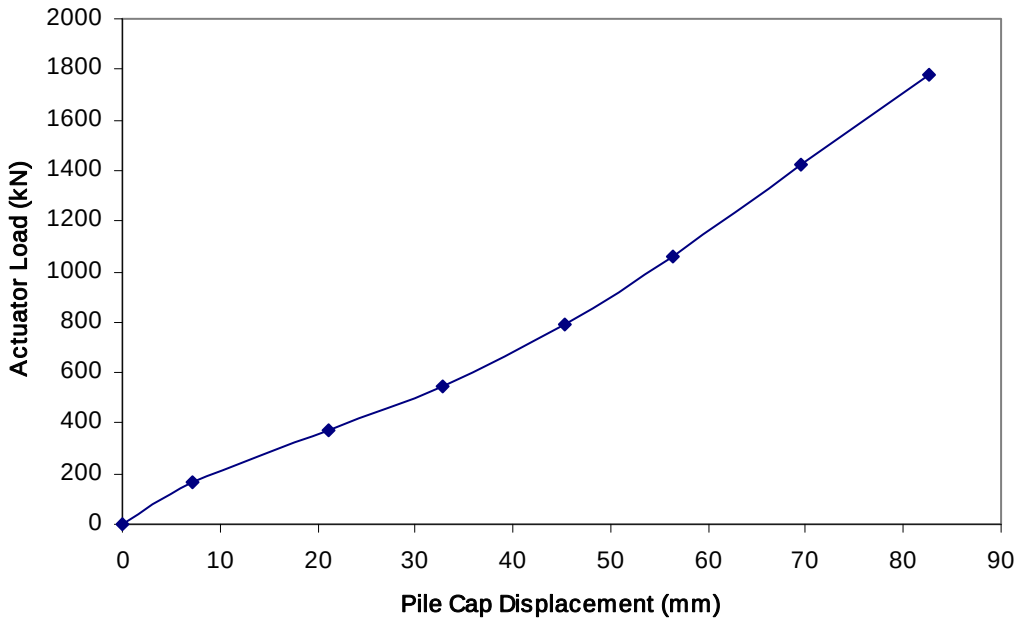

Figure 4-2 Total (and in this case, baseline) response for pile cap with no backfill

4.3 Response to Cyclic Actuator Loading

After slowly pushing the pile cap to each displacement interval, alternating combinations of small displacement cyclic actuator loads and dynamic shaker loads were applied. The response of the pile cap to the small displacement amplitude loading cycles from the actuator is presented and discussed in this section. Figure 4-3 shows the displacement amplitude, stiffness, loop area, and damping ratio for the pile cap without

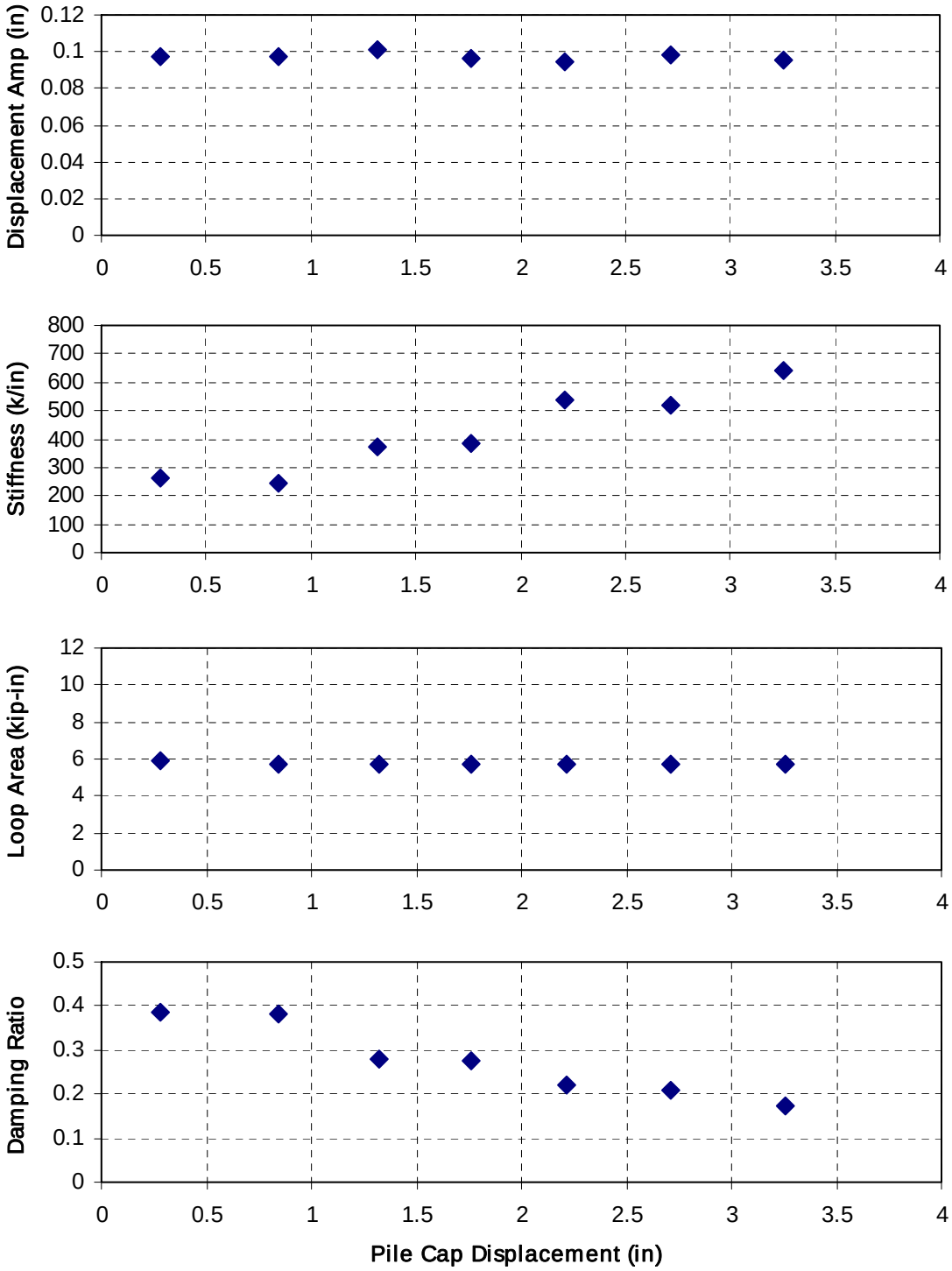

Figure 4-3 Summary of response to cyclic actuator loadings for pile cap without backfill (baseline test)

backfill as a function of cap displacement. Values are based on the median of the 15 small amplitude cycles performed at each displacement level. Although the displacement amplitude and loop areas have some variation, the increase in stiffness with increasing pile cap displacement level causes the damping to decrease from approximately 40% to just under 20% as the cap displacement increases. An interesting trend in the stiffness data is the saw-tooth shape of the trend. This shape is caused by the order of the actuator and shaker cycles. The stiffness is higher when the actuator cycles are performed before the shaker cycles because of the softening of the soil during dynamic loading (i.e., when the actuator loading occurs second, the soil has already experienced the dynamic loading from the shaker).

4.4 Response to Dynamic Shaker Loading

After slowly pushing the pile cap to each displacement interval, alternating combinations of small displacement cyclic actuator loads and dynamic shaker loads were applied. The response of the pile cap to the dynamic shaker loading is presented and discussed in this section. The first row of graphs in Figure 4-4 shows displacement amplitude as well as displacement amplitude normalized by the cyclic amplitude of net applied force from the shaker and actuators as functions of the forcing frequency and pile cap displacement level. The second and third rows of graphs show the calculated reloading stiffness and damping, respectively, of the pile cap system. In the left column, these parameters are shown in terms of forcing frequency. If non-linear behavior is present, these properties will also depend on the displacement amplitude; hence, in the right column, these parameters are shown on terms of the displacement amplitude. Based on the data, it appears that both frequency and displacement amplitude must be considered when interpreting test results. The pile cap displacement levels shown in the figures correspond to a cycling phase when the dynamic shaker cycles were applied before the slowly applied actuator cycles.

The peaks in the normalized amplitude graph occur at the damped natural frequency of the system. The damped natural frequency appears to be increasing with increasing pile cap static displacement level. This is consistent with the increasing stiffness with displacement level as also shown on the graph. The damped natural frequency of the pile cap appears to range from 5 to 6.5 Hz. Stiffness generally ranges from between 570 and 1140 kip/in (100 and 200 kN/mm). Calculated damping ratios exhibit a wide range of scatter, varying both with respect to frequency

and displacement amplitude. Damping ratios tend to be in the range of 10 to 30% at intermediate frequencies and displacement levels and then increase with increases in those parameters. Interpreting the normalized displacement amplitudes using the half-power bandwidth approach yields damping ratios of 18, 17 and 8% for the three pile cap displacement levels shown in Figure 4-4.

4.5 Comparison of Cyclic Actuator and Dynamic Shaker Responses

Included in Figure 4-4 are displacement amplitude, stiffness, and damping ratio calculated from the statically applied cycles from the actuators (~ ¾ Hz) at each represented displacement level (points in dashed ovals). The values presented are averages of the previous and subsequent actuator cycles. An average value is used to represent stiffness and damping that would have been calculated if the actuator cycles and been performed before the shaker cycles. In terms of frequency, it is difficult to make a comparison between the static and dynamic methods because of the difference in the associated displacement amplitudes (the shaker cannot generate a large force, and hence displacement, at low frequencies).

When comparing the values as a function of displacement amplitude, there is somewhat greater consistency between the stiffness and damping ratios determined from the two types of loadings. If one compares the actuator- and shaker-based parameters at similar displacement amplitude of 0.08 to 0.10 in (2 to 2.5 mm), the calculated stiffnesses are quite similar, being on the order of 430 kip/in (75 kN/mm). The damping ratios show greater variation, with the shaker-based values of 20 to 50% being higher than the 20 to 30% from the actuator-based load displacement loops. The half-power bandwidth approach gives values slightly lower than those of the actuators. Given the irregularity of the shaker-based damping ratios, it is unclear if this is a real effect or an artifact of the methodology used to interpret the dynamic shaker data. It seems reasonable, however, to state that the pile cap system has a damping ratio of about 20% and decreasing somewhat with increasing static displacement level.

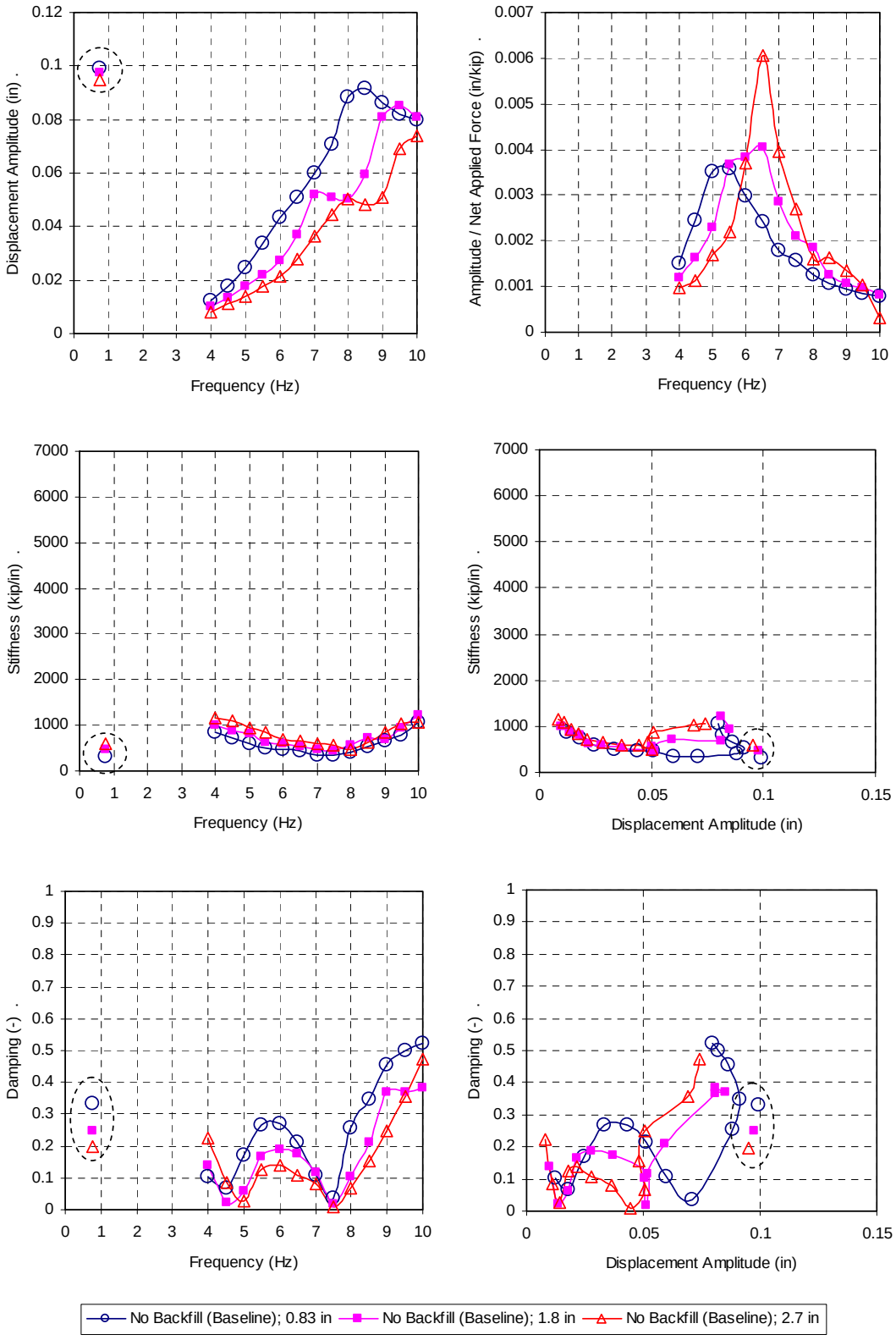

Figure 4-4 Summary of response to dynamic shaker loadings for pile cap without backfill (baseline condition)

THIS PAGE INTENTIONALLY LEFT BLANK

5.0 PILE CAP WITH NO BACKFILL PRESENT (OTHER NON-BASELINE RESPONSE TESTS)

5.1 General

As shown previously in Table 2-1, three load tests were performed on the pile cap with no backfill in place. As explained in Section 3.2, the test performed on June 21, 2007 was used as the baseline response. Basic results from the two tests not used as the baseline are presented in this Chapter. Table 5-1 and Table 5-2 summarize the tests performed on May 18 and June 1, 2007, respectively, in terms of loads and displacements measured at the end of each "static push" with the actuators. The tables also indicate the order in which cyclic loads from the actuators and dynamic loads from the shaker were applied for each test.

Table 5-1 Summary of test with no backfill (Test 1; May 18, 2007)

Displacement Interval	Displacement (in)	Actuator Load (kip)	Actuator Cycles	Shaker Cycles
1	0.22	98.7	First	Second
2	0.47	138	Second	First
3	0.75	182	First	Second
4	1.0	203	Second	First
5	1.6	293	First	Second
6	2.1	332	Second	First
7	2.7	379	First	Second
8	3.4	395	Second	First
unload	0.20	-233	---	---
9	3.5	357	None	None
unload	0.16	-199	---	---
10	0.47	0	None	None

Table 5-2 Summary of test with no backfill (Test 5; June 1, 2007)

Displacement Interval	Displacement (in)	Actuator Load (kip)	Actuator Cycles	Shaker Cycles
1	0.43	57.3	None	None
2	1.3	181	First	None
3	2.5	319	First	None
4	3.3	400	First	None

Because the two tests presented in this Chapter were not used as the baseline response for the pile cap, only limited results and interpretation are presented.

5.2 Load-Displacement Response

Figure 5-1 and Figure 5-2 show the actuator load verses pile cap displacement relationship for the May 18 and June 1, 2007, tests, respectively. The static pushes with the actuators, actuator cycles and shaker cycles being represented by green, blue, and red data points, respectively. Section 3.2 provides some discussion relative to the details of interpreting this data. Because no backfill was present, the horizontal load versus displacement relationships shown are the result of the resistance of the piles, the pile-soil interaction, and any friction due to contact of the pile cap with the underlying soil.

The first test (Test 1 on May 18) involved the initial loading of the cap, and this initial loading would not be comparable to a reloading of the cap until softening of the pile-to-cap connections had occurred after the first few complete load-displacement cycles of up to about 3.5 in (90 mm) of displacement. In addition to the loading sequence shown in Figure 5-1, the cap was unloaded and then reloaded two more times (not shown in figure) over the same range of displacement. These additional loadings, applied using only the actuators, were used to "condition" the cap and develop a consistent load-displacement response. The pile cap under these loadings exhibited slopes which were shallower than the slope from the initial loading, and these slopes were relatively consistent with each other, indicating that a constant load-displacement response had been developed. Later comparisons of the slopes of the load-displacement curves during the pulling of the cap back to its starting position at the end of each backfill test showed generally consistent values, indicating that the cap was well conditioned and that the baseline response of the cap was relatively consistent between tests.

The second test (Test 5 on June 1, 2007) did not have any dynamic effects in the load-displacement relationship since the shaker had experienced a malfunction; also, there were fewer intervals at which cyclic actuator loading were applied. The load-displacement response is quite linear with a slope of about 120 kip/in (21 kN/mm).

In general, the initial portion of the load-displacement curve during Test 1 exhibited greater load resistance than during Test 5 (indicative of the softening of the connections). At the

peak displacement level of about 3.35 in (85 mm), both tests exhibit a load resistance averaging about 400 kip (1770 kN), which is comparable with resistance exhibited during Test 11 which was used as the baseline response. The similarities between these tests with no backfill present suggest that the resistance of the pile cap does not change significantly after conditioning and remained similar throughout the duration of the testing program.

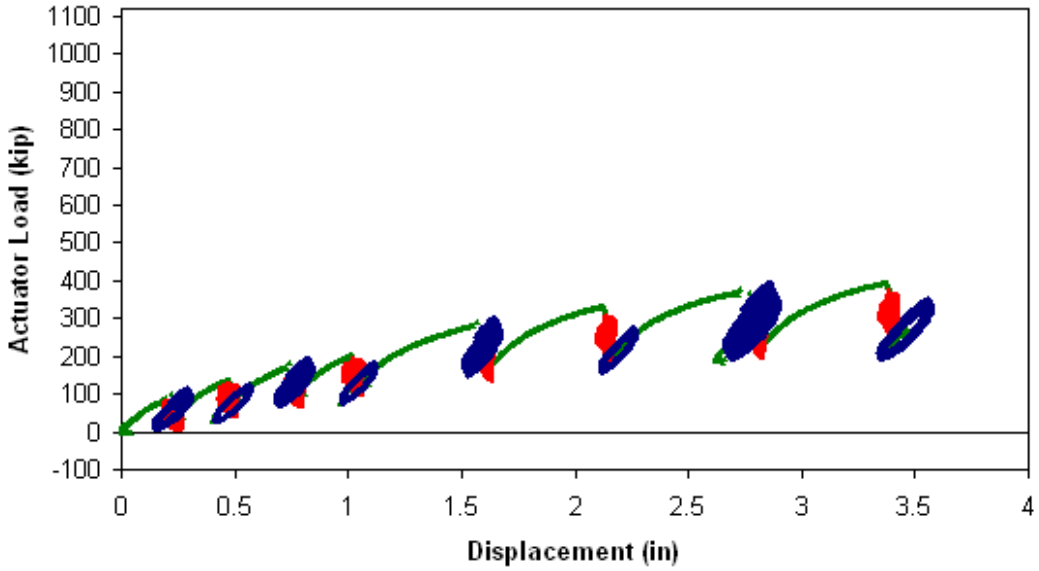

Figure 5-1 Actuator load versus pile cap displacement with no backfill (Test 1; May 18, 2007)

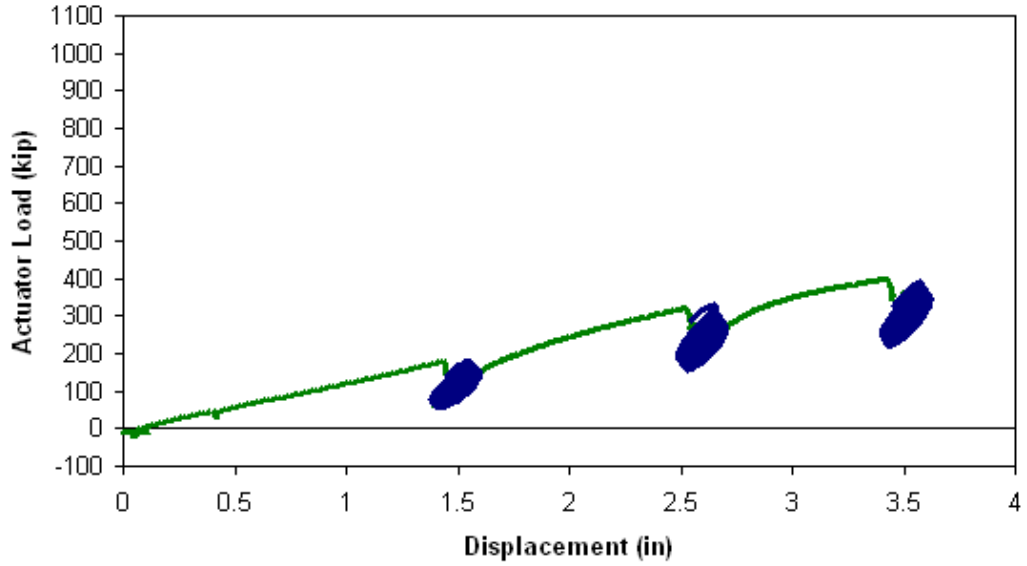

Figure 5-2 Actuator load versus pile cap displacement with no backfill (Test 5; June 1, 2007)

THIS PAGE INTENTIONALLY LEFT BLANK

6.0 PILE CAP WITH DENSELY COMPACTED CLEAN SAND BACKFILL

6.1 General

The pile cap with densely compacted clean sand backfill was tested on May 25, 2007. No significant deviations from the general test procedure occurred during this test. Table 6-1 summarizes the test in terms of loads and displacements measured at the end of each "static push" with the actuators. The table also indicates the order in which cyclic loads from the actuators and dynamic loads from the shaker were applied.

Table 6-1 Summary of test with densely compacted clean sand backfill

Displacement Interval	Displacement (in)	Actuator Load (kip)	Actuator Cycles	Shaker Cycles
1	0.11	96.2	First	Second
2	0.26	162	Second	First
3	0.43	234	First	Second
4	0.63	266	Second	First
5	0.87	363	First	Second
6	1.2	469	Second	First
7	1.5	541	First	Second
8	1.8	618	Second	First
9	2.1	659	First	Second
10	2.2	683	Second	First
11	2.5	727	First	Second

6.2 Load-Displacement Response

Figure 6-1 shows the entire actuator load verses pile cap displacement relationship for the test, with static pushes, actuator cycles and shaker cycles being represented by green, blue, and red data points, respectively. Section 3.2 provides some discussion relative to the details of interpreting this data.

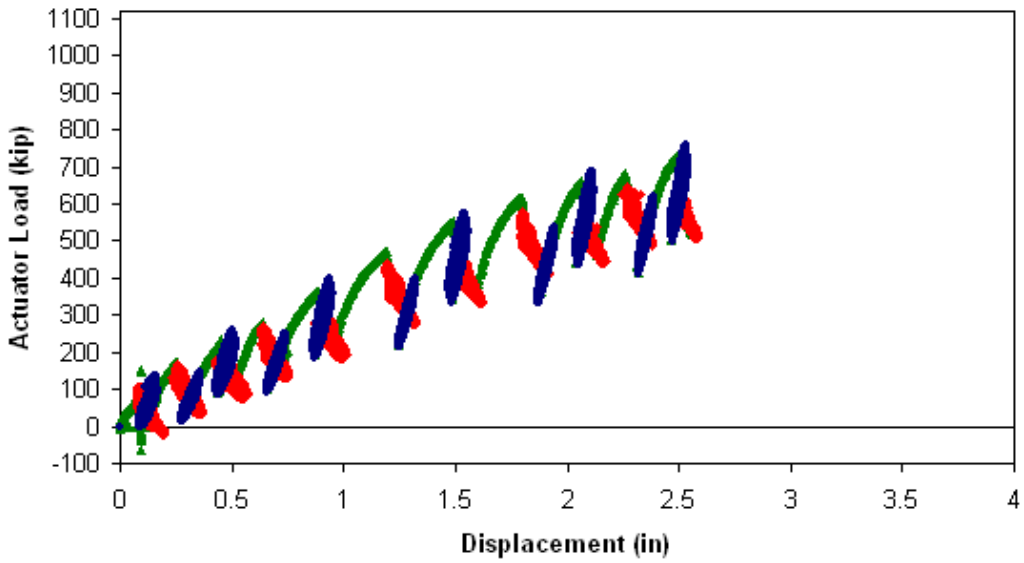

Figure 6-1 Actuator load versus pile cap displacement with densely compacted clean sand backfill (Test 2; May 25, 2007)

Figure 6-2 shows three load-displacement responses (curves) for the pile cap: one for the response with the backfill in place (referred to as the total response, which is the equivalent monotonic response or backbone curve derived from the data shown in Figure 6-1), one for the response with no backfill present (referred to as the baseline response), and one showing the passive earth response of the backfill (obtained by subtracting the baseline response from the total response).

The curves show that total response and baseline response increase at different rates until approximately 1.9 to 2.0 in (48 to 50 mm) of displacement (depending upon visual interpretation). By this point, the backfill response levels off as the baseline and total response increase at approximately the same rate. This leveling off is interpreted as the point when the backfill material is at failure. Hence, the ultimate passive resistance of the backfill, approximately 440 kip (1970 kN), is developed at a displacement of approximately 2 in (50 mm) which corresponds to a displacement to wall height ratio (Δ_{max}/H) of about 0.03.

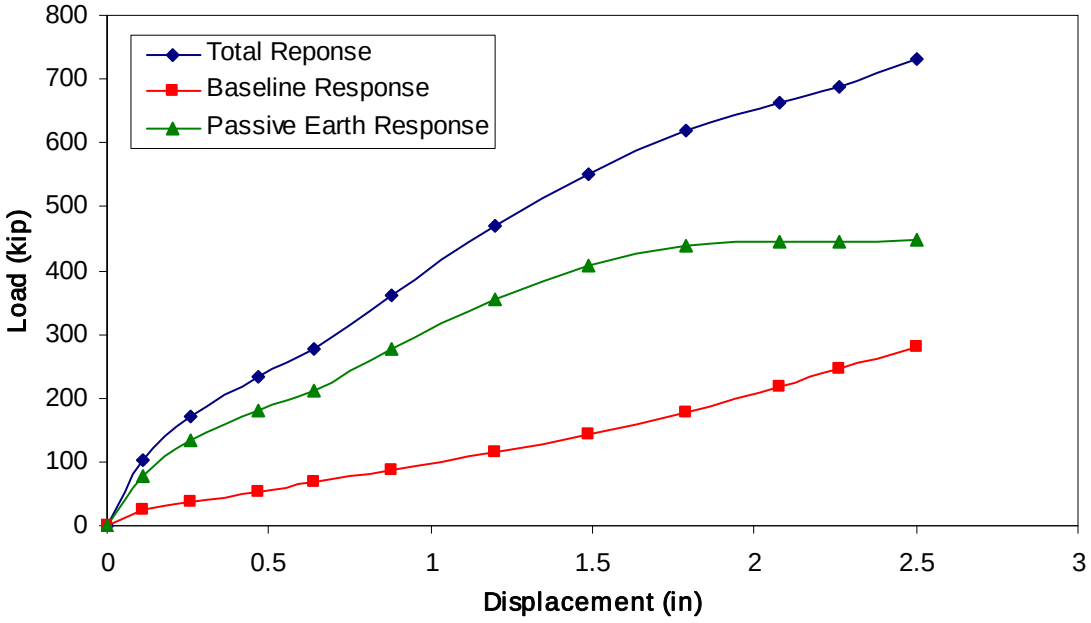

Figure 6-2 Total, baseline, and passive earth responses for pile cap with densely compacted clean sand backfill

6.3 Calculated Passive Earth Force

Commonly used methods for calculating passive earth pressure include Rankine theory, Coulomb theory, and log-spiral theory. Log-spiral theory is typically considered the most accurate of these methods (see, for example, Cole and Rollins (2006) and Duncan and Mokwa (2001)). Three methods of estimating the development of passive pressure with wall displacement are evaluated in this section. Two of these methods, PYCAP and ABUTMENT (LSH method) involve applications of log-spiral theory and a hyperbolic load-displacement relationship. The third approach evaluated in this section is an empirical load-displacement relationship based on full-scale testing of an abutment with typical backfill conditions (see discussion of CALTRANS method in Section 3.3.3)

6.3.1 Calculated Response Using PYCAP

Passive earth resistance was calculated using the modified PYCAP spreadsheet. Table 6-2 summarizes key inputs and outputs for several cases analyzed while Figure 6-3 shows the measured and calculated passive resistance curves for each case. Case I is based strictly on

laboratory-determined ultimate values for shear strength, interface friction angle (which was similar for both peak and ultimate strength states) and initial modulus. Case II is identical to Case I except that the internal friction angle is based on peak strength instead of ultimate strength. Case III is similar to Case I, except the interface friction angle has been changed to match the δ/ϕ ratio determined by Cole and Rollins (2006) for a different pile cap using the same type of backfill material, and the initial modulus has also been changed to better fit the initial slope of the measured data. For Case I, the calculated ultimate passive resistance is slightly less than the measured ultimate passive resistance. Case II predicts an ultimate passive resistance 35% greater than Case I. Case III matches the initial slope and the ultimate value of the measured resistance line. Overall the hyperbolic model used in PYCAP appears to match well with the measured data when ultimate shear strength parameters and a δ/ϕ ratio of 0.75 are used.

Table 6-2 Summary of PYCAP parameters for densely compacted clean sand backfill

Parameter	Case I	Case II	Case III
ϕ (°)	40.5	43.3	40.5
c (psf)	0	0	0
δ (°)	29	29	30.4
γ_m (pcf)	117.0	117.0	117.0
E (ksf)	830	830	600
ν	0.3	0.3	0.3
k (kip/in)	1374	1374	993
Δ_{max} (in)	1.98	1.98	1.98
Δ_{max}/H	0.030	0.030	0.030
R_f	0.84	0.79	0.77
R_{3D}	1.83	1.97	1.85
K_p	13.8	17.3	14.4

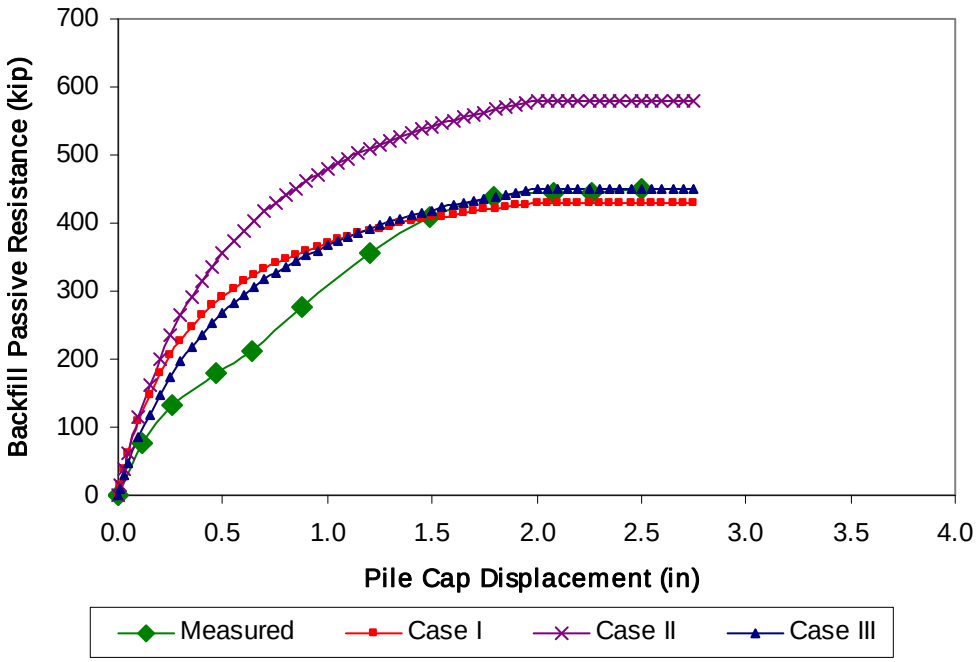

Figure 6-3 Comparison of measured and PYCAP-based calculated passive resistance for densely compacted clean sand backfill

6.3.2 Calculated Response Using ABUTMENT (LSH)

Passive earth resistance was also calculated using ABUTMENT and the LSH methodology. Table 6-3 summarizes key inputs and outputs for several cases analyzed while Figure 6-4 shows the measured and calculated passive resistance curves for each case. Case I is based strictly on laboratory-determined values for ultimate shear strength and is the same as Case I in analyses performed using PYCAP. Case II is the same as Case I except the peak friction angle has been used. The measured data lies between these two curves. Case III is a result of adjusting Case I to include 84 psf (4.0 kPa) of cohesion, a relatively small amount, to better match the measured peak resistance. This value is the same value as was used by Shamsabadi et al. (2007) in their analyses of Rollins and Cole (2006) pile cap test results with a similar backfill material. Case IV is the result of doubling the strain parameter to obtain a better match with the initial portion of the curve, but good agreement was not obtained and further increase would result in excessive displacement when the ultimate resistance is reached. The best match was obtained in Case III using the ultimate friction angle and a small amount of cohesion.

6.3.3 Calculated Response Using CALTRANS Method

Passive earth resistance based on the CALTRANS method is shown in Figure 6-5. The method under-predicts peak passive resistance by approximately 30%. The initial slopes of the calculated and measured pressure are generally comparable, although the calculated pressure in that region is lower than the measured pressure.

Table 6-3 Summary of LSH parameters for densely compacted clean sand backfill

Parameter	Case I	Case II	Case III	Case IV
ϕ (°)	40.5	43.3	40.5	40.5
c (psf)	0	0	84	84
δ (°)	29	29	29	29
γ_m (pcf)	116.4	116.4	116.4	116.4
ε_{50}	0.002	0.002	0.002	0.004
ν	0.3	0.3	0.3	0.3
R_f	0.98	0.98	0.98	0.98
R_{3D}	1.83	1.97	1.83	1.83
K_{ph}	10.8	13.4	13.2	13.2

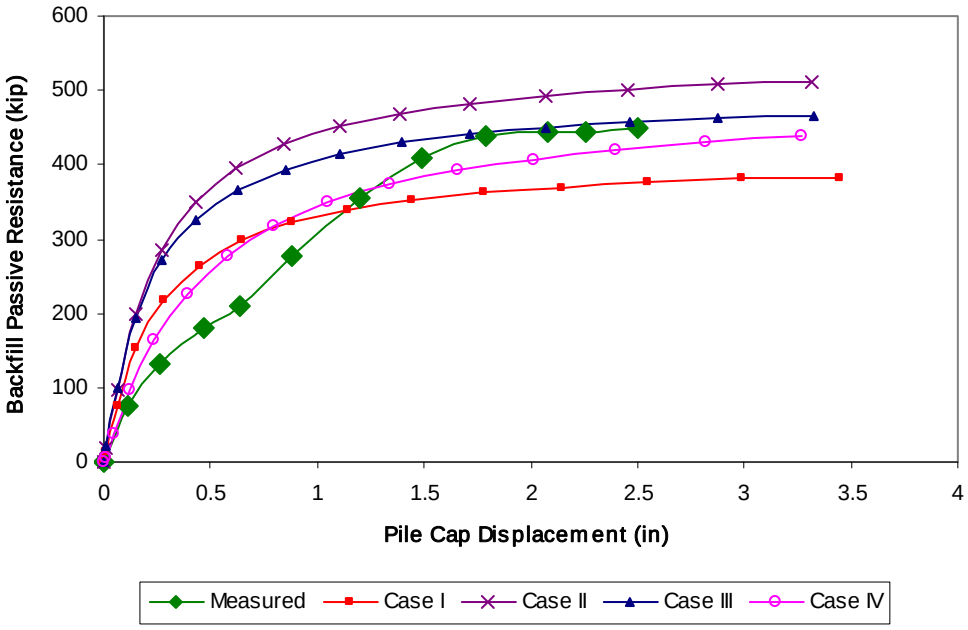

Figure 6-4 Comparison of measured and LSH-based calculated passive resistance for densely compacted clean sand backfill

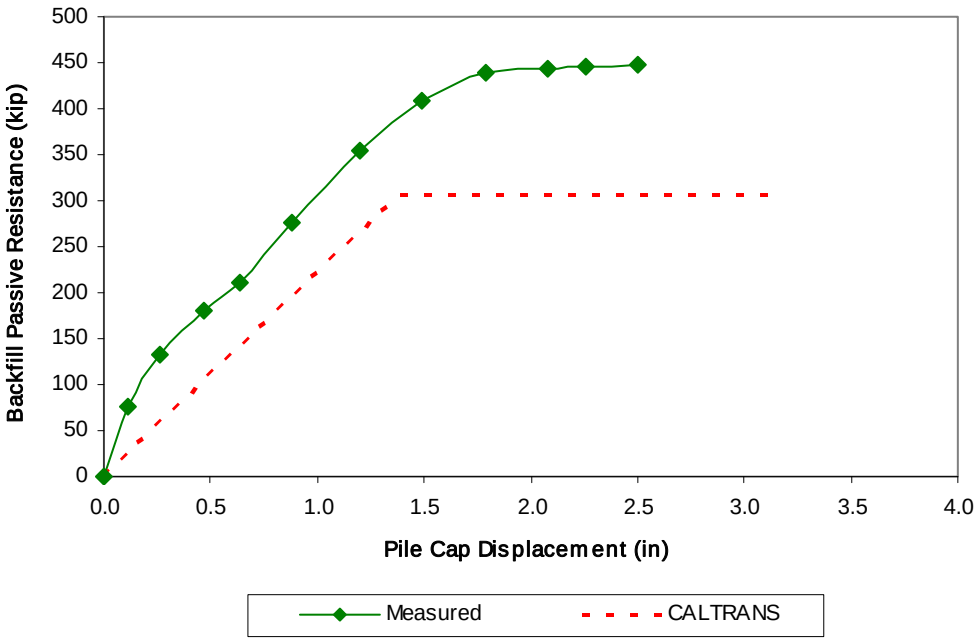

Figure 6-5 Comparison of measured and CALTRANS-based passive resistance for densely compacted clean sand backfill

6.4 Response to Cyclic Actuator Loading

After slowly pushing the pile cap to each displacement interval, alternating combinations of small displacement cyclic actuator loads and dynamic shaker loads were applied. The response of the pile cap to the small displacement amplitude loading cycles from the actuator is presented and discussed in this section. Figure 6-6 shows the loop displacement amplitude, stiffness, loop area, and damping ratio for the pile cap with backfill in place as a function of pile cap displacement. Values are based on the median of the 15 small amplitude cycles performed at each displacement level. The increase in stiffness with pile cap displacement appears to be due to greater mobilization of the backfill soil's passive strength and pile stiffness. The stiffness data particularly exhibits

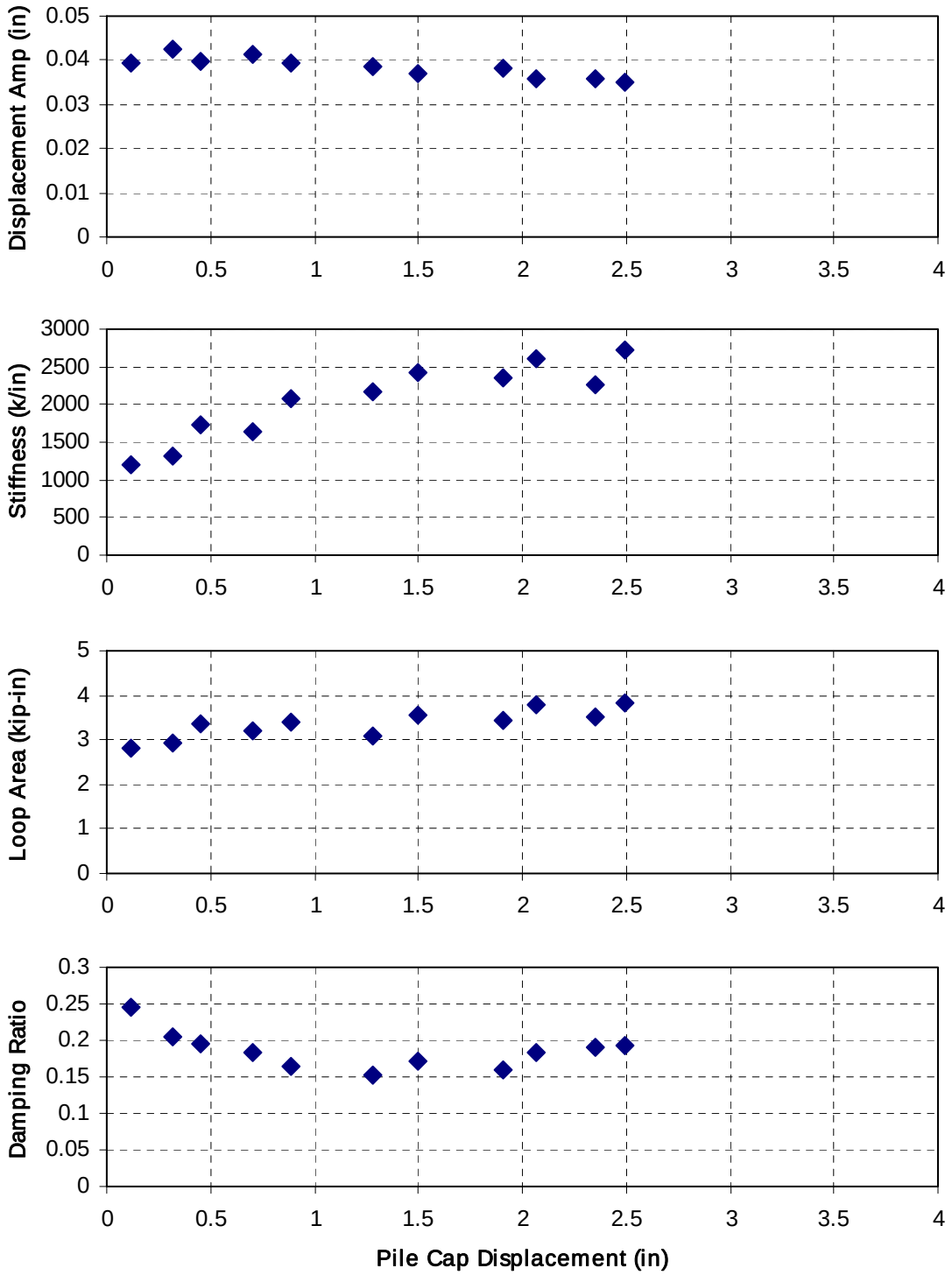

Figure 6-6 Summary of response to cyclic actuator loadings for pile cap with densely compacted clean sand backfill

the saw-tooth shaped trend as seen in other tests due to the alternating order of the static and dynamic cycling loading phases. The rate of stiffness increase appears to level off in the last several displacement intervals when the ultimate passive resistance of the backfill soil is assumed to be reached. Even with the increasing stiffness and the relatively constant displacement amplitudes and loop areas, the damping remains fairly constant with a median value of 18%.

6.5 Response to Dynamic Shaker Loading

After slowly pushing the pile cap to each displacement interval, alternating combinations of small displacement cyclic actuator loads and dynamic shaker loads were applied. The response of the pile cap to the dynamic shaker loading is presented and discussed in this section. The first row of graphs in Figure 6-7 shows loop displacement amplitude as well as loop displacement amplitude normalized by the cyclic amplitude of net applied force from the shaker and actuators as functions of the forcing frequency. The second and third rows of graphs show the calculated reloading stiffness and damping, respectively, of the pile cap system. In the left column, these parameters are shown in terms of forcing frequency. If non-linear behavior is present, these properties will also depend on the displacement amplitude; hence, in the right column, these parameters are shown on terms of the displacement amplitude. Based on the data, it appears that both frequency and displacement amplitude must be considered when interpreting test results. The individual line series shown in all of the graphs correspond to different static displacement levels of the pile cap in which dynamic shaker cycles were applied before the slowly applied actuator cycles.

The peaks in the normalized loop displacement amplitude graph correspond to the damped natural frequency of the system. The damped natural frequency appears to remain fairly constant near 7.5 Hz at all static displacement levels. Reloading stiffness values range from 1700 to just over 3400 kip/in (300 to just over 600 kN/mm), peaking just before the damped natural frequency and dropping afterward. The general trend in the stiffness data shows an increase in stiffness with increasing pile cap displacement level, but there appears to be little difference in the dynamic stiffnesses for the two largest displacement levels of 1.81 and 2.24 in (46 and 57 mm). This is consistent with the concept that at these static displacement levels the

backfill soil has already reached its ultimate strength and cannot provide more resistance with increasing pile cap displacement.

Calculated damping values vary greatly with respect to the frequency of the forcing function and displacement amplitude. Damping appears to be a minimum of 5% at about 6 Hz (just less than the damped natural frequency of the pile cap system) and at 0.01 in (0.3 mm) of displacement amplitude. At higher frequencies and displacements, the damping ratio increases up to about 35% (corresponding with the calculated decreasing stiffness) until dropping again at 8.5 Hz (where stiffness reaches a more or less constant value). Unfortunately, the normalized displacement amplitudes were such that the half-power bandwidth approach could not be used. The calculated damping ratios are comparable to those reported by Valentine (2007) for similar tests with densely compacted silty sand at another site. His damping ratios ranged from 20 and 40% at frequencies between 4 and 9 Hz.

6.6 Comparison of Cyclic Actuator and Dynamic Shaker Responses

Included in Figure 6-7 are displacement amplitude, stiffness, and damping ratio calculated from the statically applied cycles from the actuators (~ ¾ Hz) at each

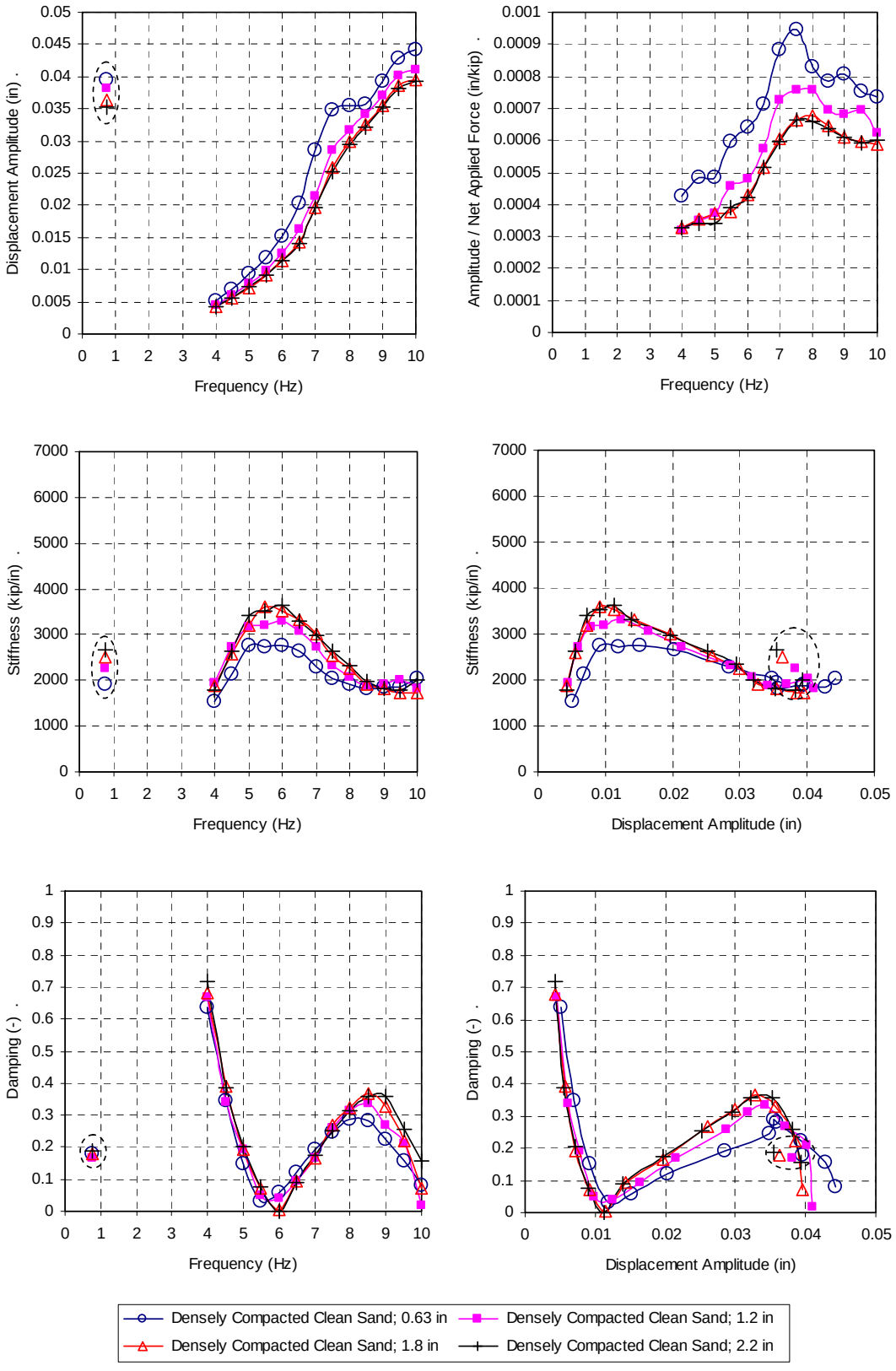

Figure 6-7 Summary of response to dynamic shaker loadings for pile cap with densely compacted clean sand backfill

represented displacement level (points in dashed ovals). The values presented are averages of the previous and subsequent actuator cycles. An average value is used to represent stiffness and damping that would have been calculated if the actuator cycles and been performed before the shaker cycles. In terms of frequency it can be difficult to make a comparison between the static and dynamic methods because of the difference in the associated displacement amplitudes (the shaker cannot generate large forces, and hence displacements, at low frequencies).

When comparing the values as a function of displacement amplitude there is somewhat greater consistency between the stiffness and damping ratios determined from the two types of loadings. The dynamic shaker loading at a frequency of 9 Hz resulted in displacement amplitudes on the order of 0.04 in (1 mm), which are comparable to those produced by the cyclic actuator loading. Comparing the two tests types at this similar displacement level, the shaker-based stiffnesses are about 1850 kip/in (325 kN/mm) whereas the range of actuator-based stiffness goes higher from 1850 to about 2570 kip/in (325 to about 450 kN/m). Damping ratios are quite similar, being between 15 and 20%. This similar amount of damping suggests that dynamic loadings do not appreciably increase the apparent resistance of the pile cap relative to slowly applied cyclic loadings.

6.7 Passive Earth Pressure Distributions

In addition to the load-displacement response data, passive earth pressure from the backfill soil was measured directly with a vertical array of six earth pressure cells evenly distributed in the central portion of the pile cap face. Figure 6-8 shows the pressure measured by the pressure cells with depth at the end of each static push interval.

The pressure cells show general trends as expected of increasing pressure with depth and increasing magnitude with increasing pile cap displacement. The bottom pressure cell seems not to follow this trend, with pressure decreasing to near zero after the first two displacement levels. This behavior could result from a rotation of the pile cap or a malfunction of the cell, and is discussed in Section 3.5. The top pressure cell also appears to not entirely follow the trend, reaching a plateau at about 2600 psf (125 kPa) at a displacement of about 1.46 in (37 mm), and then decreasing slightly in pressure to 2300 psf (110 kPa) during the last four push intervals. The peak value in the top pressure cell generally coincides with the displacement level at which

the backfill appears to reach its ultimate strength, with the lower cells (excluding the bottom one) showing progressively smaller gains in pressure with increasing displacement.

Figure 6-9 shows the backfill force calculated by multiplying each measured pressure by the respective contributory areas of the pile cap face. In general, the resulting force-displacement curve has a similar trend to that based on the actuators, but it is systematically lower. Applying a multiplier of 1.67 (the inverse of 0.6 determined in Section 3.5) to the cell-based curve provides an improved match with the actuator-based curve, although the reaching of the ultimate passive resistance is not apparent.

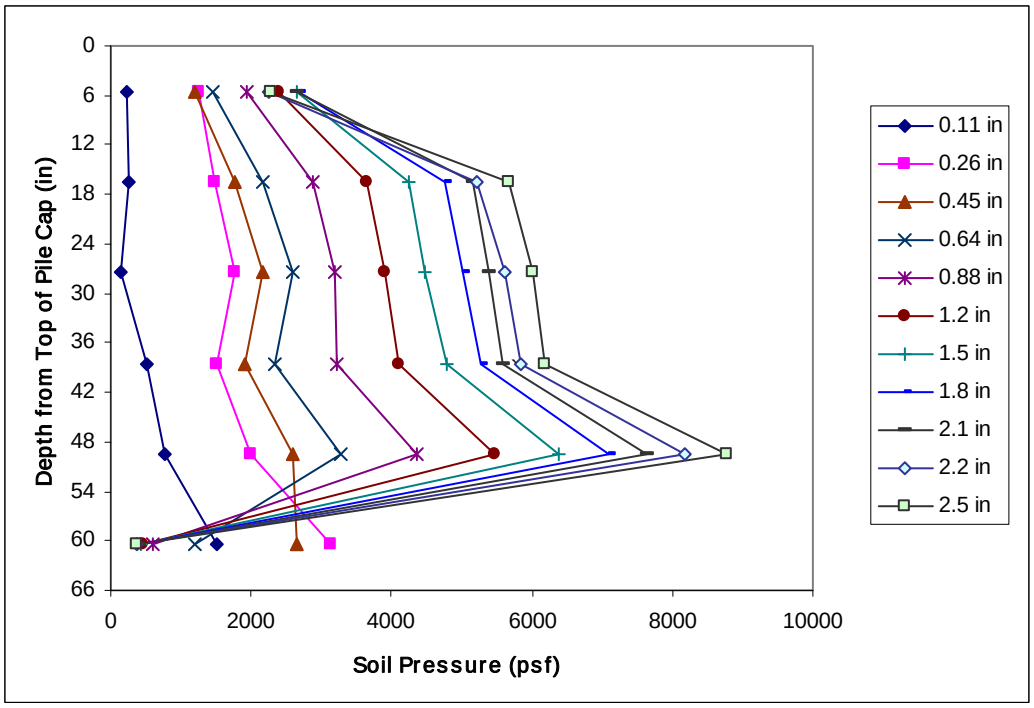

Figure 6-8 Earth pressure distribution as a function of pile cap displacement with densely compacted clean sand backfill

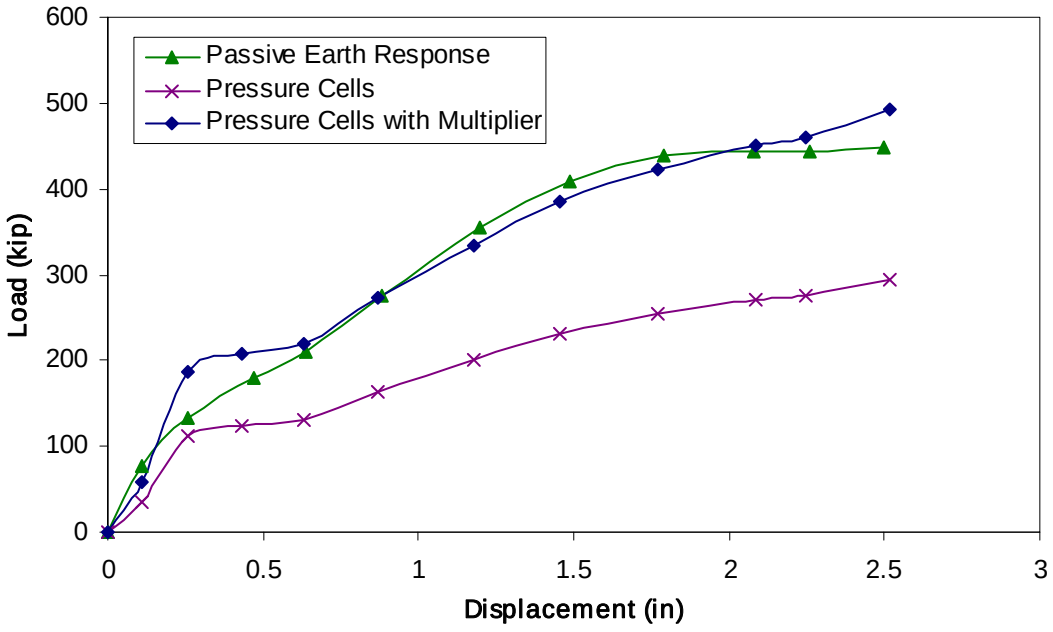

Figure 6-9 Comparison of earth forces based on actuators and pressure cells for densely compacted clean sand backfill

6.8 Cracking and Vertical Movement of Backfill

Figure 6-10 is a two part plot showing the results of static and dynamic testing on the surface of the densely compacted clean sand backfill area. The first part of the figure shows the surface cracks that developed during each static push of the pile cap. The surface cracks in the backfill indicate the presence of failure surfaces within the soil. The cohesion less nature of the material, along with the dynamic vibration due to the eccentric mass shaker, tended to cause the soil grains to shift during testing, potentially obscuring cracks. The majority of the visible cracks are concentrated around the edges of the cap face. These cracks are due to the internal shear stresses radiating out from the cap face and reflect the three dimensional shape of the failure zone. Two other distinct sets of cracks are located approximate 2 ft (0.6 m) from either side edge of the backfill zone. The distance between these two crack sets is slightly greater than 18 ft (5.5 m), which closely matches the 19.5-ft wide (6-m wide) failure wedge computed using the three dimensional correction factor from the PYCAP spreadsheet program. Cracking in the surface of the densely compacted clean sand does not indicate where the failure wedge ends.

The second part of the figure is a contour map of the change in elevation of the surface of the backfill area during testing. The typical elevation change, as represented by the median elevation change in a given row (parallel to the face of the cap) of grid nodes, is about 1.08 in (27 mm) at 4 ft (1.22 m) from the pile cap face. Calculations indicate that a log-spiral failure surface should daylight at approximately 19 ft (5.8 m) from the face of the cap. The figure shows that most of the elevation change occurred within the first 13 ft (4 m) or so of backfill; thus, it is reasonable to expect that the failure surface daylights just beyond that zone.

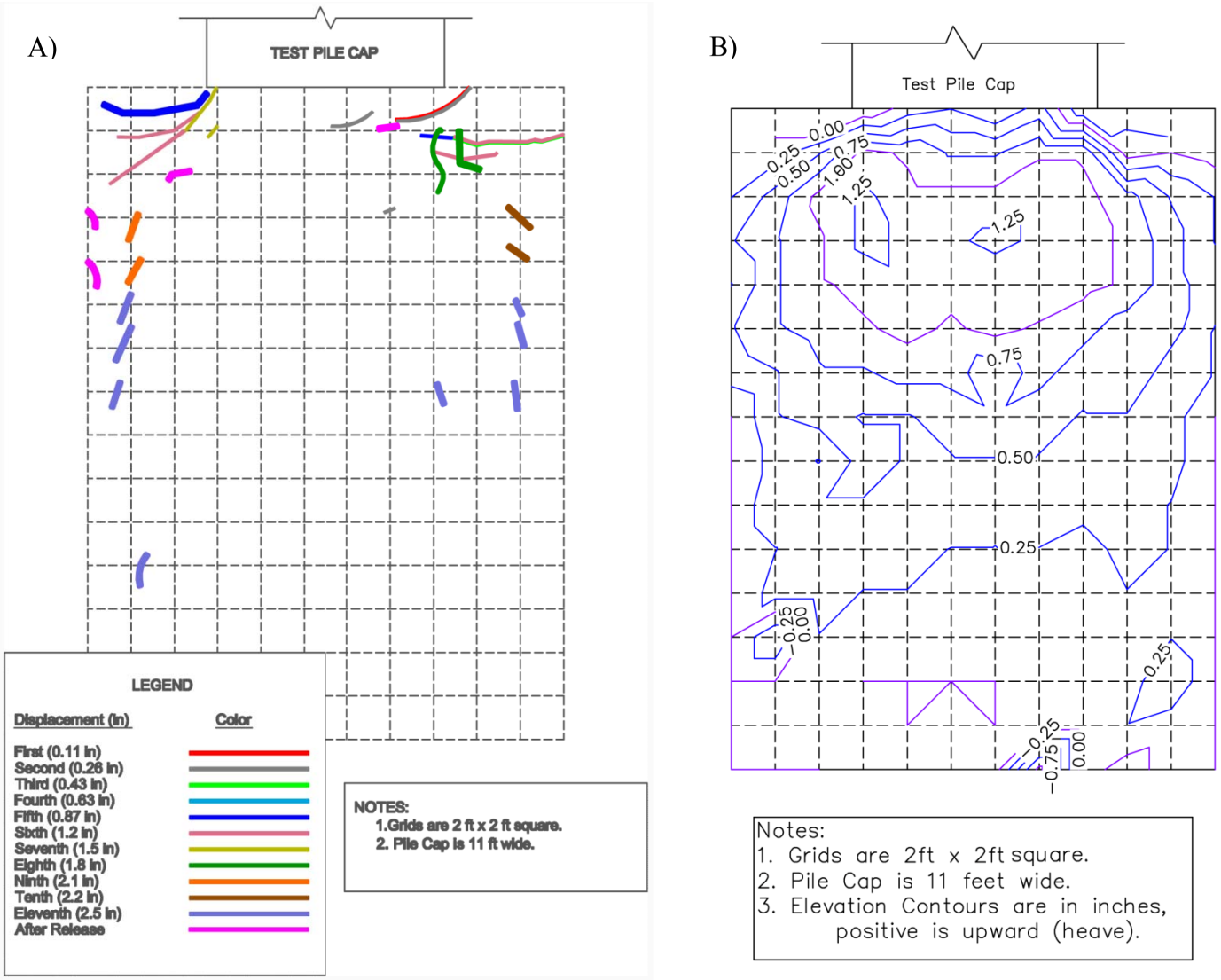

Figure 6-10 Crack pattern (A) and heave contour (B) maps for densely compacted sand backfill

The correlation between the heave characteristics of the backfill and the log-spiral failure surface is illustrated by the cross-sectional view in Figure 6-11, where the failure surface calculated in the spreadsheet program PYCAP using Case III parameters daylights for close to where heave approaches the initial elevation of the backfill surface. The heave profile in the figure is magnified ten times to make the elevation change more appreciable.

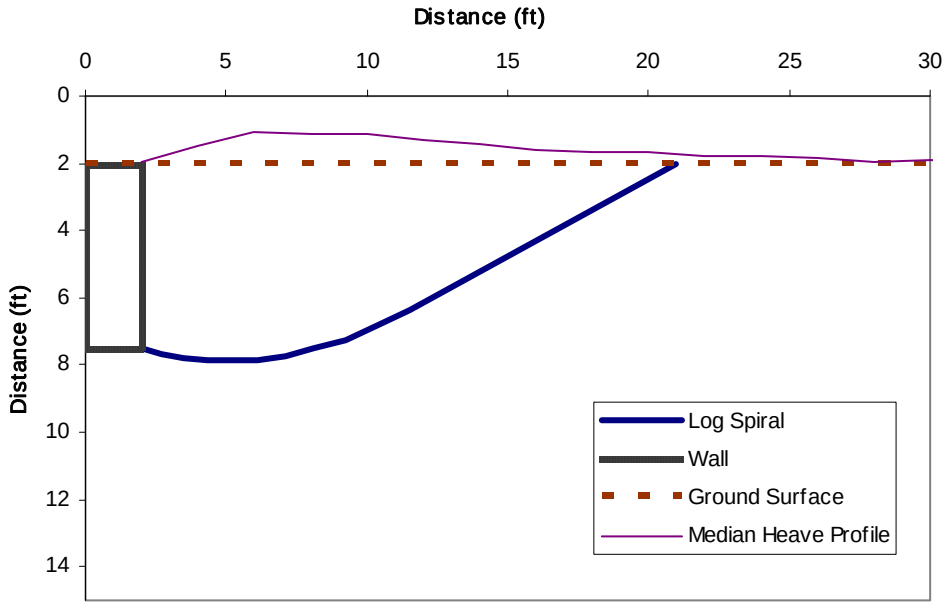

Figure 6-11 Heave profile for densely compacted clean sand compared with log spiral failure surface from PYCAP (Case III parameters)

6.9 Horizontal Movement of Backfill

String potentiometers were used to measure movement in the backfill. Figure 6-12 shows the movement of each of the monitoring points in the densely compacted clean sand backfill compared to the movement of the pile cap face. The backfill displacement ranges from 2.5 in (63 mm) (100% of cap displacement) at the cap face to 0.6 in (15 mm) (24% of cap displacement) at 18 ft (5.5 m) from the cap face. This translational movement represents the amount of the pile cap displacement not absorbed through compressive strain up to the monitoring point.

Error! Reference source not found. shows the compressive strain corresponding to each static push of the pile cap. The compressive strain ranges from 0.02 to 0.005 within the backfill

zone. The strain distribution is highest at the pile cap face, as expected, and is relatively uniform with distance away from the cap up to the maximum distance monitored. Minor variation from interval to interval may reflect the potential sensitivity of the string potentiometer measurements to differential pushing of the pile cap (not all the monitoring stakes were on the same end of the cap face) and tipping of the monitoring stakes themselves during the dynamic shaking . Movement of the stakes could explain the presence of some negative strain amounts in the calculations.

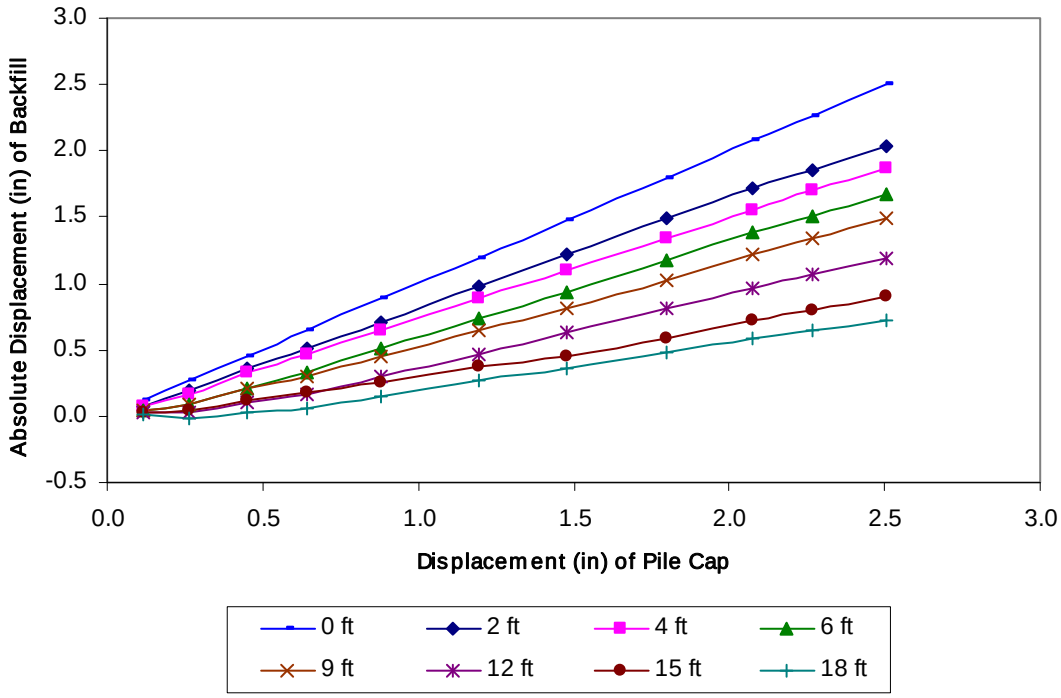

Figure 6-12 Displacement of monitoring points in densely compacted sand backfill

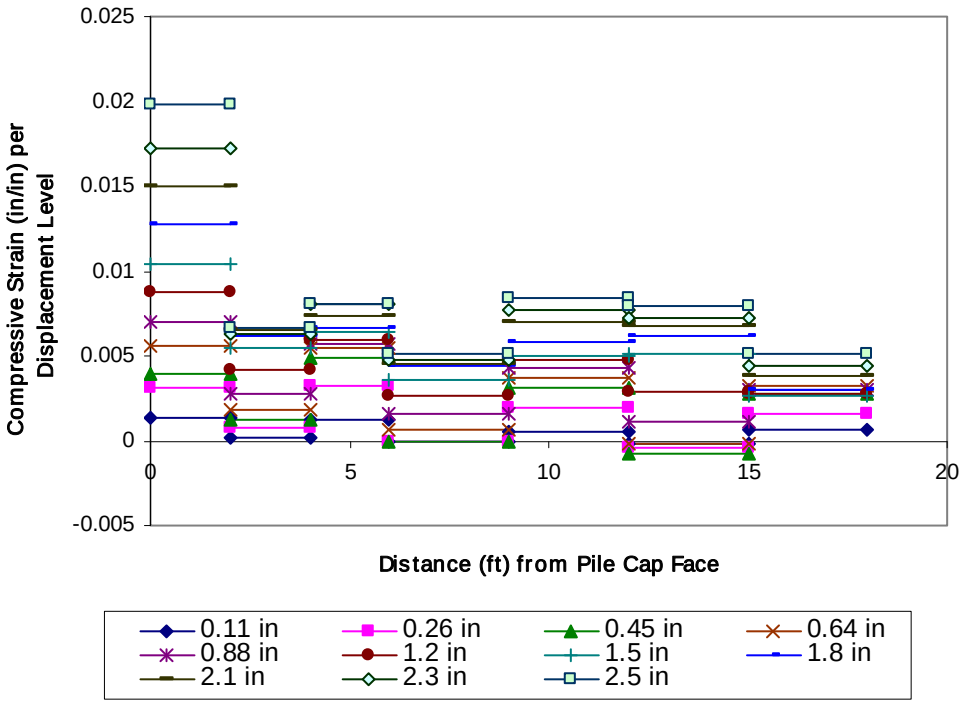
0.025
0.02
0.015
0.01
0.005
0
-0.005
0
5
10
15
20
Compressive Strain (in/in) per Displacement Level
Distance (ft) from Pile Cap Face
0.11 in
0.26 in
0.45 in
0.64 in
0.88 in
1.2 in
1.5 in
1.8 in
2.1 in
2.3 in
2.5 in

THIS PAGE INTENTIONALLY LEFT BLANK

7.0 PILE CAP WITH DENSELY COMPACTED FINE GRAVEL BACKFILL

7.1 General

The pile cap with densely compacted fine gravel backfill was tested on June 11, 2007. No significant deviations from the general test procedure occurred during this test. Table 7-1 summarizes the test in terms of loads and displacements measured at the end of each "static push" with the actuators. The table also indicates the order in which cyclic loads from the actuators and dynamic loads from the shaker were applied. At some displacement increments, no cyclic or dynamic loadings were applied in order to help assure that sufficient displacement had occurred for the load path to return to the static-backbone loading curve.

Table 7-1 Summary of test with densely compacted fine gravel backfill

Displacement Interval	Displacement (in)	Actuator Load (kip)	Actuator Cycles	Shaker Cycles
1	0.21	207	First	Second
2	0.51	291	Second	First
3	0.75	372	None	None
4	0.94	460	First	Second
5	1.2	496	None	None
6	1.4	594	Second	First
7	1.6	651	None	None
8	1.9	742	First	Second
9	2.1	802	None	None
10	2.4	894	Second	First
11	2.7	932	None	None
12	2.9	999	First	Second
13	3.2	1030	None	None
14	3.4	1090	None	None

7.2 Load-Displacement Response

Figure 7-1 shows the entire actuator load verses pile cap displacement relationship for the test, with static pushes, actuator cycles and shaker cycles being represented by green, blue, and

red data points, respectively. Section 3.2 provides some discussion relative to the details of interpreting this data.

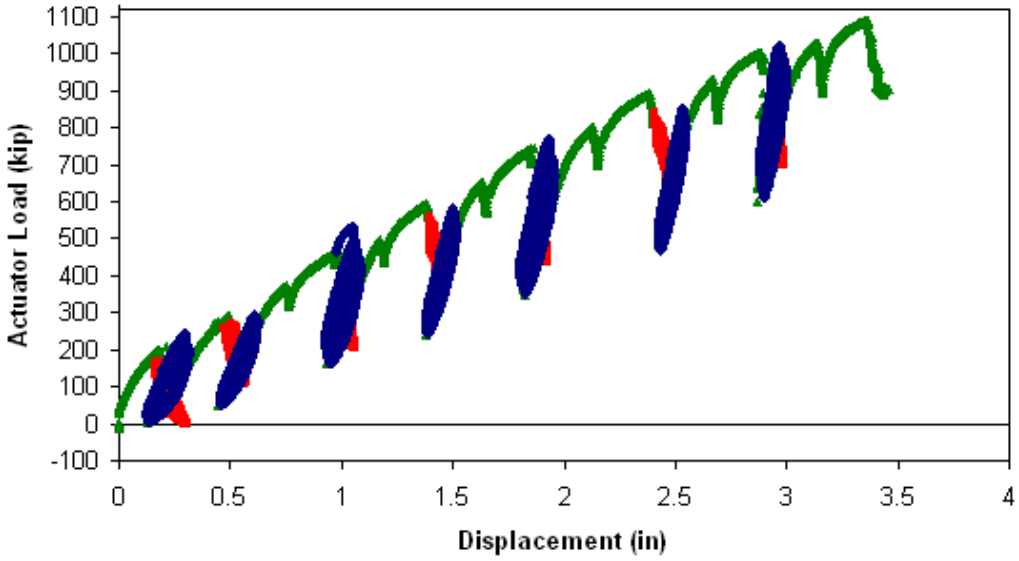

Figure 7-1 Actuator load versus pile cap displacement with densely compacted fine gravel backfill (Test 8; June 11, 2007)

Figure 7-2 shows three load-displacement responses (curves) for the pile cap: one for the response with the backfill in place (referred to as the total response, which is the equivalent monotonic response or backbone curve derived from the data shown in Figure 7-1), one for the response with no backfill present (referred to as the baseline response), and one showing the passive earth response of the backfill (obtained by subtracting the baseline response from the total response).

The curves show that total response and baseline response increase at different rates until approximately 2.4 in (62 mm) of displacement. By this point, the backfill response levels off as the baseline and total response increase at approximately the same rate. This leveling off is interpreted as the point when the backfill material is at failure. Hence, the ultimate passive resistance of the backfill, approximately 640 kip (2860 kN), is developed at a displacement of about 2.4 in (62 mm), which corresponds to a displacement to wall height ratio (Δ_{max}/H) of about 0.037.

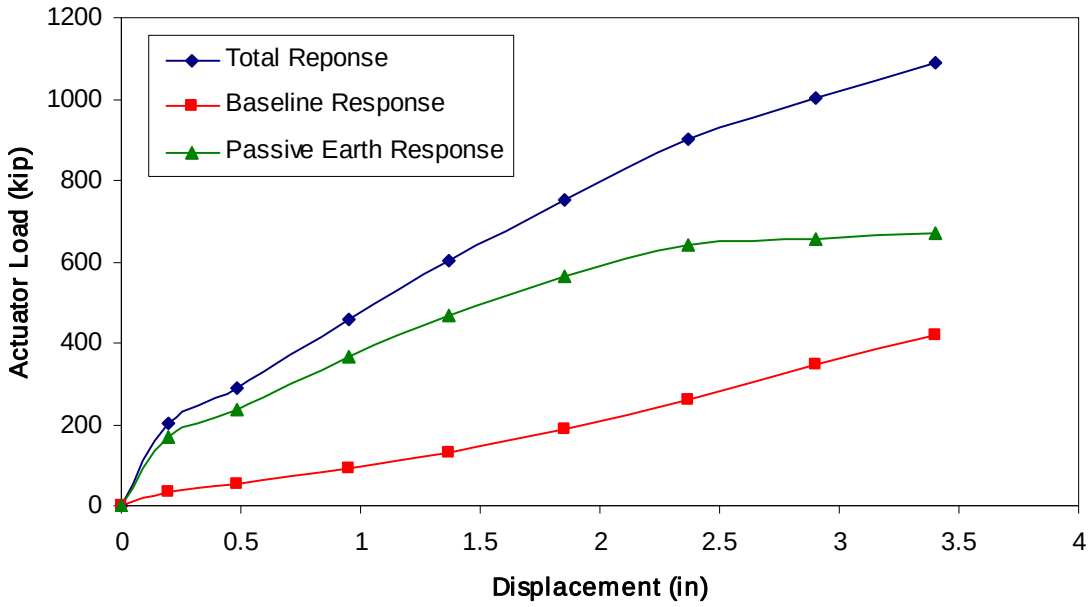

Figure 7-2 Total, baseline, and passive earth responses for pile cap with densely compacted fine gravel backfill

7.3 Calculated Passive Earth Force

Commonly used methods for calculating passive earth pressure include Rankine theory, Coulomb theory, and log-spiral theory. Log-spiral theory is typically considered the most accurate of these methods (see, for example, Cole and Rollins (2006) and Duncan and Mokwa (2001)). Three methods of estimating the development of passive pressure with wall displacement are evaluated in this section. Two of these methods, PYCAP and ABUTMENT (LSH method) involve applications of log-spiral theory and a hyperbolic load-displacement relationship. The third approach evaluated in this section is an empirical load-displacement relationship based on full-scale testing of an abutment with typical backfill conditions (see discussion of CALTRANS method in Section 3.3.3)

7.3.1 Calculated Response Using PYCAP

Passive earth resistance was calculated using the modified PYCAP spreadsheet. Table 7-2 summarizes key inputs and outputs for several cases analyzed while Figure 7-3 shows the measured and calculated passive resistance curves for each case. Case I is based strictly on laboratory-determined ultimate values for shear strength, interface friction angle (which was

similar for both peak and ultimate strength states, with a laboratory based δ/ϕ ratio of about 0.61) and initial modulus. The initial modulus of 670 ksf (32100 kPa) used in PYCAP for densely compacted fine gravel was derived from a constrained consolidation test and corresponds with the "preloaded or compacted" range for dense sands and gravels recommended by Duncan and Mokwa (2001). For Case I, the calculated load-displacement curve greatly exceeds the measured curve. Parameters for Case II are identical to Case I except that the cohesion has been neglected. The resulting load-displacement curve is closer to, but still greatly more than, the measured curve. In Case III, the interface friction angle has been iteratively reduced to obtain a good match between the calculated and measured load-displacement curves. The friction angle in Case IV is based on an in-situ direct shear test staged using a single sample over three normal pressures. The cohesion intercept from the in-situ test, 275 psf (19.7 kPa), has been reduced to a nominal value for cohesionless soils of zero, and the δ/ϕ ratio is the same laboratory-based value used in Cases I and II. The resulting curve for Case IV provides the best match with the measured resistance curve.

Table 7-2 Summary of PYCAP parameters for densely compacted fine gravel backfill

Parameter	Case I	Case II	Case III	Case IV
ϕ (°)	50.0	50.0	50.0	44.0
c (psf)	275	0	275	0
δ (°)	31	31	8	27
γ_m (pcf)	137.8	137.8	137.8	137.8
E (ksf)	670	670	670	670
ν	0.3	0.3	0.3	0.3
k (kip/in)	1110	1110	1110	1110
Δ_{max} (in)	2.44	2.44	2.44	2.44
Δ_{max}/H	0.037	0.037	0.037	0.037
R_f	0.30	0.48	0.76	0.75
R_{3D}	2.00	2.00	1.72	1.95
K_p	35.7	35.6	11.2	17.0

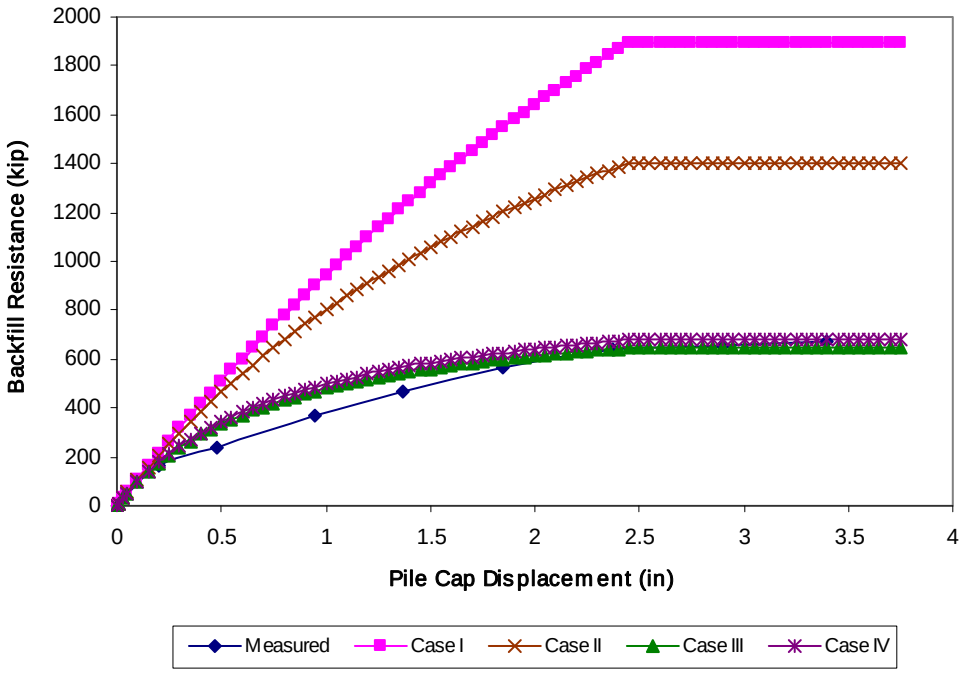

Figure 7-3 Comparison of measured and PYCAP-based calculated passive resistance for densely compacted fine gravel backfill

7.3.2 Calculated Response Using ABUTMENT (LSH)

Passive earth resistance was also calculated using the LSH method. Table 7-3 summarizes key inputs and outputs for several cases analyzed while Figure 7-4 shows the measured and calculated passive resistance curves for each case. Case I is based strictly on laboratory-determined ultimate values for shear strength and interface friction angle (which was similar for both peak and ultimate strength states, with a δ/ϕ ratio of about 0.61). The ε_{50} value was derived from laboratory testing and is within the range of values recommended in Shamsabadi et al. (2007). Similar to PYCAP, the calculated load-displacement curve from Case I parameters greatly overestimates the measured curve. The changes made in Cases II and III are the same changes made to the corresponding cases in the PYCAP analysis. If cohesion is included, the interface friction angle must be greatly reduced to obtain a good match. Case IV uses a friction angle based on an in-situ direct shear test staged using one sample over three normal pressures. In this case, the majority of apparent cohesion from that test has been neglected and an nominal amount of 84 psf (4.0 kPa) has been used. This value is the same as was used by Shamsabadi et al. (2007) in their analyses of the Cole and Rollins (2006) pile cap

test results with a similar backfill material. The resulting curve for Case IV provides a good match with the measured curve. While Case III provides the best match with the measured curve (the interface friction angle was iteratively adjusted to obtain such a match), the parameters represented by Case IV provide the most reasonable description of the measured load-displacement curve. In all cases, the calculated resistance in the middle portion of the load-displacement curves is significantly higher than the measured resistance.

Table 7-3 Summary of LSH parameters for densely compacted fine gravel backfill

Parameter	Case I	Case II	Case III	Case IV
ϕ (°)	50.0	50.0	50.0	44.0
c (psf)	275	0	275	84
δ (°)	31	31	8	27
γ_m (pcf)	137.8	137.8	137.8	137.8
ε_{50}	0.004	0.004	0.004	0.004
ν	0.3	0.3	0.3	0.3
R_f	0.98	0.98	0.98	0.98
R_{3D}	2.00	2.00	1.72	1.95
K_{ph}	36.3	25.0	17.7	16.0

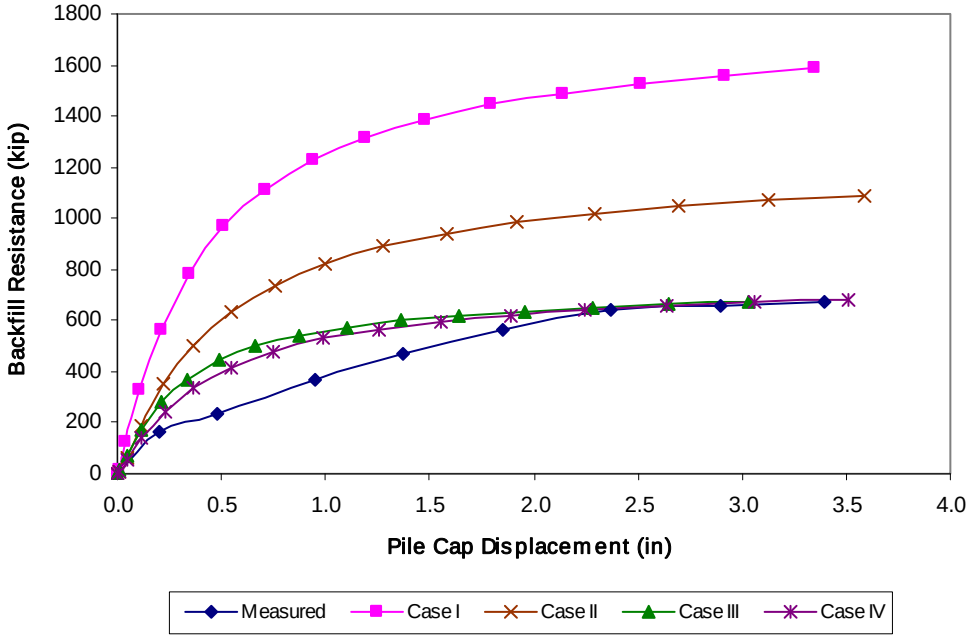

Figure 7-4 Comparison of measured and LSH-based calculated passive resistance for densely compacted fine gravel backfill

7.3.3 Calculated Response Using CALTRANS Method

Passive earth resistance based on the CALTRANS method is shown in Figure 7-5 In the case of densely compacted fine gravel, the method under-predicts peak passive resistance by approximately 50%.

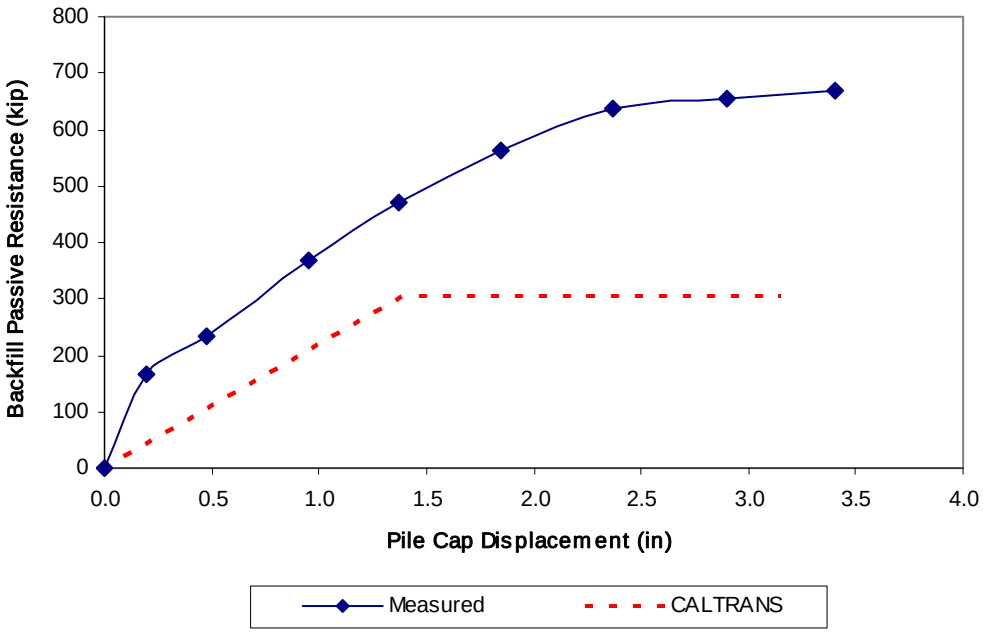

Figure 7-5 Comparison of measured and CALTRANS-based passive resistance for densely compacted fine gravel backfill

7.4 Response to Cyclic Actuator Loading

After slowly pushing the pile cap to each displacement interval, alternating combinations of small displacement cyclic actuator loads and dynamic shaker loads were applied. The response of the pile cap to the small displacement amplitude loading cycles from the actuator is presented and discussed in this section. Figure 7-6 shows the loop displacement amplitude, stiffness, loop area, and damping ratio for the pile cap with backfill in place as a function of pile cap displacement. Values are based on the median of the 15 low frequency cycles performed at each displacement level The displacement amplitude decreases fairly linearly from under 0.10 in (2.5 mm) to 0.05 in (1.25 mm). The stiffness increases from 1140 to 2860 kip/in (200 to 500 kN/mm) as the cap

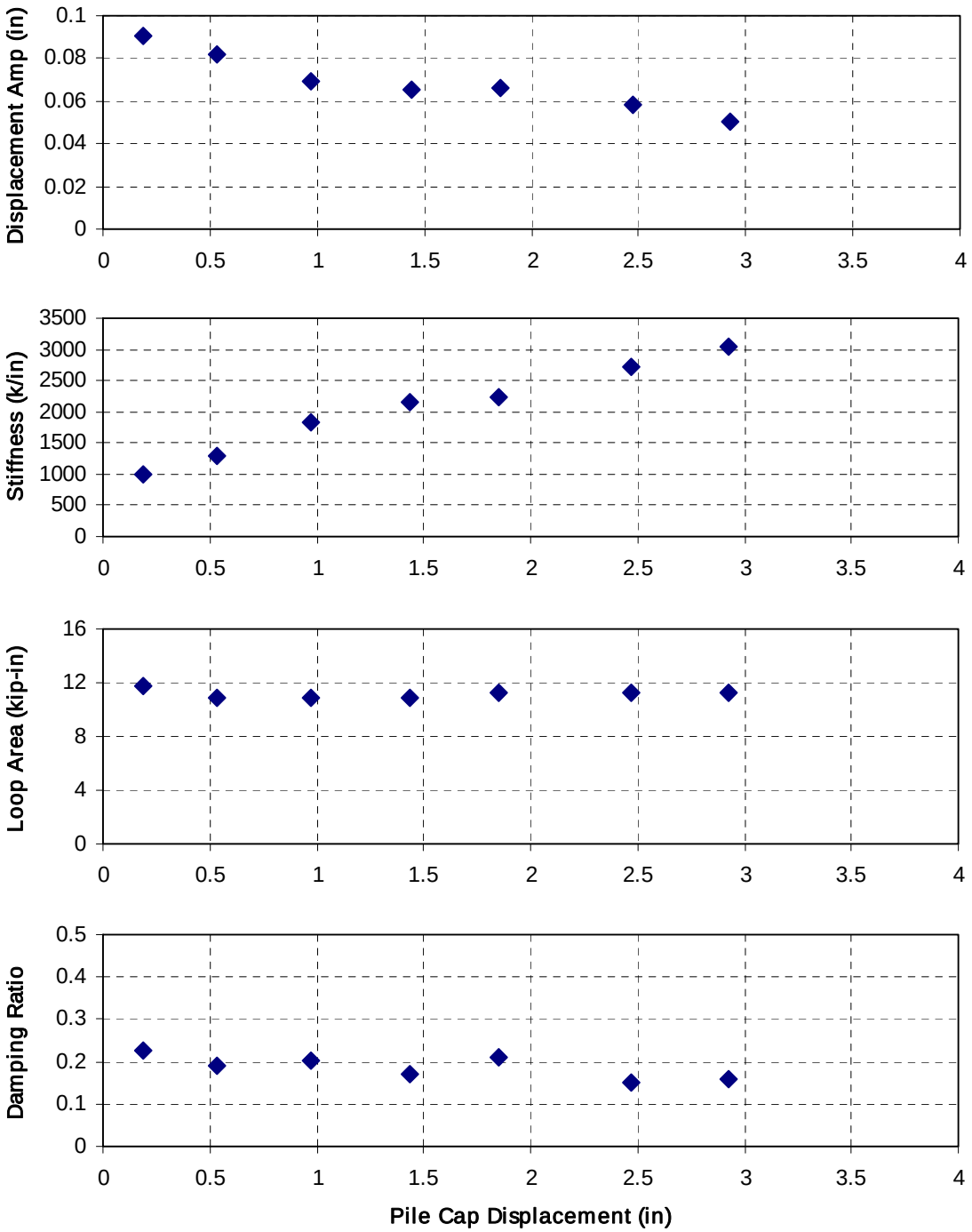

Figure 7-6 Summary of response to cyclic actuator loadings for pile cap with densely compacted fine gravel backfill

displacement increases; this appears to be due to greater mobilization of the backfill soil's passive strength and pile stiffness. Unlike the cyclic actuator loading results from densely

compacted clean sand backfill, the rate of stiffness increase for densely compacted fine gravel does not appear to level off in the last few displacement intervals when the ultimate passive resistance of the soil is assumed to be reached. The loop area remains fairly constant around 10.6 kip-in (1200 kN-mm). The damping ratio exhibits some of the saw-tooth behavior seen in other tests due to the alternating order of the static and dynamic cyclic loading phases, staying around 20% throughout testing until the last two static pushes, when it drops to about 15%.

7.5 Response to Dynamic Shaker Loading

After slowly pushing the pile cap to each displacement interval, alternating combinations of small displacement cyclic actuator loads and dynamic shaker loads were applied. The response of the pile cap to the dynamic shaker loading is presented and discussed in this section. The first row of graphs in Figure 7-7 shows loop displacement amplitude as well as loop displacement amplitude normalized by the cyclic amplitude of net applied force from the shaker and actuators as functions of the forcing frequency. The second and third rows of graphs show the calculated reloading stiffness and damping, respectively, of the pile cap system. In the left column, these parameters are shown in terms of forcing frequency. If non-linear behavior is present, these properties will also depend on the displacement amplitude; hence, in the right column, these parameters are shown on terms of the displacement amplitude. Based on the data, it appears that both frequency and displacement amplitude must be considered when interpreting test results. The individual line series shown in all of the graphs correspond to different static displacement levels of the pile cap in which dynamic shaker cycles were applied before the slowly applied actuator cycles.

The peaks in the normalized displacement amplitude graph correspond to the damped natural frequency, which ranges from about 7.5 to 8 Hz with increasing cap displacement. Dynamic stiffness ranges from slightly under 2280 to almost 5710 kip/in (400 to 1000 kN/mm) as a function of frequency, peaking about 2 Hz before the damped natural frequency and dropping afterward, then increasing again about 1 Hz after the damped natural frequency. The general trend in stiffness data shows an increase in stiffness with increasing pile cap displacement until a shaker frequency and loop displacement amplitudes of about 8.5 Hz and 0.02 in (0.5 mm), respectively, where the trend reverses.

Calculated damping values vary greatly with respect to the frequency of the forcing function and displacement amplitude. The minimum damping appears to be approximately 5% at about 5.5 Hz and 10 Hz (at least for the 0.5 in (13 mm) displacement interval), and at about 0.01 and 0.04 in (0.25 and 1 mm) of displacement amplitude. At frequencies between 5.5 and 10 Hz and displacement amplitudes between 0.01 and 0.04 in (0.25 and 1 mm), the damping ratio increases up to about 45% (corresponding with the calculated decreasing stiffness) until dropping again at about 8.5 Hz. Unfortunately, the normalized displacement amplitudes were such that the half-power bandwidth approach could not be used. As stated previously, the observed variations in stiffness and damping with frequency are likely due to variations in phase between passive earth forces (whether acting on the piles or on the pile cap itself) and the inertial force from the foundation as suggested by Tokimatsu et al. (2004) in their work

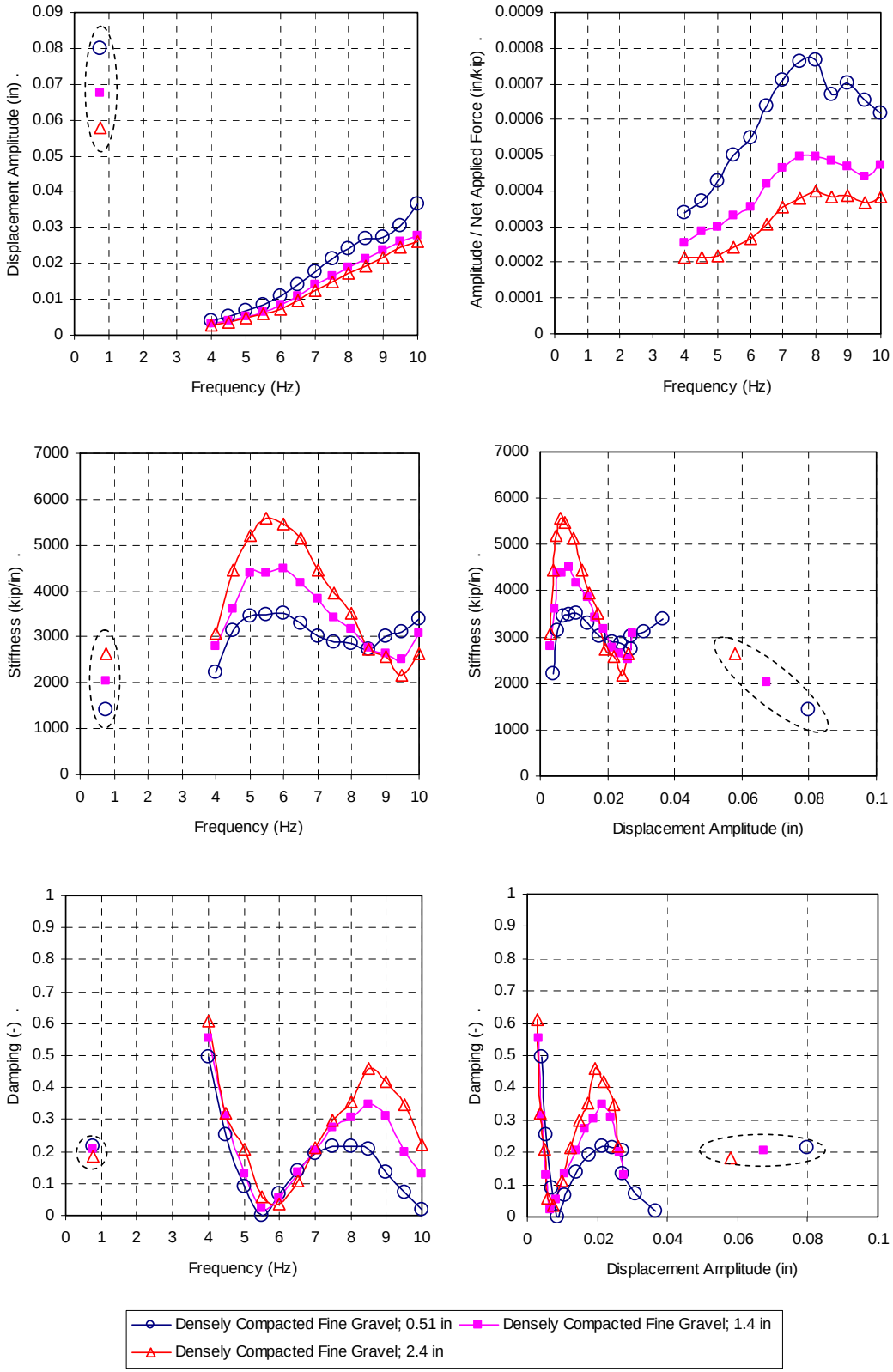

Figure 7-7 Summary of response to dynamic shaker loadings for pile cap with densely compacted fine gravel backfill

with large shaking table models of pile cap foundation systems. Some variation is also likely due to the simple lumped, constant, mass model used.

7.6 Comparison of Cyclic Actuator and Dynamic Shaker Responses

Included in Figure 7-7 are displacement amplitude, stiffness, and damping ratio calculated from the statically applied cycles from the actuators (~ ¾ Hz) at each represented displacement level (points in dashed ovals). The values presented are averages of the previous and subsequent actuator cycles. An average value is used to represent stiffness and damping that would have been calculated if the actuator cycles and been performed before the shaker cycles. In terms of frequency, it can be difficult to make a comparison between the static and dynamic methods because of the difference in the associated displacement amplitudes (the shaker cannot generate large forces, and hence displacements, at low frequencies).

The largest displacement amplitudes reached by the dynamic shaker loadings were typically 0.03 in (0.75 mm) or less. The average displacement amplitude reached by the cyclic actuator loadings was between 0.06 and 0.08 in (1.5 and 2 mm). This is a large enough disparity to make comparison between the two methods problematic, except at the highest dynamic loading frequencies. On average, the stiffness under dynamic loading conditions appears to be 30% higher than under cyclic loading conditions. The equivalent damping ratio under cyclic loading conditions (about 20%) is bracketed by the range of damping observed under dynamic loading conditions.

7.7 Passive Earth Pressure Distributions

In addition to the load-displacement response data, passive earth pressure from the backfill soil was measured directly with a vertical array of six earth pressure cells evenly distributed in the central portion of the pile cap face. Figure 7-8 shows the pressure measured by the pressure cells with depth at the end of each static push interval.

The pressure cells show general trends, as expected, of increasing pressure with depth and increasing magnitude with increasing cap displacement. It is apparent that the measured pressures at the pressure cells at 16.5 in and 49.5 in (0.42 m and 1.26 m) depart from the other pressure cells in the normal representation of pressure increasing with depth. These cells record an increase in pressure with increasing cap displacement but a decrease in pressure relative to the

cell immediately above them. In the last three static pushes, the pressure cell at 38.5 in (0.98 m) appears to manifest similar behavior, though not as pronounced, as the pressure cells at 16.5 in and 49.5 in (0.42 m and 1.26 m). Unfortunately an explanation for this behavior is not readily available, but may be due to variability of density with lift thickness during compaction. The bottom-most pressure cell appears to offer progressively smaller increases in pressure as the cap displacement increases, culminating in an apparently negligible increase in pressure during the last static push. The similarities in pressure from one push to the next at the largest displacement levels are consistent with the concept of the backfilling approaching its ultimate capacity.

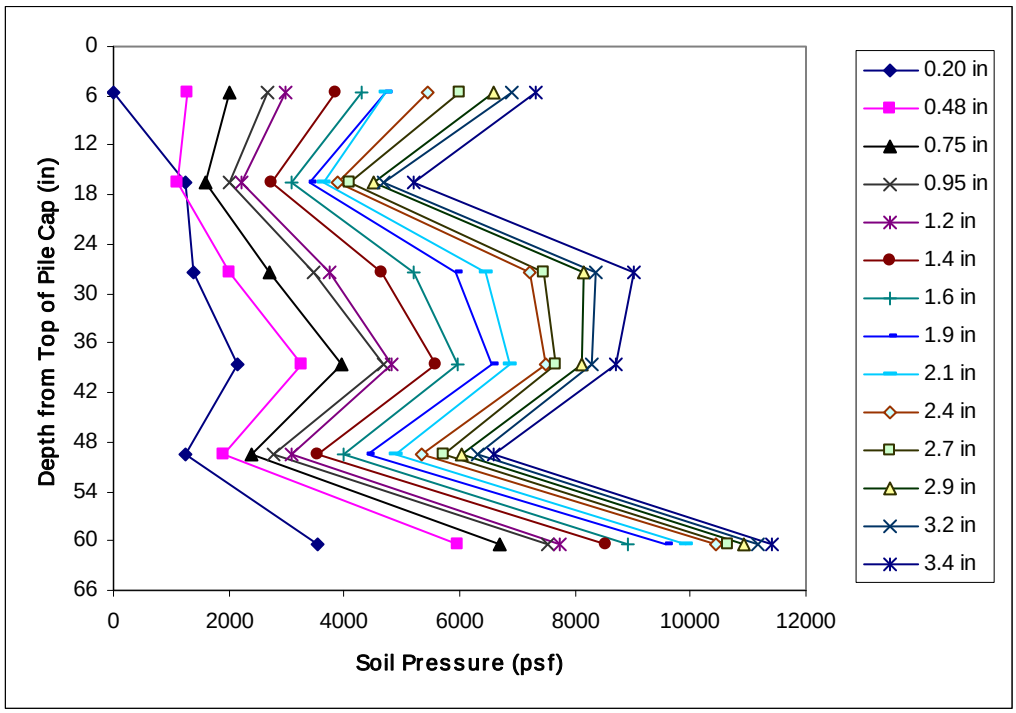

Figure 7-8 Earth pressure distribution as a function of pile cap displacement with densely compacted fine gravel backfill

Figure 7-9 shows the backfill force calculated by multiplying each measured pressure by the respective contributory areas of the pile cap face. In general, the resulting force-displacement curve has a similar trend to that based on the actuators, but it is systematically lower. Applying a multiplier of 1.67 (the inverse of 0.6 determined in Section 3.5) to the cell-based curve provides an improved match with the actuator-based curve, although the reaching of the ultimate passive resistance is not apparent.

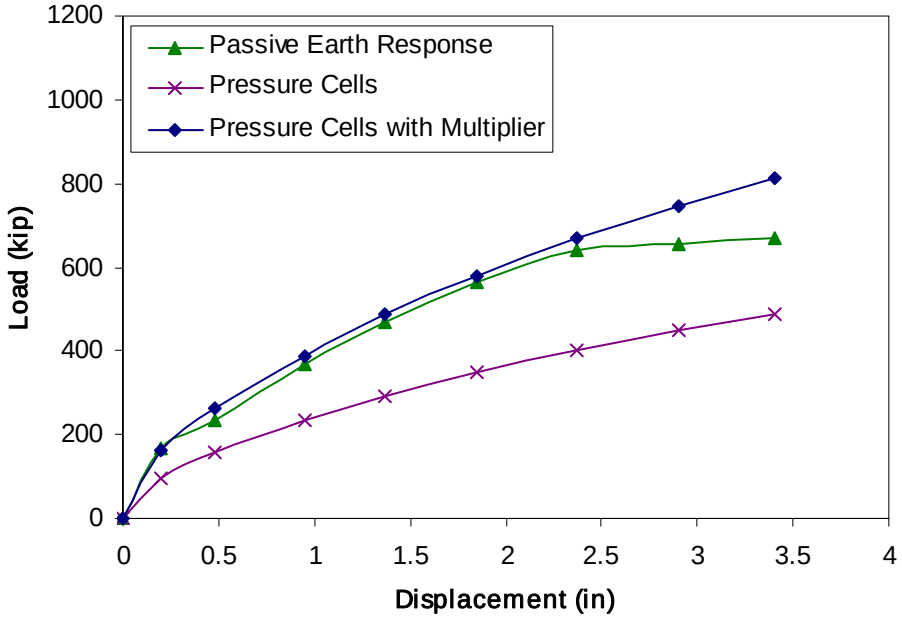

Figure 7-9 Comparison of earth forces based on actuators and pressure cells for densely compacted fine gravel backfill

7.8 Cracking and Vertical Movement of Backfill

Figure 7-10 is a two part plot showing the results of static and dynamic testing on the surface of the densely compacted fine gravel backfill area. The first part of the figure shows the surface cracks that developed during each static push of the pile cap. The surface cracks in the backfill indicate the presence of failure surfaces within the soil.

The fine gravel material has some apparent cohesion (manifest by the stability of the backfill face when excavated), which helps provide a reasonably clear indication of cracking. A significant portion of the cracks are concentrated around the edges of the cap face. These cracks are due to the internal shear stresses radiating out from the cap face and reflect the three dimensional shape of the failure zone. A horizontal group of cracks located 3 to 4 m from the center of the pile cap face may indicate the where early failure surfaces have developed and begun to daylight. The erratic cracks extending from the face of the cap out to about 3 m may be associated with near surface spalling and/or horizontal shoving rather than larger-scale shear failure.

The second part of the figure is a contour map of the change in elevation of the surface of the backfill area during testing. The typical elevation change, as represented by the median elevation change in a given row (parallel to the face of the cap) of grid nodes, is about 1.2 in (30 mm) at 6 ft (1.83 m) from the pile cap face. The contour map shows that at 10 ft (3.05 m) the maximum elevation change at one individual survey node is over 2.25 in (57 mm). Calculations indicate that a log-spiral failure surface should daylight at approximately 20 ft (6.1 m) from the face of the cap. The figure shows that most of the elevation change occurred within the first 20 ft (6 m) of backfill; thus, it is reasonable to expect that the failure surface daylights just beyond that zone.

The correlation between the backfill heave and the log-spiral failure surface is better illustrated by the cross-sectional view in Figure 7-11, where the failure surface calculated in the spreadsheet program PYCAP daylights close to where the heave profile becomes negligible. The log-spiral failure surface shown in the figure was computed using the best-fit parameters discussed in Section 7.3.1: a soil friction angle of 44° with a nominal cohesion of 84 psf (4 kPa) and an interface friction angle of 27°, corresponding to a δ/□ ratio of 0.6 as determined from laboratory direct shear testing (i.e., Case IV). The heave profile in the figure is magnified ten times to make the elevation change more appreciable.

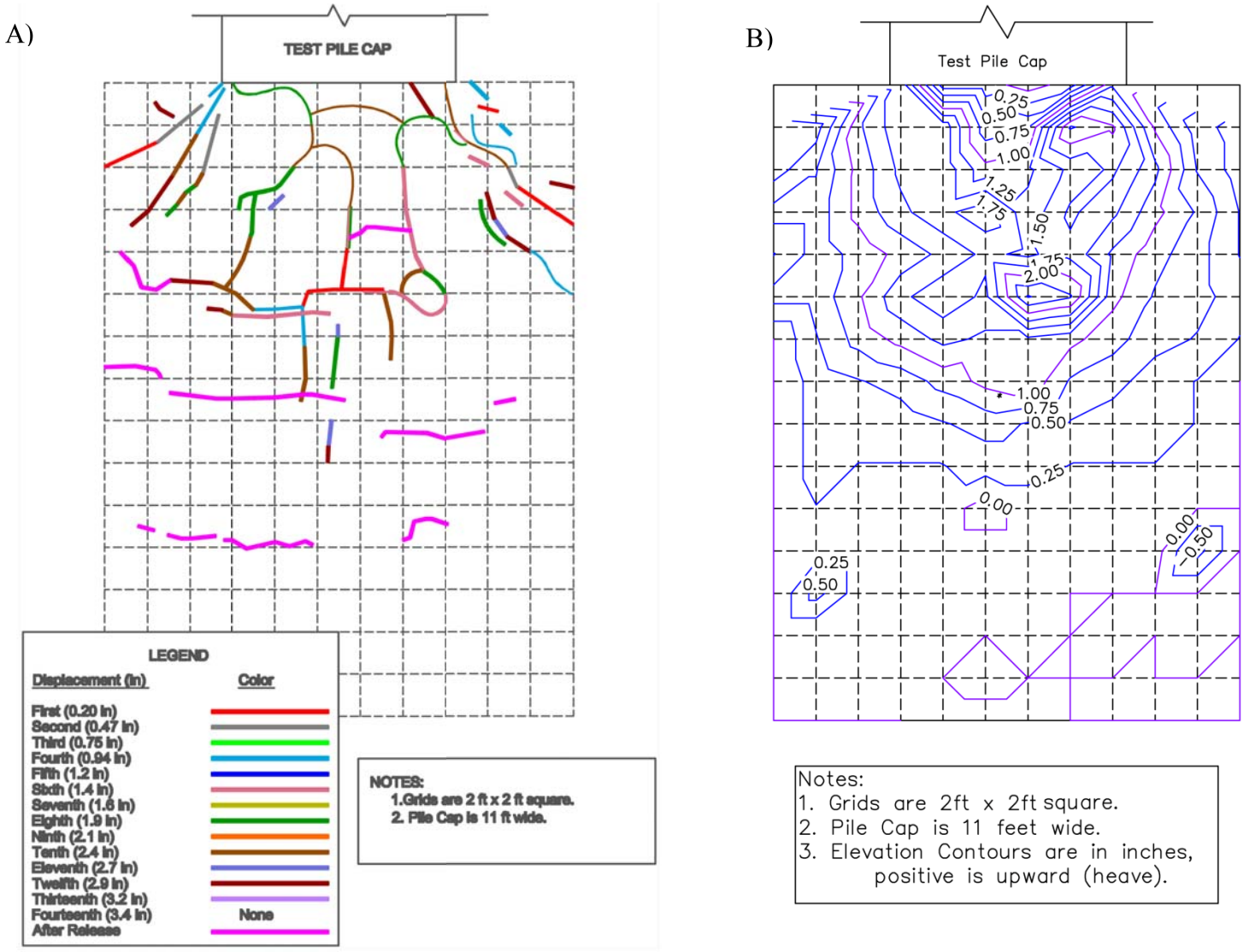

Figure 7-10 Crack pattern (A) and heave contour (B) maps for densely compacted fine gravel backfill

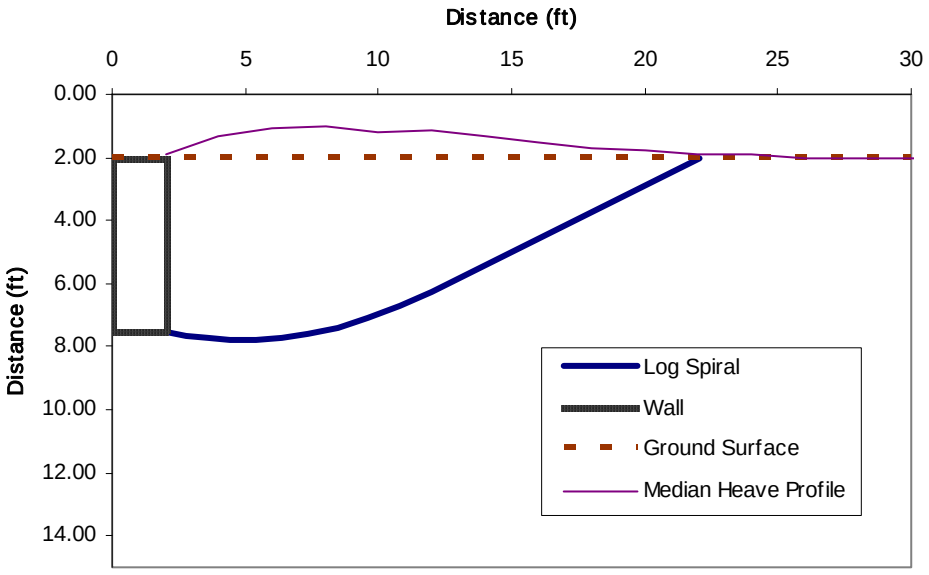

Figure 7-11 Heave profile fore densely compacted fine gravel backfill with log spiral failure surface from PYCAP (Case IV parameters)

7.9 Horizontal Movement of Backfill

String potentiometers were used to measure movement in the backfill. Figure 7-12 shows the movement of each of the monitoring points in the densely compacted fine gravel backfill compared to the movement of the pile cap face. The backfill displacement ranges from 3.43 in (87 mm) (100% of cap displacement) at the cap face to 0.35 in (9 mm) (11% of cap displacement) at 18 ft (5.5 m) from the cap face. This translational movement represents the amount of the pile cap displacement not absorbed through compressive strain up to the monitoring point.

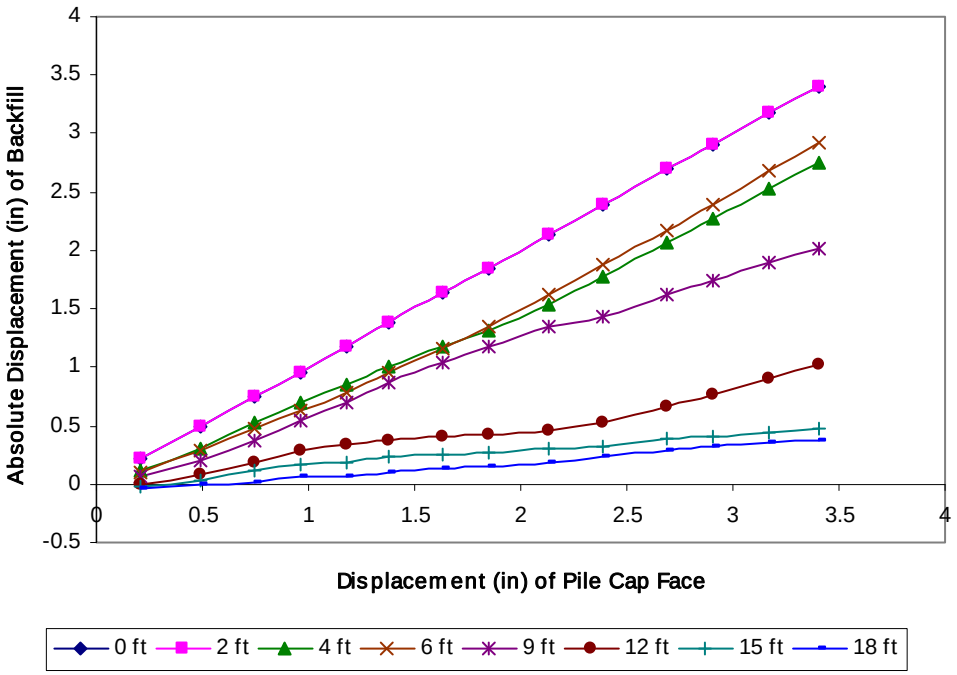

Figure 7-12 Displacement of monitoring points in densely compacted fine gravel backfill

Figure 7-13 shows the compressive strain corresponding to each static push of the pile cap. The compressive strain ranges from 0.028 to 0.003 within the backfill zone. The strain distribution is high at the cap face, as expected, but highest at about 10 ft from the cap face. This high strain level located in the middle of the backfill area may be associated with the development of progressive slip planes as soil friction is mobilized, but the exact mechanism is unclear. A simple explanation for the erratic strain behavior in the figure is not readily available; however, some of the variation from interval to interval may indicate the potential sensitivity of the string potentiometer measurements to differential pushing of the pile cap (not all the monitoring stakes were on the same end of the cap face) and tipping of the monitoring stakes themselves. Movement of the stakes could explain the presence of some negative strain amounts in the calculations. However, it does appear that stresses are transmitted some significant distance throughout this well compacted backfill.

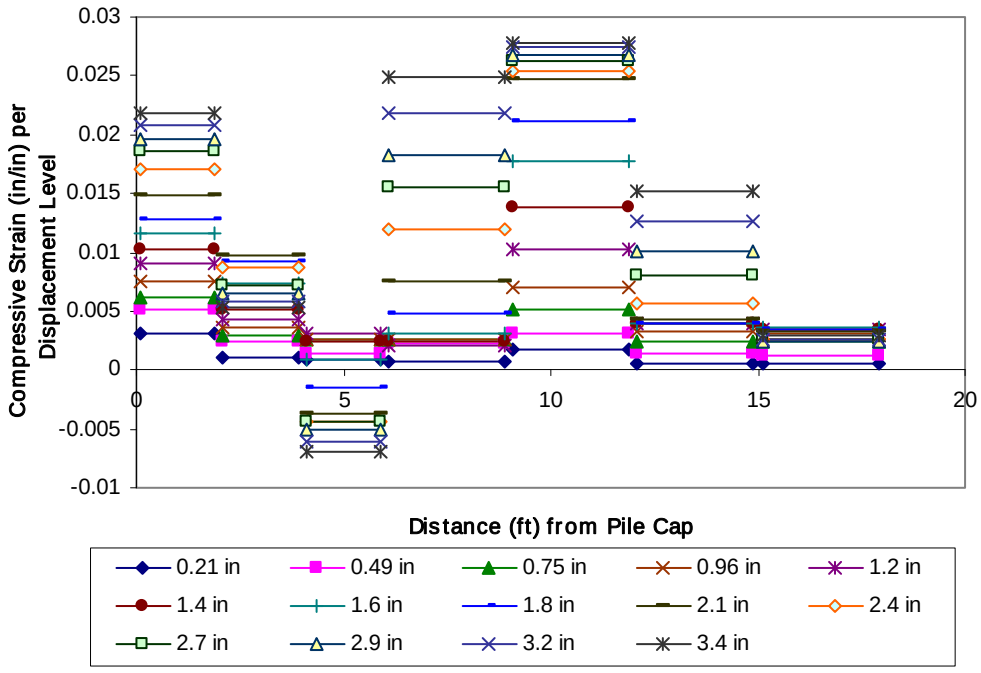

Figure 7-13 Strain per displacement level for densely compacted fine gravel backfill

8.0 PILE CAP WITH LOOSELY COMPACTED FINE GRAVEL BACKFILL

8.1 General

The pile cap with loosely compacted fine gravel backfill was tested on June 6, 2007. No significant deviations from the general test procedure occurred during this test. Table 8-1 summarizes the test in terms of loads and displacements measured at the end of each "static push" with the actuators. The table also indicates the order in which cyclic loads from the actuators and dynamic loads from the shaker were applied. At some displacement increments, no cyclic or dynamic loadings were applied in order to help assure that sufficient displacement had occurred for the load path to return to the static-backbone loading curve.

Table 8-1 Summary of test with loosely compacted fine gravel backfill

Displacement Interval	Displacement (in)	Actuator Load (kN)	Actuator Cycles	Shaker Cycles
1	0.25	119	First	Second
2	0.67	123	Second	First
3	0.94	143	First	Second
4	1.2	164	None	None
5	1.4	224	Second	First
6	1.7	253	None	None
7	1.9	328	First	Second
8	2.2	359	None	None
9	2.4	433	Second	First
10	2.7	464	None	None
11	3.0	537	First	Second

8.2 Load-Displacement Response

Figure 8-1 shows the entire actuator load verses pile cap displacement relationship for the test, with static pushes, actuator cycles, and shaker cycles being represented by green, blue, and red data points, respectively. Section 3.2 provides some discussion relative to the details of interpreting this data. As was observed with the loosely compacted clean sand, the loosely

compacted fine gravel test exhibits a loss of essentially all resistance after the cyclic and dynamic loadings accompanying the first couple of displacement intervals.

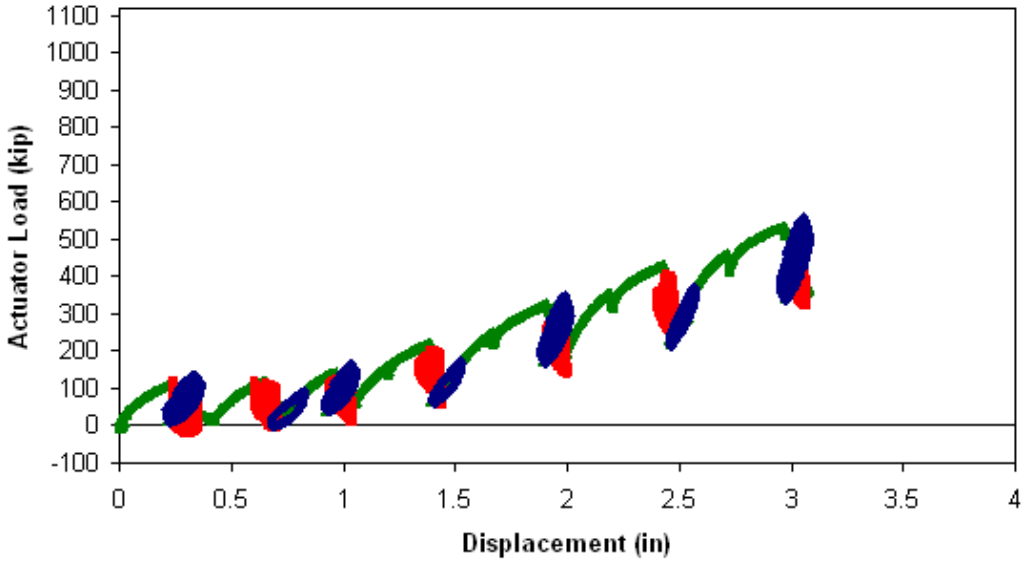

Figure 8-1 Actuator load versus pile cap displacement with loosely compacted fine gravel backfill (Test 7; June 6, 2007)

Figure 8-2 shows three load-displacement response curves for the pile cap: one for the response with backfill in place (referred to as the total response, which is the equivalent monotonic response or backbone curve derived from the data shown in Figure 8-1), one for the response with no backfill present (referred to as the baseline response), and one showing the passive earth response of the backfill (obtained by subtracting the baseline response from the total response. This figure shows that after the initial push, the loosely compacted fine gravel backfill provides an additional resistance which is slightly less than the resistance initially provided by the piles and cap acting by themselves. The test does not appear to develop a peak resistance by the conclusion of testing. This may agree with the Clough and Duncan (1991) statement that a loose or medium dense material will require two to four times more displacement to mobilize that a dense material. The final passive earth resistance, approximately 184 kip (820 kN), was recorded at the end of the last "static push" of the loosely compacted fine gravel test. The resistance may have continued to increase somewhat had greater displacement levels had been able to be realized. In the figure, it can be seen that a significant amount of resistance seems to have developed by 0.24 in (6 mm) of displacement, after which the resistance

due to passive earth pressure appears to drop and then later recovers. This behavior is surprising and may be due to the effects of cyclic and dynamic loadings, or possibly even a small error in the baseline response which effects are magnified since the passive resistance of the backfill is also relatively small.

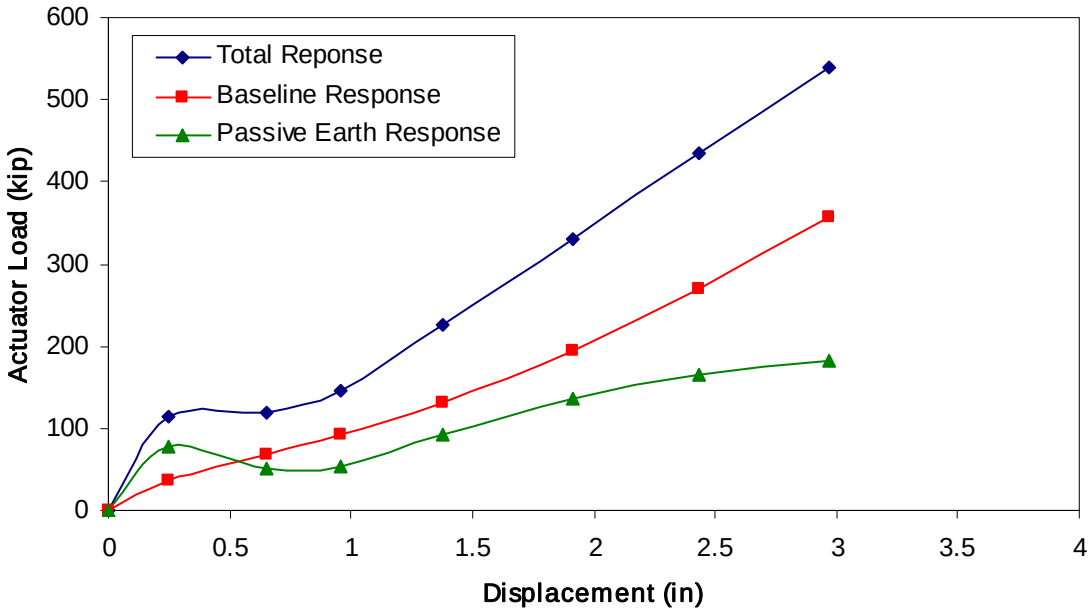

Figure 8-2 Total, baseline and passive earth responses for the pile cap with loosely compacted fine gravel backfill

8.3 Calculated Passive Earth Force

Commonly used methods for calculating passive earth pressure include Rankine theory, Coulomb theory, and log-spiral theory. Log-spiral theory is typically considered the most accurate of these methods (see, for example, Cole and Rollins (2006) and Duncan and Mokwa (2001)). Three methods of estimating the development of passive pressure with wall displacement are evaluated in this section. Two of these methods, PYCAP and ABUTMENT (LSH method) involve applications of log-spiral theory and a hyperbolic load-displacement relationship. The third approach evaluated in this section is an empirical load-displacement relationship based on full-scale testing of an abutment with typical backfill conditions (see discussion of CALTRANS method in Section 3.3.3)

8.3.1 Calculated Response Using PYCAP

Passive earth resistance was calculated using the modified PYCAP spreadsheet. Table 8-2 summarizes key inputs and outputs for several cases analyzed while Figure 8-3 shows the measured passive resistance curve alongside the calculated passive resistance curves for each case. Case I uses laboratory-determined ultimate values for shear strength parameters, and results in a predicted passive resistance nearly six times greater than the measured resistance. The initial modulus value used in Case I is consistent with the preloaded or compacted range for a loose sand or gravel given by Duncan and Mokwa (2001). The modulus value is also consistent with the normally loaded range for a medium to dense soil. In Case II, the cohesion intercept was ignored and the interface friction angle was reduced to better match the measured passive resistance. With the interface friction angle at a nominal value of 2°, Case II results in a predicted resistance that matches the measured resistance to within 5%. With so little interface friction, the solution is essentially a Rankine passive earth pressure solution using the laboratory determined soil friction angle. (In the figure, the curves for Cases II, IV, and V all essentially plot on top of one another). Case III employs in-situ direct shear test results for the shear strength parameters and a δ/ϕ ratio of 0.6 (which is equivalent to the ratio found in interface friction angle testing with densely compacted fine gravel). Case III results in a resistance estimate over 200% greater than the measured response. In Case IV, the cohesion intercept is neglected and the interface friction angle has been iteratively reduced to provide a match to the measured resistance. Like Case II, Case IV estimates the passive resistance to within 5% of the measured passive resistance curve. Using the

Table 8-2 Summary of PYCAP parameters for loosely compacted fine gravel backfill

Parameter	Case I	Case II	Case III	Case IV	Case V
ϕ (°)	44.9	44.9	43	43	31
c (psf)	566	0.0	100	0.0	0.0
δ (°)	27	2	26	4	31
γ_m (pcf)	122.6	122.6	122.6	122.6	122.6
E (ksf)	490	490	490	490	490
ν	0.3	0.3	0.3	0.3	0.3
k (kip/in)	811	811	811	811	753
Δ_{max} (in)	4.88	4.88	4.88	4.88	4.88
Δ_{max} /H	0.074	0.074	0.074	0.074	0.074

R_f	0.64	0.95	0.90	0.95	0.95
R_{3D}	2.00	1.49	1.88	1.48	1.54
K_p	18.8	6.3	15.1	6.2	6.4

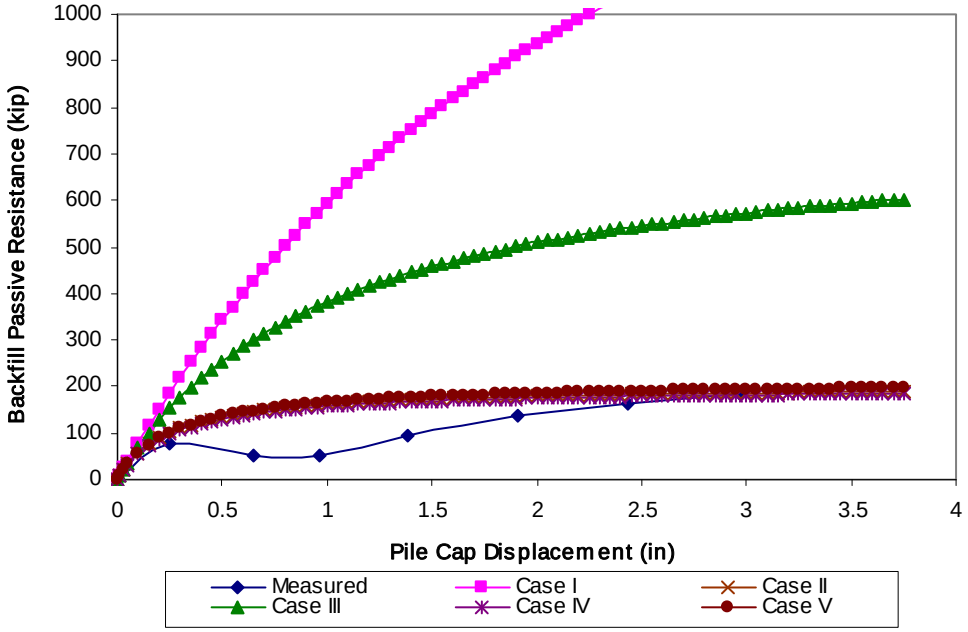

Figure 8-3 Comparison of measured and PYCAP-based calculated passive resistance for loosely compacted fine gravel backfill

Rankine method (omitting the nominal 4 degrees of interface friction) with the field test-derived soil friction angle of 43° yields an ultimate passive force of about 160 kips, which is within 15% of the measured ultimate resistance. However, a similarly close match is also obtained in Case V by reducing the peak soil friction found in the staged in-situ direct shear test, 43°, to 65% of its original value (i.e., taking the inverse tangent of 65% of the tangent of 43°) which results in a friction angle of 31 degrees. This approach is similar to the one-third reduction approach suggested by Terzaghi and Peck (1967) when evaluating bearing capacity in loose granular soils and the anticipated failure mode is local or punching shear.

8.3.2 Calculated Response Using ABUTMENT (LSH)

Passive earth resistance was also calculated using the LSH method. Table 8-3 summarizes key inputs and outputs for several cases analyzed while Figure 8-4 shows the measured passive resistance curve along with the calculated passive resistance curves for each case. In Case I, laboratory direct shear test results are used to determine ultimate strength parameters, producing a poor match with the measured earth pressure curve. In Case II, cohesion is neglected and the interface friction angle has been iteratively reduced to better match the measured resistance; this reduced interface friction angle is the same as that used in Case II of the PYCAP-based analyses. Case III employs in situ direct shear results for soil friction angle and cohesion and a δ/ϕ ratio of 0.6, as in the PYCAP analysis. Using these parameters, the Case III theoretical curve over-estimates the maximum passive resistance by about 190%, similar to the result obtained using PYCAP. The interface friction angle in Case IV was iteratively reduced to provide a match between the predicted resistance and the measured response. Both Case II and Case IV

Table 8-3 Summary of LSH parameters for loosely compacted fine gravel backfill

Parameter	Case I	Case II	Case III	Case IV
ϕ (°)	44.9	44.9	43	43
c (psf)	566	0	100	0
δ (°)	27	2	26	4
γ_m (pcf)	122.6	122.6	122.6	122.6
ε_{50}	0.005	0.005	0.005	0.005
ν	0.3	0.3	0.3	0.3
R_f	0.98	0.98	0.98	0.98
R_{3D}	2.00	1.49	1.88	1.48
K_{ph}	33.6	6.5	15.1	6.5

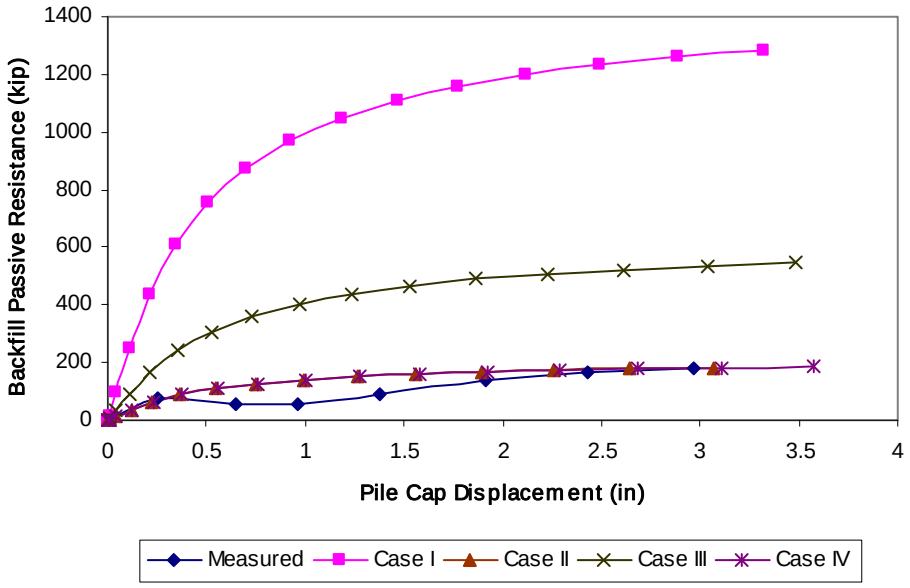

Figure 8-4 Comparison of measured and LSH-based calculated resistance for loosely compacted fine gravel backfill

provide matches within 5% of the measured resistance curve at the maximum displacement interval. It appears, in the case of the loosely compacted fine gravel that the computed prediction of passive resistance significantly overestimates the actual value unless a lower friction angle is used or the interface friction is drastically reduced, or even eliminated. Case IV appears to provide the best estimate of passive resistance for loosely compacted fine gravel backfill.

8.3.3 Calculated Response Using CALTRANS Method

Passive earth resistance based on the CALTRANS method is shown in Figure 8-5. In this case, the method over-predicts peak passive resistance by approximately 67%.

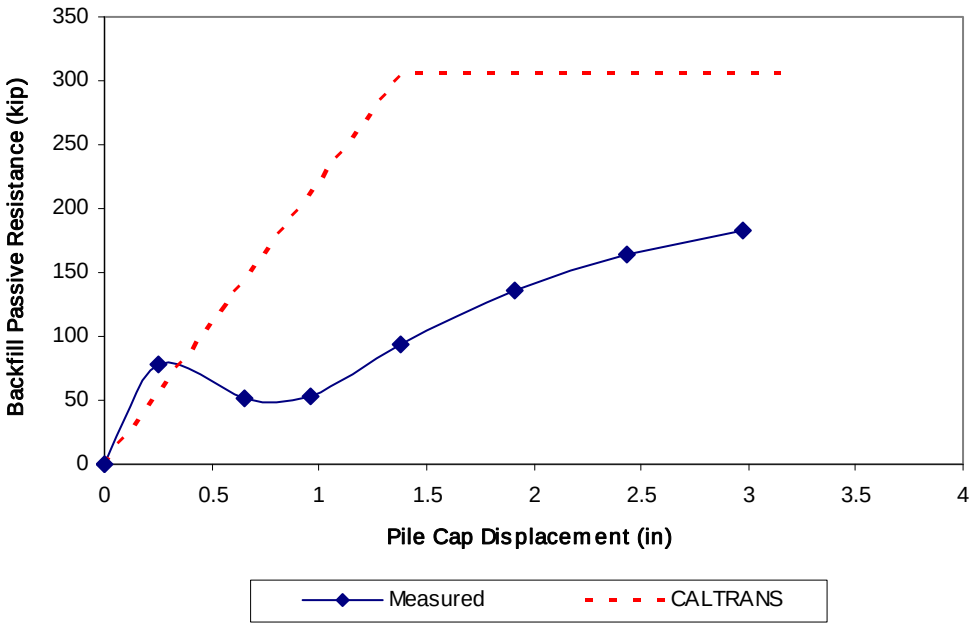

Figure 8-5 Comparison of measured and CALTRANS-based passive resistance for loosely compacted fine gravel backfill

8.4 Response to Cyclic Actuator Loading

After slowly pushing the pile cap to each displacement interval, alternating combinations of small displacement cyclic actuator loads and dynamic shaker loads were applied. The response of the pile cap to the small displacement amplitude loading cycles from the actuator is presented and discussed in this section. Figure 8-6 shows the loop displacement amplitude, stiffness, loop area, and damping ratio for the pile cap with loosely compacted fine gravel backfill in place as a function of pile cap displacement. Values are based on the median of the 15 low frequency cycles performed at each displacement level The displacement amplitude decreases slightly from about 0.07 in (1.75 mm) to just under 0.06 in (1.5 mm), with a median displacement amplitude of about 0.06 in (1.6 mm). The stiffness increases from 570 to almost 1710 kip/in (100 to 300 kN/mm) as the cap displacement increases; this appears to be due to greater mobilization of the backfill soil's passive strength and pile stiffness. The stiffness and displacement amplitude data exhibit the saw-tooth shaped trend as seen in other tests due to the alternating order of the static and dynamic cycling loading phases. The damping ratio also exhibits some oscillatory behavior with increasing cap displacement, decreasing in a somewhat linear fashion from a peak of 31% to 19% with a median value of approximately 24%. The

stiffness and damping values are more similar to those calculated without backfill present than those calculated with the densely compacted backfill present.

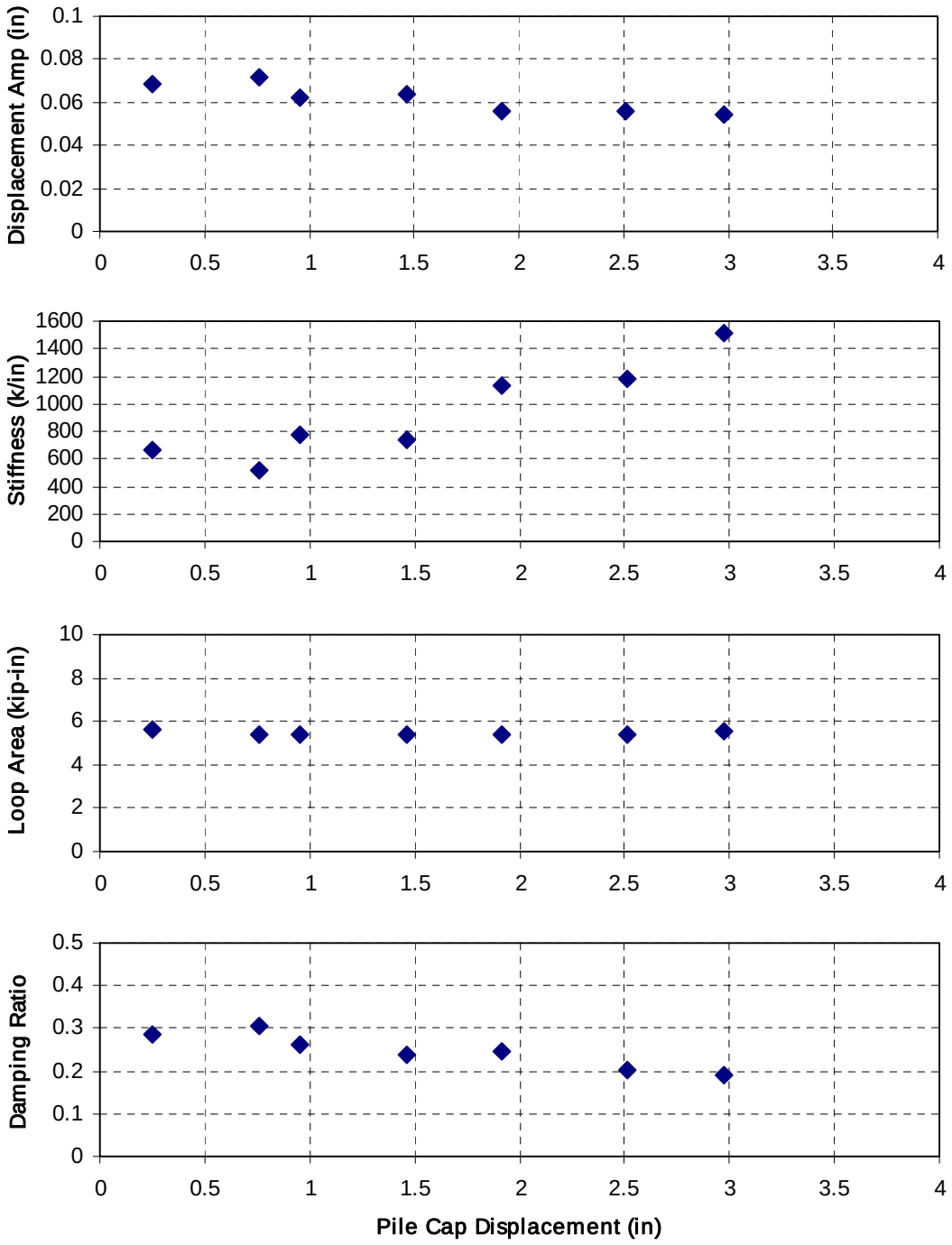

Figure 8-6 Summary of response to cyclic actuator loadings for pile cap with loosely compacted fine gravel backfill

8.5 Response to Dynamic Shaker Loading

After slowly pushing the pile cap to each displacement interval, alternating combinations of small displacement cyclic actuator loads and dynamic shaker loads were applied. The response of the pile cap to the dynamic shaker loading is presented and discussed in this section. The first row of graphs in Figure 8-7 shows loop displacement amplitude as well as loop displacement amplitude normalized by the cyclic amplitude of net applied force from the shaker and actuators as functions of the forcing frequency. The second and third rows of graphs show the calculated reloading stiffness and damping, respectively, of the pile cap system. In the left column, these parameters are shown in terms of forcing frequency. If non-linear behavior is present, these properties will also depend on the displacement amplitude; hence, in the right column, these parameters are shown on terms of the displacement amplitude. Based on the data, it appears that both frequency and displacement amplitude must be considered when interpreting test results. The individual line series shown in all of the graphs correspond to different static displacement levels of the pile cap in which dynamic shaker cycles were applied before the slowly applied actuator cycles.

The peaks in the normalized displacement amplitude graph correspond to the damped natural frequency, which ranges from 6.5 to 7 Hz with increasing cap displacement. The dynamic reloading stiffness ranges from about 1140 to about 2000 kip/in (200 to 350 kN/mm) in the range of frequencies tested. In terms of displacement amplitude, the stiffness stays close to 1140 kip/in (200 kN/mm) until approximately 0.05 in (1.25 mm) of displacement amplitude when the stiffness increases sharply. Calculated damping values vary greatly with respect to the frequency of the forcing function and displacement amplitude. The minimum damping appears to be approximately 5% at 5.5 Hz and 0.02 in (0.4 mm) of displacement amplitude. At higher frequencies, the damping ratio increases up to about 35% (corresponding with the calculated decreasing stiffness) until dropping again at 7.5 to 8 Hz. Interpreting the normalized displacement amplitudes using the half-power bandwidth approach yields damping ratios of 25, 23, and 24% for the three pile cap displacement levels shown in Figure 8-7. Generally speaking, the stiffness and damping ratio increase with increasing pile cap displacement; however, at about 9 Hz, or about 0.04 in (1 mm) of loop displacement amplitude, this trend reverses. As stated previously, the observed variations in stiffness and damping with frequency are likely due to variations in phase between passive earth forces (whether acting on the piles or on the pile cap

itself) and the inertial force from the foundation as suggested by Tokimatsu et al. (2004) in their work with large shaking table models of pile cap foundation systems. Some variation is also likely due to the simple lumped, constant, mass model used.

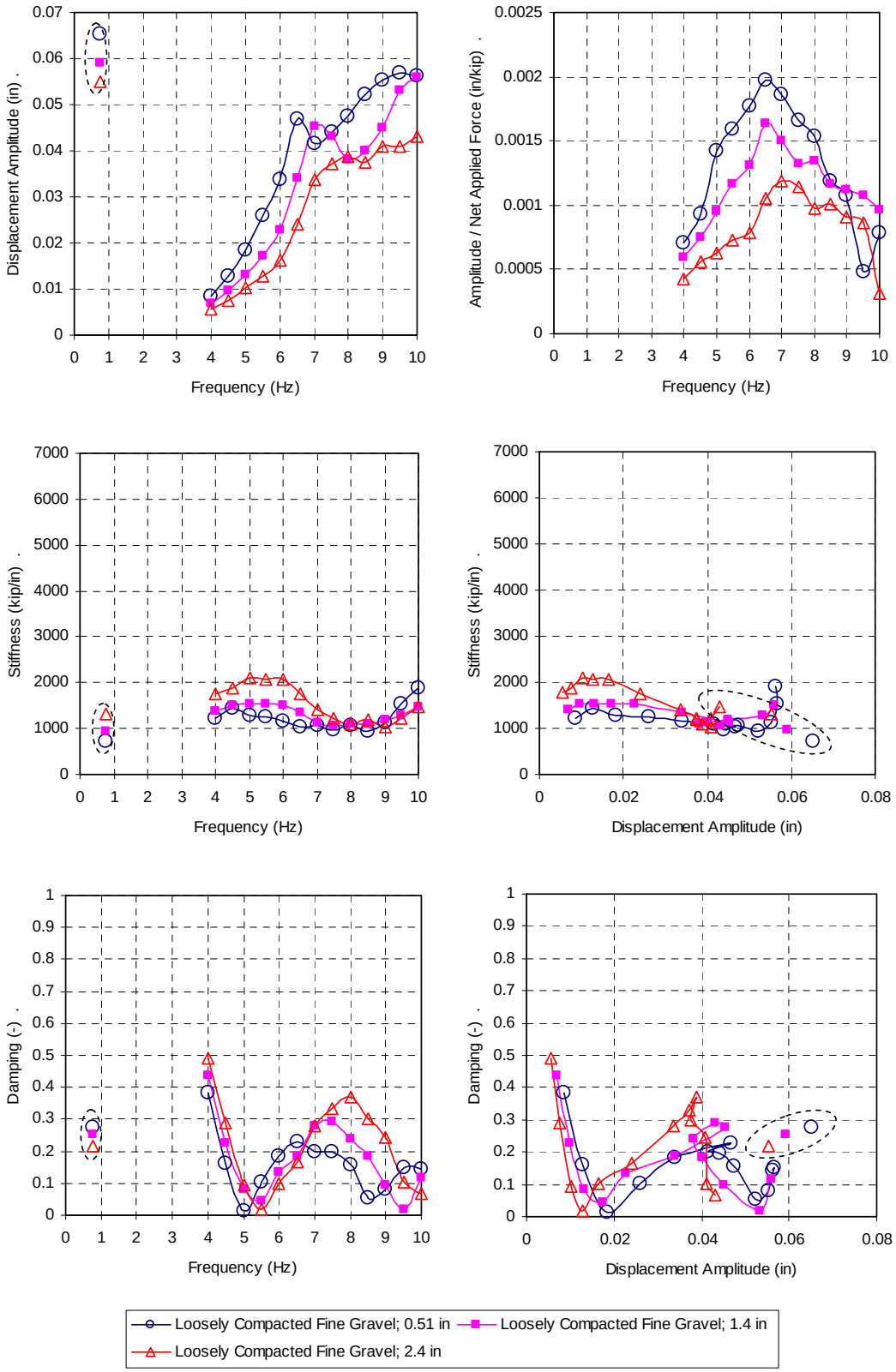

Figure 8-7 Summary of response to dynamic shaker loadings for pile cap with loosely compacted fine gravel backfill

8.6 Comparison of Cyclic Actuator and Dynamic Shaker Responses

Included in Figure 8-7 are displacement amplitude, stiffness, and damping ratio calculated from the statically applied cycles from the actuators (~ ¾ Hz) at each represented displacement level (points in dashed ovals). The values presented are averages of the previous and subsequent actuator cycles. An average value is used to represent the stiffness and damping that would have been calculated if the actuator cycles and been performed before the shaker cycles. In terms of frequency it can be difficult to make a comparison between the static and dynamic methods because of the difference in the associated displacement amplitudes (the shaker cannot generate large forces, and hence displacements, at low frequencies).

The dynamic shaker loadings at 10 Hz resulted in maximum displacement amplitudes of about 0.06 in (1.4 mm) for the first two pile cap displacement levels shown, and 0.04 in (1.1 mm) for the last pile cap displacement level shown. These values are relatively similar to those realized using the actuators. For the second and third displacement levels, the actuator-based stiffnesses are in the same range as the shaker-based stiffness, albeit at the lower bounds, near 1140 kip/in (200 kN/mm). The actuator-based damping ratio (ranging from about 20 to 30%) compares well with the 23 to 25% damping ratio determined using the half-power band width approach and is bracketed by the range calculated directly from the shaker-based load-displacement loops. This similar amount of stiffness and damping for different ranges of frequency suggests that dynamic loadings do not significantly increase the apparent resistance of the pile cap relative to slowly applied cyclic loadings.

8.7 Passive Earth Pressure Distributions

In addition to the load-displacement response data, passive earth pressure from the backfill soil was measured directly with a vertical array of six earth pressure cells evenly distributed in the central portion of the pile cap face. Figure 8-8 shows the pressure measured by the pressure cells with depth at the end of each static push interval.

The profiles suggest the reactive pressure from the backfill is concentrated at a depth near 39 in (1 m). It is apparent that the measured pressure distribution does not match the normal representation of pressure increasing with depth. However, this may be in part a result of the soil mass being far from a well defined, ultimate failure state. From the first push on, the bottom two

pressure cells show a decrease in pressure with increasing displacement, much like what was observed in the case of the densely compacted sand backfill. The topmost pressure cell shows little increase in pressure from the first push to the last, indicating that ultimate resistance near the top develops sooner than at deeper depths. While the trend in the lower most pressure cell is consistent with that observed in other tests (as also discussed in Section 3.5), the pressure cell above it also shows a similar trend by initially registering pressure, then decreasing to zero pressure after the second displacement level. Unfortunately an explanation for this behavior is not readily available. The pressure profiles for the last few displacement intervals are similar, which may suggest that the ultimate resistance for the soil adjacent to the cap has been reached.

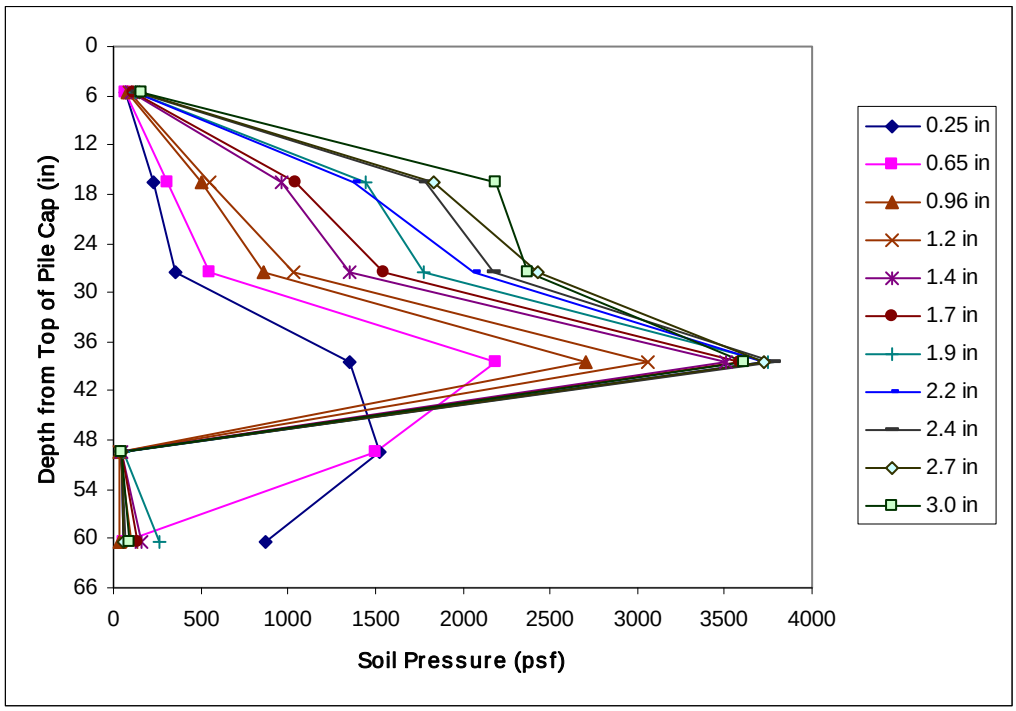

Figure 8-8 Earth pressure distribution as a function of pile cap displacement with loosely compacted fine gravel

Figure 8-9 shows the backfill force calculated by multiplying each measured pressure by the respective contributory areas of the pile cap face. In general, the resulting force-displacement curve has a similar trend to that based on the actuators, but it is systematically lower, except at the unexpected drop near 0.63 in (16 mm) after the second loading interval. Applying a multiplier of 1.67 (the inverse of 0.6 determined in Section 3.5), to the cell-based

curve provides an improved match with the actuator-based curve, although the reaching of the ultimate passive resistance appears to be more well defined and occurring at less displacement.

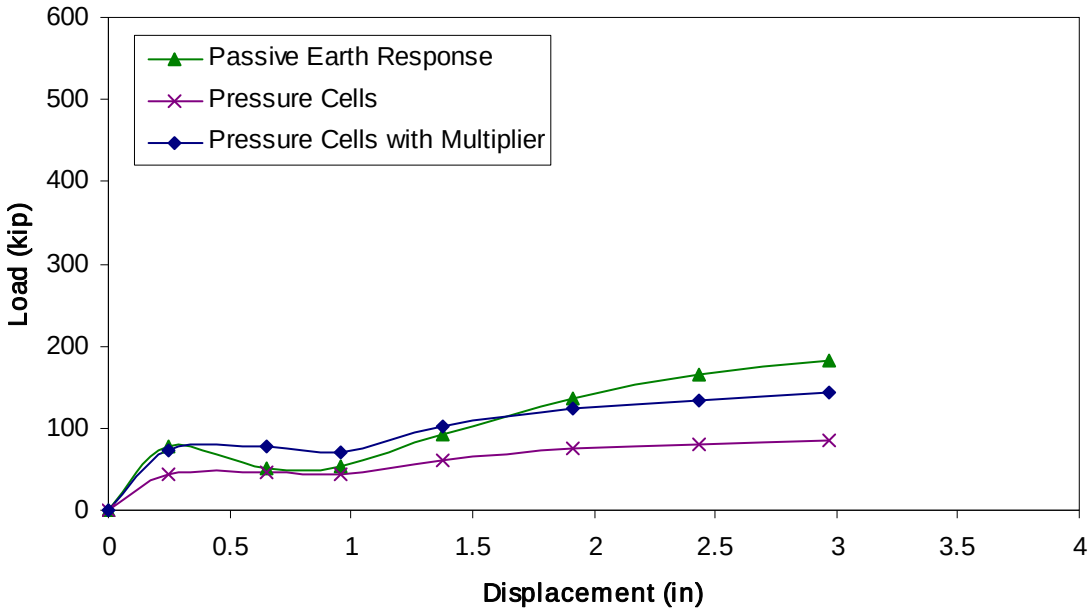

Figure 8-9 Comparison of earth forces based on actuators and pressure cells for loosely compacted fine gravel backfill

8.8 Cracking and Vertical Movement of Backfill

Figure 8-10 is a two part plot showing the results of static and dynamic testing on the surface of the loosely compacted fine gravel backfill area. The first part of the figure shows the surface cracks that developed during each static push of the pile cap. The surface cracks in the backfill indicate the presence of failure surfaces within the soil. Although the fine gravel material contains more fine material than the clean sand, low cohesion levels in the material, along with the dynamic vibration due to the eccentric mass shaker, tended to cause the soil grains to shift during testing, potentially obscuring cracks. As the figure shows, a large number of cracks formed during the first push and cycling phases with subsequent displacement intervals producing fewer cracks. Unlike the loosely compacted clean sand test, cracks from later pushes into the loosely compacted fine gravel backfill occurred largely within the 6.6 ft (2 m) closest to the cap. No radial cracking is readily evident in the loosely compacted fine gravel crack map to support the stress bulb-like failure mechanism visible in the loosely compacted clean sand

backfill. The orientation and distribution of the cracks seem to suggest a punching shear failure mechanism in the loosely compacted fine gravel backfill material.

The second part of the figure is a contour map of the change in elevation of the surface of the backfill area during testing. The typical elevation change, as represented by the median elevation change in a given row (parallel to the face of the cap) of grid nodes, is about 0.12 in (3 mm) of both heave and settlement. As much as 0.84 in (21 mm) of settlement occurred directly adjacent to the pile cap face, though some of this decrease in elevation may be due to loss of material near the boundaries of the backfill zone. Most of the heave occurred away from the pile cap face, with the settlement occurring within about 13 ft (4 m) from the pile cap face.

The correlation between the failure surface and the settlement characteristics of the backfill is better illustrated in Figure 8-11, where the median vertical displacement profile is given alongside a log-spiral failure surface. The log-spiral failure surface shown below was computed in PYCAP using the best-fit parameters discussed in section 8.3.1: a soil friction angle of 43° with no cohesion and a nominal interface friction angle of 4° (i.e., Case IV). Due to the very low interface friction angle used to compute the log-spiral solution, the failure surface appears more as a Rankine failure wedge than a log-spiral failure surface. This appears to be consistent with the backfill settlement at the pile cap face and the relative lack of heave in the backfill area.

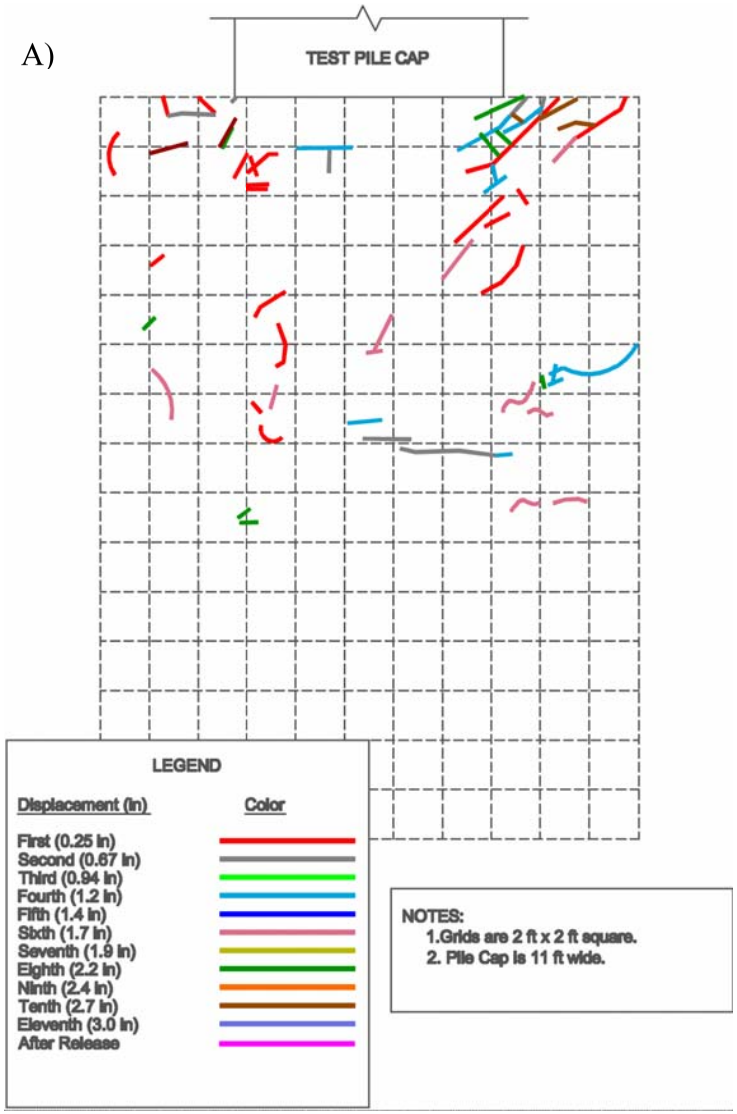

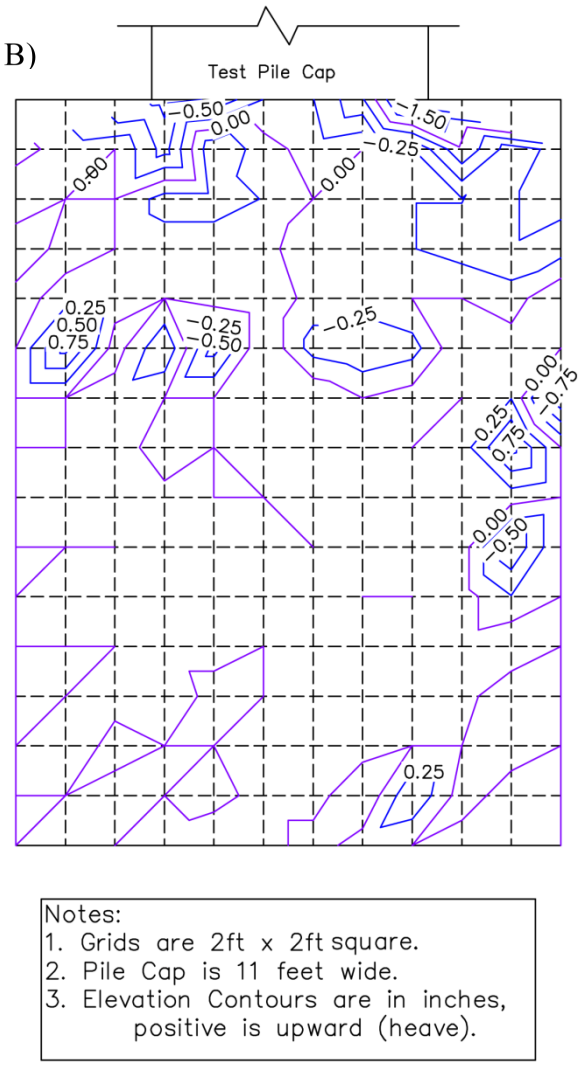

Figure 8-10 Crack pattern (A) and heave contour (B) maps for loosely compacted fine gravel backfill

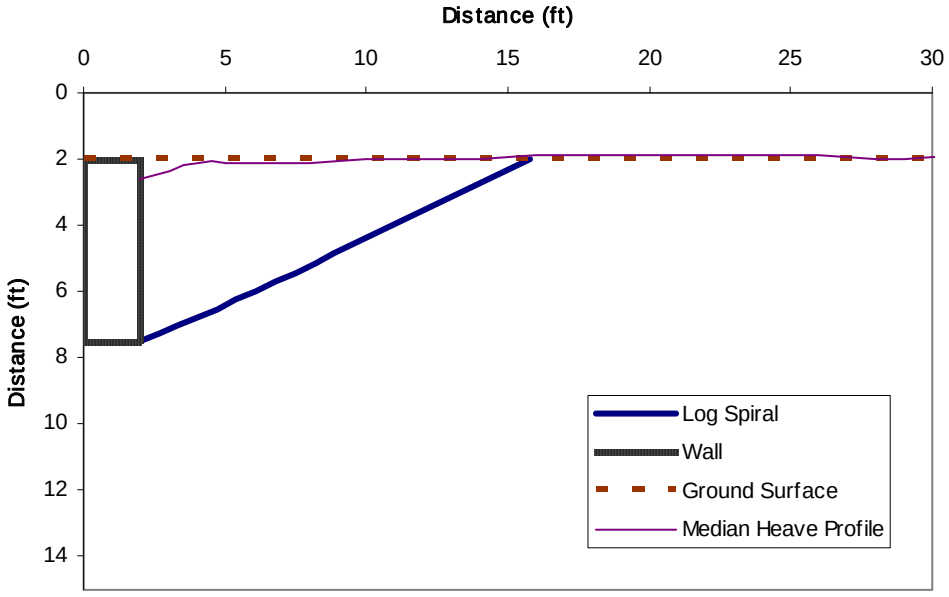

Figure 8-11 Heave profile for loosely compacted fine gravel backfill with log spiral failure surface from PYCAP (Case IV)

8.9 Horizontal Movement of Backfill

Backfill movement was measured using string potentiometers. Figure 8-12 shows the movement of each of the monitoring points in the densely compacted clean sand backfill compared to the movement of the pile cap face. The monitoring point 4 ft (1.2 m) away from the pile cap face appears to move more than the point 2 ft (0.6 m) from the face of the pile cap. This is in part due to the settlement of the backfill immediately in front of the pile cap, which may have caused the first monitoring point to move toward the pile cap while the second monitoring point experienced no such negative movement. A considerable amount of negative displacement was recorded by the string potentiometers, particularly for the monitoring points at 12 ft (3.7 m) and 18 ft (5.5 m) from the pile cap face. A negative displacement in regards to the figure below means that the monitoring point moves toward the pile cap while the pile cap moves toward the monitoring point. Background noise (spikes due to small electrical shorts) and other difficulties plague the raw data and are impossible to eliminate altogether. Despite the error that these elements may have introduced into the figure below, it is possible that small negative movements may have actually occurred. The contour map of the backfill after testing shows that the backfill

experienced a fair amount of settlement. The monitoring points were located within the zone of settlement and may have experienced negative movement by shifting along with the backfill as it settled.

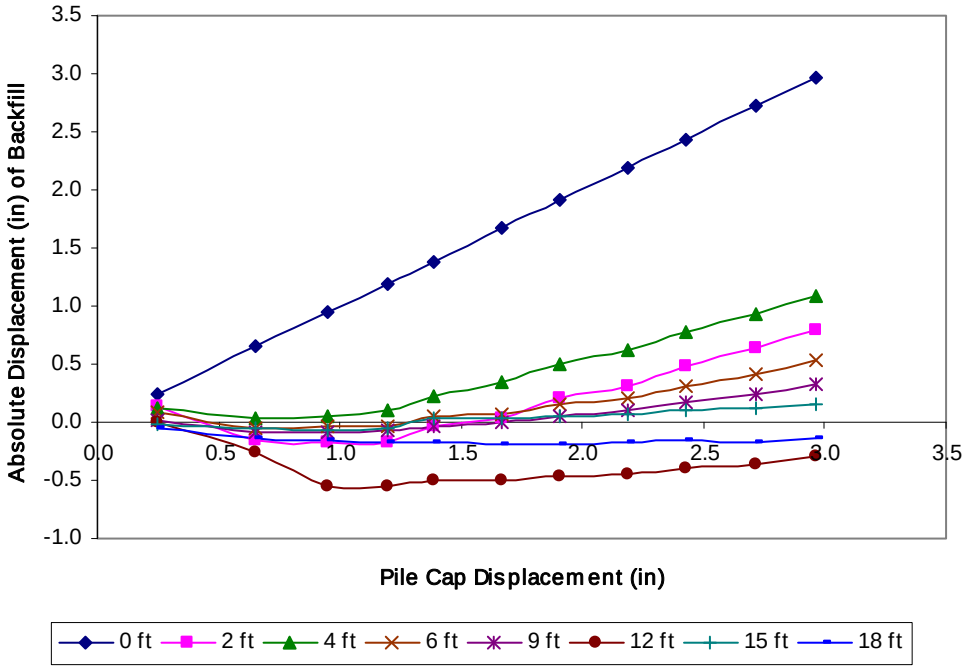

Figure 8-12 Displacement of monitoring points in loosely compacted fine gravel backfill

After the first three pushes of the pile cap, there is a general positive trend to the backfill displacement. The relatively small change in the point farthest from the pile cap face suggests that most of the displacement of the cap has been absorbed in the backfill area up to that point. It may also suggest that the initial negative displacement recorded at this displacement may be due to an unknown source of error.

Figure 8-13 shows the compressive strain corresponding to each static push of the pile cap. The compressive strain ranges from about 0.09 to 0.005 within the backfill zone. The 2 ft (0.6 m) interval closest to the cap experiences by far the most compressive strain, in this case about three times the strain in any other interval. In the loosely compacted fine gravel backfill, the compressive strain appears to decrease both rapidly and incrementally the farther from the pile cap face the strain interval is. Minor variation from interval to interval may indicate the potential sensitivity of the string potentiometer measurements to differential pushing of the pile cap (not all the monitoring stakes were on the same end of the cap face) and tipping of the

monitoring stakes themselves. Movement of the stakes could explain the presence of some negative strain amounts in the calculations, but on the whole, the strain appears to decrease logarithmically with distance away from the cap.

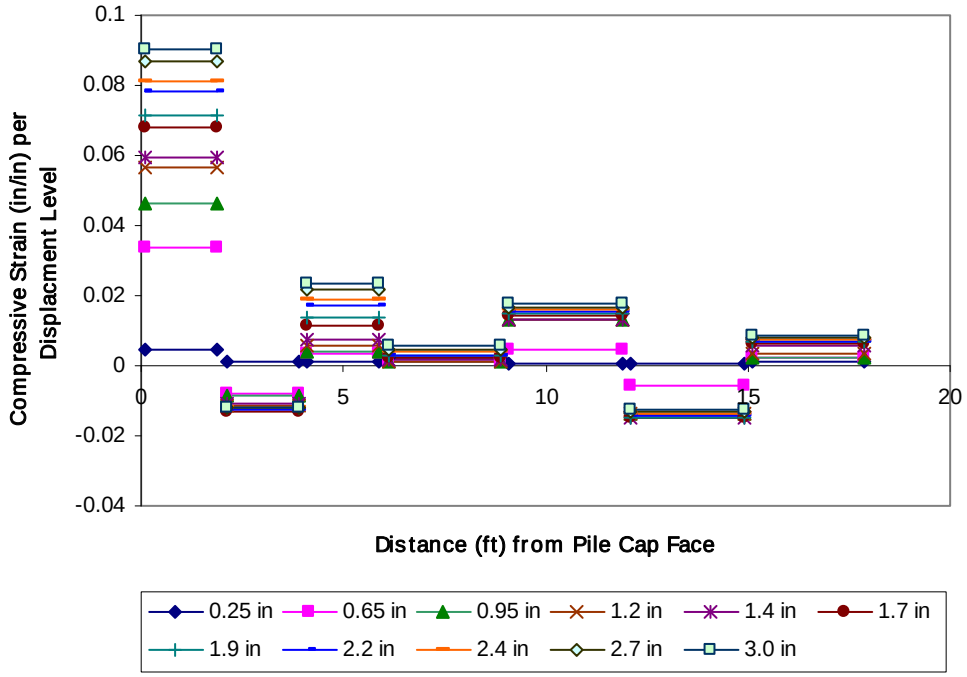

Figure 8-13 Strain per displacement level for loosely compacted fine gravel backfill

9.0 PILE CAP WITH DENSELY COMPACTED COARSE GRAVEL BACKFILL

9.1 General

The pile cap with densely compacted coarse gravel backfill was tested on June 26, 2007. Table 9-1 summarizes the test in terms of loads and displacements measured at the end of each "static push" with the actuators. The table also indicates the order in which cyclic loads from the actuators and dynamic loads from the shaker were applied. At some displacement increments, no cyclic or dynamic loadings were applied in order to help assure that sufficient displacement had occurred for the load path to return to the static-backbone loading curve. Some deviation from the general test procedure occurred during this test, being that the maximum shaker frequency for displacement interval 4 onward was limited to 9 Hz and that no shaker loadings were applied during the last displacement interval because the shaker was experiencing a progressive breakdown. The resistance of the pile cap with the densely compacted coarse gravel was near the capacity of both the actuators and the reaction foundation system.

9.2 Load-Displacement Response

Figure 9-1 shows the entire actuator load verses pile cap displacement relationship for the test, with static pushes, actuator cycles and shaker cycles being represented by green, blue, and red data points, respectively. Section 3.2 provides some discussion relative to the details of interpreting this data.

Table 9-1 Summary of test with densely compacted coarse gravel backfill

Displacement Interval	Displacement (in)	Actuator Load (kip)	Actuator Cycles	Shaker Cycles
1	0.20	198	First	Second
2	0.43	294	Second	First
3	0.67	407	First	Second
4	0.91	508	Second	First
5	1.2	601	None	None
6	1.4	704	First	Second
7	1.7	767	None	None
8	1.9	868	Second	First
9	2.2	925	None	None
10	2.4	1007	First	Second
11	2.7	1050	None	None
12	3.0	1107	First	None

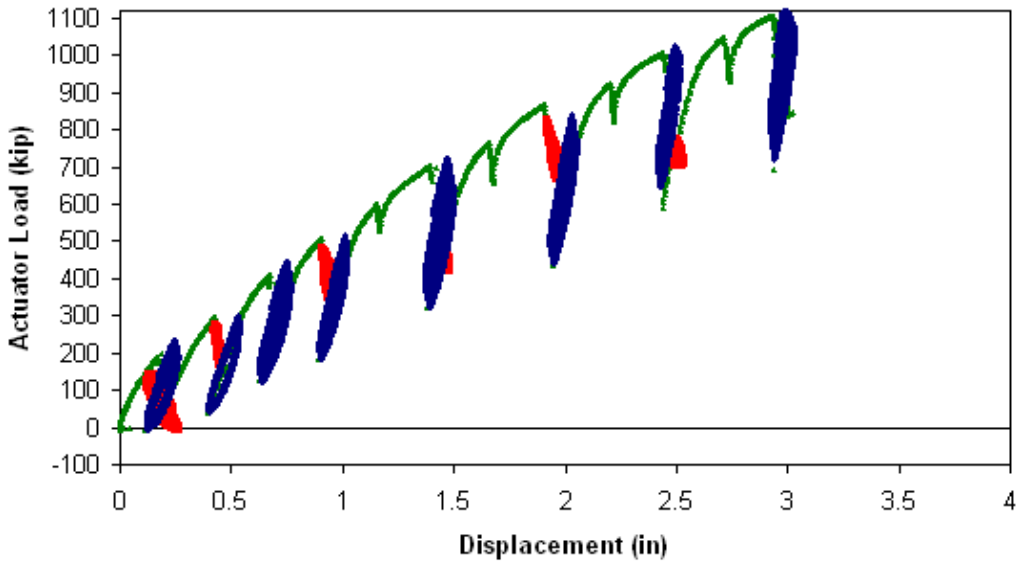

Figure 9-1 Actuator load versus pile cap displacement with densely compacted coarse gravel backfill (Test 12; June 26, 2007)

Figure 9-2 shows three load-displacement response curves for the pile cap: one for the response with backfill in place (referred to as the total response, which is the equivalent monotonic response or backbone curve derived from the data shown in Figure 9-1), one for the response with no backfill present (referred to as the baseline response), and one showing the

passive earth response of the backfill (obtained by subtracting the baseline response from the total response).

The curves show that total response and baseline response appear to increase at different rates until approximately 2.9 in (74 mm) of displacement (essentially the maximum displacement level for the test). By this point, the backfill response appears to level off as the baseline and total response appear to increase at approximately the same rate. Unfortunately, limits on equipment load capacity prevented us from displacing the pile cap to higher levels, and thus better confirm the obtaining of the ultimate resistance. Based on the data available, the ultimate passive resistance of the backfill appears to be about 760 kip (3380 kN) and is developed at a displacement of approximately 2.9 in (74 mm), which corresponds to a wall height ratio (Δ_{max}/H) of about 0.044.

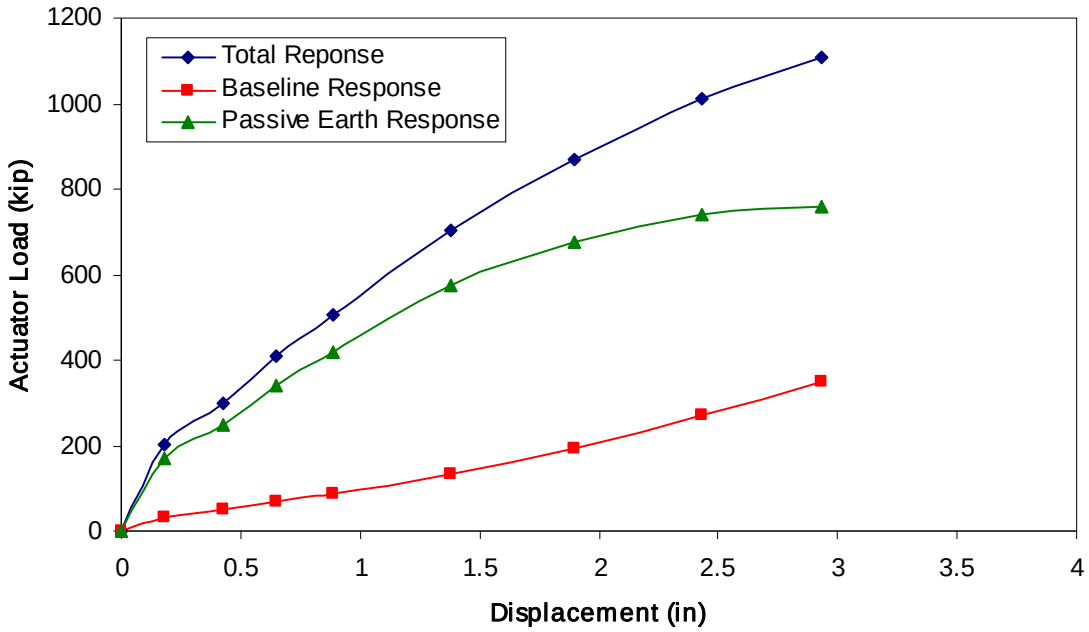

Figure 9-2 Total, baseline, and passive earth responses for pile cap with densely compacted coarse gravel backfill

9.3 Calculated Passive Earth Force

Commonly used methods for calculating passive earth pressure include Rankine theory, Coulomb theory, and log-spiral theory. Log-spiral theory is typically considered the most accurate of these methods (see, for example, Cole and Rollins (2006) and Duncan and Mokwa

(2001)). Three methods of estimating the development of passive pressure with wall displacement are evaluated in this section. Two of these methods, PYCAP and ABUTMENT (LSH method) involve applications of log-spiral theory and a hyperbolic load-displacement relationship. The third approach evaluated in this section is an empirical load-displacement relationship based on full-scale testing of an abutment with typical backfill conditions (see discussion of CALTRANS method in Section 3.3.3)

9.3.1 Calculated Response Using PYCAP

Passive earth resistance was calculated using the modified PYCAP spreadsheet. Table 9-2 summarizes key inputs and outputs for several cases analyzed while Figure 9-3 shows the measured passive resistance curve alongside the calculated passive resistance curves for each case. Case I uses a soil friction angle obtained from a correlation proposed by Duncan (2004) (as mentioned in Section 2.4.3) and a δ/φ ratio of 0.6. The initial modulus was estimated which correspond to the preloaded or compacted range presented by Duncan and Mokwa (2001). The calculated load-displacement response using Case I overestimates the measured resistance by about 200%. In Case II, the interface friction angle was iteratively reduced to obtain a good match between the calculated and measured curves. In-situ direct shear test results were used for the soil friction angle and cohesion intercept in Case III and the interface friction angle is based on a δ/ϕ ratio of 0.6 found by interface direct shear testing in the laboratory for the densely compacted fine gravel. The larger particles prevented a similar test with the coarse gravel. Case III underestimates the ultimate passive resistance by about 4%. Case IV also employs in-situ direct shear parameters, but the δ/ϕ ratio is changed to 0.75, a commonly assumed value. Case IV overestimates the ultimate passive resistance by about 16%. In Case V the interface friction angle is iteratively changed within the range used in Cases III and IV in order to match the recorded data. Case V was tailored to provide the best match between the computed and measured passive responses and will therefore be referred to as the "best fit" case. However, Case III provides an excellent match with minimal manipulation of the field-derived parameters. The Case III parameters could reasonably be used to predict the capacity of this particular soil type for design purposes.

Cole and Rollins (2006) and Rollins and Sparks (2002) also used P-154 coarse gravel materials in their tests. Their in-situ direct shear tests found friction angles of 40 and 42° with

cohesion intercepts of 150 psf and 0 psf, respectively. The gravel used in Cole and Rollins (2006) and Rollins and Sparks (2002) had unit weights of 147 and 150 pcf and required wall movements that were 3.5 and 6% of the height, respectively, to mobilize the full passive earth response. These parameters were analyzed using PYCAP for comparison with the results obtained using the Case III parameters (the in-situ direct shear results with a δ/ϕ ratio of 0.6). The Cole and Rollins, Rollins and Sparks, and Case III parameters matched the measured resistance to within roughly 10%, all underestimating the measured results. This favorable comparison with published parameters, along with a favorable match to the measured data, lends validity to the use of the field direct shear values. The friction angle based on the Duncan (2004) correlation was too large to produce a reasonable match with the measured results.

Table 9-2 Parameter summary for case comparison in PYCAP for densely compacted coarse gravel backfill

Parameter	Case I	Case II	Case III	Case IV	Case V
ϕ (°)	54	54	41	41	41
c (psf)	0	0	286	286	286
δ (°)	32.4	11.0	24.6	30.8	26.0
γ_m (pcf)	138.4	138.4	138.4	138.4	138.4
E (ksf)	830	830	830	830	830
ν	0.3	0.3	0.3	0.3	0.3
k (kip/in)	1374	1374	1374	1374	1374
Δ_{max} (in)	2.9	2.9	2.9	2.9	2.9
Δ_{max}/H	.044	.044	.044	.044	.044
R_f	0.21	0.80	0.82	0.78	0.81
R_{3D}	2.00	1.98	1.77	1.89	1.80
K_p	55.0	17.5	12.4	15.4	13.1

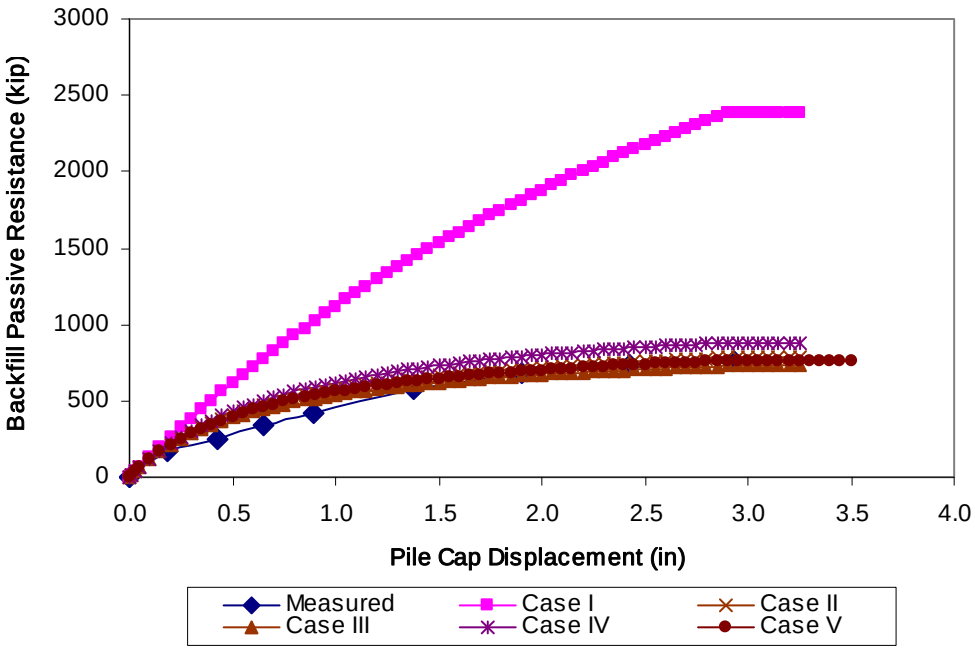

Figure 9-3 PYCAP case comparison for densely compacted coarse gravel

9.3.2 Calculated Response Using ABUTMENT (LSH)

Passive earth resistance was also calculated using ABUTMENT and the LSH methodology. Table 9-3 summarizes key inputs and outputs for several cases analyzed while Figure 9-4 shows the measured and calculated passive resistance curves for each case. The soil friction angle used in Case I was estimated using the Duncan (2004) correlation mentioned in the previous section. The strain at which 50% of the failure strength occurs (ε_{50}) was determined by finding the displacement level at which the soil mass reaches 50% of its peak resistance and then, using the displacements measured along the backfill surface as described in Section 0, averaging the corresponding strain from the two measurement intervals closest to the cap face; the resulting value was within the typical range suggested by Shamsabdi et al. (2007). The interface friction angle was determined by using a δ/ϕ ratio of 0.6, consistent with laboratory determined soil and interface friction values from the densely compacted fine gravel backfill. With the exception of the ε_{50} value, these are the same parameters used in Case I for the PYCAP analysis. Likewise, Cases II through IV use the same parameters as in the PYCAP analysis, not counting the ε_{50} value. As in the PYCAP analysis, Case I vastly overestimates the measured resistance. Case II overestimates the measured peak by about 6.5%. Case III underestimates the

measured curve by about 12.5%. The Case IV parameters estimates the resistance to within 5% of the measured resistance. The Case IV parameters provide the best match to the measured data.

Table 9-3 Parameter summary for case comparison in ABUTMENT for densely compacted coarse gravel

Parameter	Case I	Case II	Case III	Case IV
ϕ (°)	54	54	41	41
c (psf)	0	0	286	286
δ (°)	32.4	11	24.6	30.75
γ_m (pcf)	138.4	138.4	138.4	138.4
ε_{50}	0.0037	0.0037	0.0037	0.0037
ν	0.3	0.3	0.3	0.3
R_f	0.98	0.98	0.98	0.98
R_{3D}	2	1.98	1.77	1.89
K_{ph}	39.0	18.2	17.1	18.8

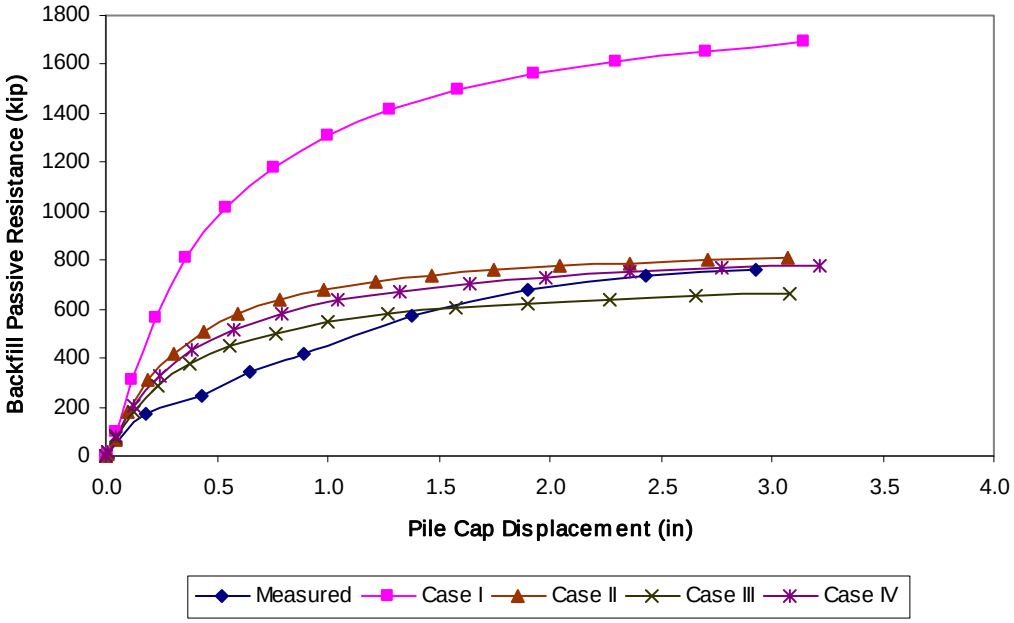

Figure 9-4 ABUTMENT case comparison for densely compacted coarse gravel backfill

9.3.3 Calculated Response Using CALTRANS Method

Passive earth resistance based on the CALTRANS method is shown in Figure 9-5. In this case, the method under-predicts peak passive resistance by almost 60%.

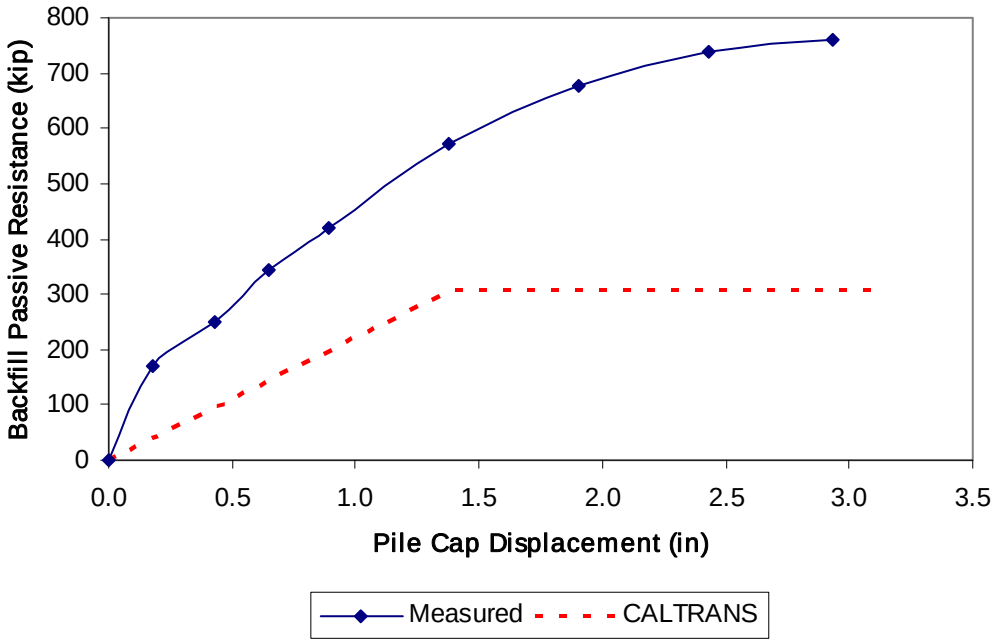

Figure 9-5 Comparison of measured and CALTRANS-based passive resistance for densely compacted coarse gravel backfill

9.4 Response to Cyclic Actuator Loading

After slowly pushing the pile cap to each displacement interval, alternating combinations of small displacement cyclic actuator loads and dynamic shaker loads were applied. The response of the pile cap to the small displacement amplitude loading cycles from the actuator is presented and discussed in this section. Figure 9-6 shows the loop displacement amplitude, stiffness, loop area, and damping ratio for the pile cap with densely compacted coarse gravel backfill in place as a function of pile cap displacement.

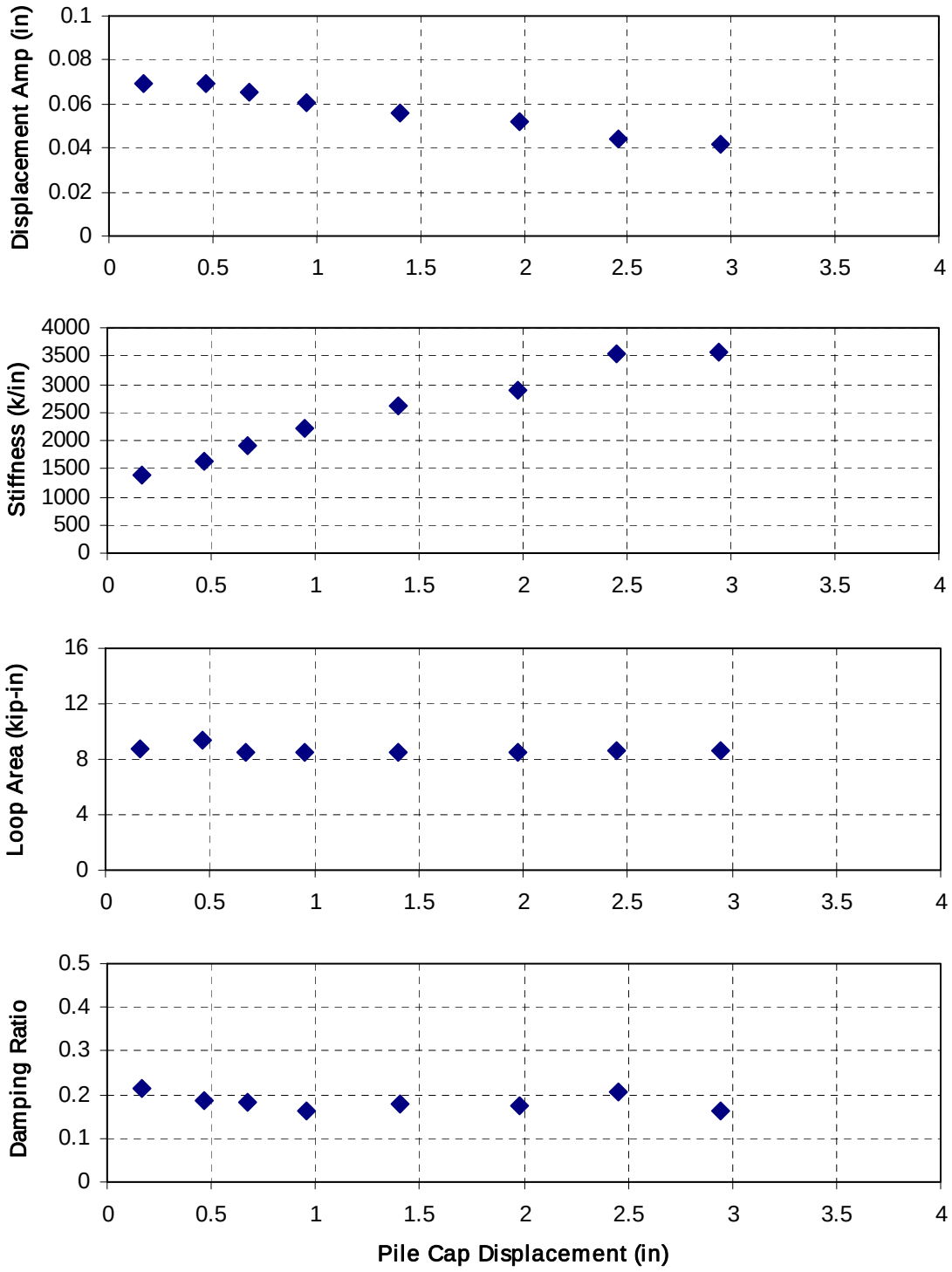

Figure 9-6 Summary of response to cyclic actuator loadings for pile cap with densely compacted coarse gravel backfill

Values are based on the median of 15 low frequency cycles performed at each displacement level. The displacement decreases almost linearly from 0.07 to 0.04 in (1.8 to 1.1 mm), with a median displacement of 0.06 in (1.5 mm). The stiffness increases from 240 to 630 kN/mm as the cap displacement increases; this appears to be due to greater mobilization of the backfill soil's passive strength and pile stiffness. The rate of stiffness increase appears to level off in the last couple of displacement intervals as the passive resistance of the backfill approaches its ultimate value. The loop area remains fairly constant at each displacement interval. The stiffness and damping data appear to exhibit the saw-tooth shaped trend seen in other tests due to the alternating order of the static and dynamic cycling loading phases. Despite a dramatic increase in stiffness and the relatively constant loop area, the damping ratio remains fairly constant with a median value of 18%.

9.5 Response to Dynamic Shaker Loading

After slowly pushing the pile cap to each displacement interval, alternating combinations of small displacement cyclic actuator loads and dynamic shaker loads were applied. The response of the pile cap to the dynamic shaker loading is presented and discussed in this section. The first row of graphs in Figure 9-7 shows loop displacement amplitude as well as loop displacement amplitude normalized by the cyclic amplitude of net applied force from the shaker and actuators as functions of the forcing frequency. The second and third rows of graphs show the calculated reloading stiffness and damping, respectively, of the pile cap system. In the left column, these parameters are shown in terms of forcing frequency. If non-linear behavior is present, these properties will also depend on the displacement amplitude; hence, in the right column, these parameters are shown in terms of the displacement amplitude. Based on the data, it appears that both frequency and displacement amplitude must be considered when interpreting test results. The individual line series shown in all of the graphs correspond to different static displacement levels of the pile cap in which dynamic shaker cycles were applied before the slowly applied actuator cycles.

The peaks in the normalized displacement amplitude graph correspond to the damped natural frequency, which appears to remain fairly constant near 7.5 Hz at all static displacement levels. Reloading stiffness values range from just over 2280 to 5710 kip/in (400 to 1000 kN/mm), peaking 1.5 to 2 Hz before the damped natural frequency and dropping thereafter.

The general trend in the stiffness data shows an increase in stiffness with increasing pile cap displacement level. The stiffness data shows similar peaking trends when plotted as a function of displacement, with peak stiffness occurring at displacement amplitudes of about 0.008 in (0.2 mm).

Calculated damping values vary greatly with respect to the frequency of the forcing function and displacement amplitude. The minimum damping appears to be approximately 5% at about 6 Hz and 0.01 in (0.2 mm) of displacement amplitude (i.e., where stiffness is greatest). At higher frequencies and displacements, the damping ratio increases up to about 30 to 40% (corresponding with the calculated decreasing stiffness) until dropping again at about 8.5 Hz (where the rate of stiffness decrease appears to start leveling off). Unfortunately, the shape of the normalized displacement amplitude curves was such that the half-power bandwidth approach could not be used.

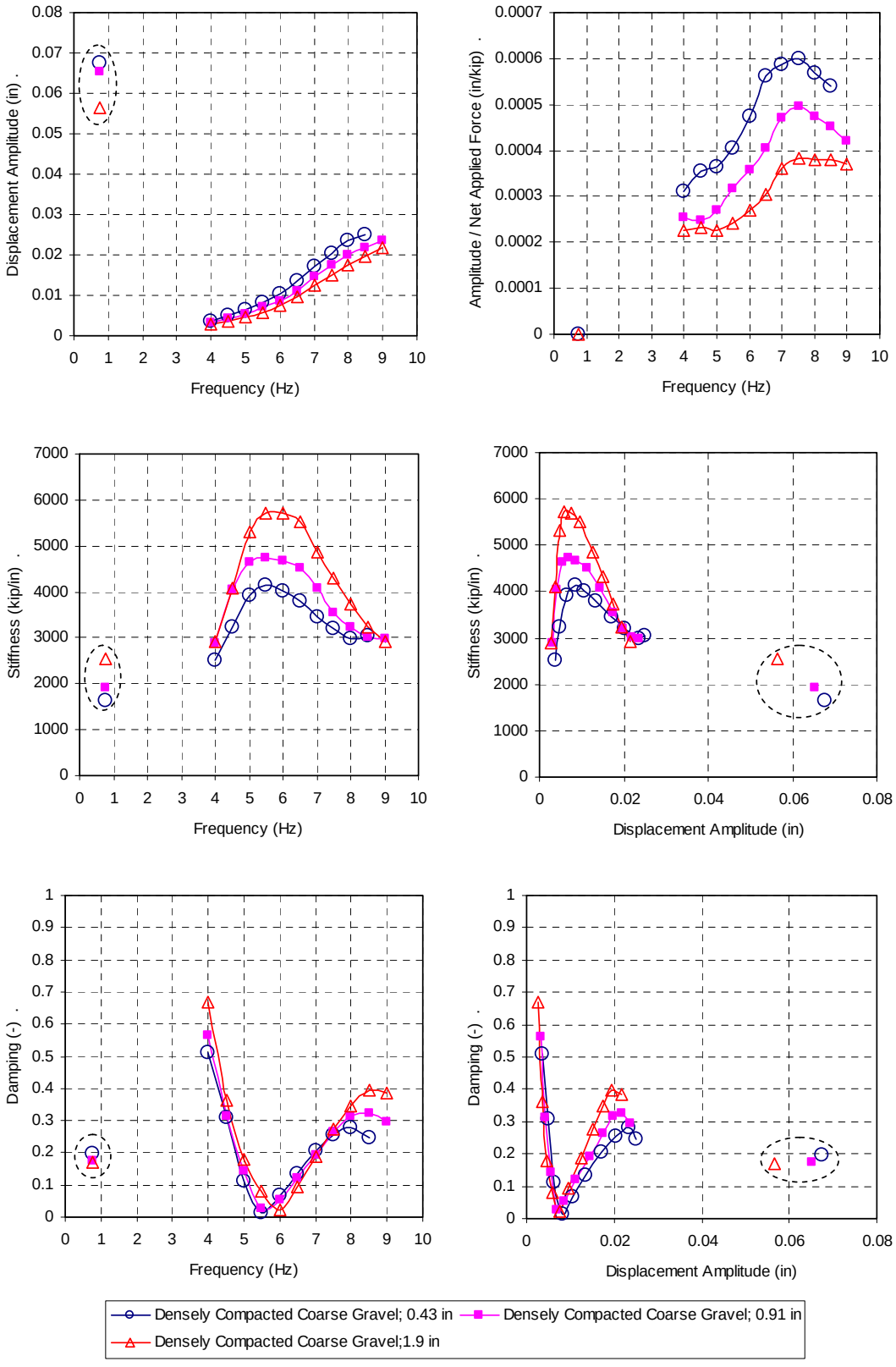

Figure 9-7 Summary of response to dynamic shaker loadings for pile cap with densely compacted coarse gravel backfill

9.6 Comparison of Cyclic Actuator and Dynamic Shaker Responses

Included in Figure 9-7 are the displacement amplitude, stiffness, and damping ratio calculated from the statically applied cycles from the actuators (~ ¾ Hz) at each represented displacement level (points in dashed ovals). The values presented are averages of the previous and subsequent actuator cycles. An average value is used to represent stiffness and damping that would have been calculated if the actuator cycles and been performed before the shaker cycles. In terms of frequency it can be difficult to make a comparison between the static and dynamic methods because of the difference in the associated displacement amplitudes (the shaker cannot generate large forces, and hence displacements, at low frequencies).

The large resistance provided the densely compacted coarse gravel caused the displacement amplitudes from the dynamic shaker loading to be too small for results to be consistent for comparison between the two types of loading (a range of 0.06 to 0.07 in (1.4 to 1.7 mm) from the actuators versus less than 0.02 in (0.6 mm) from the shaker). Extrapolation of the general trends from the dynamic shaker loading data to the displacement amplitude levels from the cyclic actuator loading is impractical due to the curvilinear nature of the trends; therefore, a comparison between the two loading types at similar displacement levels will not be attempted for the densely compacted coarse gravel backfill.

9.7 Passive Earth Pressure Distributions

In addition to the load-displacement response data, passive earth pressure from the backfill soil was measured directly with a vertical array of six earth pressure cells evenly distributed in the central portion of the pile cap face. Figure 9-8 shows the pressure measured by the pressure cells with depth at the end of each static push interval.

The pressure data shows general trends of increasing pressure with depth and increasing magnitude with increasing pile cap displacement. While all of the cells show increasing pressure with increasing pile cap displacement, the pressure cells at 16.5 in (0.42 m) and 49.5 in (1.26 m) appear to go against the trend of increasing pressure with depth. Due to the measurements at these two cells, the measured pressure distribution does not match the normal representation of pressure increasing with depth. This same behavior was observed in the case of the densely compacted fine gravel backfill, which suggests that the variations are due to either the measuring

devices themselves or variations due to differential compaction across lift thickness. (The discussion about irregularities in the pressure cell profile in Section 3.5 does not apply in this case because the bottom-most pressure cell appears to behave as expected.) The rate of pressure increase appears to slow substantially in the last several pile cap displacement intervals, suggesting that the passive resistance of the backfill is approaching its maximum value.

Figure 9-9 shows the backfill force calculated by multiplying each measured pressure by the respective contributory areas of the pile cap face. In general, the resulting force-displacement curve has a similar trend to that based on the actuators, but it is systematically lower. Applying a multiplier of 1.67 (the inverse of 0.6 determined in Section 3.5), to the cell-based curve provides an improved match with the actuator-based curve, although the curve suggests that the ultimate passive resistance may not be realized until a further displacement level (although such a conclusion depends on the validity of an assumed, constant multiplier).

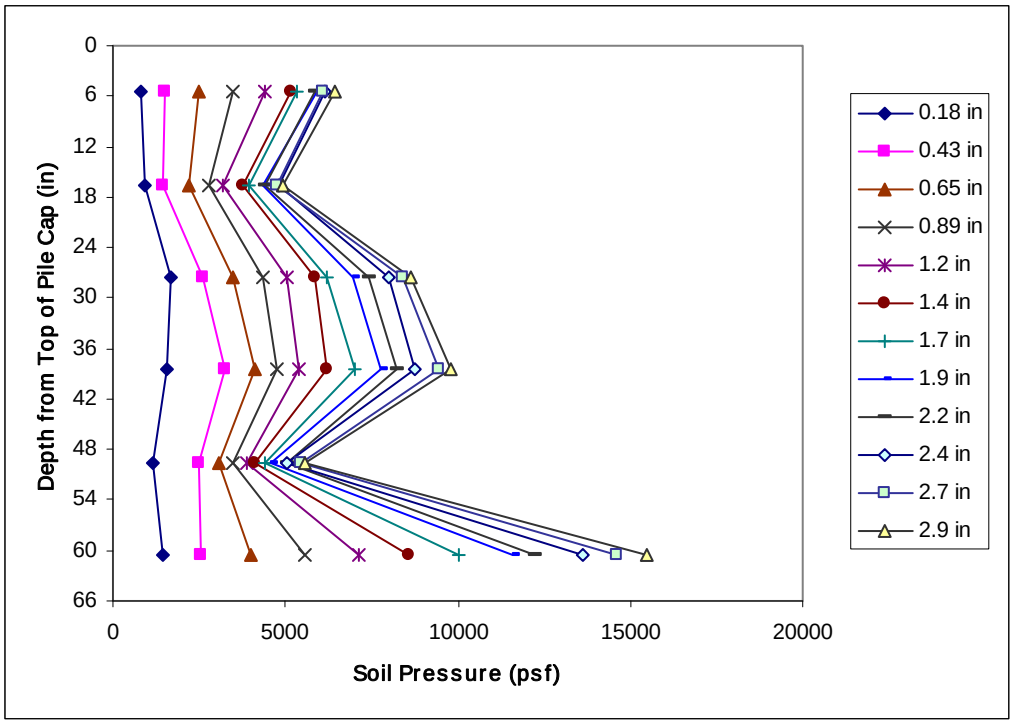

Figure 9-8 Earth pressure distribution as a function of pile cap displacement with densely compacted coarse gravel

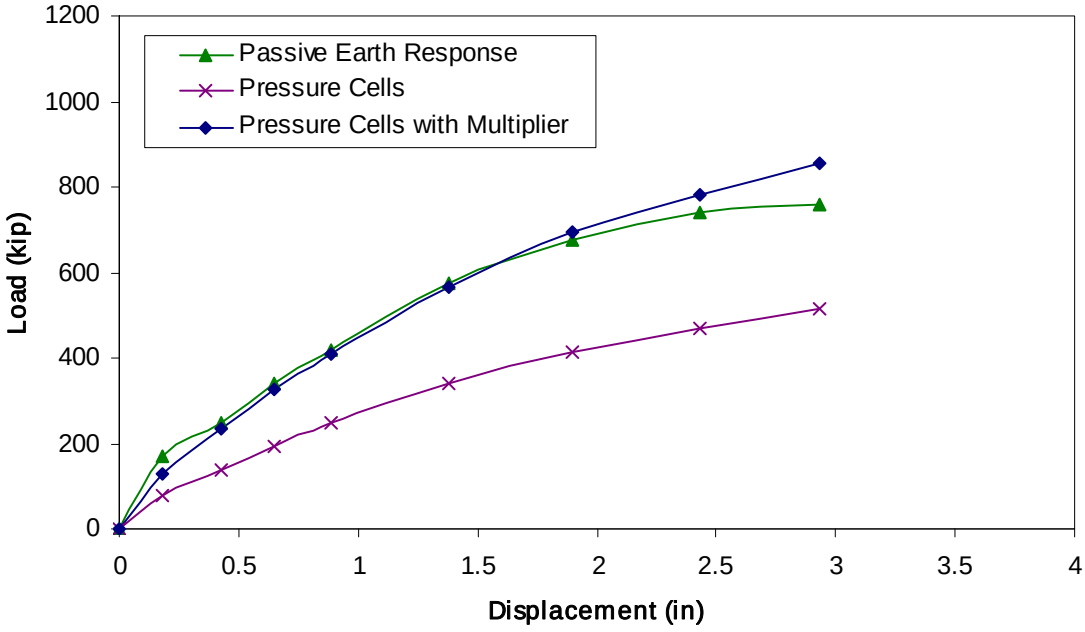

Figure 9-9 Comparison of earth forces based on actuators and pressure cells for densely compacted coarse gravel backfill

9.8 Cracking and Vertical Movement of Backfill

Figure 9-10 is a two part plot showing the results of static and dynamic testing on the surface of the densely compacted clean sand backfill area. The first part of the figure shows the surface cracks that developed during each static push of the pile cap. The surface cracks in the backfill indicate the presence of failure surfaces within the soil. The cohesionless, coarse-grained nature of the material, along with the dynamic vibration due to the eccentric mass shaker, tended to cause the soil grains to shift during testing, potentially obscuring cracks. A thin layer of fine material was spread over the densely compacted coarse gravel to avoid crack obfuscation during the course of the test. The majority of the cracks are concentrated around the edges of the pile cap face. These cracks are due to internal shear stresses radiating out from the cap face and reflect the three dimensional shape of the failure zone. Another group of cracks occur in the center of the backfill zone and include several cracks oriented in the direction of pile cap movement. These central cracks may be due to localized failure surfaces resulting from particles shifting as the backfill moves. The pink horizontal cracks distributed through the central region of the backfill zone are from the soil relaxing after the pile cap was unloaded and are not forcibly related to shear failure planes that occur during loading.

The second part of the figure is a contour map of the change in elevation of the surface of the backfill area during testing. The typical elevation change, as represented by the median elevation change in a given row (parallel to the face of the cap) of grid nodes, is about 1.4 in (35 mm) at 4 ft (1.2 m)from the pile cap face. The heave ranges to about 1.8 in (45 mm) within 3 to 5 ft (1 to 1.5 m) from the pile cap face. Calculations in PYCAP indicate that a log-spiral failure surface should daylight at approximately 20 ft (6 m) from the face of the cap. While the contour map shows heave occurring throughout

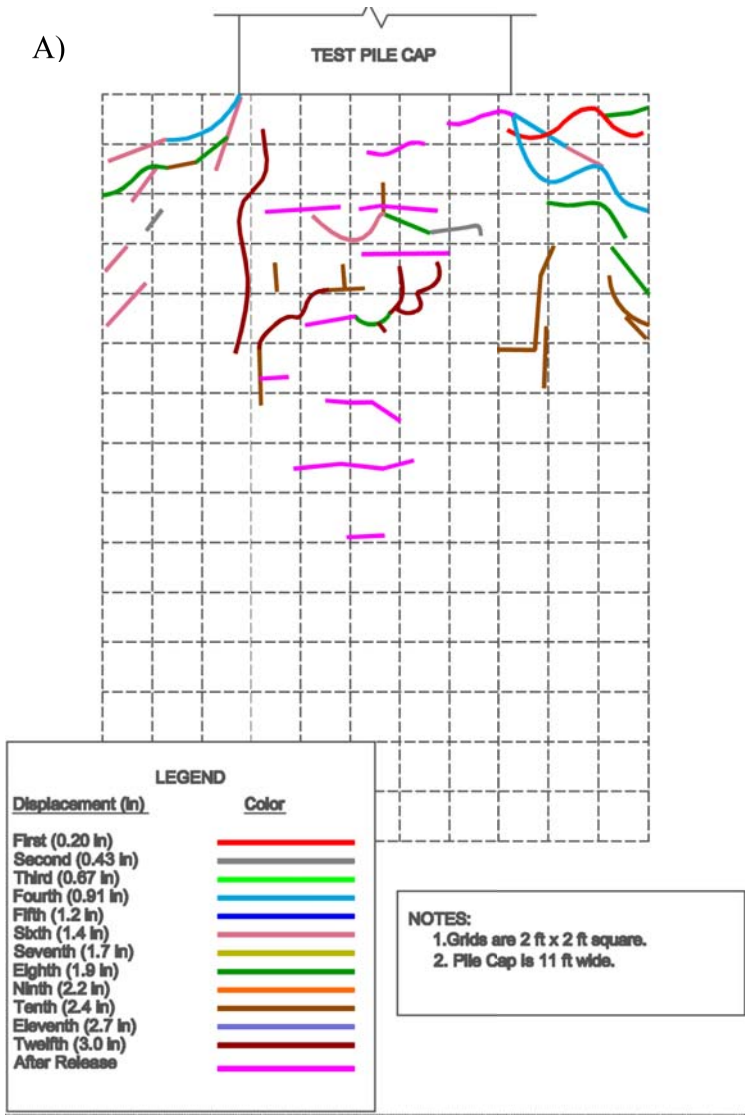

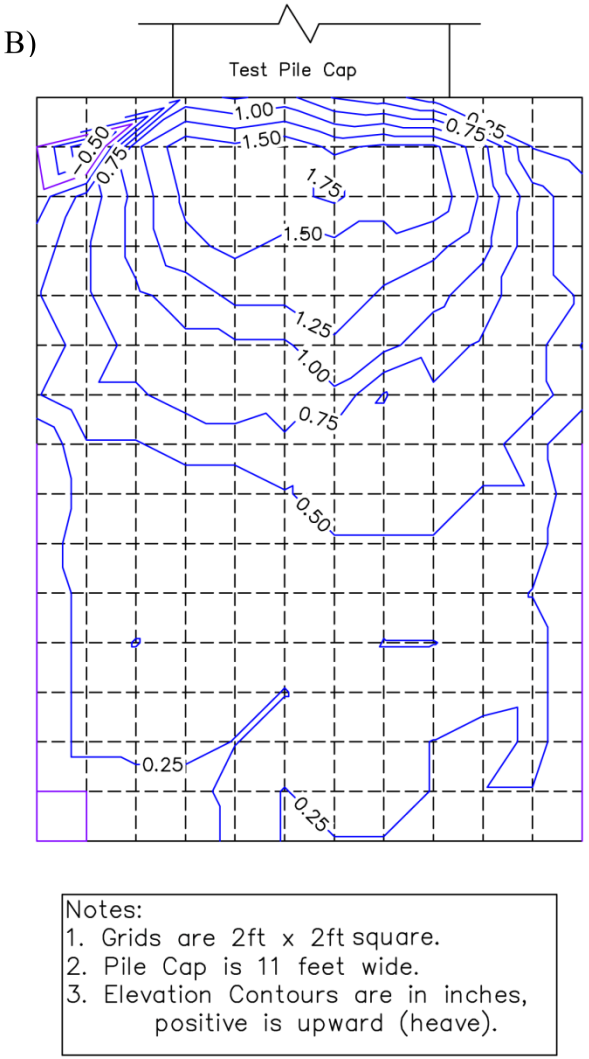

Figure 9-10 Crack pattern (A) and heave contour (B) maps for densely compacted coarse gravel backfill

the entire backfill, the bulk of the heave occurs within the first 13 to 16 ft (4 to 5 m) of the backfill zone, with the heave at greater distances generally less than 0.4 in (10 mm) higher than the original backfill surface elevation. As the observated rate of elevation change beyond 20 ft (6 m) is minimal, it is reasonable to expect that the failure surface daylights in the vicinity of the PYCAP prediction. The correlation between the heave profile and log-spiral failure surface is illustrated by the cross-sectional view in Figure 9-11, in which the failure surface calculated in the spreadsheet program PYCAP using the best-fit parameters discussed in Section 0: in-situ test-based soil friction and cohesion values of 44° and 13.7 kPa, respectively, with an interface friction angle of 26° iterated to match the measured response (i.e., Case V). The log-spiral surface daylights close to where the elevation change becomes negligible. In the densely compacted coarse gravel backfill, the sudden change in elevation in the area immediately in front of the pile

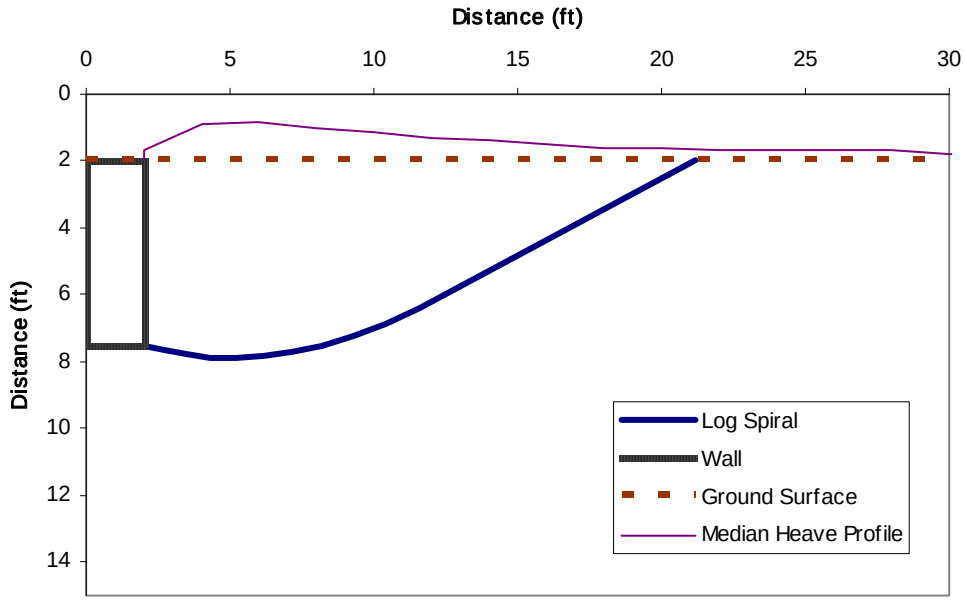

Figure 9-11 Heave profile for densely compacted coarse gravel compared with log spiral failure surface from PYCAP (Case V parameters)

cap suggests a fairly strong interaction between the backfill and the wall surface; hence, the best-fit parameters were chosen to reflect that interaction. The heave profile shown in the figure is magnified ten times to make the elevation change more appreciable.

9.9 Horizontal Movement of Backfill

String potentiometers were used to measure movement in the backfill. Figure 9-12 shows the movement of each of the monitoring points in the densely compacted coarse gravel backfill compared to the movement of the pile cap face. The backfill displacement ranges from 3.0 in (75 mm) (100% of cap displacement) at the cap face to 0.59 in (15 mm) (20% of cap displacement) at 18 ft (5.5 m) from the cap face. The translational movement at the monitoring point 18 ft (5.5 m) from the cap face represents

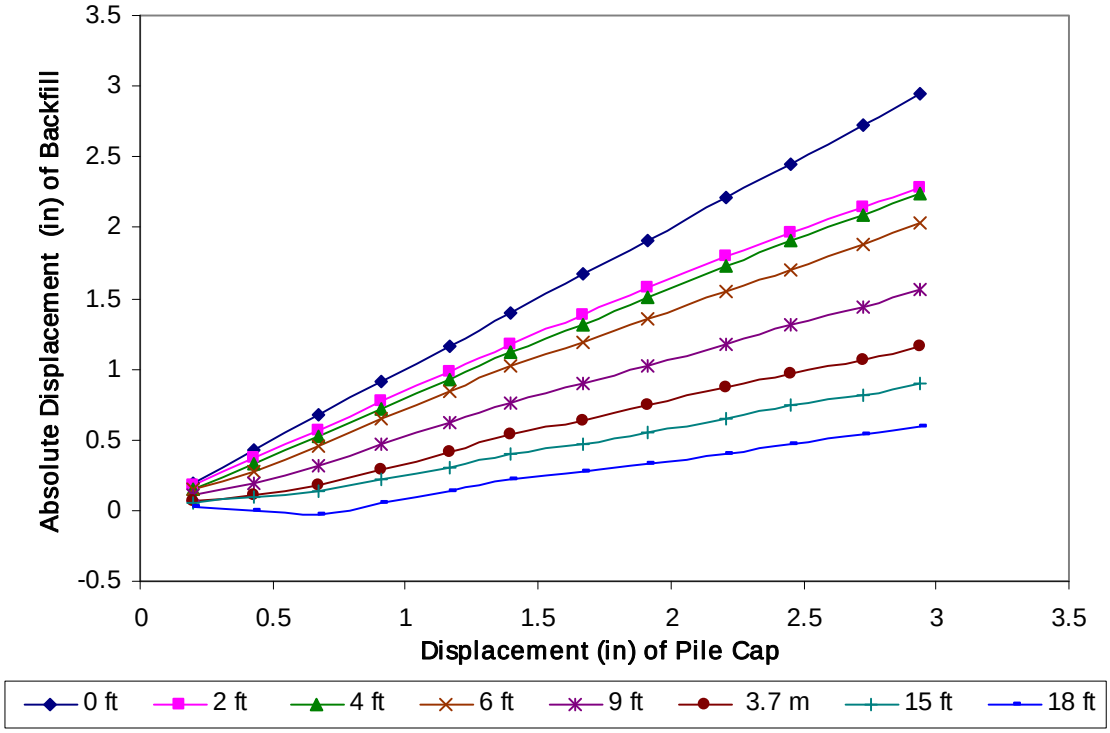

Figure 9-12 Displacement of monitoring points in densely compacted coarse gravel backfill

the amount of the pile cap displacement not absorbed through compressive strain up to that point.

Figure 9-13 shows the compressive strain corresponding to each static push of the pile cap. The 2-ft (0.6-m) interval closest to the cap experiences the most compressive strain for a given displacement level, in this case almost twice the strain in any other interval. With the exception of the second 2-ft (0.6-m) interval, the strain in the remainder of the intervals is fairly evenly distributed. The compressive strain ranges from 0.027 to 0.002 within the backfill zone. Minor variation from interval to interval may indicate the potential sensitivity of the string

potentiometer measurements to differential pushing of the pile cap (not all the monitoring stakes were on the same end of

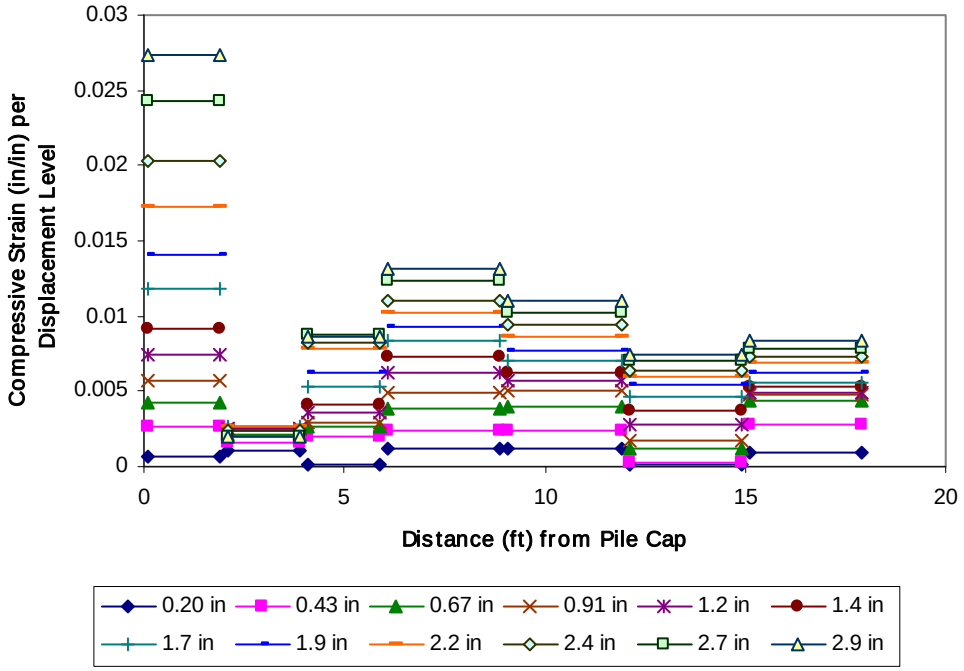

Figure 9-13 Strain per displacement level for densely compacted coarse gravel backfill

the cap face) and tipping of the monitoring stakes themselves. In this particular case, some of the strain shown in the first interval likely occurs in the second interval, making the distribution more uniform with distance, but still highest near the face of the pile cap.

10.0 PILE CAP WITH LOOSELY COMPACTED COARSE GRAVEL BACKFILL

10.1 General

The pile cap with loosely compacted coarse gravel backfill was tested on June 21, 2007. No significant deviations from the general test procedure occurred during this test. Table 10-1 summarizes the test in terms of loads and displacements measured at the end of each "static push" with the actuators. The table also indicates the order in which cyclic loads from the actuators and dynamic loads from the shaker were applied. At some displacement increments, no cyclic or dynamic loadings were applied in order to help assure that sufficient displacement had occurred for the load path to return to the static-backbone loading curve.

Table 10-1 Summary of test with loosely compacted coarse gravel backfill

Displacement Interval	Displacement (in)	Actuator Load (kip)	Actuator Cycles	Shaker Cycles
1	0.27	110	First	Second
2	0.59	144	None	None
3	0.87	223	Second	First
4	1.1	208	None	None
5	1.4	295	First	Second
6	1.7	295	None	None
7	1.9	383	Second	First
8	2.1	391	None	None
9	2.3	485	First	Second
10	2.5	500	None	None
11	2.8	596	Second	First
12	3.0	611	None	None
13	3.2	693	First	Second

10.2 Load-Displacement Response

Figure 10-1 shows the entire actuator load verses pile cap displacement relationship for the test, with static pushes, actuator cycles and shaker cycles being represented by green, blue,

and red data points, respectively. Section 3.2 provides some discussion relative to the details of interpreting this data.

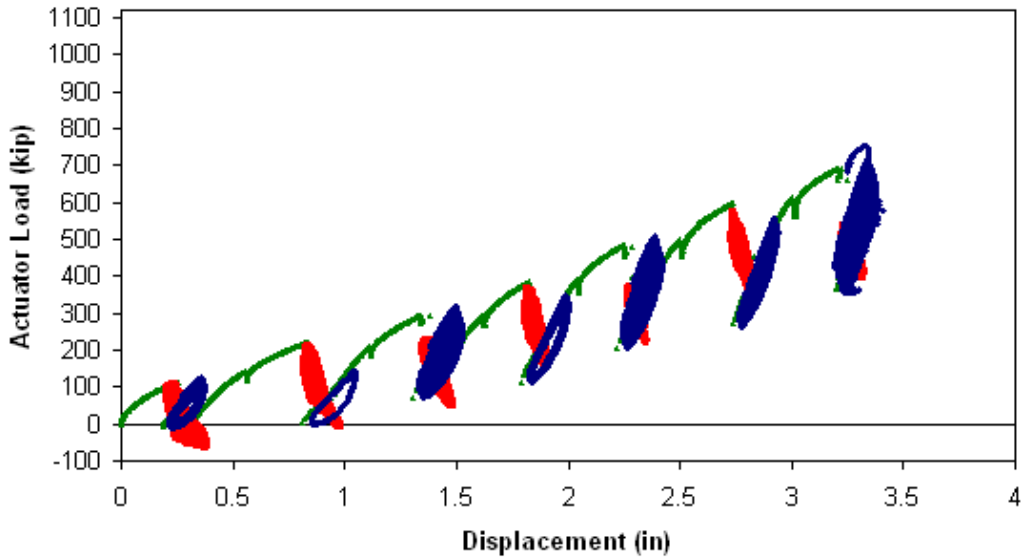

Figure 10-1 Actuator load versus pile cap displacement with loosely compacted coarse gravel backfill (Test 10; June 21, 2007)

Figure 10-2 shows three load-displacement response curves for the pile cap: one for the response with backfill in place (referred to as the total response, which is the equivalent monotonic response or backbone curve derived from the data shown in Figure 10-1), one for the response with no backfill present (referred to as the baseline response), and one showing the passive earth response of the backfill (obtained by subtracting the baseline response from the total response).

The curves show that total response and baseline response increase at different rates until the end of testing for the loosely compacted coarse gravel backfill material. At about 2.4 in (60 mm), the total response and baseline response curves appear to increase at a similar rate, but the backfill response merely seems to experience a gentle slope change. The apparent absence of a leveling off makes it difficult to determine when the backfill is at failure; the resistance likely would have increased somewhat past 301 kip (1340 kN) had the test continued to higher displacement levels. For subsequent analysis purposes, however, the ultimate passive resistance of the backfill is assumed to develop at a displacement of 5.8 in (148 mm) – twice that of the densely compacted coarse gravel backfill as suggested by Clough and Duncan (1991) for a loose

or medium dense material as compared to a dense material. The displacement to wall height ratio for this material is thus assumed to be about 0.088.

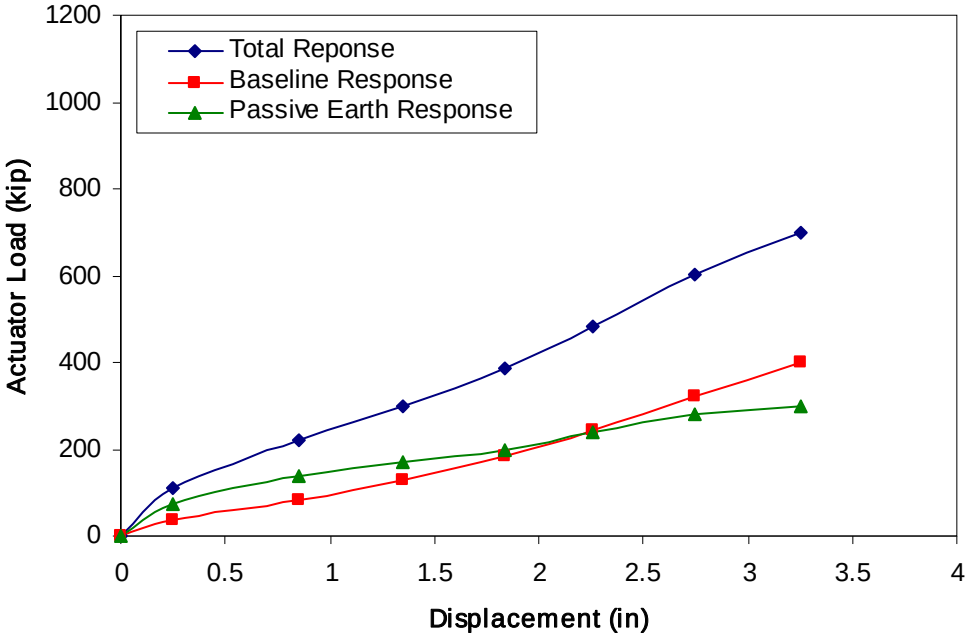

Figure 10-2 Total, baseline, and passive earth responses for pile cap with loosely compacted coarse gravel backfill

10.3 Calculated Passive Earth Forces

Commonly used methods for calculating passive earth pressure include Rankine theory, Coulomb theory, and log-spiral theory. Log-spiral theory is typically considered the most accurate of these methods (see, for example, Cole and Rollins (2006) and Duncan and Mokwa (2001)). Three methods of estimating the development of passive pressure with wall displacement are evaluated in this section. Two of these methods, PYCAP and ABUTMENT (LSH method) involve applications of log-spiral theory and a hyperbolic load-displacement relationship. The third approach evaluated in this section is an empirical load-displacement relationship based on full-scale testing of an abutment with typical backfill conditions (see discussion of CALTRANS method in Section 3.3.3)

10.3.1 Calculated Response Using PYCAP

Passive earth resistance was calculated using the modified PYCAP spreadsheet. Table 10-2 summarized key inputs and outputs for the various cases analyzed while Figure 10-3 shows

the measured passive resistance curve alongside the calculated passive resistance curves for each case. Case I is the best estimate case based on the friction angle correlation developed by Duncan (2004) as discussed in Chapter 2. The ultimate passive resistance from Case I is 233% greater than the measured resistance. The initial modulus value used in Case I, and in all other cases, is consistent with the normally loaded range given by Duncan and Mokwa (2001). Case II is similar to Case I, except the interface friction angle was iteratively reduced to provide a better match to the ultimate passive resistance. The resistance calculated from the Case II parameters is within 5% of the measured resistance. The soil friction angle in Case III is based on the results of an in-situ direct shear test and the interface friction angle was estimated using a δ/ϕ ratio of 0.6, based on laboratory results using densely compacted fine gravel material and concrete with roughness comparable to the pile cap. The Case III curve does not match the measured ultimate passive resistance as nicely as that provided by Case II parameters, however, the Case III parameters provide an estimate that is within 16% of the measured resistance and provides a good representation of the soil behavior. Case IV is similar to Case III, except an assumed δ/ϕ ratio of 0.75 is used. Case IV overestimates the measured response by about 40%. The Case II parameters obviously provide the best match to the measured passive earth response and are referred to as the "best fit" parameters for this soil. Case III provides a reasonable match with little parameter manipulation, which makes it a good choice for design situations. Hence, the Case III parameters are considered the "most representative" parameters. In Case V, the shear strength parameters found during the in-situ direct shear test for the loosely compacted coarse gravel are reduced to 85% of their original value (the tangent of the original densely compacted coarse gravel friction angle was multiplied by 0.85 and the inverse tangent of that value became the new soil friction angle for the loosely compacted coarse gravel). As Figure 10-3 shows, the match obtained using the reduced parameters is quite reasonable. As stated previously, this approach resembles that suggested by Terzaghi and Peck (1967) for dealing with local shear effects for the bearing capacity of loose to medium sands; however, the fraction of shear strength used is 85% rather than 67% as suggested by Terzaghi and Peck.

Table 10-2 Parameter summary for case comparison in PYCAP for loosely compacted coarse gravel backfill

Parameter	Case I	Case II	Case III	Case IV	Case V
ϕ (°)	50	50	40	40	35.5
c (psf	0	0	0	0	0
δ (°)	30	4.2	24	30	35.5
γ_m (pcf)	128.7	128.7	128.7	128.7	128.7
E (ksf)	400	400	400	400	400
ν	0.3	0.3	0.3	0.3	.3
k (kip/in)	662	662	662	662	662
Δ_{max} (in)	148	148	148	148	148
Δ_{max}/H	0.088	0.088	0.088	0.088	0.088
R_f	0.67	0.92	0.90	0.88	0.91
R_{3D}	2.00	1.64	1.72	1.82	1.72
K_p	33.9	9.3	11.1	13.7	9.2

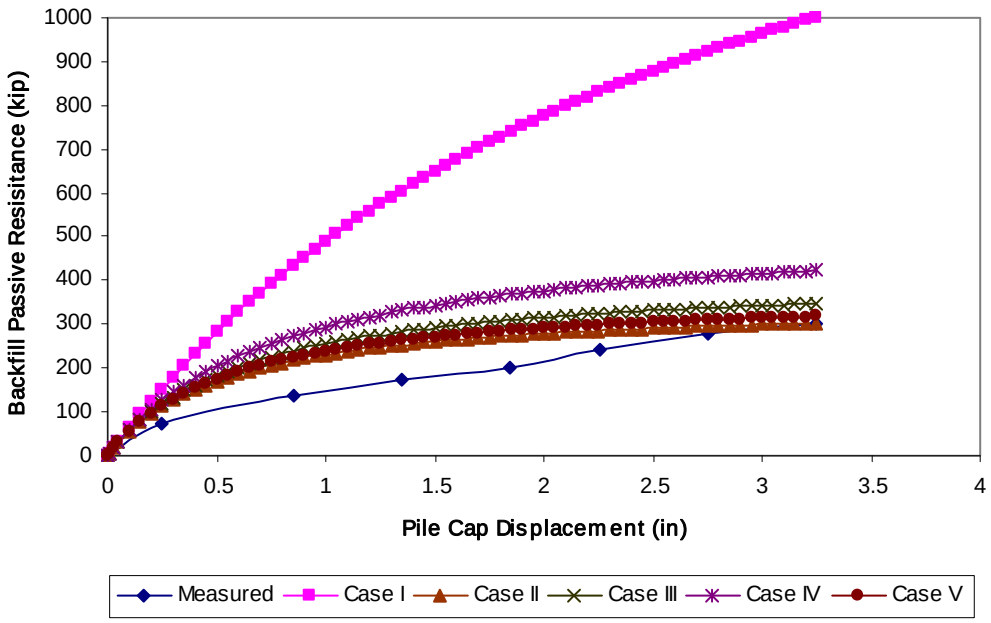

Figure 10-3 PYCAP case comparison for loosely compacted coarse gravel backfill

10.3.2 Calculated Response Using ABUTMENT (LSH)

Passive earth resistance was also calculated using the LSH method. Table 10-3 summarizes key inputs and outputs for several cases analyzed while Figure 10-4 shows the measured and calculated passive resistance curves for each case. Case I is based on a correlation equation given by Duncan (2004) (see Section 2.4.3 for further discussion) and greatly overestimates the measured resistance. In Case II, the interface friction angle is reduced to better match the measured data using the correlated friction angle. Case III uses a field derived soil friction angle and a δ/ϕ ratio of 0.6, resulting in a calculated hyperbolic curve that compares favorably with the measured passive resistance. Both Case II and Case III provide excellent estimates of the measured resistance. Case IV is similar to Case III, except the δ/ϕ ratio is assigned a typical value of 0.75. Case IV overestimates the measured curve by about 15%, but matches the initial portion of the curve about as well as Cases II and III.

10.3.3 Calculated Response Using CALTRANS Method

Passive earth resistance based on the CALTRANS method is shown in Figure 10-5. In the case of loosely compacted coarse gravel, the method estimates the passive resistance to within 5% of the final measured resistance; thus, the CALTRANS method provides a good match to the measured resistance at the displacement levels reached during testing for this material, although the loading slope is much too steep and it appears that the method would underestimate the resistance if the pile cap could have been pushed to higher displacement levels.

Table 10-3 Parameter summary for case comparison in ABUTMENT for loosely compacted coarse gravel backfill

Parameter	Case I	Case II	Case III	Case IV
ϕ (°)	50	50	40	40
c (psf)	0	0	0	0
δ (°)	30	4.2	24	30
γ_m (pcf)	128.7	128.7	128.7	128.7
ε_{50}	0.0074	0.0074	0.0074	0.0074
ν	0.3	0.3	0.3	0.3

R_f	0.98	0.98	0.98	0.98
R_{3D}	2.00	1.64	1.72	1.82
K_{ph}	24.4	9.8	9.7	10.6

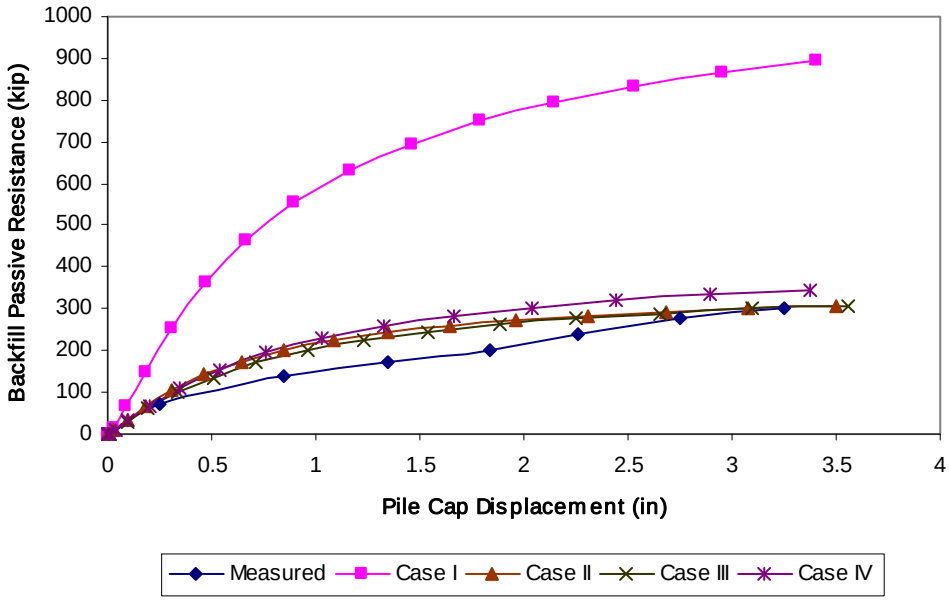

Figure 10-4 ABUTMENT case comparison for loosely compacted coarse gravel backfill

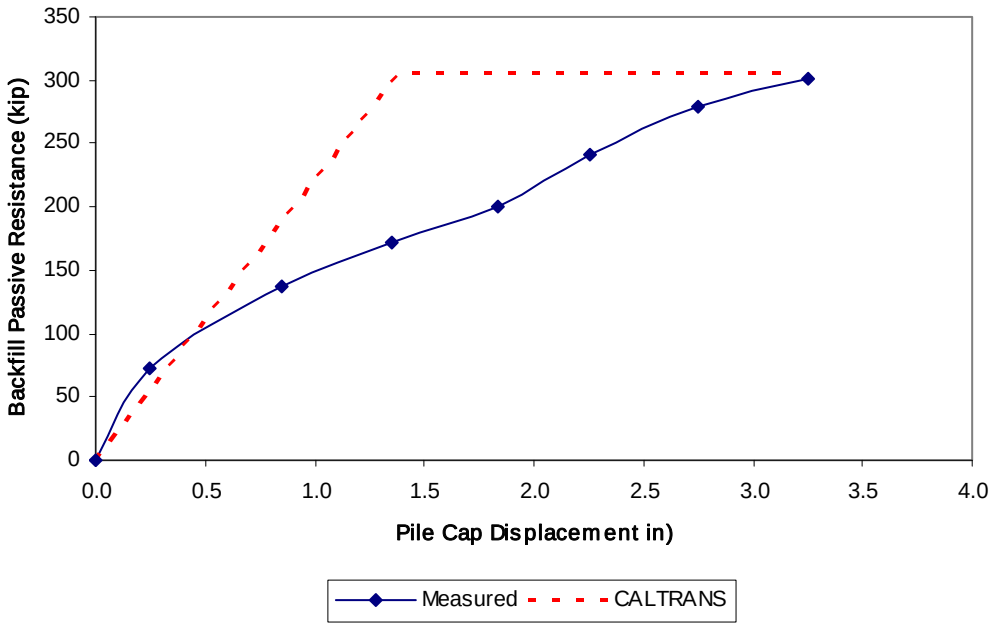

Figure 10-5 Comparison of measured and CALTRANS-based passive resistance for loosely compacted coarse gravel backfill

10.4 Response to Cyclic Actuator Loading

After slowly pushing the pile cap to each displacement interval, alternating combinations of small displacement cyclic actuator loads and dynamic shaker loads were applied. The response of the pile cap to the small displacement amplitude loading cycles from the actuator is presented and discussed in this section. Figure 10-6 shows the loop displacement amplitude, stiffness, loop area, and damping ratio for the pile cap with loosely compacted coarse gravel backfill in place as a function of pile cap displacement. Values are based on the median of the 15 low frequency cycles performed at each displacement level. Displacement amplitude ranges from about 0.07 to 0.1 in (1.9 to 2.5 mm), with a general trend of decreasing amplitude with pile cap displacement level.

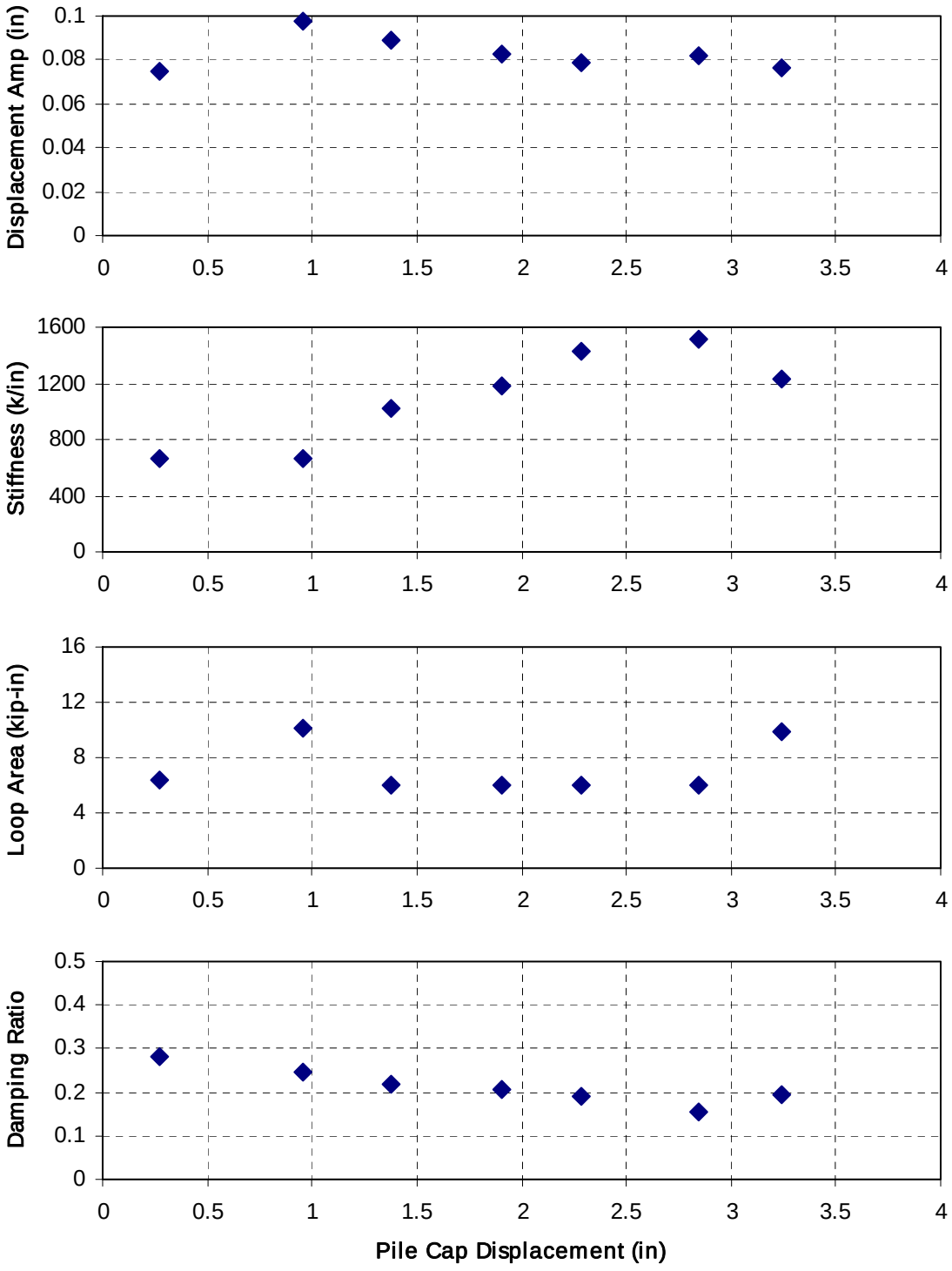

Figure 10-6 Summary of response to cyclic actuator loadings for pile cap with loosely compacted coarse gravel backfill

The stiffness increases from 571 to nearly 1710 kip/in (100 to 300 kN/mm) as the cap displacement increases to about 2.6 in (67 mm), excepting a small decrease at the last displacement level of 3.2 in (82 mm). The damping ratio decreases fairly linearly from 28% to 15% until about 2.6 in (67 mm) of cap displacement, after which the damping ratio increases to about 20%. The median damping ratio for the cyclic actuator loading over the course of the test is 21%. Each data type in Figure 10-6 exhibits, to some degree, the saw-tooth shaped trend seen in other tests due to the alternating order of the static and dynamic cycling loading phases. The stiffness and damping values reflect the presence of backfill, but are more similar to those calculated for the pile cap without backfill present than those calculated with the densely compacted coarse gravel backfill present.

10.5 Response to Dynamic Shaker Loading

After slowly pushing the pile cap to each displacement interval, alternating combinations of small displacement cyclic actuator loads and dynamic shaker loads were applied. The response of the pile cap to the dynamic shaker loading is presented and discussed in this section. The first row of graphs in Figure 10-7 shows loop displacement amplitude as well as loop displacement amplitude normalized by the cyclic amplitude of net applied force from the shaker and actuators as functions of the forcing frequency. The second and third rows of graphs show the calculated reloading stiffness and damping, respectively, of the pile cap system. In the left column, these parameters are shown in terms of forcing frequency. If non-linear behavior is present, these properties will also depend on the displacement amplitude; hence, in the right column, these parameters are shown on terms of the displacement amplitude. Based on the data, it

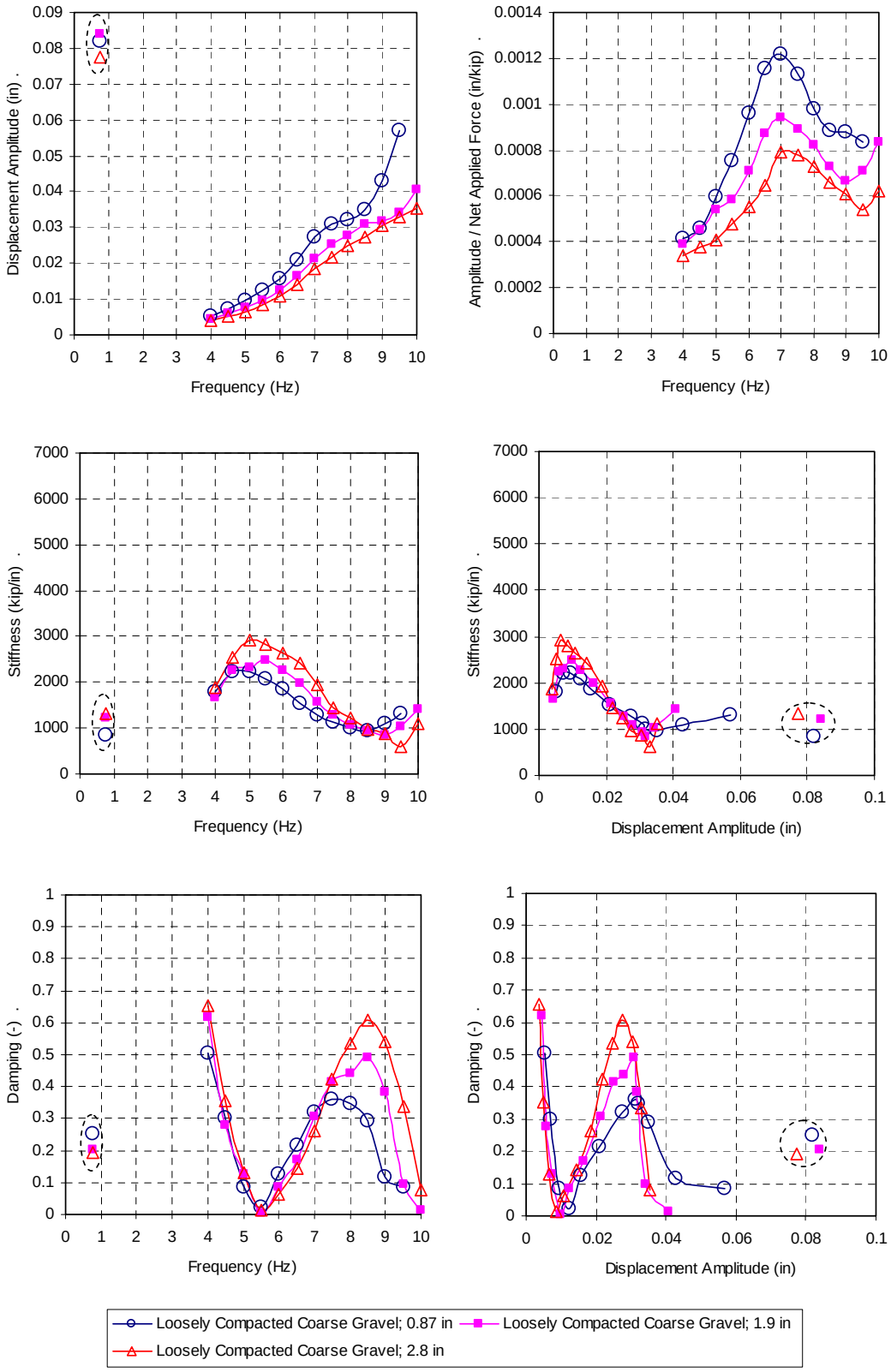

Figure 10-7 Summary of response to dynamic shaker loadings for pile cap with loosely compacted coarse gravel backfill

appears that both frequency and displacement amplitude must be considered when interpreting test results. The individual line series shown in all of the graphs correspond to different static displacement levels of the pile cap in which dynamic shaker cycles were applied before the slowly applied actuator cycles.

The peaks in the normalized displacement amplitude graph correspond to the damped natural frequency of the system. The damped natural frequency appears to remain fairly constant near 7 Hz with increasing static displacement levels. Dynamic stiffness initially ranges from 1710 to over 2860 kip/in (300 to 500 kN/mm) as a function of frequency, peaking at about 5 Hz, and then decreasing to values from just under 1140 to just over 570 kip/in (200 to 100 kN/mm) between 8.5 and 9.5 Hz. Calculated damping values vary greatly with respect to the frequency of the forcing function and displacement amplitude. The minimum damping appears to be approximately 5% at 5.5 Hz and at 0.01 in (0.3 mm) of displacement amplitude. At higher frequencies and displacements, the damping ratio increases up to about 60% (approximately corresponding with the calculated decreasing stiffness) until dropping again at 8.5 Hz (where stiffness begins to increase again). The damping curve corresponding to the 0.87 in (22 mm) static push reaches a maximum damping ratio at a lower frequency and higher displacement level than the other two recorded pile cap displacement intervals. Interpreting the normalized displacement amplitudes using the half-power bandwidth approach yields a damping ratio of 23% for the 0.87 and 1.9 in (22 and 47 mm) displacement intervals, while the distribution of values for the 2.8 in (70 mm) displacement interval result in a curve shape such that the half-power bandwidth approach could not be used.

10.6 Comparison of Cyclic Actuator and Dynamic Shaker Responses

Included in Figure 10-7 are displacement amplitude, stiffness, and damping ratio calculated from the statically applied cycles from the actuators (~ ¾ Hz) at each represented displacement level (points in dashed ovals). The values presented are averages of the previous and subsequent actuator cycles. An average value is used to represent the stiffness and damping that would have been calculated if the actuator cycles had been performed before the shaker cycles. In terms of frequency, it can be difficult to make a comparison between the static and dynamic methods because of the difference in the associated displacement amplitudes (the shaker cannot generate large forces, and hence displacements, at low frequencies).

Maximum displacement levels due to dynamic shaker loading were just less than 0.06 in (1.5 mm) for the 0.87 in (22 mm) static push and decreased to about 0.04 in (1 mm) for the subsequent 1.9 and 2.8 in (47 and 70 mm) static pushes. Average displacement levels due to cyclic actuator loading were about 0.08 in (2 mm), which means that, in the case of loosely compacted coarse gravel backfill, it is difficult to make a comparison between the static and dynamic methods because of the difference in the associated loop displacement amplitudes. Although the shaker was unable to generate enough force at the frequencies tested to produce comparable displacement amplitudes for precise comparisons, the actuator- and shaker-based stiffnesses appear to be generally comparable for displacement amplitudes in the range of 0.04 to 0.08 in (1 to 2 mm). The equivalent damping ratio under cyclic loading conditions (about 20%) is bracketed by the range of damping observed under dynamic loading conditions.

10.7 Passive Earth Pressure Distributions

In addition to the load-displacement response data, passive earth pressure from the backfill soil was measured directly with a vertical array of six earth pressure cells evenly distributed in the central portion of the pile cap face. Figure 10-8 shows the pressure measured by the pressure cells with depth at the end of each static push interval.

The pressure cells show general trends of increasing pressure with depth and increasing magnitude with increasing pile cap displacement. The bottom pressure cell seems not to follow this trend, with pressure decreasing to near zero after the first displacement level. This behavior is consistent with that observed in other tests as mentioned in Section 3.5. Inspection of the figure shows that after the first five displacement increments, there is a drop in measured pressure for every other increment. The behavior is consistent with the overall loss in resistance observed after the application of the actuator and shaker loadings. In these instances, no cyclic or dynamic loadings were applied during the next interval (as shown previously in Table 10-1) in order to help assure that sufficient displacement had occurred for the load path to return to the static-backbone loading curve before applying the cyclic and dynamic loadings again. Figure 10-9 shows the backfill force calculated by multiplying each measured pressure by the respective contributory areas of the pile cap face. In general, the resulting force-displacement curve has a similar trend to that based on the actuators, but it is systematically lower. Applying a multiplier of 1.67 (the inverse of 0.6 determined in Section 3.5) to pressures for the even numbered

displacement intervals (i.e., those intervals for which the load path returned to the backbone) provides a very good match with the actuator-based curve. The data suggests that the loosely compacted coarse gravel backfill does not reach its ultimate passive resistance before the end of testing.

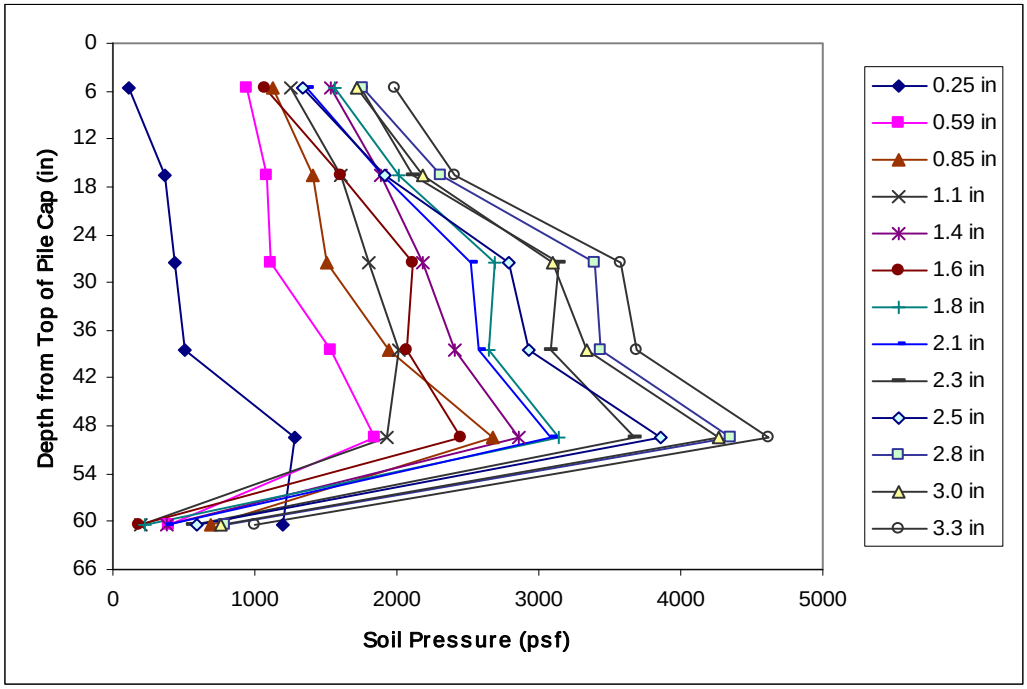

Figure 10-8 Earth pressure distribution as a function of pile cap displacement with loosely compacted coarse gravel

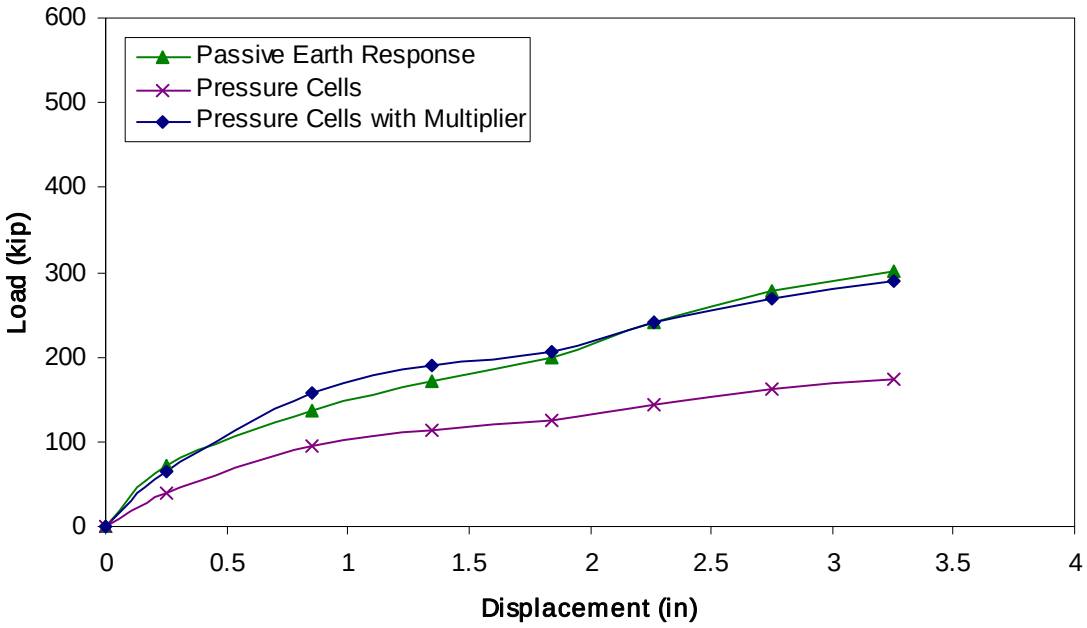

Figure 10-9 Comparison of earth forces based on actuators and pressure cells for loosely compacted coarse gravel backfill

10.8 Cracking and Vertical Movement of Backfill

Figure 10-10 is a two part plot showing the results of static and dynamic testing on the surface of the loosely compacted coarse gravel backfill area. The first part of the figure shows the surface cracks that developed during each static push of the pile cap. The surface cracks in the backfill indicate the presence of failure surfaces within the soil. The cohesionless, coarse-grained nature of the material, along with the dynamic vibration due to the eccentric mass shaker, tended to cause the soil grains to shift during testing, potentially obscuring cracks. No veneer of fine-grained material was placed on the surface of the loosely compacted coarse gravel backfill, making it extremely difficult to identify individual cracks in the open, granular, backfill surface. Unfortunately, too few cracks were observable to clearly identify a pattern of stress distribution and/or failure.

The second part of the figure is a contour map of the change in elevation of the surface of the backfill area during testing. The typical elevation change, as represented by the median elevation change in a given row (parallel to the face of the cap) of grid nodes, is about 2.46 in (62 mm) of subsidence directly adjacent to the pile cap face. The settlement ranges from 0 to

over 4 in (100 mm) of subsidence at individual survey nodes near the pile cap face, though some of the larger settlements may be due to loss of material near the boundaries of the backfill area. This material loss may also affect the accuracy of the value given for typical settlement near the face of the pile cap. The figure shows that most of the elevation change occurred within the first meter or so of backfill. Beyond about 13 ft (4 m) from the face of the pile cap, very little elevation change occurs at all.

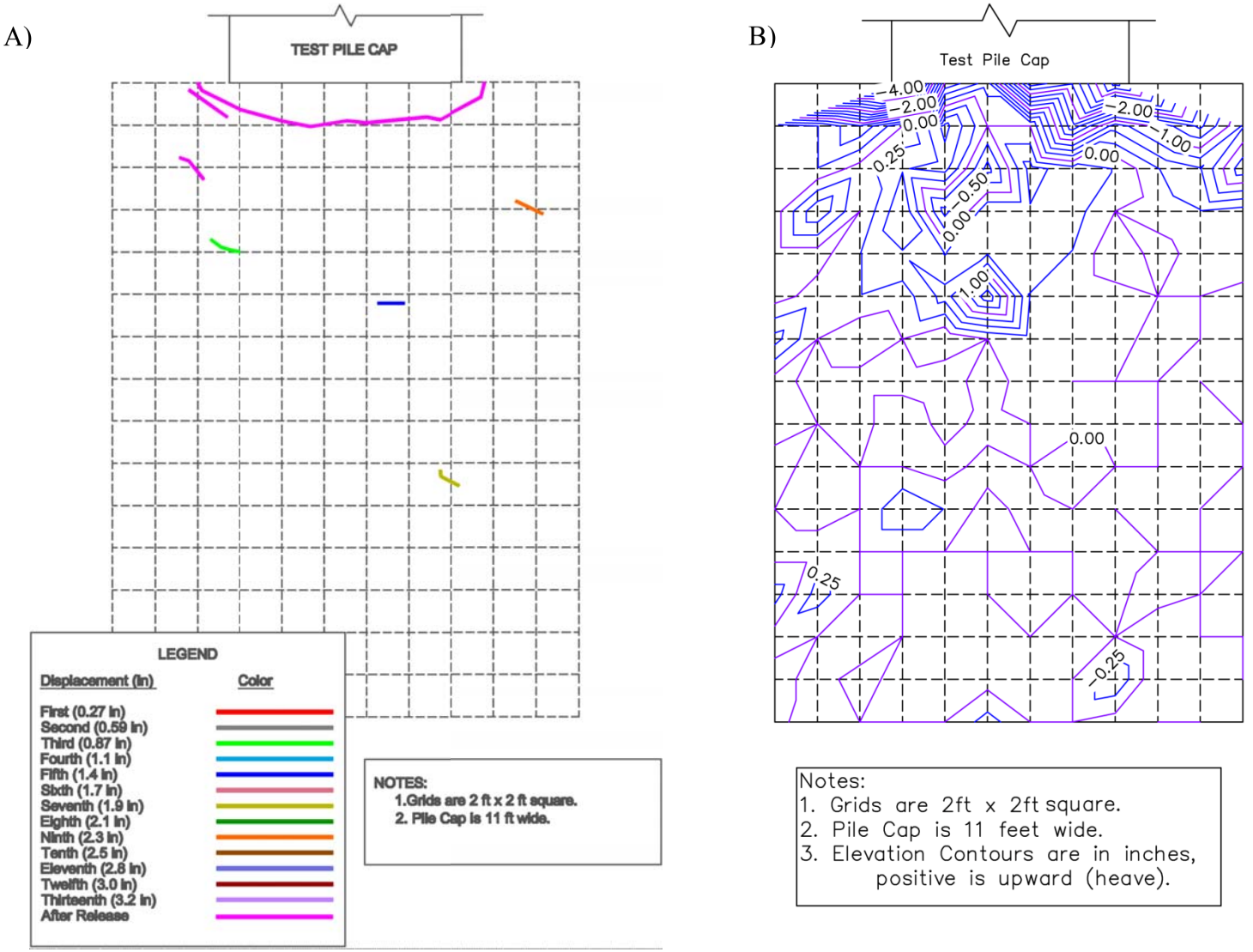

Figure 10-10 Crack pattern (A) and heave contour (B) maps for loosely compacted coarse gravel backfill

The contour map in Figure 10-10 shows that the majority of the elevation change in the loosely compacted coarse gravel backfill was settlement. Figure 10-11 illustrates the correlation between the vertical movement in the backfill and the log-spiral failure surface calculated using using Case III parameters for PYCAP discussed in Section 0: a friction angle of 40° based on the in-situ direct shear test results and a δ/□ ratio of 0.6. Also shown is the failure surface derived from Case II, which is more linear. As the figure illustrates, there is some to little curve to the log-spiral failure surface (depending on the case), suggesting that loosely compacted coarse gravel may fail according to mechanism similar to a Rankine passive failure wedge. The vertical displacement profile in the figure is magnified ten times to make the elevation change more appreciable.

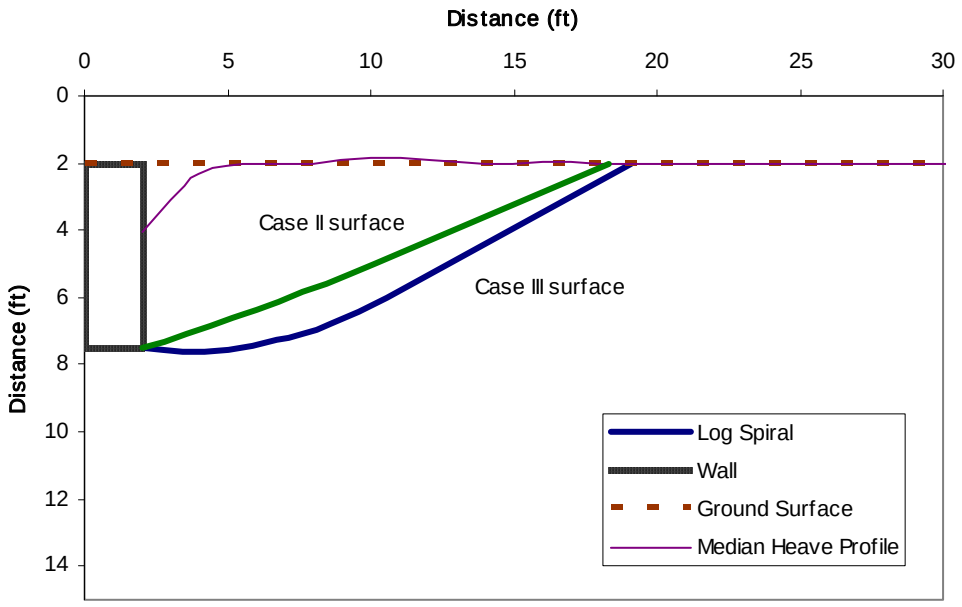

Figure 10-11 Heave profile for loosely compacted coarse gravel backfill with log spiral failure surfaces from PYCAP with best-fit" (Case II) and "most-representative" (Case III) parameters

10.9 Horizontal Movement of Backfill

String potentiometers were used to measure movement in the backfill. Figure 10-12 shows the movement of each of the monitoring points in the densely compacted clean sand backfill compared to the movement of the pile cap face. The backfill displacement ranges from

3.3 in (83 mm) (100% of cap displacement) at the cap face to 0.23 in (5.9 mm) (7% of cap displacement) at 18 ft (5.5 m) from the cap face. This translational movement represents the amount of the pile cap displacement not absorbed through compressive strain up to the monitoring point.

Figure 10-13 shows the compressive strain corresponding to each static push of the pile cap. The compressive strain ranges from 0.055 to 0.003 within the backfill zone. As expected, the strain is highest in the interval closest to the pile cap face and is relatively uniform with distance away from the cap up to the maximum distance monitored. Minor variation from interval to interval may indicate the potential sensitivity of the string potentiometer measurements to differential pushing of the pile cap (not all the monitoring stakes were on the same end of the cap face) and tipping in the monitoring stakes themselves during the dynamic shaking. Movement of the stakes could explain the presence of some negative strain amounts in the calculations.

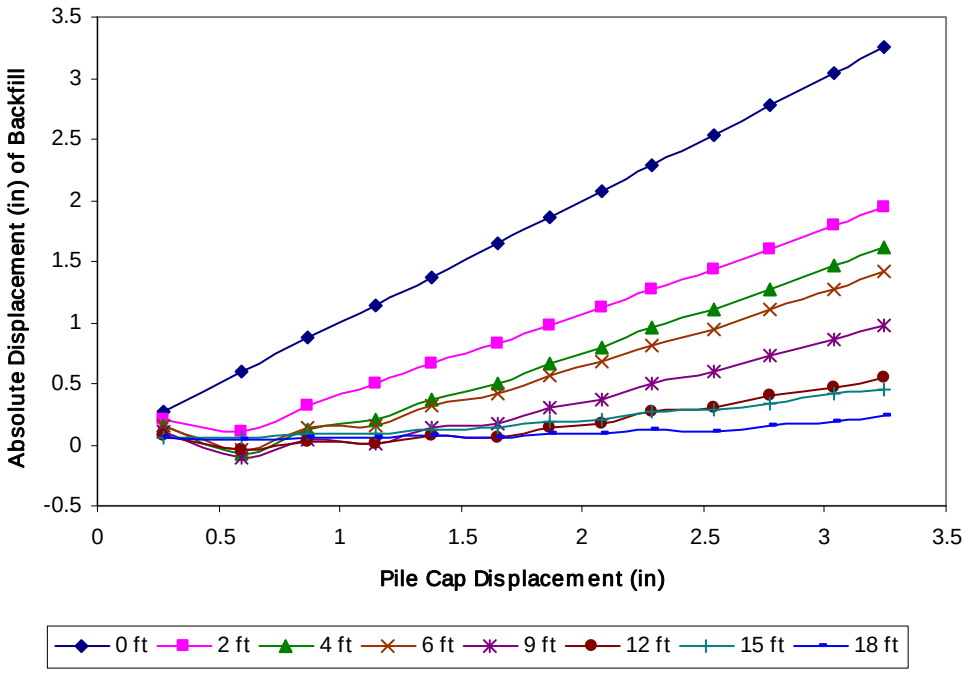

Figure 10-12 Displacement of monitoring points in loosely compacted coarse gravel backfill

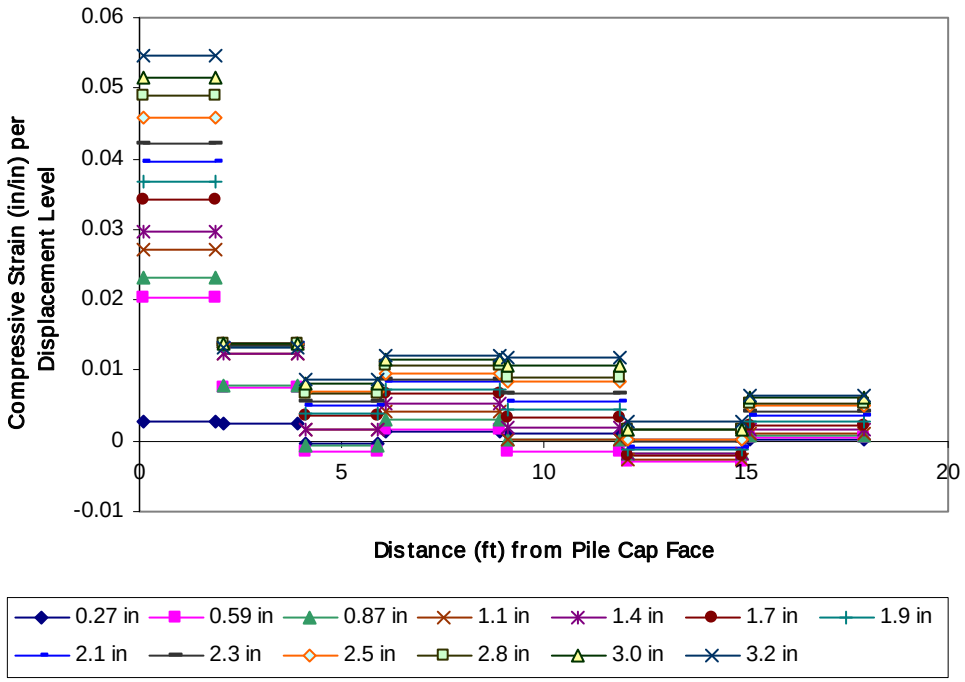

Figure 10-13 Strain per displacement level for loosely compacted coarse gravel backfill

11.0 PILE CAP WITH 3-FOOT WIDE DENSELY COMPACTED FINE GRAVEL ZONE AND LOOSELY COMPACTED CLEAN SAND BACKFILL

11.1 General

The pile cap with a 3-ft (0.91-m) wide gravel zone and loosely compacted clean sand backfill was tested on June 1, 2007. No significant deviations from the general test procedure occurred during this test, excepting a breakdown of the shaker prior to the final two displacement levels. Table 11-1 summarizes the test in terms of loads and displacements measured at the end of each "static push" with the actuators. The table also indicates the order in which cyclic loads from the actuators and dynamic loads from the shaker were applied.

Table 11-1 Summary of test with 3-ft wide gravel zone and loosely compacted clean sand backfill

Displacement Interval	Displacement (in)	Actuator Load (kN)	Actuator Cycles	Shaker Cycles
1	0.17	121	First	Second
2	0.38	175	Second	First
3	0.67	259	First	Second
4	0.98	343	Second	First
5	1.2	378	First	Second
6	1.4	441	Second	First
7	1.7	508	First	Second
8	1.9	568	Second	First
9	2.2	633	First	Malfunction
10	2.5	699	Second	Malfunction

11.2 Load-Displacement Response

Figure 11-1 shows the entire actuator load verses pile cap displacement relationship for the test, with static pushes, actuator cycles and shaker cycles being represented by green, blue, and red data points, respectively. Section 3.2 provides some discussion relative to the details of interpreting this data.

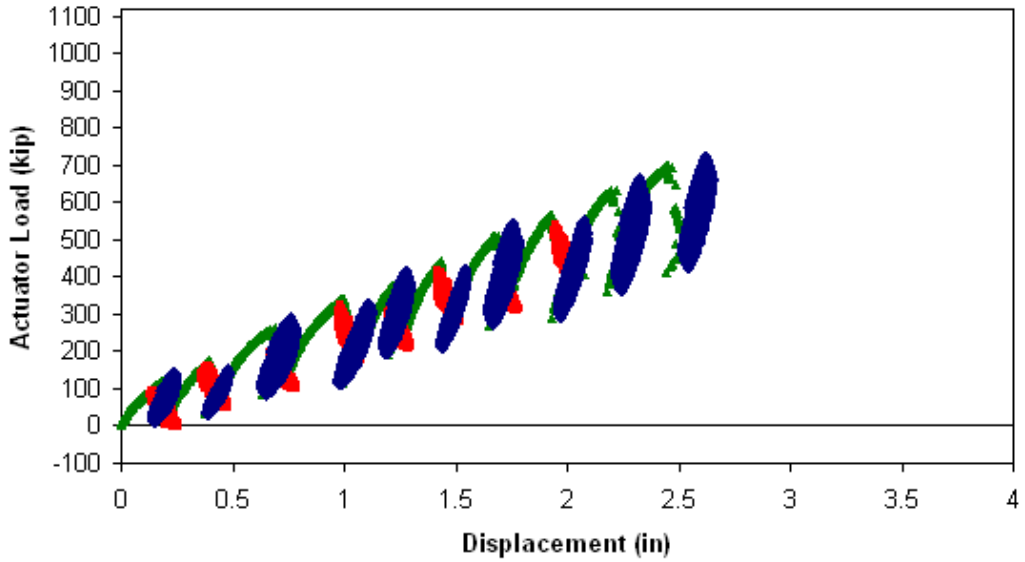

Figure 11-1 Actuator load versus pile cap displacement with 3-ft wide gravel zone and loosely compacted clean sand backfill (Test 4; June 1, 2007)

Figure 11-2 shows three load-displacement response curves for the pile cap: one for the response with backfill in place (referred to as the total response, which is the equivalent monotonic response or backbone curve derived from the data shown in Figure 11-1), one for the response with no backfill present (referred to as the baseline response), and one showing the passive earth response of the backfill (obtained by subtracting the baseline response from the total response.

The curves show that total response and baseline response increase at different rates until approximately 2.4 in (62 mm) of displacement, which is essentially the maximum 2.5 in (64 mm) displacement level for the test. By this point, the backfill response levels off as the baseline and total response seem to increase at approximately the same rate. Unfortunately, the pile cap was not pushed further for this test (and thus better confirm the obtaining of the ultimate resistance)

due to concerns of prematurely damaging the pile cap connections and altering the baseline response. Based on the data available, the ultimate passive resistance of the backfill, about 405 kip (1800 kN), appears to develop at a displacement of approximately 2.4 in (62 mm), which corresponds to a displacement to wall height ratio (Δ_{max}/H) of about 0.037.

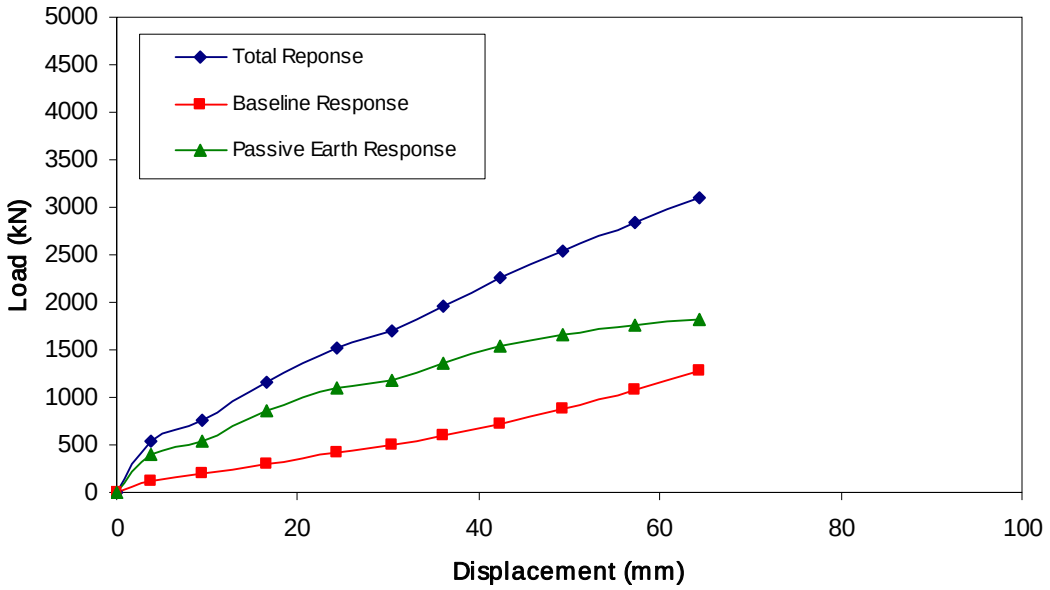

Figure 11-2 Total, baseline, and passive earth responses for pile cap with 3-ft densely compacted fine gravel zone and loosely compacted clean sand backfill

11.3 Response to Cyclic Actuator Loading

After slowly pushing the pile cap to each displacement interval, alternating combinations of small displacement cyclic actuator loads and dynamic shaker loads were applied. The response of the pile cap to the small displacement amplitude loading cycles from the actuator is presented and discussed in this section. Figure 11-3 shows the loop displacement amplitude, stiffness, loop area, and damping ratio for the pile cap with backfill in place as a function of pile cap displacement. Values are based on the median of the 15 low frequency cycles performed at each displacement level. Aside from a jump to about 0.07 in (1.8 mm) during the third and fourth static pushes, the displacement amplitude remains fairly constant with a median value of about 0.06 in (1.5 mm). The stiffness increases from about 1000 to 2050 kip/in (175 to 360 kN/mm) as the cap displacement increases; this appears to be due to greater mobilization of the backfill soil's passive strength and pile stiffness. The stiffness data particularly exhibits the

saw-tooth shaped trend as seen in other tests due to the alternating order of the static and dynamic cycling loading phases. The damping ratio decreases somewhat linearly from 24% to 19% with a median value of approximately 20%. The stiffness and damping values are closer to the values for the full width, densely compacted fine gravel backfill than for the full width, loosely compacted clean sand backfill.

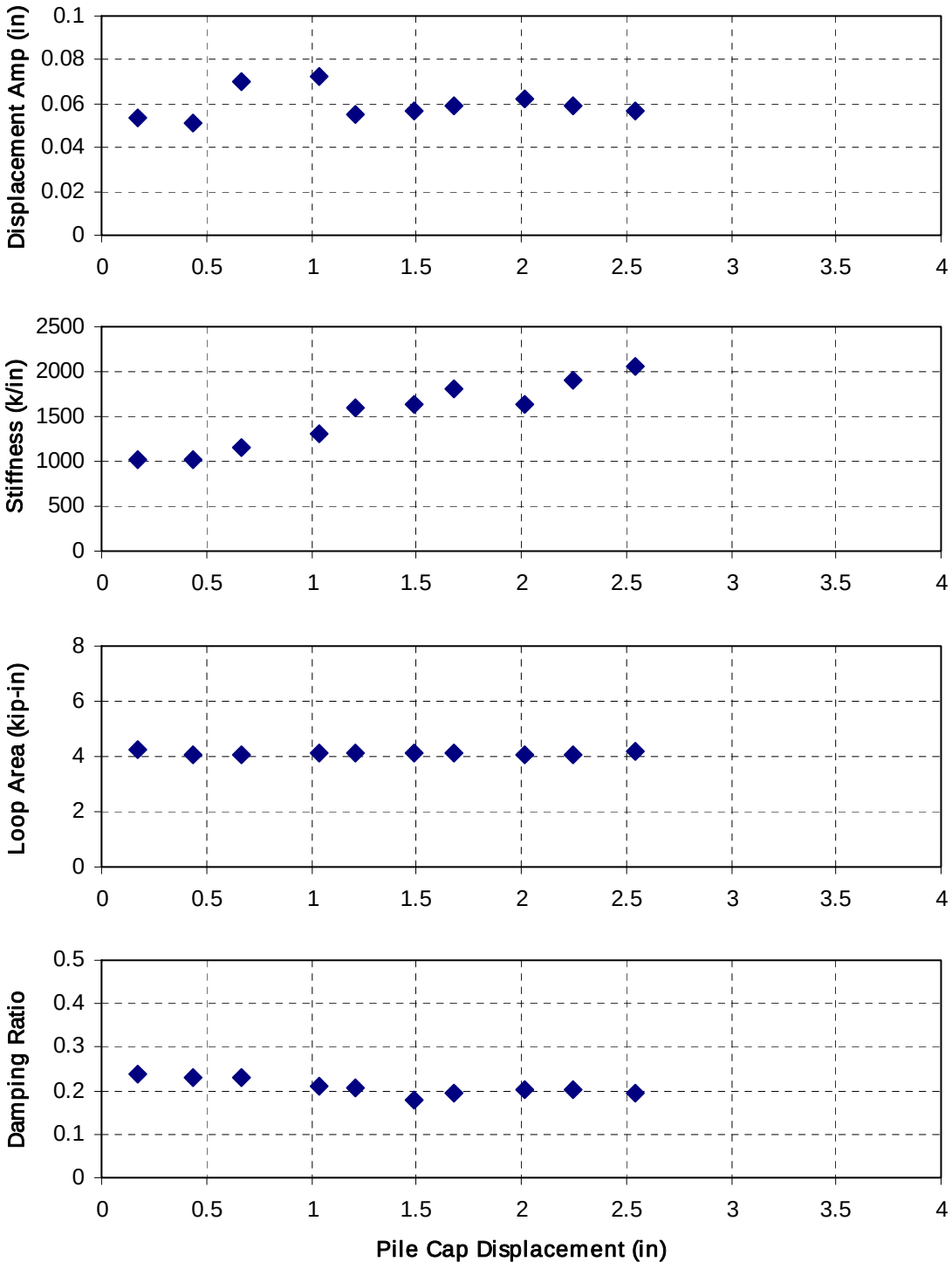

Figure 11-3 Summary of response to cyclic actuator loadings for pile cap with 3-ft densely compacted fine gravel zone and loosely compacted clean sand backfill

11.4 Passive Earth Pressure Distributions

In addition to the load-displacement response data, passive earth pressure from the backfill soil was measured directly with a vertical array of six earth pressure cells evenly distributed in the central portion of the pile cap face. Figure 11-4 shows the pressure measured by the pressure cells with depth at the end of each static push interval.

The pressure cell data show that earth pressure is relatively uniform with depth along the pile cap until the near the bottom where the pressure increases (becoming nearly double that occurring at the next highest pressure cell under maximum loading conditions). Figure 11-5 shows the backfill force calculated by multiplying each measured pressure by the respective contributory areas of the pile cap face. In general, the resulting force-displacement curve has a nearly identical trend to that based on the actuators, but it is systematically lower. Applying a multiplier of 1.67 (the inverse of 0.6 determined in Section 3.5) to the cell-based curve provides a better match with the actuator-based curve, but it is still systematically lower; the agreement could be improved by using a larger multiplier. From these two figures, there is no definite indication that the maximum earth pressure is realized much before the maximum displacement level.

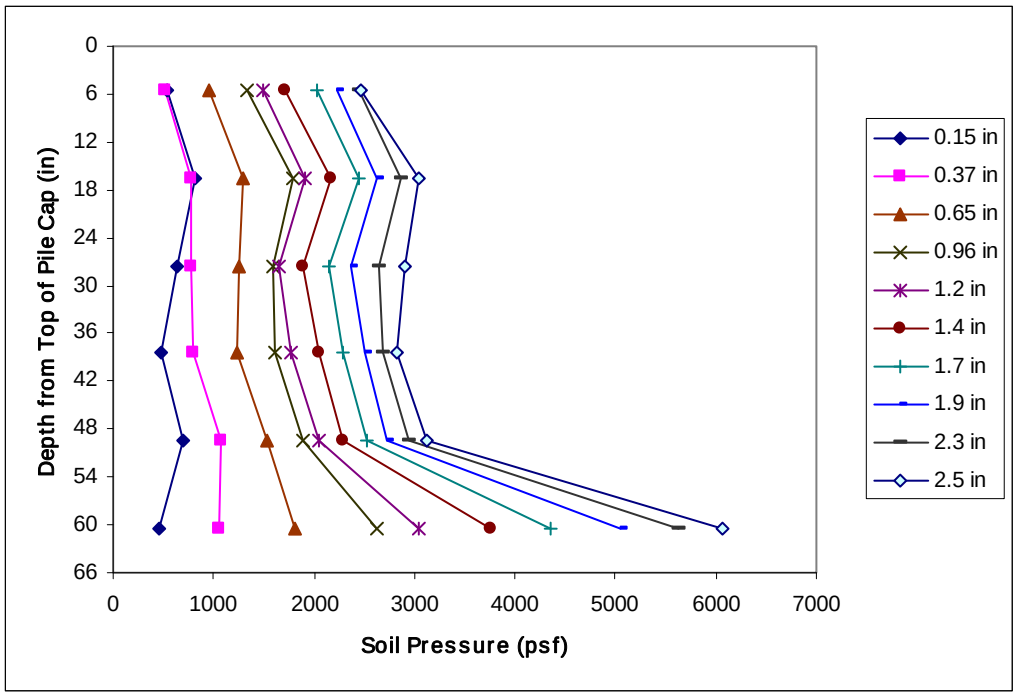

Figure 11-4 Earth pressure distribution as a function of pile cap displacement with 3-ft wide gravel zone and loosely compacted clean sand

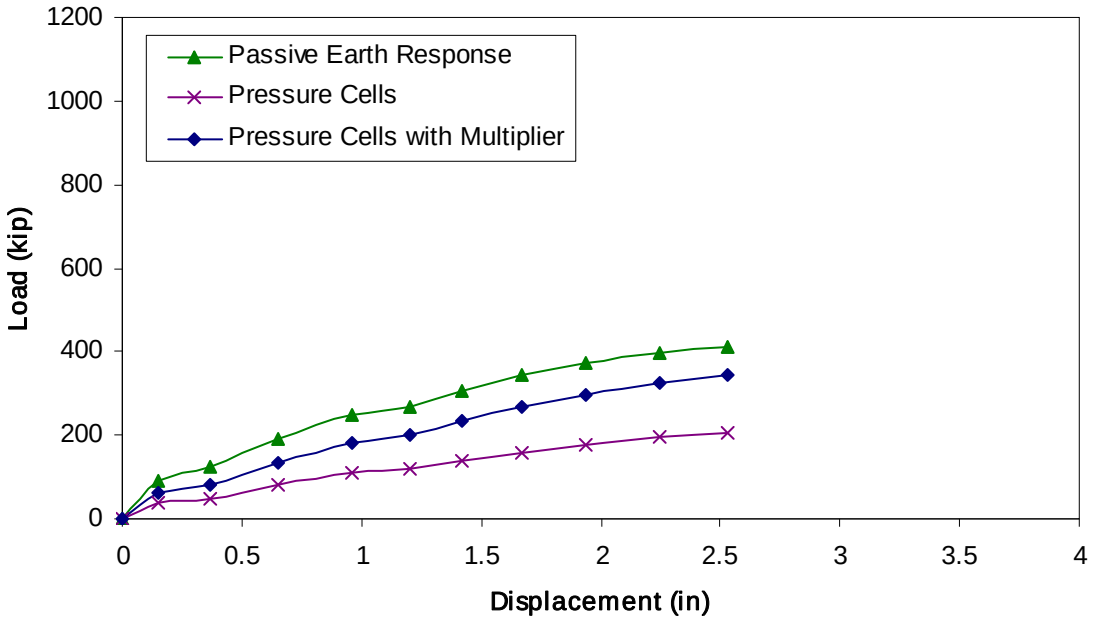

Figure 11-5 Comparison of earth forces based on actuators and pressure cells for 3-ft densely compacted fine gravel zone with loosely compacted clean sand backfill

11.5 Cracking and Vertical Movement of Backfill

Figure 11-6 is a two part plot showing the results of static and dynamic testing on the surface of the 3-ft (0.91-m) densely compacted fine gravel zone with loosely compacted clean sand backfill test area. The first part of the figure shows the surface cracks that developed during each static push of the pile cap. The surface cracks in the backfill likely indicate the presence of failure surfaces within the soil. Cracking within the 3-ft (0.91-m) wide zone of densely compacted fine gravel is characterized by pronounced cracks radiating out from the corner of the pile cap to the outer corners of the gravel zone. These cracks then become less pronounced and terminate within a distance of a meter in the loosely compacted clean sand. Most of the cracking in the clean sand is in the transverse direction, bounded by the radial cracks projecting from gravel zone. The concentration of cracks extending out from the edges of the cap face are similar to those seen in the densely compacted backfill material, while the horizontal cracking

beyond the gravel zone recalls the stress-bulb shaped cracking pattern observed in the full width loosely compacted clean sand backfill.

The second part of the figure is a contour map of the change in elevation of the surface of the backfill during testing. The typical elevation change, as represented by the median elevation change in a given row (parallel to the face of the cap) of grid nodes, is about 0.9 in (23 mm) at 8 ft (2.44 m) from the pile cap face, which is in the loosely compacted clean sand portion of the backfill. The contour map shows some heave in the vicinity of the gravel zone, but the amount of heave more than doubles in the first 12 in (0.3 m) of the loosely compacted clean sand backfill. The muted elevation change in the gravel zone may suggest that much of the stress from the cap is transmitted through the gravel zone into the backfill beyond. Most of the elevation change occurs within about

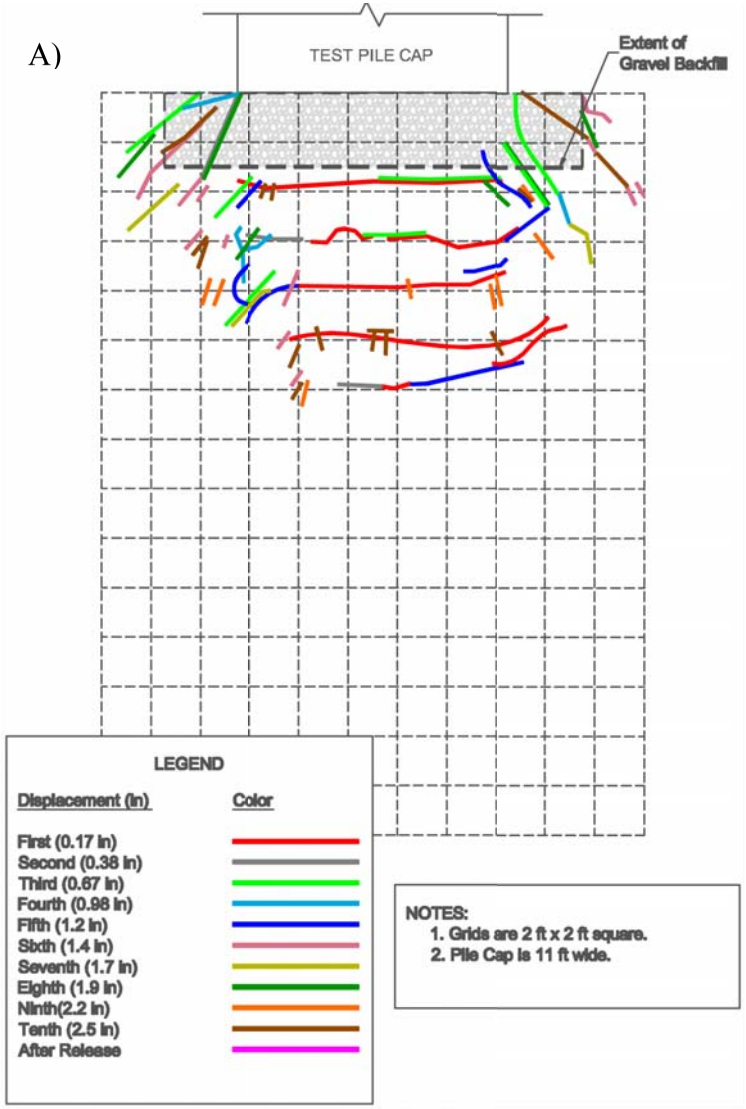

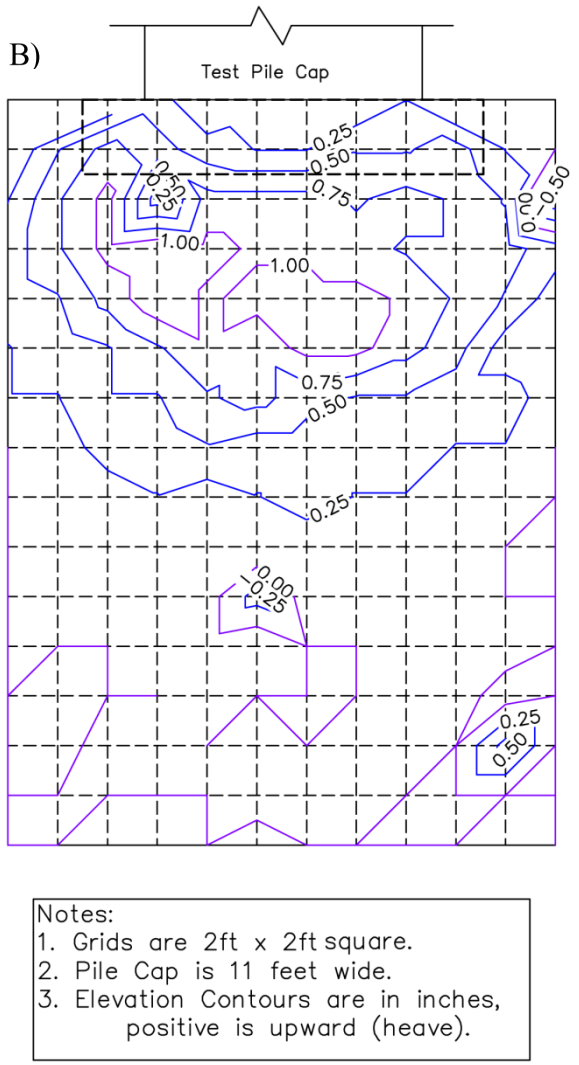

Figure 11-6 Crack patterns (A) and heave contours (B) for 3-ft gravel zone with loosely compacted clean sand

16 ft (5 m) from the pile cap face, which suggests that the failure surface daylights around 13 ft (4 m) past the end of the 3 ft (0.91 m) fine gravel zone.

11.6 Horizontal Movement of Backfills

String potentiometers were used to measure movement in the backfill. Figure 11-7 shows the movement of each of the monitoring points in the densely compacted clean sand backfill compared to the movement of the pile cap face. The monitoring point farthest from the cap did not move appreciably during the last static push. This lack of translational movement indicates that the displacement of the pile cap is absorbed through compressive strain. Displacement in the backfill ranged from 2.5 in (64 mm) (100% of the pile cap movement) at the cap face to 0.24 in (6.2 mm) (10% of the pile cap movement) at 18 ft (5.5 m) from the pile cap face. The monitoring point at 2 ft (0.6 m) from the cap face experienced almost 97% of the displacement of the pile cap, suggesting that the 3 ft (0.91 m) gravel zone moved as an integral block into the backfill behind it. The monitoring point at 15 ft (4.5 m) from the cap face appears to move less than the point 3 ft (0.91 m) farther from the cap. This might be explained by the location where the potentiometers were attached to the pile cap, with the potentiometer monitoring the 15 ft (4.5 m) point being on the other side of the pile cap from the potentiometer monitoring the 18 ft

(5.5 m) point. Differential movement of the pile cap face from east to west sides would cause one point to appear to move slightly more than the other. However, it is clear that most of the pile cap displacement has already been absorbed by compressive strain by the time it is transmitted to the 15 ft (4.5 m) point.

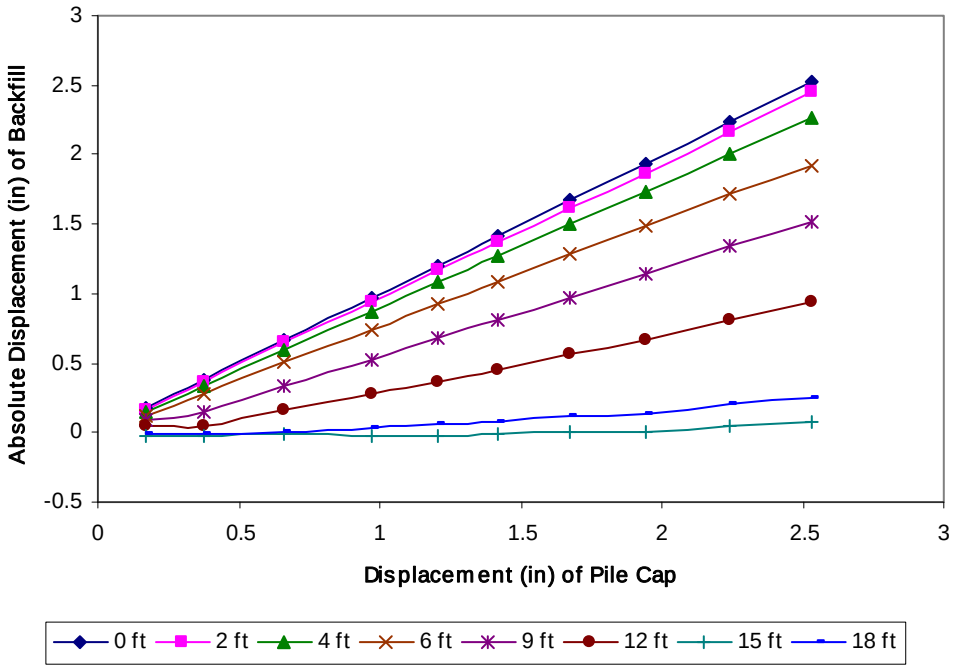

Figure 11-7 Displacement of monitoring points in 3-ft wide densely compacted fine gravel zone with loosely compacted clean sand backfill

Figure 11-8 shows the compressive strain corresponding to each static push of the pile cap. In this case, the 2-ft (0.6-m) interval closest to the cap experiences very little compressive strain over the course of the test. Compressive strains reach more significant levels in the intervals beyond the gravel zone in the loosely compacted clean sand. The strains in the regions beyond the gravel zone are fairly evenly distributed, except for the last interval, which initially appears to not experience any compressive strain; however, given the potential for differential movement from one side of the cap to the other, it seems likely that the amount of strain is actually a relatively small, compressive amount.

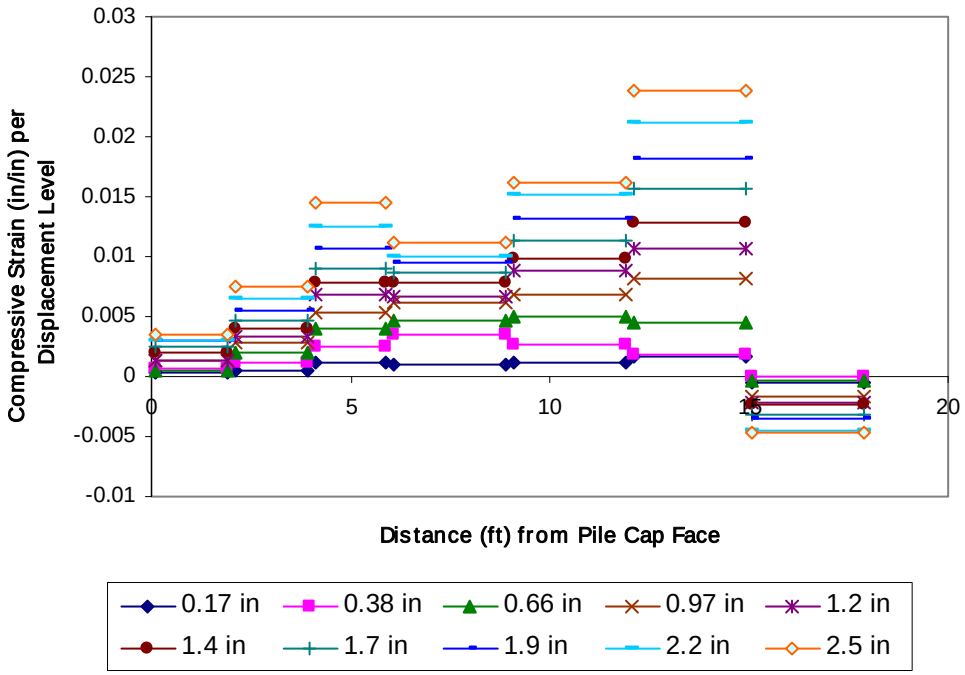

Figure 11-8 Strain per displacement level for a 3-ft wide densely compacted fine gravel zone with loosely compacted sand backfill

12.0 PILE CAP WITH 6-FOOT WIDE DENSELY COMPACTED FINE GRAVEL ZONE AND LOOSELY COMPACTED CLEAN SAND BACKFILL

12.1 General

The pile cap with a 6-ft wide gravel zone and loosely compacted clean sand backfill was tested on June 4, 2007. No significant deviations from the general test procedure occurred during this test. Table 12-1 summarizes the test in terms of loads and displacements measured at the end of each "static push" with the actuators. The table also indicates the order in which cyclic loads from the actuators and dynamic loads from the shaker were applied. During this test, the load-displacement response unexpectedly appeared to be very similar to that of the previous test with a 3-ft wide gravel zone.

Table 12-1 Summary of test with 6-ft wide gravel zone and loosely compacted clean sand backfill)

Displacement Interval	Displacement (in)	Actuator Load (kip)	Actuator Cycles	Shaker Cycles
1	0.13	120	First	Second
2	0.43	234	Second	First
3	0.67	281	First	Second
4	0.94	352	Second	First
5	1.3	421	First	Second
6	1.5	473	Second	First
7	1.8	523	First	Second
8	2.0	569	Second	First
9	2.2	614	First	Second
10	2.5	652	Second	First
11	2.8	696	None	None
12	3.0	763	Second	First

In order to help determine if there was a significant difference in the ultimate passive forces between the two tests, and if the ultimate soil resistance was being significantly affected by the cyclic and dynamic loads, the pile cap was pushed in excess of the maximum previous

amount of about 2.5 in to 3.0 in (64 mm to 75 mm), and the cyclic and dynamic loads were omitted for one displacement interval.

12.2 Load-Displacement Response

Figure 12-1 shows the entire actuator load verses pile cap displacement relationship for the test, with static pushes, actuator cycles and shaker cycles being represented by green, blue, and red data points, respectively. Section 3.2 provides some discussion relative to the details of interpreting this data.

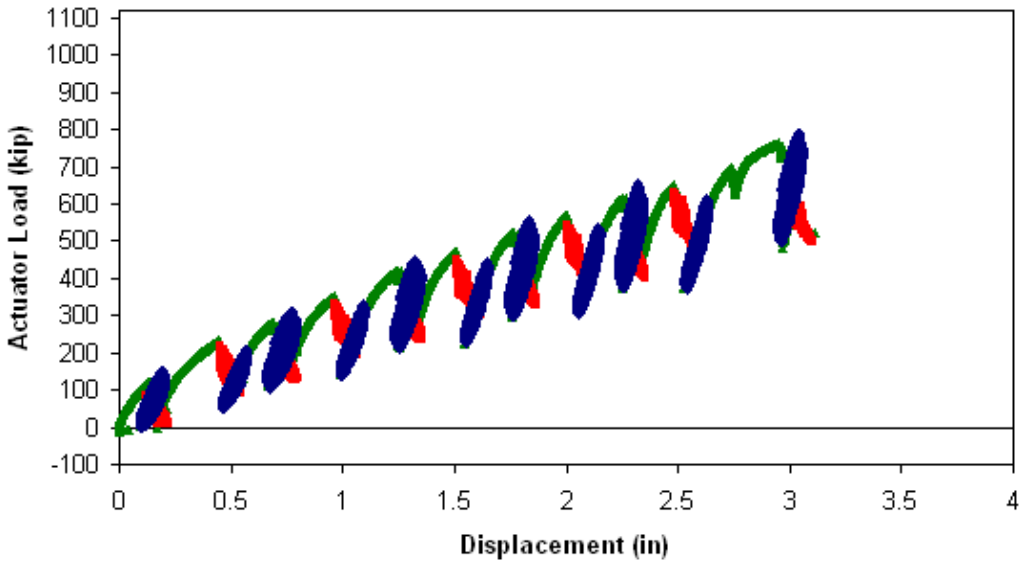

Figure 12-1 Actuator load versus pile cap displacement with 6-ft wide grave zone and loosely compacted clean sand backfill (Test 6; June 4, 2007)

Figure 12-2 shows three load-displacement response curves for the pile cap: one for the response with backfill in place (referred to as the total response, which is the equivalent monotonic response or backbone curve derived from the data shown in Figure 12-1), one for the response with no backfill present (referred to as the baseline response), and one showing the passive earth response of the backfill (obtained by subtracting the baseline response from the total response.

The curves show that total response and baseline response increase at different rates until approximately 2.4 in (62 mm) of displacement. By this point, the backfill response levels off as the baseline and total response increase at approximately the same rate. However, with

additional displacement to nearly 3.0 in (75 mm), there appears to be a 10% increase in passive earth resistance, suggesting that the ultimate state has not quite been reached by the end of the test and/or this is the approximate effect of the omitting the cyclic and dynamic loadings in the previous displacement increment of 0.47 in (12 mm). The maximum passive resistance of the backfill at the end of the test is

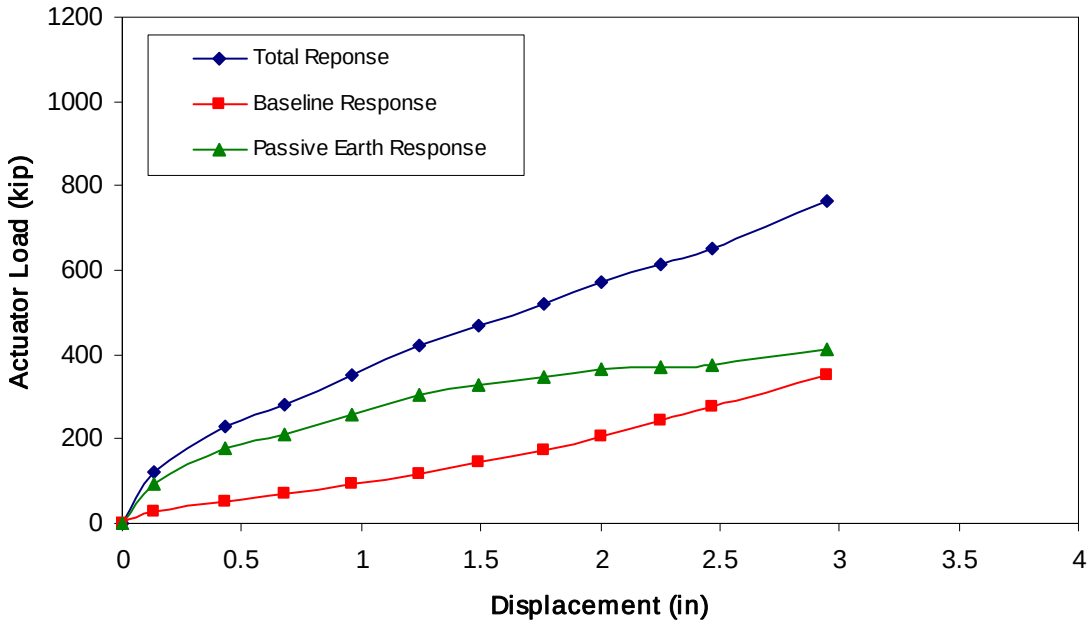

Figure 12-2 Total, baseline, and passive earth responses for pile cap with 6-ft densely compacted fine gravel zone and loosely compacted clean sand backfill

about 411 kip (1830 kN) and ultimate resistance is developed at a displacement to wall height ratio (Δ_{max}/H) somewhat greater than 0.045.

12.3 Response to Cyclic Actuator Loading

After slowly pushing the pile cap to each displacement interval, alternating combinations of small displacement cyclic actuator loads and dynamic shaker loads were applied. The response of the pile cap to the small displacement amplitude loading cycles from the actuator is presented and discussed in this section. Figure 12-3 shows the loop displacement amplitude, stiffness, loop area, and damping ratio for the pile cap with backfill in place as a function of pile cap displacement. Values are based on the median of the 15 low frequency cycles performed at each displacement level. Despite minor variation from one pile cap displacement to the next, the

displacement amplitude remains fairly constant with a median value of approximately 0.05 in (1.3 mm). The stiffness increases from 1140 to 2280 kip/in (200 to 400 kN/mm) as the cap displacement increases; this appears to be due to greater mobilization of the backfill soil's passive strength and pile stiffness. The damping ratio decreases from 25% to 18% with a median damping ratio of approximately 20%. The stiffness, damping, and displacement amplitude data exhibit the saw-tooth shaped trend as seen in other tests due to the alternating order of the static and dynamic cycling loading phases. Stiffness and damping values for the 6-ft (1.83-m) fine gravel zone are more consistent with the full width, densely compacted fine gravel backfill results than the loosely compacted clean sand results.

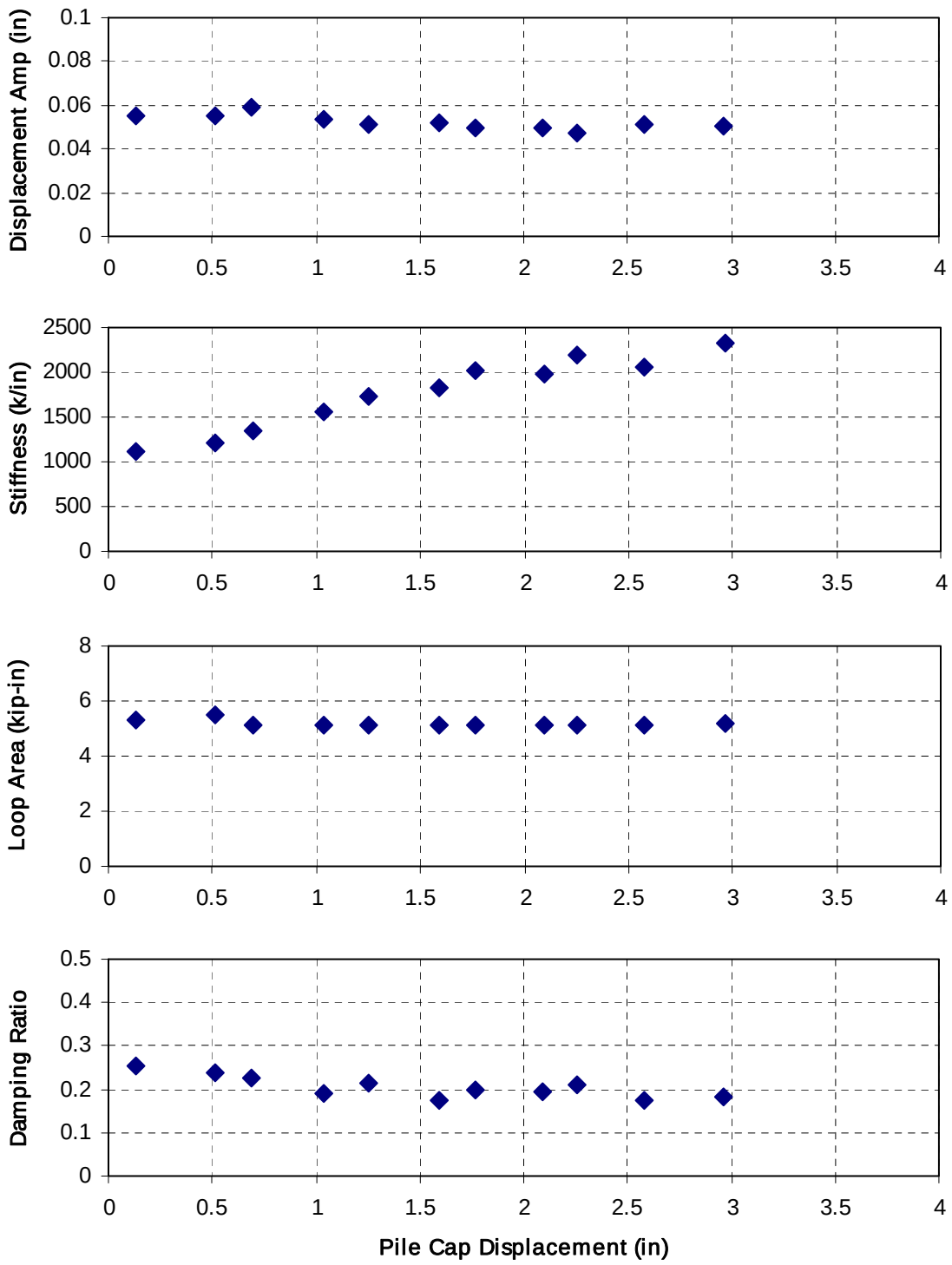

Figure 12-3 Summary of response to cyclic actuator loadings for pile cap with 6-ft densely compacted fine gravel zone with loosely compacted clean sand backfill

12.4 Passive Earth Pressure Distributions

In addition to the load-displacement response data, passive earth pressure from the backfill soil was measured directly with a vertical array of six earth pressure cells evenly distributed in the central portion of the pile cap face. Figure 12-4 shows the pressure measured by the pressure cells with depth at the end of each static push interval.

The profiles suggest that the soil pressure is concentrated in the upper two-thirds of the tip cap height. It is apparent that the measured pressure distribution does not match the normal representation of pressure increasing with depth. After the first several pushes, the bottom pressure cell shows a decrease in pressure with increasing displacement. While the trend in the lower most pressure cell is consistent with that observed in other tests (as also discussed in Section 3.5), the pressure cell above it also displays unexpected behavior by measuring significant increases in pressure for the first two or three pile cap displacement intervals, then grouping the measurements for the remaining cap displacements between 1880 and 2190 psf (90 and 105 kPa); the pressure cell still appears to measure increasing pressure with increasing pile cap displacement, but the increases are relatively insignificant. Another interesting aspect of the pressure distribution in Figure 12-4 is the steady increase in pressure in the upper-most pressure cell. After the 0.94 in (24 mm) pile cap displacement, the measurements in the top pressure cell are larger than the bottom cell, eventually resulting in what resembles an inverted pressure distribution. This inversion of pressure concentration may be in part due to rotation effects.

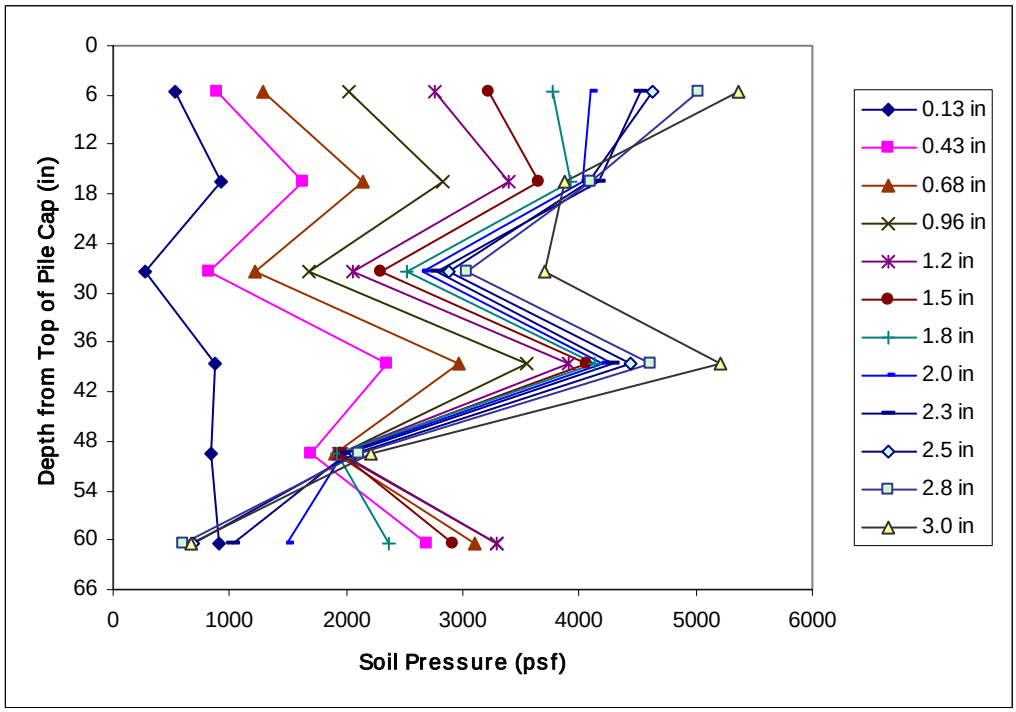

Figure 12-4 Earth pressure distribution as a function of pile cap displacement with 6-ft wide gravel zone with loosely compacted clean sand

Figure 12-5 shows the backfill force calculated by multiplying each measured pressure by the respective contributory areas of the pile cap face. In general, the resulting force-displacement curve has a similar trend to that based on the actuators, but it is systematically lower. Applying a multiplier of 1.67 (the inverse of 0.6 determined in Section 3.5), to the cell-based curve provides an improved match with the actuator-based curve. In this case, the modified pressure cell-based curve matches the actuator-based curve very well until about the 1.2 in (31 mm) pile cap displacement interval, where the modified pressure cell-based curve begins to underestimate the actuator-based curve. For the last four pile cap displacement intervals, the modified cell-based curve parallels the actuator-based curve, staying about 45 kip (200 kN) lower than it until the end of the test.

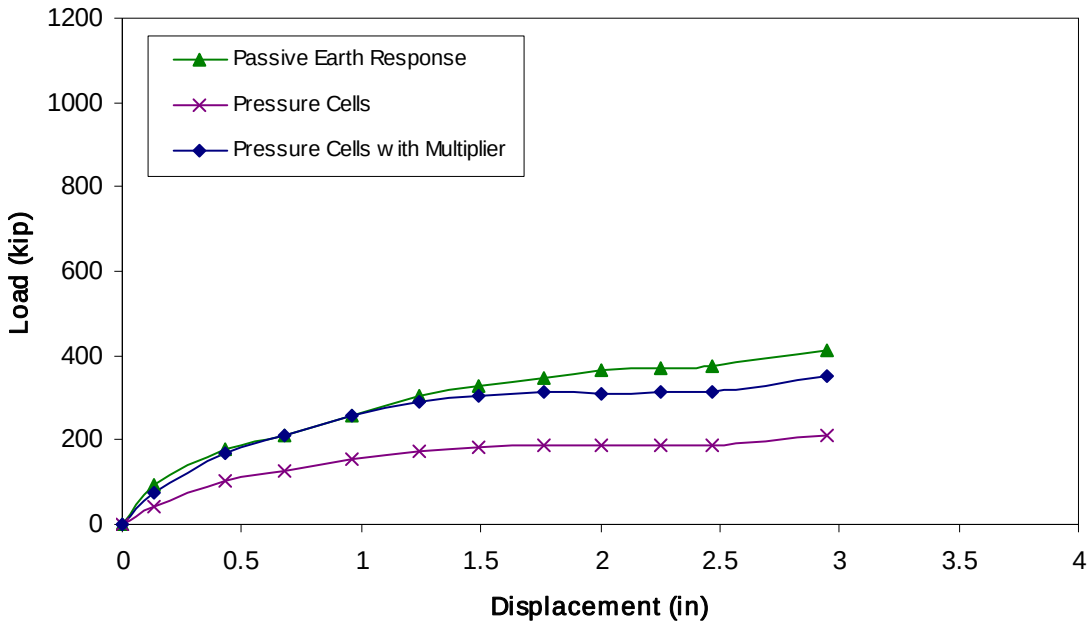

Figure 12-5 Comparison of earth forces based on actuators and pressure cells for 6-ft densely compacted fine gravel zone with loosely compacted clean sand backfill

12.5 Cracking and Vertical Movement of Backfill

Figure 12-6 is a two part plot showing the results of static and dynamic testing on the surface of the 6-ft (1.83-m) wide densely compacted fine gravel zone with loosely compacted clean sand backfill test area. The first part of the figure shows the surface cracks that developed during each static push of the pile cap. The surface cracks in the backfill potentially indicate the presence of failure surfaces within the soil. The combination of the cracking behavior seen in the densely compacted fine gravel and in the loosely compacted clean sand backfill materials is similar to that observed in the 3-ft (0.91-m) wide fine gravel zone backfill condition. A large group of cracks extending out from the edges recalls the behavior of other densely compacted backfill materials, while the horizontal cracking in the loosely compacted region beyond the gravel zone is characteristic of other loosely compacted backfill conditions. In this case, less transverse cracking is observed in the loosely compacted clean sand portion of the backfill.

The second part of the figure is a contour map of the change in elevation of the surface of the backfill area during testing. After an initial heave within the fine gravel zone at the pile cap face, the ground surface progressively heaves across the gravel zone, until the loosely compacted clean sand is reached, at which point greater heave occurs. The typical elevation change, as

represented by the median elevation change in a given row (parallel to the face of the cap) of grid nodes, is over 1.2 in (30 mm) at a distance between 8 and 10 ft (2.44 and 3.05 m) from the pile cap face, with the maximum recorded elevation change at a single node (about 1.5 in (40 mm)) occurring 10 ft from the face of the pile cap. Globally, the bulk of the elevation change occurs between the cap face and 13 ft (4 m) from the edge of the gravel zone; thus, it is reasonable to expect that the failure surface daylights about 20 ft (6 m) from the pile cap face.

12.6 Horizontal Movement of Backfill

String potentiometers were used to measure movement in the backfill. Figure 12-7 shows the movement of each of the monitoring points in the 6-ft (1.83-m) wide densely compacted fine gravel zone with loosely compacted clean sand backfill compared to the movement of the pile cap face. Backfill displacement ranged from 3.0 in (75 mm) (100% of pile cap displacement) at the cap face to 0.24 in (6 mm) (8% of pile cap deflection) at the monitoring point 18 ft (5.5 m) away from the cap face. Unlike the 3-ft (0.91-m) wide fine gravel zone backfill condition, the first 2 ft (0.6 m) of the 6-ft (1.83-m) wide gravel zone backfill condition compressed slightly, although the monitoring point still moved 2.4 in (62 mm) (89% of pile cap deflection). The difference

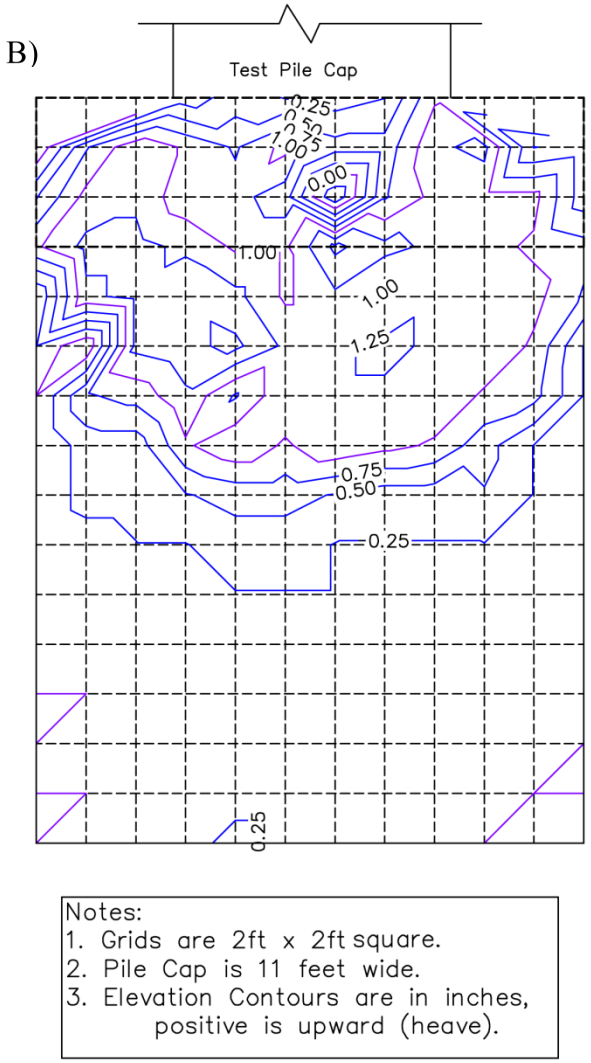

Figure 12-6 Crack pattern (A) and heave contour (B) maps for 6-ft gravel

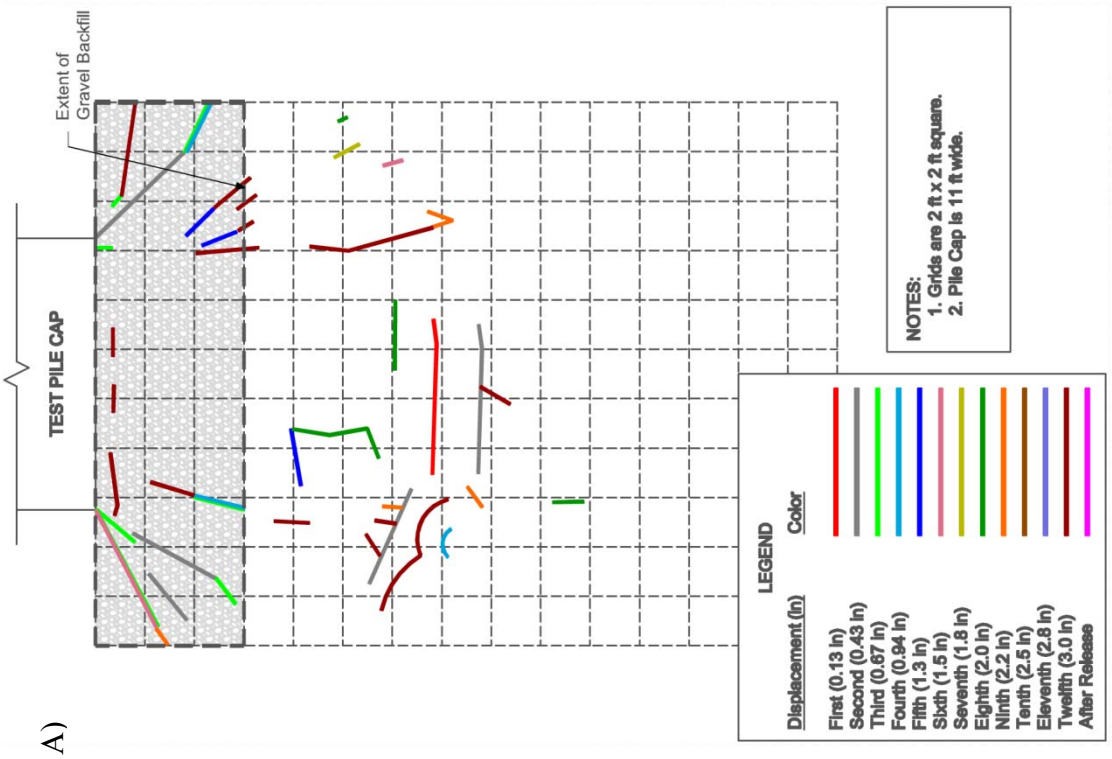

A)

in movement between the 2 and the 6 ft (0.6 and the 1.8 m) monitoring points is about 0.04 in (1 mm), suggesting that after initially compressing the gravel zone, the zone moved as a single body and transmitted almost all of the motion of the pile cap into the loosely compacted clean sand backfill behind it; this phenomenon can also be seen in the 3-ft (0.91-m) wide gravel zone condition. The motion of the monitoring points represents the movement of the backfill due to the displacement of the pile cap that has not be absorbed by compressive strain in the backfill up to that point. String pots attached to monitoring points beyond the gravel zone record that absorption is fairly uniform in the loosely compacted sand backfill.

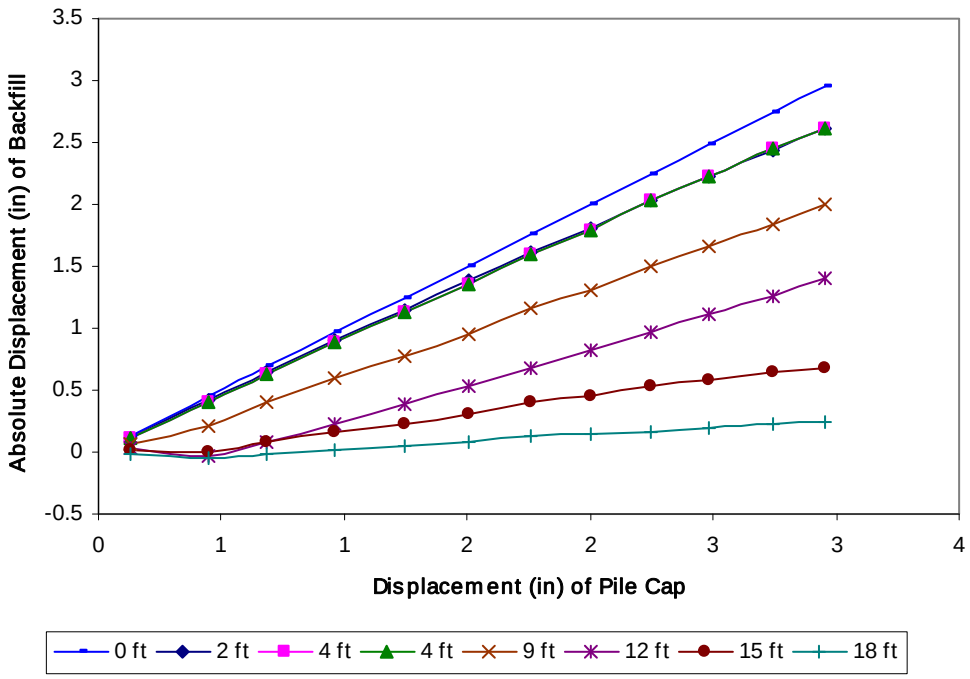

Figure 12-7 Displacement of monitoring points in 6-ft wide densely compacted fine gravel zone with loosely compacted sand backfill

Figure 12-8 shows the compressive strain corresponding to each static push of the pile cap. In this case, the 2-ft (0.6-m) interval closest to the cap experiences a moderate amount of compressive strain with the following 4 ft (1.2 m) experiencing almost no appreciable strain. Compressive strains reach more significant levels in the intervals beyond the densely compacted gravel zone, within the loosely compacted clean sand. The strains in the regions beyond the zone are fairly evenly distributed. Minor variation from interval to interval may indicate the potential sensitivity of the string potentiometer measurements to differential pushing of the pile cap (not all the monitoring stakes were on the same end of the cap face) and tipping of the monitoring stakes themselves.

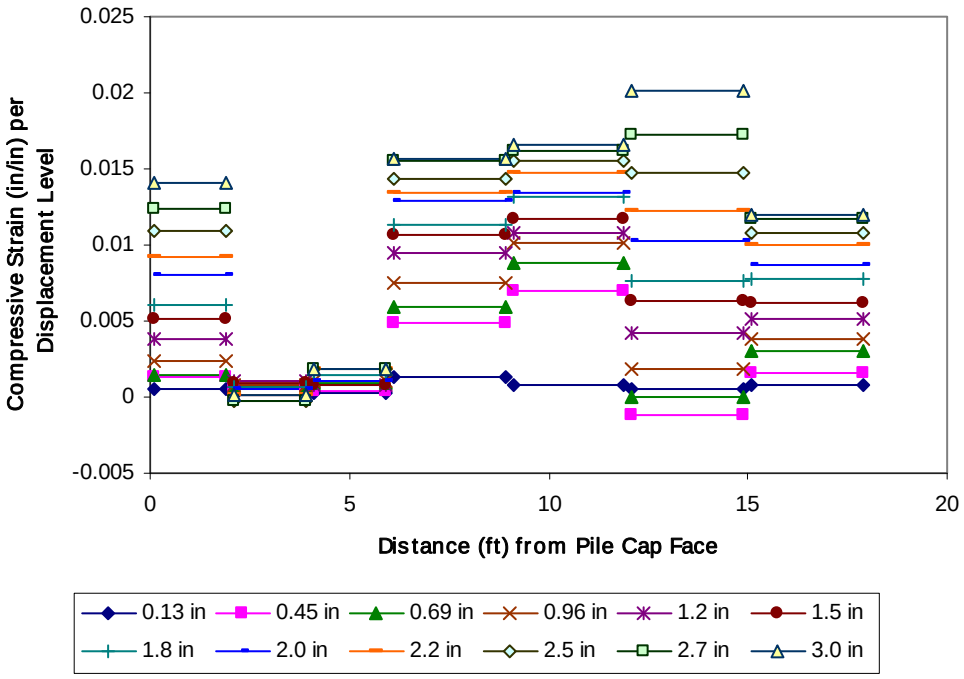

Figure 12-8 Strain per displacement level for a 6-ft wide densely compacted gravel zone with loosely compacted sand backfill

THIS PAGE INTENTIONALLY LEFT BLANK

13.0 EVALUATION AND COMPARISON OF DIFFERENT BACKFILL CONDITIONS

13.1 Measured Passive Earth Resistance Based on Soil Type and Compactive Effort

Quantifying the passive earth resistance of different backfill soil types with differing compactive efforts was of primary interest during this research. As described in Section 2.4, three backfill soil types, each in two different density states, were tested. Two partial widths of dense gravel backfill with otherwise loosely compacted clean sand were also tested. Table 13-1 summarizes the peak resistance provided by each of the backfill soil conditions along with the displacement at which the soil reaches failure. Comparisons of the passive force-displacement curves for each backfill material in its loosely and densely compacted states are subsequently shown in Figure 13-1 to Figure 13-3, while the passive force-displacement curves of the three densely and loosely compacted soil types are shown in Table 13-1 and Table 13-2, respectively.

As shown in the table and figures, the densely compacted coarse gravel provided the most passive resistance, followed by the densely compacted fine gravel and then the densely compacted sand. In their loosely compacted state and out to the displacement levels tested, the clean sand, fine gravel, and coarse gravel backfill provided only 20, 27, and 40%, respectively, of their densely compacted load capacity. The clear disparity in the peak values and shapes of the backfill resistance curves for the densely and loosely compacted backfills highlights the importance of obtaining adequate compaction. When considered in light of the differing patterns of horizontal strain, vertical heaving / settlement, and cracking observed, it appears that different resistance-developing mechanisms are in play. In the densely compacted soils, resistance appears to develop as shear is developed along a curvilinear failure plane. This contention is further substantiated by the generally good agreement between measured and calculated passive earth forces (presented previously for each soil type) obtained with strength parameters obtained from in-situ field testing. However, in the loosely compacted backfills, the soils appear to compress in an area very near the face of the pile cap without significant strains occurring farther away in the backfill, and resistance is significantly less than the calculated ultimate resistance, even at otherwise relatively large displacement levels. This behavior is akin to a punching

failure in a bearing capacity analysis where shear failure planes are not well defined and the resistance developed is due to incremental compression of the soil soft or loose soil beneath.

Table 13-1 Peak passive earth resistance and associated displacement for various backfill conditions

Backfill Type	Peak Resistance (kip)	Δ_{max} (in)	Δ_{max}/H
Densely Compacted Clean Sand	443	2.0	0.030
Loosely Compacted Clean Sand	88	1.5	0.023
Densely Compacted Fine Gravel	643	2.4	0.037
Loosely Compacted Fine Gravel	184	≥ 2.5	--
Densely Compacted Coarse Gravel	760	≈ 2.9	0.044
Loosely Compacted Coarse Gravel	301	≥ 2.9	--
3-ft Fine Gravel Zone	405	≈ 2.5	0.037
6-ft Fine Gravel Zone	411	≥ 3.0	--

Note: the presence of the "≥" symbol indicates that the backfill did not appear to reach its ultimate strength by the maximum displacement level of the test; peak resistance in such cases are the maximum observed resistance.

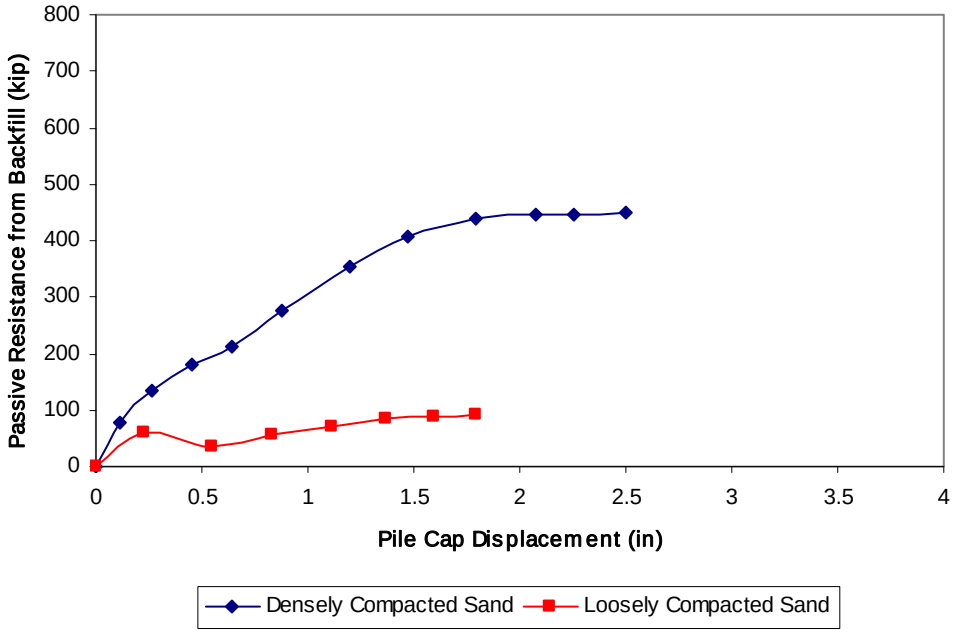

Figure 13-1 Comparison of passive earth force-displacement curves for densely and loosely compacted clean sand backfill

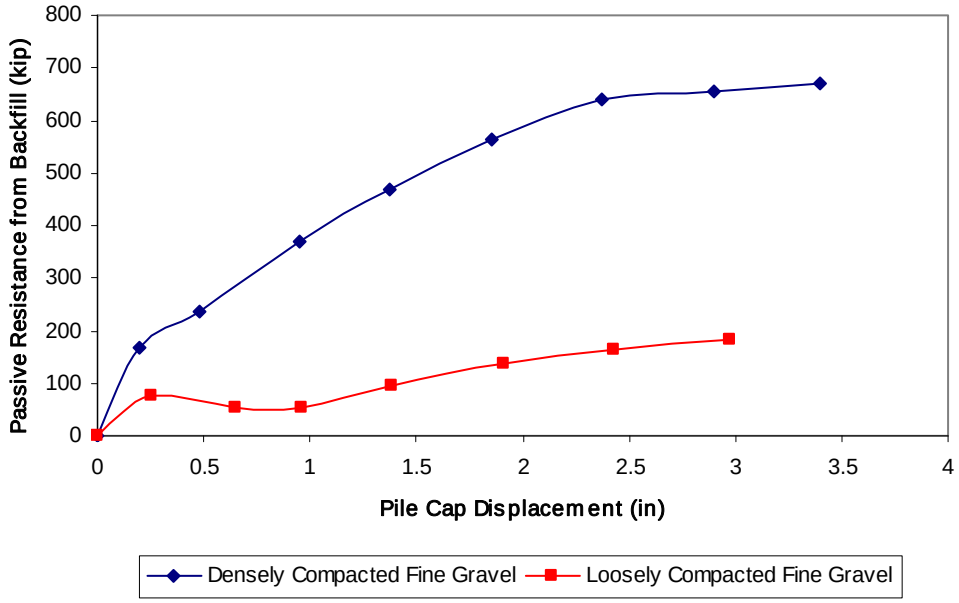

Figure 13-2 Comparison of passive earth force-displacement curves for densely and loosely compacted fine gravel backfill

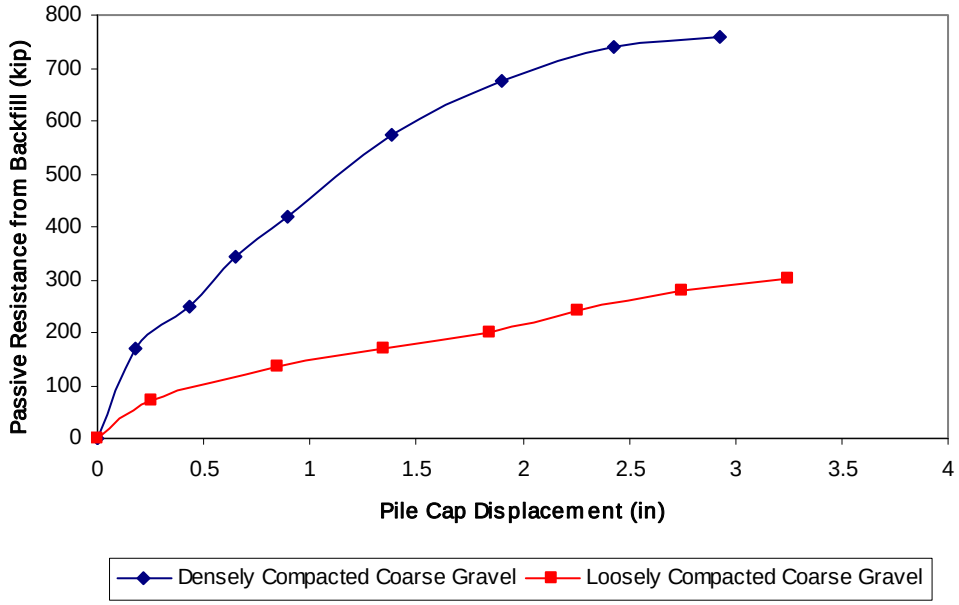

Figure 13-3 Comparison of passive earth force-displacement curves for densely and loosely compacted coarse gravel backfill

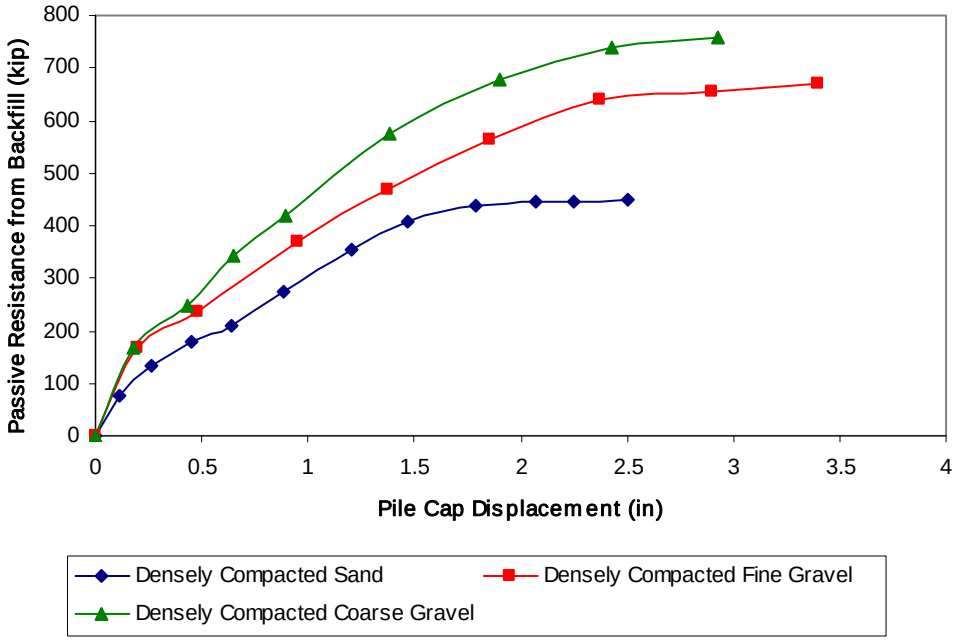

Figure 13-4 Comparison of earth force-displacement curves for densely compacted backfills

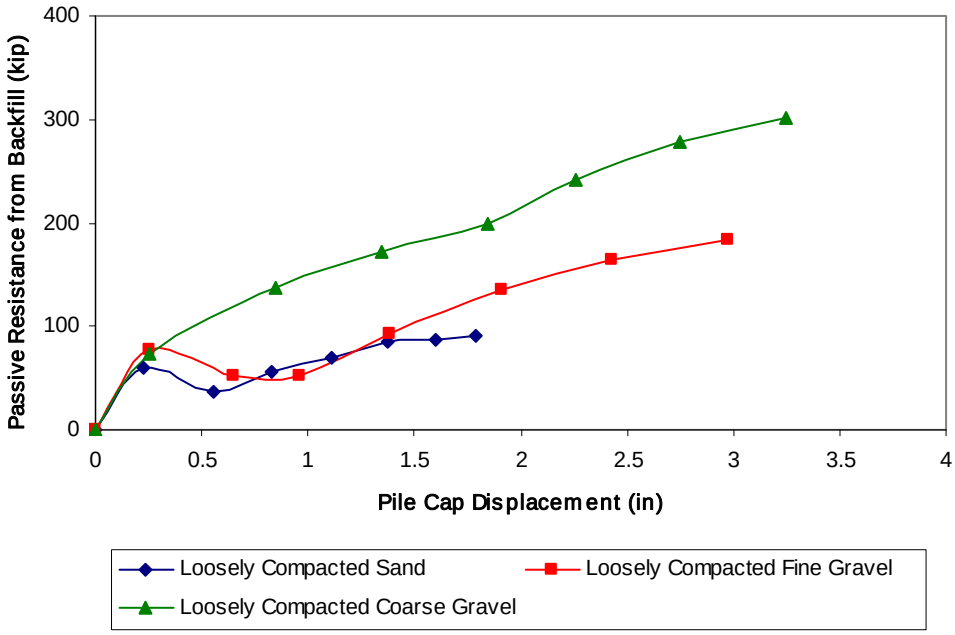

Figure 13-5 Comparison of earth force-displacement curves for loosely compacted backfills

For the loosely compacted soils, the peak passive resistance cited in the table generally corresponds to the load at the end of each test; more resistance may have developed if the tests could have been conducted to higher displacement levels. (Maximum displacement levels during testing were limited by equipment capacities as well as concern of damaging the pile-to-cap connections when subjected to greater displacements). Because the loosely compacted fine and coarse gravel (see Figure 13-5) exhibit a gradually increasing load resistance up to the maximum displacement in the test, it may be misleading to identify this displacement as $\square_{max}$; hence, values for this parameter have not been provided in the table for the fine and coarse gravel backfill soils.

In general, the development or mobilization of passive earth force for the densely compacted backfills was observed to occur by a pile cap displacement-to-height- ratio of approximately 0.02 to 0.04. By way of comparison, the upper bound is relatively close to the 0.05 wall displacement-to-height ratio recently proposed for design by Shamsabadi and Yan (2008), but the lower bound is still appreciably larger than the 0.01 proposed by AASHTO (2007) for dense soils. The load-displacement curves tend to follow a hyperbolic curve, although the initial loading portion is flatter than one typically associates with a static, monotonic load-displacement curve. This softened initial response is believed to be an effect of the dynamic and cyclic loadings.

13.2 Engineering Parameters to Calculate Earth Forces for Backfill

Starting with field and laboratory measured values of shear strength, load-displacement relationships were calculated for each backfill soil using the a modified version of the spreadsheet program PYCAP, developed by Duncan and Mokwa (2001), which implements the classical log-spiral solution for passive force with a hyperbolic displacement curve; and the computer program entitled ABUTMENT, which implements the Log Spiral Hyperbolic (LSH) approach presented by Shamsabadi et al. (2007). Parameters were varied until a good match (within 5% of the peak observed resistance) was obtained between measured and calculated curves for each method. Typically, adjustments were made only to cohesion and the interface friction angle. Emphasis was placed on comparing measured and calculated ultimate passive

forces rather than initial loading stiffnesses. In general, the initial stiffnesses of the load-displacement curves from the testing presented in this thesis tend to be flatter by about 50% than the slope generally associated with static, monotonic load-displacement curves. Dynamic and cyclic loading effects seem to contribute to this behavior, although creep displacement of the cap between the time of backfill placement and the start of load testing (typically about a day) may also be a contributing factor. However, it is anticipated that the underlying piles were able to resist the at-rest earth forces resulting from backfill placement without appreciable movement of the pile cap.

A summary of the engineering parameters which provide the best match with the measured backfill response as calculated using the PYCAP spreadsheet and the ABUTMENT program is provided in Table 13-2. The load-displacement curves corresponding to the given parameters are shown in preceding chapters for each backfill type. In contrast to Table 13-2, Table 13-3 summarizes the engineering parameters believed to best represent field conditions and have not been optimized to obtain a "best fit" between measured and calculated ultimate passive earth pressures. The corresponding load-displacement curves are presented in Figure 13-6 and Figure 13-7.

Table 13-2 "Best fit" engineering parameters used to calculate passive earth forces for backfills

Backfill Type	$\gamma_{m,avg}$ (pcf)	ϕ (°)	PYCAP		ABUTMENT	
			c (psf)	δ (°)	c (psf)	δ (°)
Densely Compacted Clean Sand	116.4	40.5	0.0	30.4	84	29.0
Loosely Compacted Clean Sand	105.0	37.3	0.0	0.0	0.0	0.0
Densely Compacted Fine Gravel	137.8	44.0	0.0	27.0	84	27.0
Loosely Compacted Fine Gravel	122.6	43.0	0.0	4.0	0.0	4.0
Densely Compacted Coarse Gravel	138.4	41.0	286	26.0	286	30.8
Loosely Compacted Coarse Gravel	128.7	50.0	0.0	4.2	0.0	4.2

Table 13-3 "Most-representative" engineering parameters used to calculate passive earth forces for backfills

Backfill Type	$\gamma_{m,avg}$ (pcf)	ϕ (°)	c (psf)	δ (°)	Calculated and Measured Force Difference (%)
Densely Compacted Clean Sand	116.4	40.5	0.0	29.0	-3
Loosely Compacted Clean Sand	105.0	37.3	0.0	0.0	+10
Densely Compacted Fine Gravel	137.8	44.0	84*	27.0	+5*
Loosely Compacted Fine Gravel	122.6	43.0	0.0	0.0	-16
Densely Compacted Coarse Gravel	138.4	41.0	286	24.6	-4
Loosely Compacted Coarse Gravel	128.7	40.0	0.0	24.0	+15

* Cohesion reduced to a nominal value; with c=410 psf from in-situ test, the resulting difference is +76%

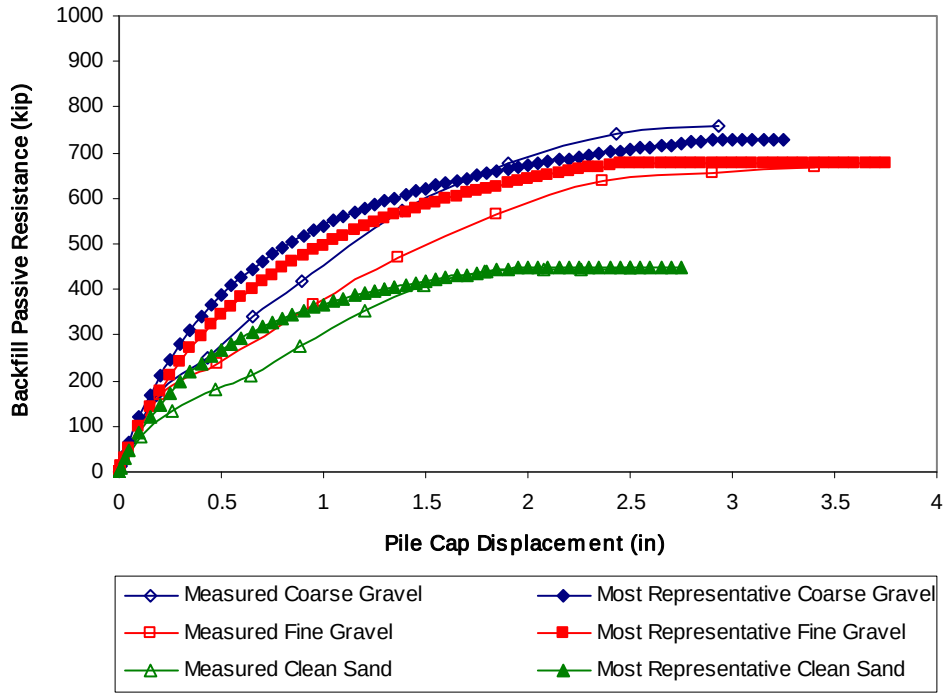

Figure 13-6 Summary of measured versus calculated load-displacement curves for densely compacted backfill materials using "most representative" parameters

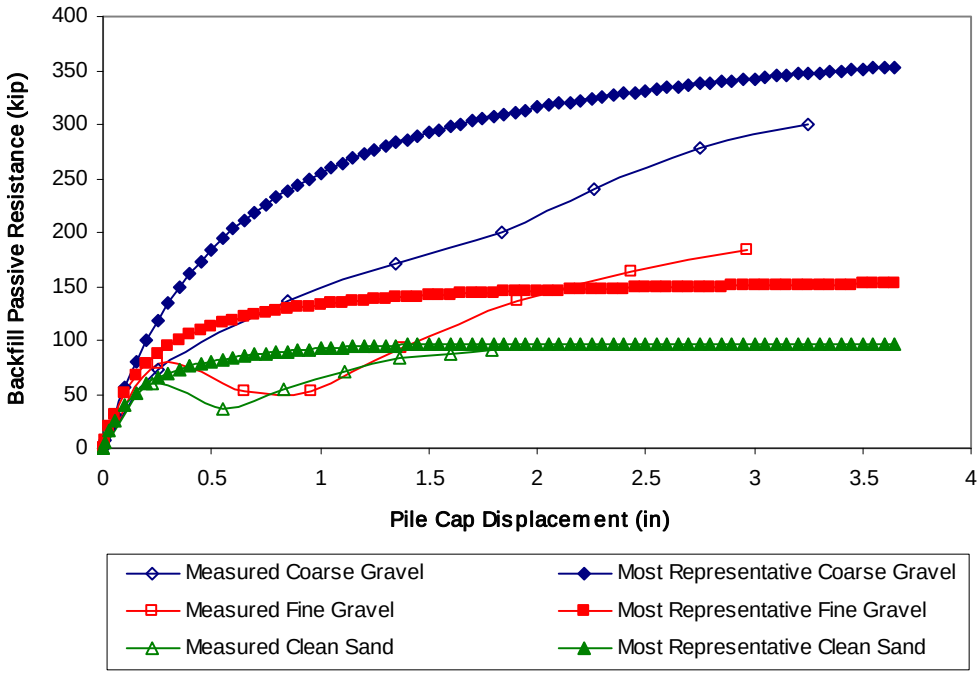

Figure 13-7 Summary of measured versus calculated load-displacement curves for loosely compacted backfill materials using "most-representative" parameters

Passive earth pressure calculations using both PYCAP and ABUTMENT (LSH) generally matched well against the measured data for the densely compacted soils without significant adjustment to the strength parameters, provided that in-situ field test parameters were used. It was observed that the addition of approximately 84 psf (4 kPa) of cohesion in the ABUTMENT model was often required to obtain agreement with the PYCAP model.

In contrast with the more densely compacted soils, judicial manipulation of the strength parameters was required to match model-based response to the measured data for the less densely compacted soils. The interface friction generally had to be reduced and the displacement required to mobilize the ultimate passive force was typically assumed to be double that required for the densely compacted soil (thereby setting the displacement to failure beyond the displacement range in the test). The reduction or elimination of the interface friction (thereby creating conditions corresponding to Rankine earth pressure conditions) dramatically reduces the computed earth pressure coefficient and typically produces better matches with field data for the loosely compacted soils. The reduction in interface friction also seems consistent with the settlement observed near the pile cap face when loosely compacted backfill was used.

Given the belief that the failure of the loosely compacted backfills deform primarily due to punching rather than general shear failure, another approach to modeling the response of the loosely compacted backfills was also used. Rather than reducing the interface friction, the frictional strength of the backfill soil was reduced by an iteratively determined factor. This approach is similar to the one-third strength reduction method suggested by Terzaghi and Peck (1967) for dealing with local shear effects for the bearing capacity of loose to medium sands. The shear strength parameters used for each of the loosely compacted materials examined were the laboratory-determined ultimate friction angle for the clean sand (reliable field test data for this material was not available), the friction angle from in-situ testing (the nominal cohesion was neglected) for the loosely compacted fine gravel, and the friction angle from in-situ testing (there was no cohesion) for the loosely compacted coarse gravel. The reduced friction angle was obtained by taking the inverse tangent of the tangent of the original friction angle multiplied by 0.60, 0.65, and 0.85 for the clean sand, fine gravel, and coarse gravel, respectively. These reduced parameters were used with the log-spiral method implemented in the spreadsheet program PYCAP. Figure 13-8 gives a summary of the matches obtained from the log-spiral

computations for the reduced parameters. The 0.6 and 0.65 factors for the clean sand and fine gravel are quite consistent with the 0.67 factor suggested by Terzaghi and Peck for bearing capacity with a localized punching failure mode. The previously discussed Rankine solution also produces a reasonably accurate match for both the loosely compacted clean sand and the loosely compacted fine gravel (although the resulting failure surfaces are different from those obtained with the reduction method); however, the loosely compacted coarse gravel is not well represented by Rankine passive earth theory. With respect to the coarse gravel and the 0.85 factor, this higher factor could stem from the intermediate relative density of the loosely compacted coarse gravel and a failure mode which may be between pure punching and pure general shear.

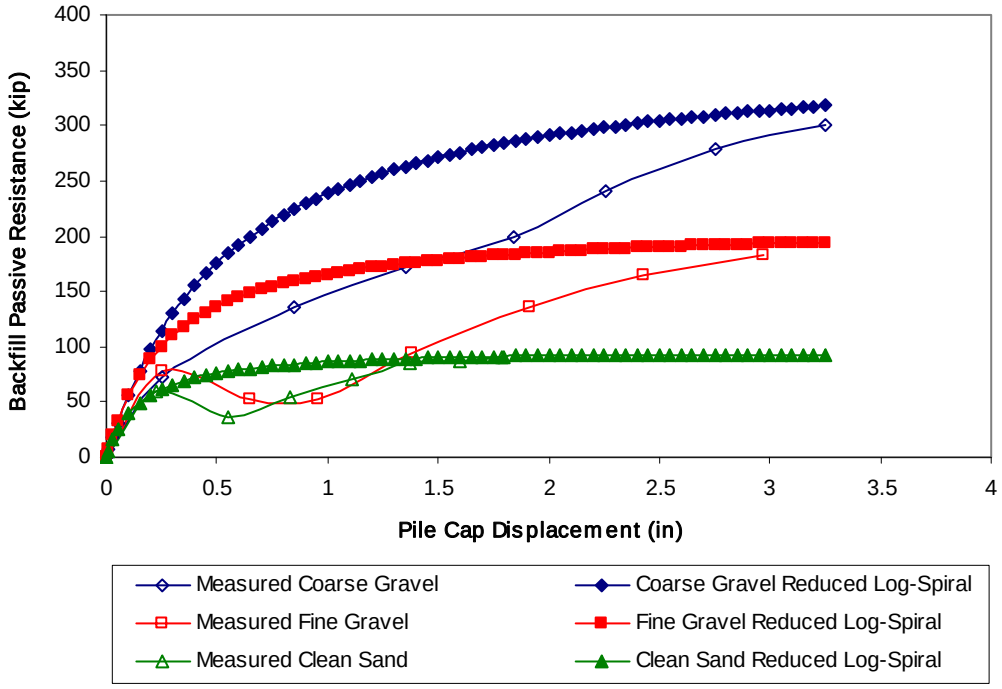

Figure 13-8 Comparison of measured load-displacement curves for loosely compacted backfill materials and those computed using reduced shear strength parameters in the log-spiral approach

13.3 Response of Pile Cap and Backfill to Cyclic Actuator and Dynamic Shaker Loadings

Quantifying the variations in response of the pile cap response with backfill soil types when subject to cyclic and dynamic loadings was also of interest during this research. Table 13-4 summarizes the reloading stiffness and damping ratio for the pile cap with each backfill

condition due to slowly applied, cyclic actuator loadings while Table 13-5 summarizes the natural frequency, reloading stiffness, and damping ratio for the pile cap with each backfill condition subject to dynamic shaker loadings in the frequency range of 4 to 10 Hz.

Table 13-4 Summary of pile cap with backfill response due to cyclic actuator loadings

Pile Cap with Backfill Condition	Displacement Amplitude (in)	Reloading Stiffness (kip/in)	Damping Ratio (%)
No Backfill (Baseline Response)	0.094 to 0.10	230 to 660	15 to 38
Densely Compacted Clean Sand	0.035 to 0.043	1140 to 2860	15 to 25
Loosely Compacted Clean Sand	0.051 to 0.063	570 to 1140	21 to 31
Densely Compacted Fine Gravel	0.051 to 0.091	1030 to 3030	15 to 23
Loosely Compacted Fine Gravel	0.055 to 0.071	510 to 1540	20 to 30
Densely Compacted Coarse Gravel	0.043 to 0.071	1370 to 3600	17 to 22
Loosely Compacted Coarse Gravel	0.075 to 0.098	690 to 1540	16 to 28

Table 13-5 Summary of pile cap with backfill response due to dynamic shaker loadings

Pile Cap with Backfill Condition	Natural Freq. (Hz)	Max. Disp. Amp (in)	Reloading Stiffness (k/in)	Damping Ratio (%)	
				Half-power Bandwidth	Load-Disp. Loops
No Backfill (Baseline Response)	5.0 to 6.5	0.091	570 to 1140	8 to 18	1 to 52
Densely Compacted Clean Sand	7.5 to 8.0	0.043	1710 to 3430	--	1 to 37
Loosely Compacted Clean Sand	5.0 to 6.5	0.059	1140 to 1710	15 to 25	1 to 28
Densely Compacted Fine Gravel	7.5 to 8.0	0.035	2280 to 5710	--	1 to 46
Loosely Compacted Fine Gravel	6.5 to 7.0	0.059	1140 to 2000	23 to 25	2 to 37
Densely Compacted Coarse Gravel	7.5	0.028	2280 to 5710	--	1 to 40
Loosely Compacted Coarse Gravel	7	0.059	1710 to 2860	23	1 to 60

In Table 13-4 (for cyclic actuator loadings), it is seen that the placement of backfill material significantly increases the reloading stiffness of the pile cap system, most particularly

when the backfill is densely compacted. The range in reloading stiffness for each backfill condition reflects increasing stiffness as the static displacement level of the pile cap increases during each test. Typically, reloading stiffness of the pile cap is at least doubled when densely compacted backfill is used instead of loosely compacted backfill. The average damping ratio of the pile cap by itself without backfill is approximately 26% and changes little with the placement of loosely compacted backfill. However, the damping ratio decreases to about 19 or 20% when the backfill is densely compacted for each of the granular soil types tested.

The response of the pile cap is somewhat different for dynamic shaker loadings as shown Table 13-5. However, comparisons between actuator- and shaker-based loadings are qualified by the differences in displacement amplitude for the two types of loadings (displacements from the shaker range from near 0 to 0.04 or 0.08 in (1 or 2 mm)) as well as the static displacement level of the pile cap. In general, damping ratios determined using the half-power bandwidth method are in the same range as, but with median values somewhat lower than, those measured from the actuator-based load displacement loops (15 to 25% when loosely compacted backfill was present). Reloading stiffness and damping determined from the shaker-based load-displacement loops are highly variable with frequency and displacement, but when displacement amplitudes from the shaker- and actuator-based load-displacement loops are similar (as they are with densely compacted clean sand backfill (see Figure 6-7), the loosely compacted clean sand backfill (see 7-7), and the loosely compacted fine gravel backfill (see Figure 8-7)), stiffness and damping are comparable. The stiffness and damping of the pile cap – backfill system varies significantly with forcing frequency because the backfill acts in and out of phase with the pile cap, which prevents simple quantification of dynamic parameters.

13.4 Cracking, Vertical Movement, and Horizontal Movement of Backfill

In certain cases, as with the clean sand and the loosely compacted coarse gravel backfill materials, the crack maps suggest much less movement than the heave contours. It was particularly difficult to map cracking in the clean sand backfills because the sand along the surface of the backfill, having little binder, tended the shift during the dynamic loading, obscuring the occurrence of cracking. The poorly graded nature and the relatively open matrix between particles in the coarse gravel made differentiation between individual cracks and natural gaps between particle contacts difficult. In some instances, a thin veneer of finer material was

placed over the backfill to help highlight the occurrence of cracking in the underlying gravel. It is for this reason that the crack map for the densely compacted coarse gravel is so much more detailed than the crack map for the less dense placement of this same material.

In general, cracking in the loosely compacted materials tended to be manifest as an arching or bulb pattern in front of the pile cap. Contrastingly, in the densely compacted materials, cracking generally appears to be oriented in an echelon pattern radiating out from the edge of the cap out to the periphery of the backfill. The loosely and densely compacted soils also exhibited distinctly different behaviors with respect to changes in elevation. The loosely compacted soil backfills, most particularly the clean sand, experienced settlement which decreased with increasing distance from the face of the pile cap. On the other hand, the densely compacted soil backfills exhibited heaving. For example, for the clean sand backfill, the loosely compacted soil experienced approximately 0.8 in (20 mm) of settlement immediately adjacent to the pile cap face whereas the densely compacted soil experienced approximately 1.2 in (30 mm) of heave at a distance of 6 ft (1.8 m) from the pile cap face. The occurrence of backfill heave or settlement appears to be strongly correlated with the amount of horizontal resistance developed by the backfill. Subsequent analyses showed that the loosely compacted soils fail to mobilize a large amount of their theoretical passive pressure within the range of displacements achieved during testing.

With respect to horizontal movement and compressive strain in the backfill, compressive strains on the order of 0.05 to 0.1 were experienced near the pile cap face when loosely compacted soils were present. For the densely compacted soils, the compressive strains were lower, being on the order of 0.02 to 0.25 in the same vicinity. Strains were much more evenly distributed in the densely compacted backfills. The distributions of measured horizontal strain for the different backfill conditions appear to correspond well with the heave/settlement patterns presented in the respective cracking and vertical movement sections for each backfill condition.

13.5 Effect of Partial Width Backfill

Figure 13-9 illustrates the effect of including a partial width of densely compacted fine gravel adjacent to the pile cap face in an otherwise loosely compacted clean sand. Without any gravel present, the resistance of the sand acting by itself is about 90 kip (400 kN) (at a displacement level of 1.8 in (45 mm)). The inclusion of either a 3- or 6-ft (0.91- or 1.83-m) wide

zone of densely compacted gravel increases the resistance of the loosely compacted sand backfill by almost 300% to approximately 360 kip (1600 kN) (at the same displacement level). This equates to over 60% of the resistance developed if the entire backfill area consisted of densely compacted fine gravel at a pile cap displacement level of 1.8 in (45 mm). The peak resistance and displacements at which the backfill reached failure is shown in Table 13-1. With the partial width gravel zone backfill conditions, ultimate resistance appears to be reached near the same displacement as the full-width, densely compacted fine gravel backfill (that is about 2.4 in (62 mm)). At 2.4 in (62 mm), the 3-ft (0.91-m) gravel zone provides approximately 34 kip (150 kN) more resistance than the 6-ft (1.83-m) gravel zone. This behavior was not expected; however, the 6-ft (1.83-m) zone continues to provide slightly increased resistance at later pile cap displacement levels, offering a resistance of 411 kip (1830 kN) after the final pile cap displacement interval.

At a pile cap displacement of 1.8 in (45 mm), the backfill with a 6-ft (1.83-m) zone of densely compacted fine gravel exhibits similar resistance to that of the 3-ft (0.91-m) wide zone. The reason for this behavior is unclear; one would likely expect an increase in resistance with increasing width of dense soil. This behavior differs from that observed during testing conducted at the I-15/South Temple test site using a smaller height pile cap (3.67 ft (1.12 m)) with 3- and 6-ft (0.91- and 1.82-m) wide zones of densely compacted gravel adjacent to the pile cap with the remaining backfill consisting of loosely compacted silty sand. As described in Rollins et al. (2010), "despite being thin relative to the overall shear length, the 0.92- and 1.82-m (3- and 6-ft) wide gravel zones increase lateral resistance to approximately 52% and 77%, respectively, of the resistance that would be provided by a backfill entirely composed of dense gravel." Figure 13-10, included for comparison with Figure 13-9, shows the increase in resistance with increasing width of gravel during testing at the I-15/South Temple test site. It is possible that the different pile cap face aspect ratios (4.6 and 2.0 for the South Temple and Airport pile caps, respectively) for the two sites (thus affecting the three-dimensional fanning of the failure plane), together with the differing ratios of partial gravel zone width to pile cap height (thus affecting the amount of the failure zone occupied by the compacted gravel), both contribute to the differences in observed increases in resistance with increasing partial gravel zone width. A possible scenario which might explain the differences observed between the two sites is that with increasing width of the gravel zone at the South Temple test site, the shear/failure plane

remained well within the gravel zone, thus providing greater shear resistance with increasing width of the gravel zone. Contrastingly, with increasing width of the gravel zone at the Airort site, the shear/failure plane may have exited the bottom of the gravel zone near the first 3 ft (0.91 m) of gravel and then picked up negligible resistance passing through the underlying soft, saturated clay before spiraling back up into the loosely compacted clean sand beyond the compacted gravel zone. In both cases, however, the partial widths of dense gravel do also appear to act as an extension of the pile cap, transferring load from the face of the cap to the face of the loosely compacted sand backfill. It is hoped that current finite element modeling efforts for the different tests at the two sites will better quantify the actual mechanisms involved. What does appear certain based on the tests conducted at both sites is that a nominal 3 ft (0.91 m) of densely compacted gravel zone backfill in

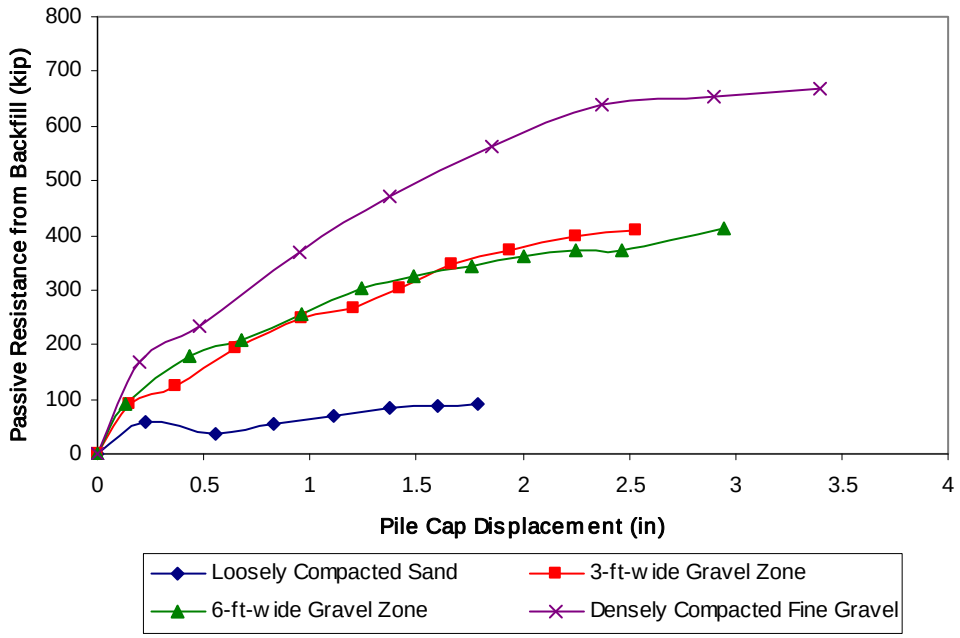

Figure 13-9 Comparison of earth force-displacement curves for loosely compacted clean sand backfill with varying widths of densely compacted gravel

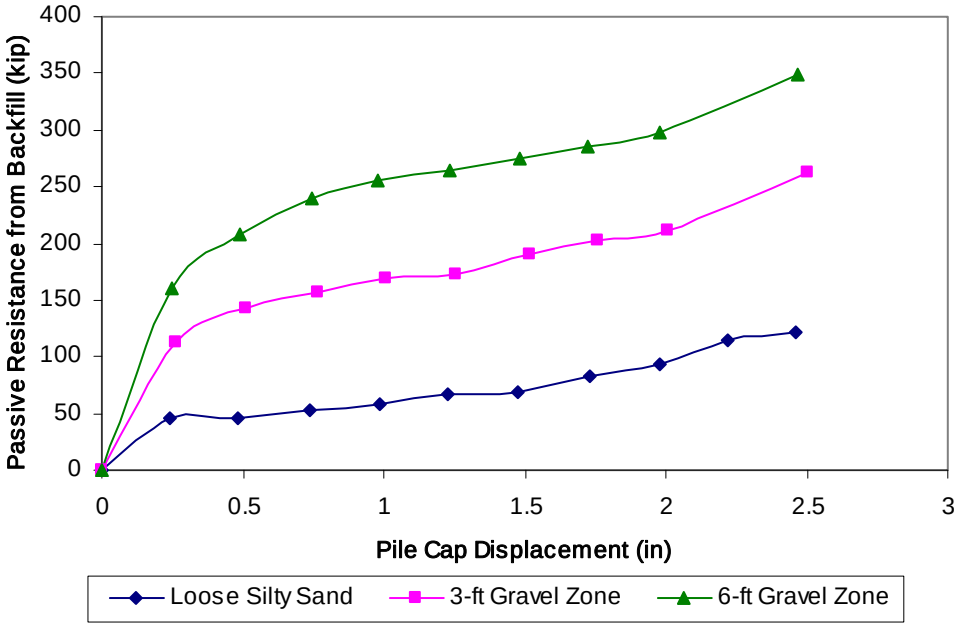

Figure 13-10 Comparison of earth force-displacement curves for loose silty sand backfill with varying widths of densely compacted gravel from tests at the I-15/South Temple site

front of looser material can provide at least 50% (actual tests values are 52% to 60%) of the ultimate capacity otherwise expected if all of the material surrounding the pile cap had been composed of the densely compacted gravel.

13.6 Effect of Pile Cap Height

Cole and Rollins (2006) conducted a lateral load test on a 3.67 ft (1.12 m) high pile cap with a densely compacted clean sand backfill similar to that used in the current tests with a 5.5 ft (1.68 m) high pile cap at the Salt Lake City International Airport (also see Cole, 2003). By comparing the results of these two tests, the effect of pile cap height on passive earth pressure can be evaluated. Parameters from the test of Cole and Rollins at the South Temple / I-15 site are shown in Table 13-6 together with the corresponding parameters from the test at the Airport. Soil parameters are based on laboratory values and have not been adjusted to improve the match between measured and theoretical passive earth pressures.

Table 13-6 Summary of load test parameters from South Temple and Airport sites

Parameter	South Temple	Airport
Cap height, H (ft)	3.67	5.5
Cap width, B (ft)	17	11
Horiz. passive earth force,P_{ph} (kip)	245	442
Friction angle, ϕ (°)	39	40.5
Cohesion, c (psf)	0	0
Interface friction angle, δ (°)	30	29
Moist unit weight, γ_m (pcf)	117.0	116.4
Disp. for max. soil force, Δ_{max} (in)	1.50	1.97
Δ_{max}/H	0.034	0.030
Three dimensional factor, R_{3D}	1.36	1.83
Passive earth pressure coeff., K_p	15.6	14.2
P-S passive earth force,P_{phps} (kip/ft)	10.6	21.9

The horizontal passive earth force and displacement at which this force is developed are based on the load-displacement curves for the two tests shown in Figure 13-11 and Figure 13-12. The three-dimensional loading effect due to different pile cap face aspect ratios was determined using the correction factor (R_{3D}) developed by Brinch-Hansen (1966). The passive earth pressure coefficient was calculated using the expression shown in Equation 14-1, whereas the normalized or plane-strain passive earth force (i.e., passive earth force normalized per unit width after removing three dimensional effects) was calculated using Equation 14-2.

$$P_{ph} = \frac{1}{2}\left(K_p \gamma_m H\right) H \; B \, R_{3D} \cos(\delta) \qquad \text{Equation 13-1}$$

$$P_{phps} = \frac{P_{ph}}{B \, R_{3D}} \qquad \text{Equation 13-2}$$

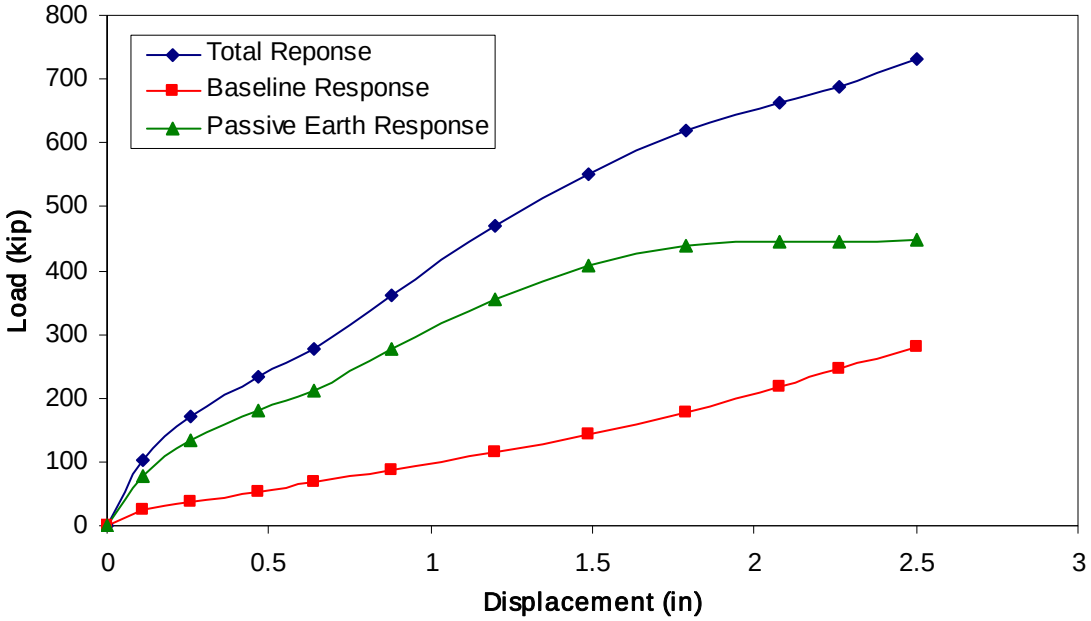

Figure 13-11 Load-displacement response for pile cap with densely compacted clean sand backfill at Airport site

From the data shown in Table 13-6, it can be seen that the passive earth pressure coefficients are quite similar (within 9%), despite some variances in the measured soil properties at the two sites. This suggests that it is reasonable to compare the results of these two tests to assess the effect of pile cap height on the passive resistance of backfill soil.

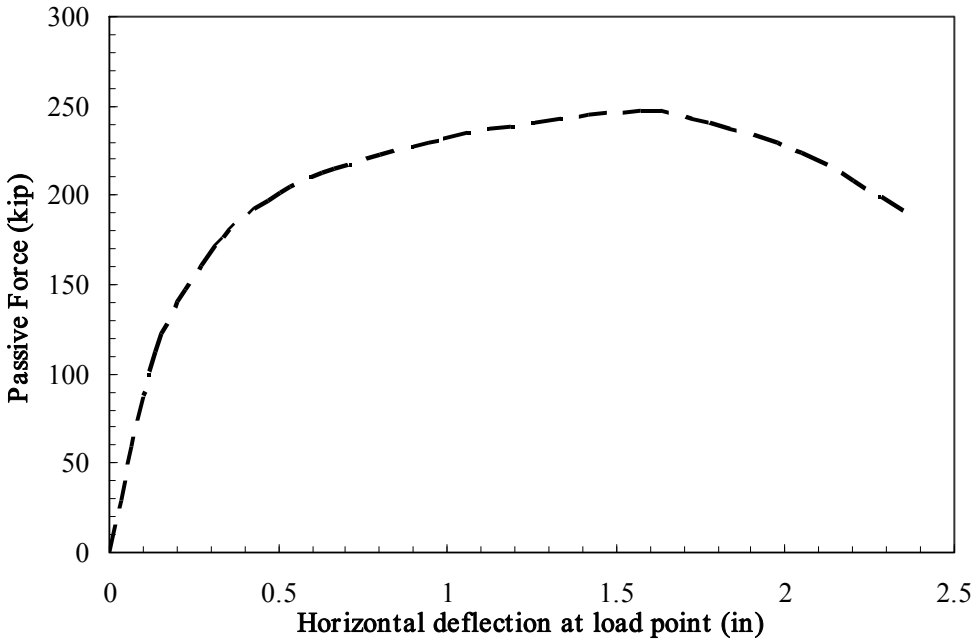

Figure 13-12 Load-displacement response for pile cap with densely compacted clean sand backfill at South Temple site (after Cole and Rollins, 2006)

Despite differing aspect ratios of 4.6 and 2.0 for the South Temple and Airport pile caps, respectively, the displacement to height ratio (Δ_{max}/H) is similar for both caps, being on the order of 3%. Expressed in terms of an equivalent fluid pressure, the term K_p □$_m$ is similar for both caps, being 1830 and 1650 pcf (287 and 260 kN/m^3), which averages to 1740 pcf (274 kN/m^3). Hence, for pile caps of different heights with the same backfill material, the ratio Δ_{max}/H appears to be constant (as expected), and the passive earth force is closely a function of the square of the height (as indicated by earth pressure theory).

The two tests can also be compared to assess the effect of height on foundation stiffness. Unfortunately, the initial portion of the load-displacement curve for the Airport pile cap appears to be unusually soft (perhaps due to cyclic/dynamic loading effects), thus preventing a definitive comparison of initial stiffness conditions. However, a comparison of stiffness at the maximum passive earth resistance can be made. Using the relationship shown in Equation 14-3, the equivalent stiffness (k_{equiv}) for the South Temple and Airport backfills is approximately 23.3 and 60.9 kip/in (4.08 and 10.67 kN/mm), respectively.

$$k_{equiv} = \frac{P_{phps}}{\Delta_{max}}$$

Equation 13-3

Using the Airport pile cap whose height is 5.5 ft (1.68 m) as a reference, Equation 14-4 was used to determine an appropriate cap (wall) height scaling parameter, n.

$$k_{southtemple} = k_{airport}\left(\frac{H_{southtemple}}{H_{airport}}\right)^{n}$$ Equation 13-4

An exponent, n, of 2.38 (about 19/8) satisfies Equation 14-4. Given the initial variation in earth pressure coefficients between the two sites and given that the height term is squared in Equation 14-1, and although wall height does somewhat effect the passive earth pressure coefficient determined by the log-spiral method, it seems reasonable to approximate the exponent n as 2.0, indicating that wall stiffness is a function of the square of the height ratio.

14.0 CLOSURE

14.1 Summary

This report presents results from lateral load tests performed on a full-scale pile cap with nine different backfill conditions. The results from each condition are presented in the following order: no backfill present (baseline response), densely compacted clean sand, loosely compacted clean sand, densely compacted fine gravel, loosely compacted fine gravel, densely compacted coarse gravel, loosely compacted coarse gravel, a 3-ft (0.91-m) wide densely compacted fine gravel zone with loosely compacted clean sand backfill, and a 6-ft (1.83-m) wide densely compacted fine gravel zone with loosely compacted clean sand backfill. Static load induced displacement was accompanied by low frequency small amplitude loading cycles and higher frequency small amplitude dynamic loading cycles. Analysis and interpretation of the results are presented for each backfill condition, and comparisons are made between backfill conditions.

14.2 Conclusions

Based on the data, analyses, and interpretations presented in this report, the following conclusions and recommendations have been developed:

14.2.1 Clean Sand Backfill

1. Passive earth pressure from the backfill significantly increased the lateral load capacity of the pile cap. At the fully mobilized passive earth pressure, the densely compacted clean sand backfill contributes about 67% of the total load capacity of the pile cap system. In contrast, the loosely compacted clean sand contributes about 36% of the total lateral load capacity of the test foundation.
2. At a displacement of about 2.0 in (corresponding to a displacement-to-cap-height ratio of about 0.030), the passive resistance of the densely compacted clean sand appears to be fully mobilized, and the placement of the densely compacted clean sand produced a 204% increase in capacity over the pile cap acting alone. In contrast, the loosely compacted coarse gravel increased the total capacity of the pile cap system by 56% relative to the pile cap without backfill. The dramatic increase in resistance

3. Both the log-spiral method (as represented by the spreadsheet program PYCAP) and the LSH method (as represented by ABUTMENT) provide reasonably accurate predictions of passive resistance for the densely compacted clean sand. The Rankine passive earth approach appears to provide a good match to the measured ultimate resistance for the loosely compacted clean sand. Reducing the shear strength parameters to 60 to 65% of their original values and setting the interface friction angle equal to the soil friction angle (similar to the approach Terzaghi and Peck (1967) took regarding the bearing capacity of loose to medium granular soils) also provides a reasonable estimate of the ultimate passive resistance of the loosely compacted soil. The CALTRANS simplified bilinear method did not provide a good prediction for either density state of the clean sand.
4. Under low frequency cyclic loadings, the stiffness of the pile cap system increases with the presence of the backfill material. The loosely compacted backfill provided about twice the stiffness of the no backfill case. The densely compacted sand provided double the stiffness of the loosely compacted sand, thus quadrupling the stiffness of the pile cap relative to the case with no backfill present.
5. Under low frequency cyclic loadings, the damping ratio of the pile cap system decreases with cap displacement and with increasing stiffness of backfill material. The median damping ratio is about 18% for the densely compacted clean sand and about 24% for the loosely compacted clean sand.
6. Under higher frequency cyclic loading (up to 10 Hz), the dynamic stiffness of the pile cap system increases with the presence of backfill material. The loosely compacted backfill provided on the order of twice the stiffness of the pile cap acting without backfill. The densely compacted backfill provided on the order of three times more stiffness than the no backfill case.
7. Under higher frequency cyclic loading, the damping ratio of the pile cap system appears to vary with frequency. In fact, the damping ratio varies similarly with frequency for all the backfill conditions tested: a wave-like pattern of high and low values as the frequency increases; however, specific values vary from one backfill

8. Comparison of damping ratios at similar displacement amplitudes for low frequency (~0.75 Hz) and higher frequencies (4 to 10 Hz) yielded reasonable agreement for applicable backfill conditions. The similarity in damping for different frequency ranges suggests that dynamic loadings do not appreciably increase the apparent resistance of the pile cap relative to slowly applied cyclic loadings.
9. Comparison of stiffness values at similar displacement amplitudes for low frequency (~0.75 Hz) and higher frequencies (4 to 10 Hz) yielded comparable results for the no backfill case and the loosely and densely compacted clean sand.
10. Measured earth pressure distributions generally increased with depth, except near the bottom of the pile cap where, for both compaction levels of clean sand, the observed pressure was negligible. The trends in earth pressure forces versus displacement calculated from these pressure distributions are similar to the trends seen in the passive earth force versus displacement calculated from actuator forces, except they are systematically lower. Using a multiplier of approximately 1.67 to adjust the earth pressure cell measurements to account for three-dimensional and other effects provided a reasonable match between the passive earth force-displacement curves based on the actuator loads and those derived from the earth pressure cells.
11. Vertical movement, horizontal strain, and surface cracking patterns seem to relate well with each other. For the densely compacted clean sand, these patterns also appeared to correlate well with the computed log-spiral failure surface. The movement and surface cracking patterns manifest in the loosely compacted clean sand appear to suggest that development of the soil's resistance as the pile cap is displaced is due to progressive densification of the backfill, or perhaps a punching shear failure mechanism, instead of shear resistance along a well-defined log-spiral failure surface as is seemingly the case with the densely compacted clean sand.

14.2.2 Fine Gravel Backfill

1. Passive resistance from the backfill dramatically improved the lateral load capacity of the pile cap. At the fully mobilized passive earth pressure, the densely compacted

fine gravel contributes about 70% of the total lateral load capacity of the test foundation. The loosely compacted fine gravel contributes about 37% of the total lateral load capacity of the test foundation for the maximum displacement reached during testing. In other words, the resistance offered by the densely compacted fine gravel was about 2.4 times the resistance offered by the loosely compacted fine gravel.

2. At a displacement of about 2.4 in (corresponding to a displacement-to-cap height ratio of about 0.037), the passive resistance of the densely compacted fine gravel appears to be fully mobilized, and placement of the densely compacted fine gravel produced a 235% increase in capacity over the pile cap acting alone. In contrast, the capacity observed with the loosely compacted fine gravel backfill test was about 60% greater than the pile cap acting by itself. The dramatic increase in resistance offered by the densely compacted backfill compared to that offered by the loosely compacted backfill demonstrates the importance of adequate backfill compaction.
3. The log-spiral methods presented in PYCAP and in the LSH method are sensitive to variation in interface friction parameters (particularly as the soil friction angle becomes large) and can produce a wide range of predictions of the ultimate passive force. Due to constraints presented by oversized aggregates in laboratory tests and potential shortcomings with staged in-situ tests, it is difficult to assess the shear strength parameters for the gravel materials. Log-spiral methods can provide reasonable predictions of passive resistance as long as input parameters are judiciously selected. Recommendations for computing passive earth forces for gravelly soils are presented at the end of this chapter. In-situ shear strength parameters appeared to provide the best matches to the measured resistance curve. The Rankine passive earth approach appears to provide a good match to the measured ultimate resistance for the loosely compacted fine gravel. Reducing the shear strength parameters to 65% of their original values and setting the interface friction angle equal to the soil friction angle (similar to the approach Terzaghi and Peck (1967) took regarding the bearing capacity of loose to medium granular soils) also provides a reasonable estimate of the ultimate passive resistance of the loosely compacted soil. The CALTRANS simplified bilinear method performed poorly in the

prediction of the ultimate resistance of the backfill for either density state of the fine gravel.

4. The fine gravel backfill material increases the stiffness of the test foundation under slowly applied cyclic loadings. The presence of the loosely compacted fine gravel roughly doubled the stiffness of the pile cap system, compared to the no backfill case. With densely compacted fine gravel present, the stiffness of the test foundation more than quadrupled in comparison to the test with no backfill present.
5. Under low frequency cyclic loadings, the median damping ratio of the pile cap with densely compacted fine gravel is approximately 19%, while the median damping ratio of the loosely compacted fine gravel is about 24%. This represents a decrease in damping ratio with increasing cap displacement and increasing backfill stiffness.
6. Fine gravel backfill increased the dynamic stiffness of the test foundation when the cap was subjected to higher frequency cyclic loading (up to 10 Hz). Loosely compacted fine gravel approximately doubled the stiffness of the test foundation with no backfill. Densely compacted fine gravel roughly quadrupled the stiffness of the pile cap relative to the no backfill case. The densely compacted backfill also offers a proportionally larger range of stiffness than that obtained with no backfill behind the pile cap.
7. Damping ratio appears to vary with frequency when the pile cap system is subjected to higher frequency cyclic loading. This variation applies to all the backfill conditions tested and can be described as a wave-like pattern of high and low values as the frequency increases; however, specific values vary from one backfill condition to another. The densely compacted fine gravel backfill appeared to provide slightly more dynamic damping, in a broader range, than the loosely compacted fine gravel.
8. A comparison of damping ratios at similar displacement amplitudes for the loosely compacted fine gravel appeared to result in reasonable agreement between low frequency (~0.75 Hz) and higher frequency (4 to 10 Hz) loadings. Similar damping for different frequency ranges suggests that higher frequency loadings do not appreciably increase the apparent resistance of the pile cap compared to slowly applied cyclic loadings.

9. Comparable stiffness between the two cyclic loading types was found at similar loop displacement amplitudes for the loosely compacted fine gravel.
10. Earth pressure distributions compiled from earth pressure cell data generally showed an increase with depth and with increasing pile cap displacement. The loosely compacted fine gravel pressure distribution displayed unusual behavior in that the measured pressure appeared to be negligible near the bottom of the pile cap. The trends in earth pressure forces versus displacement calculated from these pressure distributions are similar to the trends seen in the passive earth force versus displacement calculated from actuator forces, except they are systematically lower. Using a multiplier of approximately 1.67 to adjust the earth pressure cell measurements to account for three-dimensional and other effects provided a reasonable match between the passive earth force-displacement curves based on the actuator loads and those derived from the earth pressure cells.
11. Vertical movement, horizontal strain, and surface cracking patterns seem to relate well with each other. For the densely compacted fine gravel, these patterns also appeared to correlate well with the computed log-spiral failure surface. The movement and surface cracking patterns manifest in the loosely compacted fine gravel appear to suggest that development of the soil's resistance as the pile cap is displaced is due to progressive densification of the backfill, or perhaps a punching shear failure mechanism, instead of shear resistance along a well-defined log-spiral failure surface as is seemingly the case with the densely compacted fine gravel.

14.2.3 Coarse Gravel Backfill

1. Passive resistance from the backfill dramatically improved the lateral load capacity of the pile cap. At fully mobilized passive earth pressure, the densely compacted coarse gravel contributes about 68% of the total lateral load capacity of the test foundation. In contrast, the loosely compacted coarse gravel contributed about 43% of the total lateral load capacity of the test foundation for the maximum displacement reached during testing.
2. At a displacement of about 2.9 in (corresponding to a displacement-to-cap-height ratio of about 0.044), the passive resistance of the densely compacted coarse gravel appears to be fully mobilized, and the placement of the densely compacted coarse

gravel produced a 217% increase in capacity over the pile cap acting alone. In contrast, the loosely compacted coarse gravel increased the total capacity of the pile cap system by 82% relative to the pile cap without backfill. The dramatic increase in resistance offered by the densely compacted backfill compared to that offered by the loosely compacted backfill demonstrates the importance of adequate backfill compaction.

3. The log-spiral methods presented in PYCAP and in the LSH method are sensitive to variation in interface friction parameters (particularly as the soil friction angle becomes large) and can produce a wide range of predictions of the ultimate passive force. Due to constraints presented by oversized aggregates in laboratory tests and potential shortcomings with staged in-situ tests, it is difficult to assess the shear strength parameters for the gravel materials. Log-spiral methods can provide reasonable predictions of passive resistance as long as input parameters are carefully chosen. In-situ shear strength parameters appeared to provide the best match to the measured response with the least amount of manipulation for the densely compacted coarse gravel, whereas the correlation-based friction angle with a significantly discounted interface friction angle was found to provide a good match for the loosely compacted coarse gravel. However, the use of Duncan's engineering correlation can produce friction angles not in the range commonly used by designers. Reducing the shear strength parameters to 85% of their original value and setting the interface friction angle equal to the soil friction angle (similar to the approach Terzaghi and Peck (1967) took regarding the bearing capacity of loose to medium granular soils) also provides a reasonable estimate of the ultimate passive resistance of the loosely compacted soil. The CALTRANS simplified bilinear method provided a good prediction for loosely compacted coarse gravel, but severely underestimated the densely compacted coarse gravel.
4. The coarse gravel backfill material increases the stiffness of the test foundation under slowly applied cyclic loadings. The presence of loosely compacted coarse gravel roughly doubled the stiffness of the test foundation acting with no backfill. The densely compacted coarse gravel provided nearly 6 times the stiffness offered by the pile cap with no backfill present.

5. Under low frequency cyclic loadings, the median damping ratio of the pile cap with densely compacted coarse gravel is approximately 18%, while the median damping ratio for the loosely compacted coarse gravel test is 21%.
6. Coarse gravel backfill increased the dynamic stiffness of the test foundation when the cap was subjected to higher frequency cyclic loading (up to 10 Hz). Loosely compacted coarse gravel nearly tripled the stiffness offered by the test foundation with no backfill. Densely compacted coarse gravel provided over four times the stiffness of the pile cap acting without backfill.
7. Damping ratio appears to vary with frequency when the pile cap system is subjected to higher frequency loading. This variation applies to all the backfill conditions tested and can be described as a wave-like pattern of high and low values as the frequency increases; however, specific values vary from one backfill condition to the next. Significantly more damping, in a wider range of values, was observed in the loosely compacted coarse gravel test than in the densely compacted coarse gravel test.
8. Neither compaction state of the coarse gravel yielded comparable loop displacement amplitudes between the slowly applied (~0.75 Hz) and the higher frequency (up to 9 or 10 Hz) loadings. The shaker was not able to produce enough force to displace the backfill adequately to make a comparison of damping ratio for the densely and loosely compacted soil at the same displacement amplitude.
9. Earth pressure distributions compiled from earth pressure cell data generally showed an increase with depth and with increasing pile cap displacement. The loosely compacted coarse gravel pressure distribution exhibited unusual behavior when the measured pressure fell to negligible levels after the first push, then rose incrementally with increasing cap displacement for the pressure cell nearest the bottom of the pile cap. Even with the incremental increase in pressure following the drop, the final observed pressure for the bottom cell was well below the observed pressure from the cell above after the final cap displacement. The trends in earth pressure forces versus displacement calculated from these pressure distributions are similar to the trends seen in the passive earth force versus displacement calculated from actuator forces, except they are systematically lower. Using a multiplier of approximately 1.67 to adjust the earth pressure cell measurements to account for three-dimensional and

other effects provided a reasonable match between the passive earth force-displacement curves based on the actuator loads and those derived from the earth pressure cells.

10. Vertical movement, horizontal strain, and surface cracking patterns seem to relate well with each other. For the densely compacted coarse gravel, these patterns also appeared to correlate well with the computed log-spiral failure surface. The movement and surface cracking patterns manifest in the loosely compacted coarse gravel appear to suggest that development of the soil's resistance as the pile cap is displaced is due to progressive densification of the backfill, or perhaps a punching shear failure mechanism, instead of shear resistance along a well-defined log-spiral failure surface as is seemingly the case with the densely compacted coarse gravel.

14.2.4 Partial Widths of Densely Compacted Gravel with Loosely Compacted Sand Backfill

1. Passive earth pressure from the backfill significantly increased the lateral load capacity of the pile cap, relative to the cap without any backfill. At the displacement levels where the ultimate passive earth pressures appear to be reached, the 3-ft (0.91-m) and 6-ft (1.83-m) densely compacted fine gravel zones with loosely compacted clean sand backfill offered 60% and 58%, respectively, of the total passive resistance of the pile cap system
2. At about 2.4 in (62 mm), the displacement level where both of the partial width densely compacted fine gravel backfill conditions appear to start failing, the 3-ft (0.91-m) and 6-ft (1.83-m) fine gravel zones increased the total capacity of the pile cap without backfill by 148% and 136%, respectively.
3. Using relatively narrow zones of densely compacted gravel immediately adjacent to a pile cap face significantly increased the capacity of otherwise weak fill or native soil. In the tests conducted at the Airport site, at a pile cap displacement of about 1.5 in (38 mm) (the displacement level at which the loosely compacted clean sand appears to fail), the 3-ft (0.91-m) and the 6-ft (1.83-m) densely compacted fine gravel zones with loosely compacted clean sand backfill improved the resistance offered by the loosely compacted clean sand backfill by approximately 260% and 270%, respectively. This equates to approximately 64% and 66% of the resistance offered

by the full length densely compacted fine gravel backfill condition at 1.5 in (38 mm) for the 3- and 6-ft (0.91- and 1.83-m) wide fine gravel zones with loosely compacted sand backfill, respectively.

4. Based on the observed pattern of backfill cracking and calculated strains, the relatively narrow zones of densely compacted gravel next to the pile cap appear to behave somewhat as an extension of the pile cap. After a small amount of initial strain in the densely compacted fine gravel zones, the majority of the pile cap displacement in the 3-ft (0.91-m) and 6-ft (1.83-m) densely compacted fine gravel zone with loosely compacted clean sand backfill tests was transferred directly into the loosely compacted sand. As displacement increases, radial cracking develops from the corners of the pile cap and propogates through the densely compacted gravel to the dense gravel/loose sand interface.
5. Under low frequency cyclic loadings, the stiffness of the pile cap system increases with the presence of backfill material. The partial width densely compacted gravel zones with loosely compacted clean sand backfill provided close to 4 times the stiffness of the pile cap system without backfill.
6. Under low frequency cyclic loadings, the damping ratio of the pile cap system decreases with cap displacement and with increasing stiffness of backfill material. The median damping ratio is about 20% for the partial width gravel zones.
7. Measured earth pressure distributions generally increased with depth for the 3-ft (0.91-m) fine gravel zone with loosely compacted sand backfill condition. For the 6-ft (1.83-m) zone of densely compacted fine gravel with loosely compacted clean sand backfill, the measured pressure at the bottom pressure cell initially increased, then decreased as the pile cap advanced; the top of the pressure distribution increases steadily until, by the end of the test, the distribution appears to be inverted from the typical representation of earth pressure. The trends in earth pressure forces versus displacement calculated from these pressure distributions are similar to the trends seen in the passive earth force versus displacement calculated from actuator forces, except they are systematically lower. Using a multiplier of approximately 1.67 to adjust the earth pressure cell measurements to account for three-dimensional and other effects provided a reasonable match between the passive earth force-

displacement curves based on the actuator loads and those derived from the earth pressure cells.

8. Observed heave and cracking patterns seem to correspond well with each other. In both the 3-ft (0.91-m) and 6-ft (1.83-m) cases, the zone of densely compacted gravel heaves, as was observed with the conditions of the full width placement of the same densely compacted fine gravel backfill. In terms of cracking, the cases of the 3-ft (0.91-m) and 6-ft (1.83-m) wide densely compacted gravel zones with otherwise loosely compacted clean sand exhibit a combination of the behaviors similar to that observed in the full-width densely compacted fine gravel backfill and the full-width loosely compacted clean sand backfill.

14.2.5 Effect of Pile Cap Height on Passive Earth Pressure

1. A comparison of the passive earth pressure test results in a densely compacted clean sand material between two different pile cap foundations showed similar displacement to height ratios despite drastically different aspect ratios between the two pile cap systems. The two pile caps have similar equivalent fluid pressure terms (being on the order of 10% different from each other); hence, for pile caps with different heights with the same backfill material, Δ_{max}/H appears to be constant.
2. Despite initial stiffness differences between the two foundations (the Airport site foundation had unusually low initial stiffness), a comparison of the foundation stiffness at maximum passive earth pressure was made. The stiffness at maximum earth pressure for the Airport foundation was about 2.6 times the stiffness of the South Temple foundation at maximum earth pressure.
3. A cap (wall) height scaling parameter was determined using the results from the comparison of the two test foundations. The exponent, n, applies to Equation 13-4, and can be approximated as 2.0, indicating that backfill stiffness is a function of the square of the height ratio.

14.3 Recommendations for Implementation

Based on the data, analyses, and interpretations presented in this report, the following recommendations have been developed:

1. Given the dramatically different load-displacement response of loosely and densely compacted soils, engineering professionals should take significant measures to assure that backfill compaction requirements are met and that those requirements result in a high relative density if significant passive earth force is required.
2. For the design of concrete foundations and abutments backfilled with well-compacted granular materials, say on the order of 95% modified Proctor density or 75% relative density, the log-spiral approach can be used with a soil friction angle of 40° and a δ/□ ratio of 0.6 to 0.75 to determine the passive earth force. These parameters should give a lower-bound solution to the passive response of backfill subjected to static, cyclic, and dynamic loadings. The designer who has performed field shear strength testing and is confident in the resulting parameters can use them in determining a larger passive earth force, noting that calculated passive earth coefficients increase 10 to 15% for each 1° increase in □beyond 40°.
3. In the case of loosely compacted granular fills, say on the order of 85 to 90% modified Proctor or 35% relative density, Rankine passive earth theory may be used to determine the passive earth force. However, the Rankine method may underestimate the capacity of granular backfill soil as the failure mode transitions from punching to general shear. Alternatively, shear strengths can be reduced by a factor ranging from 0.6 to 0.85 (perhaps increasing with relative density) when using the log-spiral method to compute the passive earth force. This approach is similar to that suggested by Terzaghi and Peck (1967) for the bearing capacity of loose to medium dense granular soils.
4. For densely compacted granular backfills, the load-displacement response can be modeled as a hyperbolic curve and the ultimate passive force is realized at a displacement-to-height ratio of approximately 3 to 4%. Computer programs such as PYCAP and ABUT can be used to reasonably calculate hyperbolic passive earth load versus displacement relationships for densely compacted granular backfills.
5. Three-dimensional loading effects for pile caps with varying aspect ratios and densely compacted granular backfills can be reasonably accounted for using Brinch-Hansen's (1966) relationship.

6. Under cyclic and dynamic loadings, the passive earth force acting on the face of a pile cap or abutment can contribute a significant portion of the overall resistance and stiffness. The response of pile cap structures subject to variable frequency loadings can be quantified using an average damping ratio of at least 15%, but the precise ratio will vary as inertial and total earth forces act in and out of phase. Consideration should be given to changes in structural period due to changes in dynamic stiffness and damping ratio with forcing frequency and displacement amplitude.
7. Placement of a relatively narrow zone of densely compacted gravel immediately adjacent to a foundation where the surrounding soil is otherwise relatively loose can significantly increase the passive resistance provided by the soil backfill. A nominal 3 ft (0.91 m) wide (i.e., horizontal) zone of densely compacted gravel should provide at least 50% of the ultimate capacity otherwise expected if all of the material surrounding the pile cap had been composed of the densely compacted gravel. The densely compacted backfill should also extend vertically below the bottom of the foundation 25% of the pile cap height. The effect of a wider zone of densely compacted gravel is less certain and requires more analysis.
8. When accounting for the effect of wall height on the ultimate passive force and backfill stiffness, both parameters should be scaled by the square of the ratio of the wall heights.

THIS PAGE INTENTIONALLY LEFT BLANK

REFERENCES

AASHTO (2007). *AASHTO LRFD Bridge Design Specifications, 4th Ed.* American Association of State Highway and Transportation Officials, Washington, D.C.

Borowicka, H. (1938). "Distribution of pressure under a uniformly loaded elastic strip resisting on elastic-isotropic ground." *2nd Cong. Int. Assoc. Bridge Struct. Engrg.* Vol. 8 (3).

Brinch-Hansen, J. (1966). "Resistance of a rectangular anchor slab." *Bulletin No. 21,* Danish Geotechnical Institute, Copenhagen, 12–13.

Christensen, D.S. (2006). "Full scale static lateral load test of a 9 pile group in sand," *MS Thesis*, Dept. of Civil and Environmental Engineering, Brigham Young University, Provo, Utah.

Clough, G.W. and Duncan, J.M. (1991). Earth retaining structures, *In Foundation engineering handbook*. 2nd Ed. H.Y. Fang, Ed. Van Nostrand Reinholdt, New York

Cole, R.T. (2003). "Full-scale effects of passive earth pressure on the lateral resistance of pile caps." *PhD Dissertation*, Brigham Young University, Provo, Utah.

Cole, R.T. and Rollins, K.M. (2006). "Passive earth pressure mobilization during cyclic loading." *Journal of Geotechnical and Geoenvironmental Engineering*, ASCE, 132(9), 1154-1164.

Douglas, D. J. and Davis, E. H. (1964). "The movements of buried footings due to moment and horizontal load and the movement of anchor plates." *Geotechnique*, London, 14(2), 115–132.

Duncan, J.M. (2004). "Friction angles for sand, gravel, and rockfill." Kenneth L. Lee Memorial Seminar, Long Beach, CA, April 2004.

Duncan, J.M. and Mokwa, R. L. (2001). "Passive earth pressures: theories and tests." *J. Geotechnical and Geoenv. Engrg.*, ASCE, 127(3), 248-257

Johnson, S.R. (2003). "Static lateral load testing a full-scale pile group spaced at 5.65 pile diameters." *MS Thesis*, Dept. of Civil and Environmental Engineering, Brigham Young University, Provo, Utah.

Lee, K.L. and Singh, A. (1971). "Relative density and relative compaction." *Journal of the Soil Mechanics and Foundations Division,* ASCE, 97(7), 1049-1052.

Maroney, B.H. (1995). "Large scale bridge abutment tests to determine stiffness and ultimate strength under seismic loading," *Ph.D. Dissertation*, University of California, Davis

Peterson, K.T. (1996). "Static and dynamic lateral load testing a full-scale pile group in clay." *MS Thesis*, Dept. of Civil and Environmental Engineering, Brigham Young University, Provo, Utah.

Rollins, K.M. and Cole, R.T. (2006). "Cyclic lateral load behavior of a pile cap and backfill." *Journal of Geotechnical and Geoenvironmental Engineering*, ASCE, 132(9), 1143-1153.

Rollins, K.M., Gerber, T.M., and Kwon, K.H. (2010). "Increased lateral abutment resistance from gravel backfills of limited width." *Journal of Geotechnical and Geoenvironmental Engineering*, ASCE. 136(1) ,230-238.

Rollins, K.M., King, R., Snyder, J.E., and Johnson, S.R. (2005b). "Full-scale lateral load tests of pile groups and drilled shafts in clay." *Procs. Intl. Conf. on Soil-Structure Interaction, Calculation Methods and Engineering Practice*, Vol. 1, Ulitsky, V.M., Ed., ASV Publishers, Moscow: 287-292.

Rollins, K.M., Snyder, J.L., and Broderick, R.D. (2005a). "Static and dynamic lateral response of a 15 pile group." *Procs. 16th Intl. Conf. on Soil Mechanics and Geotechnical Engineering*, Vol. 4, Millpress, Rotterdam, Netherlands: 2035-2040.

Runnels, I.K. (2007). "Cyclic and dynamic full-scale testing of a pile cap with loose silty sand backfill." *MS Thesis*, Dept. of Civil and Environmental Engineering, Brigham Young University, Provo, Utah.

Shamsabadi, A., Ashour, M., and Norris, G. (2005). "Bridge abutment nonlinear force-displacement-capacity prediction for seismic design." *Journal of Geotechnical and Geoenvironmental Engineering*, ASCE, 131(2), 151-161.

Shamsabadi, A., Rollins, K.M., and Kapaskur, M. (2007). "Nonlinear soil-abutment-bridge structure interaction for seismic performance-based design." *Journal of Geotechnical and Geoenviromental Engineering.*, ASCE, 133(6), 707-720.

Shamsabadi, A. and Yan, L. (2008). "Closed-form force-displacement backbone curves for bridge abutment-backfill systems." *Proc. of Geotechnical Earthquake Engineering and Soil Dynamics IV*, Geotechnical Special Publication 181, ASCE.

Taylor, A.J. (2006). "Full-scale-lateral-load test of a 1.2 m diameter drilled shaft in sand." *MS Thesis*, Dept. of Civil and Environmental Engineering, Brigham Young University, Provo, Utah.

Terzaghi, K. and Peck, R. B. (1967). *Soil Mechanics in Engineering Practice*. Wiley, New York.

Tokimatsu, K., Suzuki, H., and Sato, M. (2004). "Influence of initial and kinematic components on pile response during earthquakes." *Procs. 11th Intl. Conf. on Soil Dynamics and Earthquake Engineering* and *3rd Intl. Conf. on Earthquake Geotechnical Engineering.* University of California, Berkeley. Doolin, D., Kammerer, A., Nogami, T., Seed, R.B., and Towhata, I., Eds. Vol. 1, 768-775.

U.S. Navy. (1986). *Foundations and Earth Structures - Design Manual 7.2*. Navy Facilities Engineering Command, Alexandria, Va.

Valentine, T.J. (2007). "Dynamic testing of a full-scale pile cap with dense silty sand backfill." *MS Thesis*, Dept. of Civil and Environmental Engineering, Brigham Young University, Provo, Utah.